# Sex-specific Gene Expression in Embryonic Mouse Germ Cells during Commitment to Spermatogenesis or Oogenesis

**Luke Lewis**

**MPhil Degree**

**The University of Edinburgh**

**2009**

# Abstract

The default developmental choice for both female and male Murine Germ Cells (GCs) is to commit to oogenesis and begin meiosis, which occurs *in vivo* in the developing ovary, and *in vitro*, at E12.5-E13.5. Prior to this commitment, female and male GCs are receptive to masculinising signals from the developing male gonad that induce GCs to commit to spermatogenesis at E11.5-E12.5, followed by temporary mitotic arrest. A previous differential expression study identified 2 candidate genes upregulated sex-specifically. *Inhibitor of DNA Binding 1* (*Id1*) mRNA was upregulated in female E13.5 GCs and has not been studied in relation to this developmental paradigm; while *Lipocalin-Type Prostaglandin $D_2$-Synthase* (*Ptgds*) mRNA was upregulated in XY E13.5 GC preparations and precious studies show that its high expression by male supporting cells augments masculinisation of cells in the developing male gonad. This thesis aims to firstly confirm sex-specific GC expression of these genes at E13.5, a stage when GCs have committed to spermatogenesis or oogenesis, and secondly, to use this sex-specific expression to shed light upon the molecular events driving GC sexual commitment.

Id1 belongs to the Basic Helix-loop-helix (bHLH) family of transcriptional effectors that operate as homo- or heterodimers. Id1 suppresses cellular commitment and exit from the cell cycle partly by binding to and inhibiting the action of pro-differentiation bHLHs. A 40-fold female-specific enrichment of *Id1* mRNA and protein in E13.5 XX GCs was confirmed by Quantitative Real-time PCR and by Quantitative Immunofluorescence, respectively. Male GC nuclei had very low levels of Id1 immunofluorescence, whereas female GC nuclei had heterogeneous but significantly higher average Id1 immunofluorescence levels. GCs in both XX and XY E11.5 gonads had heterogeneous Id1 immunofluorescence levels, similar to E13.5 female GCs, but no obvious sex-specific difference was seen at E11.5. However, in E12.5 gonads a sex-specific difference was seen, with XY GCs expressing very low Id1 levels. It appears, therefore, that XY GCs' Id1 protein expression drops sharply at E11.5-E12.5, coinciding with the time that XY GCs commit to spermatogenesis and arrest

mitotically. Female GCs on the other hand continually express heterogeneous Id1 protein levels at E11.5-E13.5.

In order to discover candidate Id1-interacting bHLHs in female E13.5 GCs, a Quantitative Real-time PCR expression screen was performed to identify bHLHs enriched sex-specifically in E13.5 GC cDNA. 5 bHLH genes were significantly enriched or detected only in male E13.5 GC cDNA and 16 bHLH genes (including *Id2* and *Id3*, close family members to *Id1*) were significantly enriched or detected only in female E13.5 GC cDNA. *Mnt*, a negative regulator of the oncogene *Myc*, was one of the male-enriched genes and male-specific enrichment of Mnt protein was confirmed by Quantitative Immunofluorescence on E13.5 gonad sections, and qualitatively by immunofluorescence on E12.5 gonad sections. Both female and male GCs expressed high Mnt protein levels at E11.5, so sex-specific Mnt protein expression probably first appears at E11.5-E12.5 due to a downregulation by female GCs. To conclude, 21 genes were enriched or expressed sex-specifically in E13.5 GC cDNA, 16 in female cDNA and are interesting candidates for Id1 interaction in female GCs during commitment to oogenesis and meiotic entry. Mnt protein was enriched male-specifically in E12.5 and E13.5 GC nuclei, when female GCs appear to downregulate Mnt protein levels.

Semi-quantitative PCR detected weak *Ptgds* in purified E13.5 male, but not female, GC cDNA. Also, weak *Ptgds* immunofluorescence was seen in male, but not female, GC cytoplasm. In conclusion, weak *Ptgds* mRNA and protein expression was detected sex-specifically in male GCs. A study was then undertaken to test whether molecular signals that are known to affect *Ptgds* expression in other tissues were able to affect *Ptgds* expression in developing GCs. E11.5 and E12.5 XX or XY genital ridges were cultured with the phorbol ester Phorbol 12-myristate 13-acetate, Ionomycin, Dexamethoasone or Thyroid Hormone for 3 days and *Ptgds* expression examined by whole mount *in situ* hybridisation. All 4 compounds failed to induce or suppress *Ptgds* expression levels detectably. This suggests that *Ptgds* expression in GCs may be stimulated by distinct molecular pathways.

# Abbreviations

| | |
|---|---|
| AP: | Alkaline phosphatase |
| Amh: | Anti-mullerian hormone |
| bHLH: | Basic helix-loop-helix |
| BCIP: | 5-bromo-4-chloro-3-indolyl-phosphate |
| BMP: | Bone morphogenic protein |
| BrdU: | Bromodeoxyuridine |
| BSA: | Bovine serum albumin |
| $C_{(t)}$: | Threshold cycle |
| CDKI: | Cyclin-dependent kinase inhibitor |
| ESCs: | Embryonic stem cells |
| FACS: | Fluorescence-activated cell sorting |
| GC: | Germ cell |
| GCNA: | Germ cell nuclear antigen |
| GFP: | Green fluorescent protein |
| GR: | Genital ridge |
| Ig: | Immunoglobulin |
| LIF: | Leukemia inhibitory factor |
| Mvh: | Mouse vasa homologue |
| NBT: | 4-nitro blue tetrazolium chloride |
| nt: | nucleotide(s) |
| PBS: | Phosphate buffered saline |
| $PgD_2$: | Prostaglandin $D_2$ |
| PolyA: | Polyadenosine |
| Ptgds: | Lipocalin-type prostaglandin $D_2$ synthase |
| RA: | Retinoic acid |
| Rb: | Retinoblastoma protein |
| RT: | Reverse transcription |
| RtPCR: | Real-time PCR |
| TPA: | 12-O-tetradecanoylphorbol-13-acetate |
| T3: | Thyroid hormone |
| WISH: | Wholemount *in situ* hybridisation |

# Chapter 1:
# Introduction

Unlike the somatic cells making up most mammalian tissues, germline cells undergo meiosis to form mature germ cells (GCs) that generate the zygote of the next generation. Primordial GCs are the progenitors of the germline and differentiate sex-specifically during embryogenesis, after a period of non-sex-specific development, to produce populations of self-renewing spermatogonial stem cells in the adult male testis or meiotically-arrested oocytes in the adult female ovary. In the adult testes of normal XY males, the germline stem cells undergo repeated rounds of mitosis followed by meiosis to give rise to mature sperm. In the adult ovary of normal XX females, meiotically-arrested oocytes reside in primordial follicles until estrous hormones direct their maturation into fertilisation-competent oocytes.

## 1.1. Germ Cell (GC) Specification and Migration

As with other organisms –flies, worms and chickens for example - mammalian GCs are specified and initially develop outside of the gonads then actively migrate to them once they are formed (McLaren, 2000). Mammalian GC progenitors (primordial GCs) are specified after implantation from proximal epiblast cells that contribute to both germline and somatic cell lineages. due to extracellular signals emanating from the extraembryonic ectoderm (Saitou et al., 2002). *Bmp4*, *Bmp2* , *Bmp8b* and Smad signaling are involved in GC specification (Saitou et al., 2002; Saitou et al., 2003). Once specified, the founder GCs are distinguished from their non-germline neighbouring cells by the expression of several molecular markers, including *Tissue non-specific alkaline phosphatase*, *Oct4*, *SSEA1*, *Stella*, *Blimp1* and *Fragilis1* (McLaren, 1984; Ohinata et al., 2005; Saitou et al., 2002).

Molyneaux and Wiley describe several stages of mouse GC migration from the proximal epiblast to the gonad (Molyneaux and Wylie, 2004; Molyneaux et al., 2001). Specified GCs migrate through the forming hindgut, and from about

E9.5-E10.5, GCs are seen exiting the hindgut and actively migrating towards the forming genital ridges. Some ectopic GCs do not migrate to the genital ridges and find themselves in ectopic locations. In wildtype embryos, these ectopic GCs fragment and apoptose (Stallock et al., 2003).

On leaving the hindgut at E9.5, the migrating GCs begin to link up with each other via extended processes, and by E10.5 have formed interconnected networks that migrate together towards the genital ridges then form even tighter aggregates when in the genital ridges (Gomperts et al., 1994). *In vitro* aggregates were seen to consist of non-sister as well as sister GCs, showing that this interconnectivity is an active, rather than passive, process. This aggregation behaviour may be a mechanism to ensure proper germ cell organisation in the gonad, to aid in the colonisation/migration of GCs into the genital ridge, and/or to prevent ectopic GCs from migrating to inappropriate places with the possibility of forming tumorigenic cells.

Various experiments have shown that Stl/c-kit and SDF1/CXCR4 signaling is involved in the survival and migration of migratory GCs and additionally show that Stl/c-kit may be involved in post-migratory GC survival and/or proliferation (McLaren, 2003; Molyneaux and Wylie, 2004). Migratory GCs change their adhesive properties to extracellular matrix substrates found along their migration path during their embryonic development (Garcia-Castro et al., 1997). Further work has shown that GCs actively participate in their migration during migration and genital ridge colonisation (Donovan et al., 1986; Gomperts et al., 1994; Molyneaux et al., 2001), and this involves the action of several cellular adhesion/receptor proteins, including β1-integrins (Anderson et al., 1999), E-cadherins (Okamura et al., 2003) and possibly c-kit (Molyneaux and Wylie, 2004).

The initial founder population of 40 or so specified GCs expands via several rounds of mitosis during migration to a population of approximately 3000 cells on reaching the genital ridges by E11.5 (Lawson and Hage, 1994; Tam and Snow, 1981). Experiments have also identified FGF2 and leukaemia-inhibitory

factor (LIF) as having positive mitogenic effects on migratory and post-migratory GCs *in vitro* (Matsui et al., 1991). However, others (Takeuchi et al., 2005) find that FGF2 affects motility, but not proliferation, of migratory GCs in cultured embryo slices. This suggests that the mitogenic affects of FGF2 on migratory GCs *in vitro* (Matsui et al., 1991) might be an artificial phenomenon induced by culture conditions, or that the lack of mitogenic effect on FGF2 in embryo slices (Takeuchi et al., 2005) indicates the presence of compensatory factors provided in the embryo. Another indication that FGF2 has a redundant role *in vivo* is that embryonic GC development proceeds normally in *Fgf2* knockout mice (Ortega et al., 1998). Migratory GCs express multiple FGF receptors and signaling through them specifically controls either the motility or the number of migratory GCs (Takeuchi et al., 2005).

The precise *in vivo* role of LIF is not completely clear at present, because embryonic GC development proceeds normally in LIF (Stewart et al., 1992) or LIF receptor (Ware et al., 1995) knockout mice. The shared receptor Gp130 for the IL-6 family of cytokines (of which LIF belongs) is expressed by GCs at multiple stages during their embryonic development (Molyneaux et al., 2003) and treatment of post-migratory, and to a much lesser extent of migratory, GCs with antibodies against Gp130 blocks the mitogenic action of LIF *in vitro* (Koshimizu et al., 1996). Knockout of *Gp130* results in a sex-specific reduction in male GC numbers at E13.5, whereas embryonic female GC development is unaffected (Molyneaux et al., 2003). This *in vitro* and *in vivo* data suggests that LIF has a sex-specific role in survival/migration of post-migratory, rather than migratory, GCs.

## 1.2. GC Markers Associated With Pluripotency

GCs express several genes associated with pluripotency during their development – including *Stella*, *Oct4*, *Nanog* and *Blimp1*. GC expression of these genes is dynamic and for some is sensitive to sex-specific developmental choices.

*Oct4* is a Pou-domain containing transcription factor and has a crucial role in maintenance of pluripotency in cells of the early embryo (Nichols et al., 1998; Niwa et al., 2000). Embryonic stem cells (ESCs) in culture lose *Oct4* expression when they differentiate, as do cells of the inner cell mass when overt differentiation and body patterning begins (Rosner et al., 1990). The only cells to retain detectable expression after E8.5 are GCs. Conditional knockout of *Oct4* in GCs resulted in loss of GCs due to apoptosis in late migration between the hindgut and the genital ridges (Kehler et al., 2004). Oct4 protein is expressed highly by both male and female post-migratory GCs between E11.5 and E13.5, but at E14.5 female GCs transiently downregulate Oct4 protein levels as they proceed through the earliest stages of meiosis, while mitotically-arrested XY GCs retain Oct4 protein expression (Pesce et al., 1998). Down-regulation of Oct4 protein by E14.5 female GCs is mirrored by downregulation of *Oct4* mRNA at E13.5/E14.5 that occurs in an anterior-to-posterior wave (Menke et al., 2003). After birth, female GCs once again begin to express Oct4, and this expression becomes high in most, if not all, female GCs by 7 days post partum. In adult testes, the undifferentiated A-type spermatogonia are the highest expressing cell type. B-type spermatogonia and more mature male GCs, on the other hand, do not express Oct4 protein (Pesce et al., 1998).

The way in which *Oct4* mediates pluripotency is complex, as both ectopic expression or reduction of expression of *Oct4* cause cultured embryonic stem cells to differentiate (Niwa et al., 2000). *Nanog*, together with *Oct4* and other pluripotency-associated genes such as *Sox2*, regulates the pluripotency in the pre-gastrula embryo and cultured ESCs (Chambers and Tomlinson, 2009).

*Nanog*, *Sox2* and *Oct4*, along with other ESC-expressed transcripts such as *Esg1*, are all expressed by post-migratory GCs before sex-specific differentiation (Western et al., 2005), indicating that these 3 pluripotency-associated transcription factors may regulate GC pluripotency. GCs begin expressing *Nanog* when they enter the hindgut and retain expression while migrating. Both male and female GCs downregulate *Nanog* expression after colonising the genital ridges but with a slight sex-specific difference in timing (Yamaguchi et al., 2005). Female GCs downregulate *Nanog* concomitantly with meiotic entry at E13.5-E14.5, while male GCs retain expression until E14.5-E15.5. Ectopic expression of *Nanog* in cultured ESCs relieves their dependence on LIF for maintenance of pluripotency and proliferative capacity (Chambers et al., 2003; Mitsui et al., 2003). *Nanog* overexpression also reduces differentiation of ESCs in response to differentiation factors like retinoic acid (Chambers et al., 2003), while *Nanog* knockout embryos develop abnormally and die, with loss of pluripotent inner cell mass between E3.5 and E5.5 (Mitsui et al., 2003). Therefore, *Nanog* appears to be a potent pluripotency factor that is required to maintain inner cell mass cells in the pre-implantation embryo. On the other hand, *Nanog* is not required for maintenance of ESC pluripotency because removal of *Nanog* does not prevent ESCs from contributing to all 3 germ layers in chimaeric mice (Chambers et al., 2007). Removal of *Nanog* does, however, prevent post-migratory GC development beyond E11.5 (Chambers et al., 2007). Currently, the cause of loss of *Nanog* knockout GCs after E11.5 is not known, but this loss does coincide with epigenetic changes in GCs at this time (Allegrucci et al., 2005). Therefore, *Nanog* may be required for these epigenetic changes to take place in post-migratory GCs.

*Blimp1* is a transcriptional repressor associated with the repression of somatic gene expression programs and is required for the earliest stages of GC development after primordial GC specification (Ohinata et al., 2005). *Blimp1* is expressed in the founder GC population in the proximal epiblast concomitantly with GC specification (Ohinata et al., 2005; Saitou et al., 2002), and is believed to repress *Hox* gene expression in specified GCs by recruiting other histone methyl

transferases (Ancelin et al., 2006). *Blimp1* is reported to silence certain genomic loci, such as that containing *Dhx38*, the mouse homologue of *C. elegans Mog1*, which is involved in the *C. elegans* spermatogenesis-oogenesis switch (Graham and Kimble, 1993), in migratory GCs, but not in post-migratory female and male E11.5 GCs (Ancelin et al., 2006).

*Stella* is another gene whose expression begins in GCs around the time when they are specified (Saitou et al., 2002) and is downregulated with slightly different sex-specific timing in post-migratory GCs (Bowles et al., 2003). However, *Stella* appears not to have an *in vivo* role in GC development, instead being required during pre-implantation embryonic development in some mouse strains (Bortvin et al., 2004; Payer et al., 2003).

# 1.3. Mouse Gonad Development

## 1.3.1. Non-Sex-Specific Gonad Development

Development of the gonads begins as thickenings of the ventrolateral surfaces of the mesonephroi at each side of the intermediate mesoderm, and the gonads become visible by ~E10.0 (Swain and Lovell-Badge, 1999). These earliest stages of gonad development are identical in XX (female) and XY (male) embryos, and the gonad is therefore described as indifferent, until obvious sex-specific differences appear at ~E12.0. Early development of the indifferent gonad depends upon the presence of, among other genes, *SF-1*, *Lim1*, *Wt1* and *Emx2*, as homozygous knockout of these genes results in either a complete lack of gonads or severely underdeveloped gonads.

## 1.3.2. Sex-Specific Gonad Development

Between E10.5 and E12.5 sex-specific differentiation of the various gonadal cell populations begins, resulting in the development of ovaries in XX embryos or testes in XY embryos. Release of sex hormones, such as testosterone and anti-Mullerian hormone (Amh), by the testes results in masculinisation of the XY embryo (Parker et al., 1999). In the absence of testes in the XX embryo, this masculinisation does not occur and the embryo develops female genitalia and secondary sexual characteristics.

***Morphological Characteristics of Sex-specific Gonad Development***

Sex-specific gonad development begins at ~E10.5 with the expression of *Sry* in the XY gonad, and this leads to the formation of testis cords and pronounced vasculature that clearly distinguishes the testes from the ovary by E12.0-E12.5 (Parker et al., 1999). The testis cords, themselves surrounded by muscle-like peritubular myoid cells, consist of Sertoli cells surrounding spermatogenic GCs bunched in the middle of the cords. 2 cellular events following *Sry* expression

are crucial to the formation of characteristic testes morphology and gene expression. Firstly, proliferation of *Sry*-expressing pre-Sertoli cells between ~E10.8-E11.2 is required for the differentiation of Sertoli cells, which is itself a requirement for testes formation (Schmahl and Capel, 2003; Schmahl et al., 2000). Secondly, endothelial and peritubular myoid cells migrate into the XY gonad from the mesonephros and contribute to the formation of testis cords and pronounced vasculature (Buehr et al., 1993; Martineau et al., 1997; Merchant-Larios et al., 1993; Tilmann and Capel, 1999). This migration is induced by the differentiating XY gonad (Merchant-Larios et al., 1993) and is critical for the formation of testis cords, because XY gonads cultured without a mesonephros, even though Sertoli cell differentiation still occurs, do not form testis cords (Tilmann and Capel, 1999). Recent work shows that it is the migration of endothelial cells that is critical to the formation of basal lamina of the testis cords and cord formation (Combes et al., 2009), rather than peritubular myoid cells (Cool et al., 2008).

The E12.0-E14.0 XX ovary is more unstructured and less well defined, with GCs spread homogeneously throughout the gonad and intermingled with somatic cells, some of which are differentiating into stromal cells (Swain and Lovell-Badge, 1999). There is some vasculature throughout the ovary, and this is irregular and indistinct rather than clearly pronounced as in age-matched testes.

### *Sry and Sox9 Drive Sertoli Cell Differentiation and Maintenance*

Experiments by Palmer and Burgoyne (Palmer and Burgoyne, 1991) showed that in the embryonic testes of male chimaeras composed of XX and XY cells, Sertoli cells are the only major cell type in the testes that have a bias towards having an XY rather than an XX sex chromosome complement. The other major gonadal cell populations – peritubular myoid cells, Leydig cells and germ cells – were equally comprised of XX and XY cells. These experiments revealed 2 important aspects of sex-specific gonad development. Firstly, that Sertoli cells

are the only cell type to differentiate due to cell-autonomous expression of a testis-determining factor on the Y chromosome, and secondly that Sertoli cell differentiation then triggers the masculinisation of the other cell types in the gonad. Therefore, Sertoli cell development is the defining event of testis development.

A critical region of the Y chromosome, the *Sxr* region, is the minimum piece of DNA required to induce testis formation, because natural transposition of this *Sxr* region to the pseudoautosomal region on the X chromosome results in sex reversal of $XX^{Sxr}$ mice (Roberts et al., 1988). This region contains a number of genes that were suggested as testis-determining genes. However, several lines of evidence show that *Sry* is the one gene contained in this region that is required for testis-determination. Firstly, Sry is an active Sox family transcription factor (Polanco and Koopman, 2007). Secondly, mutations in Sry, many of which occur in its HMG DNA-binding domain (Hawkins 1993) and impair DNA-binding (Polanco and Koopman, 2007), are commonly associated with XY sex reversal in mouse and humans (Gubbay et al., 1990; Hawkins, 1993). Thirdly, *Sry* expression begins just before the morphological events of early testis development (Bullejos and Koopman, 2001). The most crucial piece of evidence is that a 14kb region of DNA containing *Sry* and its flanking regulatory sequences is sufficient to drive complete testis formation and masculinisation of XX embryos (Koopman et al., 1991).

*Sry* mRNA expression in the XY gonad occurs in a dynamic and transient centre-to-pole pattern, first appearing at the centre of the indifferent gonad at ~E10.5 and receding at the poles by ~E12.5 (Bullejos and Koopman, 2001; Wilhelm et al., 2005), and is closely followed by Sry protein expression (Wilhelm et al., 2005). This transient Sry expression results in cell-autonomous differentiation of the vast majority of Sertoli cells (Sekido et al., 2004; Wilhelm et al., 2005), from sexually bipotential supporting cells that become granulosa cells in the absence of *Sry* expression in an XX embryo (Albrecht and Eicher, 2001). The centre-to-pole pattern of Sry expression means that testis formation is slightly delayed at the gonadal poles. Delayed expression of Sry and testis formation at

the poles is probably what causes development of ovarian regions at the poles of partially sex-reversed testes, or ovotestes, in mice in which *Sry* expression is generally delayed such as in C57BL/6 mice (Wilhelm et al., 2009). The further delay in *Sry* expression may allow the ovarian program to suppress testis development at the poles.

The transient expression pattern of *Sry* mRNA and protein suggests that *Sry* acts as a trigger, rather than a mechanism for maintaining, Sertoli cell differentiation and testis formation. There is now evidence showing that *Sox9* is a major downstream target of Sry that maintains Sertoli cell fate and directs testis development. Appearance of abundant *Sox9* transcript and protein expression mirrors that of *Sry* except with a slight delay (Kent et al., 1996; Wilhelm et al., 2005) and occurs in the same pre-Sertoli cells that express Sry for ~90% of Sertoli cells (Sekido et al., 2004; Wilhelm et al., 2005). *Sox9* expression continues throughout embryonic gonad development in Sertoli cells, consistent with a gene that maintains Sertoli cell differentiation (Kobayashi et al., 2005). There is also compelling genetic evidence for *Sox9* being the only required testis-determining gene downstream of *Sry*. Artificial knockouts of *Sox9* in mice show that *Sox9* is required for development of testes and phenotypically male embryos (Barrionuevo et al., 2006; Chaboissier et al., 2004), while certain mutations in *Sox9* cause campomelic dysplasia in humans, a developmental syndrome usually linked with sex reversal (Foster et al., 1994; Kwok et al., 1995). Conversely, *Sox9* overexpression in the bipotential gonads of XX mice, due to the insertion of an ectopic enhancer or a *Sox9* transgene, results in complete testis formation without *Sry* expression (Bishop et al., 2000; Vidal et al., 2001). Recently, chromatin immunoprecipitation experiments have shown that Sry, in conjunction with SF-1, binds to a testis-specific region of the *Sox9* promoter in E11.5 XY gonads to drive *Sox9* expression (Sekido and Lovell-Badge, 2008). Numerous studies have also reported testis-specific expression of *Sox9* in a wide range of vertebrate species, ranging from turtles to chickens (Morais da Silva et al., 1996; Spotila et al., 1998), suggesting a conserved role of

*Sox9* in vertebrate testis formation despite diverse sex-determination triggers in these species.

It is unclear how *Sox9* ensures Sertoli cell differentiation and maintenance. Hundreds of genes have been identified as being sex-specifically-expressed in XY gonads after *Sry* expression (Cory et al., 2007; Nef et al., 2005), and many of these are expressed specifically in Sertoli cells. Many of these genes are probably indirectly downstream of *Sox9*, and studies have identified some as direct Sox9 target genes. For example, Sox9 and SF-1 work in concert to drive the expression of a variety of Sertoli cell-specific genes, as has been shown for *Amh* (Arango et al., 1999; De Santa Barbara et al., 1998) and *Vanin-1* (Wilson et al., 2005). Sox9 also binds directly to the *Ptgds* promoter in E11.5 XY gonads and drives testis-specific *Ptgds* expression in Sertoli cells from E11.5 (Wilhelm et al., 2007). Also, it is known that autoregulation of the *Sox9* promoter, also with the aid of SF-1, is probably what maintains *Sox9* expression in Sertoli cells once they downregulate Sry (Sekido and Lovell-Badge, 2008). *Ptgds* and *Fgf9*, both sex-specifically upregulated from E11.5/E12.5 in Sertoli cells in response to *Sox9* expression, also have masculinisation properties that feedback positively upon *Sox9* expression (Kim et al., 2006; Malki et al., 2005; Moniot et al., 2009; Wilhelm et al., 2005). The masculinisation properties of these genes might reside completely in their ability to maintain *Sox9* expression/Sertoli cell differentiation or might be due to triggering other downstream pathways (Kim et al., 2007).

### Fgf9 *and* Ptgds *Maintain and Augment Sertoli Cell Differentiation*

*Fgf9* and *Ptgds* are both expressed sex-specifically from E12.5 or E11.5, respectively, in the XY gonad in response to *Sry* and *Sox9* (Kim et al., 2006; Wilhelm et al., 2007), and have independent positive effects on masculinisation of the E11.5 gonad. Fgf9 is a member of the fibroblast growth factor of peptide signaling molecules and acts downstream of *Sry* to ensure testes development. Fgf9 is required for adequate levels of Sertoli cell proliferation (Kim et al., 2006;

Schmahl et al., 2004), and maintenance, rather than initiation, of *Sox9* expression (Kim et al., 2006) and Sertoli cell differentiation (DiNapoli et al., 2006) in gonads of XY C57BL/6 mice. This is known because *Sox9* expression is initially upregulated in the *Fgf9* knockout gonads at E11.5-E12.0, but is almost completely lost by E12.5 (Kim et al., 2006). Fgfr2 appears to be the main receptor mediating these effects of Fgf9 in XY gonads, because knockout of *Fgfr2* results in a very similar phenotype (Bagheri-Fam et al., 2008; Kim et al., 2007). It is not completely clear whether the effects of Fgf9 are solely due to maintenance of Sertoli cell *Sox9* expression and/or proliferation, which is required for testis formation (Schmahl and Capel, 2003), or whether Fgf9 has other masculinising effects, such as repression of female-specific genes like *Wnt4*, *Follistatin* and *Bmp2*, which are upregulated in *Fgf9* knockout XY gonads (Kim et al., 2007).

In the XX-XY chimera experiments by Palmer & Burgoyne approximately 10% of Sertoli cells in these mice were XX and therefore must have been induced by the masculinising environment rather than cell-autonomous *Sry* expression (Palmer and Burgoyne, 1991). More recently Adams & McLaren found that *Ptgds* is expressed sex-specifically from E11.5 in embryonic XY gonads, and Prostaglandin D2 ($PgD_2$), its enzymatic product, can partially masculinise cultured bipotential XX gonads (Adams and McLaren, 2002). Further study showed that $PgD_2$ induces Sertoli cell differentiation by enhancing *Sox9* expression and nuclear localisation (Malki et al., 2005), and could account for the small population of non-cell-autonomously induced Sertoli cells (Wilhelm et al., 2005). *Ptgds* knockout on C57BL/6 background results in a delay rather than a complete block of testis development (Moniot et al., 2009), suggesting that the Ptgds/$PgD_2$ masculinisation pathway, at least in mice, is less critical than Fgf9.

### *Genetic Pathways Controlling Ovary Development*

Expression screens examining sex-specific gene expression differences in gonads during the earliest stages of sex-specific gonad development have revealed that many genes are sex-specifically enriched in the somatic cells of the developing ovary (Bouma et al., 2005; Cory et al., 2007; Nef et al., 2005), showing that ovary development is an active process. Furthermore, studies have shown that expression of these genes, such as *Wnt4* (Kim et al., 2006), in the supporting cell lineage of XX gonads, actively represses testis formation by suppressing various aspects of testis development, such as Sertoli cell differentiation. The prevailing current model is that the testis-determining genes, like *Fgf9* (DiNapoli et al., 2006; Kim et al., 2006) and *Sox9* (Qin and Bishop, 2005) counterbalance the ovary-determining genes like *Wnt4* (Kim et al., 2006) and *Rspo1* (Chassot et al., 2008), and *vice versa*, and that the testis-determining switch, *Sry*, acts to initiate the male pathway (Hiramatsu et al., 2009), which then feeds-back positively on itself, and feeds-back negatively on the ovary-determining genes. In the absence of *Sry* expression, the ovary-determining genes are not repressed and are automatically upregulated.

*Wingless-related MMTV integration site 4* (*Wnt4*) and *R-spondin1* (*Rspo1*) are the two most prominent upstream positive regulators of ovary development that are currently known. *Wnt4* is expressed non-sex-specifically in the genital ridge at E10-E11, but is then downregulated in XY gonads from E11.5 and maintained in XX gonads (Vainio et al., 1999). Knockout of *Wnt4* results in dose-dependent increases in *Fgf9* and *Sox9* expression, resulting in partial masculinisation of XX gonads (Vainio et al., 1999). This finding raises two important points for sex-specific mouse gonad development. Firstly, initiation of the male pathway can occur in the absence of *Sry* expression, and secondly, *Wnt4* dose-dependently represses this initiation in XX gonads. *Wnt4* is also required in XX gonads to repress other aspects of gonad masculinisation such as mesonephric cell migration (Jeays-Ward et al., 2003), although some or all of these effects might be a consequence of inhibition of Sertoli cell differentiation. Surprisingly, *Wnt4* is also required early on in XY gonad development to ensure Sertoli cell

differentiation and proper development of testes (Jeays-Ward et al., 2004). However, because Wnt4 is downregulated at E11.5-E12.5, this is seemingly due to a requirement for *Wnt4* in the indifferent gonad, probably to prevent precocious masculinisation of the indifferent gonad.

Mutation of *Rspo1* in humans is linked with the development of XX males, also in the absence of *Sry* expression (Parma et al., 2006) and analysis in mice shows that *Rspo1* is expressed much more highly in XX compared to XY gonads at E12.5-E14.5 in somatic cells (Chassot et al., 2008; Parma et al., 2006), suggestive of a role in promoting ovary development. Knockout of the gene in mice results in partial masculinisation of embryos on a C57BL/6 background (Chassot et al., 2008). The XX gonads of these knockouts develop as ovotestes with varying degrees of masculinisation, in which meiotic entry and survival of oocytes is impaired, and male markers are slightly upregulated (Chassot et al., 2008). *Rspo1* knockout also results in reduced *Wnt4* expression in E11.5-E12.5 XX gonads (Tomizuka et al., 2008), so this could account for partial masculinisation of *Rspo1* knockout XX gonads. R-spondin signaling upregulates *β-catenin* and analysis of embryonic gonads showes that β-catenin reporters are sex-specifically active in XX gonads from E12.5 in somatic cells (Chassot et al., 2008). β-catenin reporter activity is lost in the XX gonads of *Rspo1* knockouts mice, while ectopic expression of a constitutively-active β-catenin driven by an *SF-1* transgene was able to rescue normal ovarian development in surviving embryos (Chassot et al., 2008), showing that the feminisation activity of *Rspo1* involves downstream β-catenin signaling.

Because XX sex-reversal is not complete in either the *Wnt4* or *Rspo1* knockout XX mice, *Rspo1* and *Wnt4* may be redundant and compensate for the loss of each other. Nobody has yet carried out a *Wnt4*/*Rspo1* double knockout. β-catenin activation is also a common consequence of Wnt signaling, raising the possibility that *Rspo1* and *Wnt4* act in concert to maximally activate *β-catenin* expression in the XX gonad. In support of this theory, one patient showing complete XY sex reversal was found with a duplication of the chromosomal region containing both *Rspo1* and *Wnt4* (Jordan et al., 2001). Further genetic

studies are required to ascertain whether *Wnt4* and *Rspo1* work together to activate β-catenin to promote ovary development. However, one recent study has shown that ectopic expression of a stable form of β-catenin in *SF-1*-expressing cells results in a complete block of testis formation in XY gonads, but does not impair ovary formation of XX gonads (Maatouk et al., 2008). At E13.5, the transgenic XY gonads show loss of Sox9 protein expression, testis cord formation and coelomic vessel formation and an increase of female-specific markers, clearly displaying that active β-catenin is a potent inhibitor of testis formation.

Other genes upregulated sex-specifically in XX gonadal supporting cells around the time of sex determination include *Follistatin*, *Bmp2* and *Foxl2*, which are believed to act downstream of *Wnt4* and *Rspo1*, after initiation of ovary development. *Follistatin* is a member of the TGF-beta family of peptide signaling molecules and is downregulated in partially-masculinised *Wnt4* knockout XX gonads (Yao et al., 2004). *Follistatin* knockout results in development of the coelomic vessel in XX gonads and eventual GC loss, but does not perturb expression of *Bmp2* or absence of *Sox9* expression (Yao et al., 2004). *Bmp2* is another ovary-enriched gene that is also downregulated in XX gonads of *Wnt4* knockout mice (Yao et al., 2004), and is upregulated in XY gonads of *Fgf9* knockout mice (DiNapoli et al., 2006). Its role in ovary determination has not yet been explored in much detail, but studies have shown that *Decapentaplegic*, the Drosophila *Bmp2/4* orthologue, is required to maintain female germline stem cells in the Drosophila ovary (Xie and Spradling, 1998). A similar ovary-specific role for *Bmp2* is possible in mice but to find out its exact role will require a gonad-specific conditional knockout because *Bmp2* knockout embryos die before E10.5 (Zhang and Bradley, 1996). *Foxl2* appears to represent a complementary ovary determination pathway (Garcia-Ortiz et al., 2009), that genetically interacts with either absence of GCs in $Kit^{Wv/Wv}$ mice or with knockout of *Wnt4*, to produce partial or complete, respectively, masculinisation of XX gonads (Ottolenghi et al., 2007).

### *Other Genes Involved in Sex-Specific Gonad Development*

*I*t is not clear whether *Dax1* is required for testis development, ovary development and/or both. *Dax1* knockout results in incomplete sex-reversal of XY gonads in *129Sv/J* mice (Meeks et al., 2003a), and complete sex-reversal of XY gonads in *C57BL/6* or *XY$^{POS}$* mice (Bouma et al., 2005; Meeks et al., 2003b). In completely sex-reversed knockout XY gonads, *Sry* upregulation is not affected, whereas the *Sox9* upregulation is impaired (Bouma et al., 2005), suggesting that *Dax1* is involved in the *Sry*-mediated stimulation of *Sox9* transcription, a critical event in male-specific gonad development. On the other hand, female knockout mice appear to be unaffected and are fertile (Meeks et al., 2003a), implying that *Dax1* is not involved in female-specific gonad development in mice. However, studies in humans (Swain et al., 1996) and mice (Swain et al., 1998) show that multiple copies of *Dax1* can block, rather than augment, development of functional testes. Swain and colleagues introduced multiple copies of *Dax1* into mice and found that testis development was slightly delayed in mice with the highest transgenic *Dax1* expression (Swain et al., 1998). Additionally, multiple copies of *Dax1* were able to increase incidences of ovotestes and sex reversal in XY$^{POS}$ mice, indeed suggesting that *Dax1* does have an anti-testes effect. The fact that a single extra copy of Dax1 in humans is able to cause sex reversal (Swain et al., 1996) suggests there are species-specific differences in the potency of the feminising effects of Dax1 and/or the way in which Dax1 interacts with other sex determining factors in mice and humans. Functional data of *Dax1* suggest that *Dax1* is able to inhibit SF-1-mediated gene transcription of genes such as *Amh* (Ludbrook and Harley, 2004), and this can explain the anti-testes effect of *Dax1*, but not necessarily why the removal of *Dax1* predisposes mouse XY gonads towards ovarian development (Bouma et al., 2005; Meeks et al., 2003b).

Signaling through insulin and Dhh receptors is also involved in testes development. Knockout of all 3 insulin receptors results in complete XY sex-reversal (Nef et al., 2003), which is characterised by massively reduced expression of testis markers and increased expression of ovary markers at

E12.5, a loss of the initiating pulse of *Sry* expression in E10.5-E12.0 testes and the absence of testis cord formation. The percentage of Bromo Deoxyuridine-stained cells was reduced in triple knockout testes and both XX and XY knockout gonads were smaller than controls, suggesting that insulin receptor signaling mediates proliferation of gonadal cells. Blocking proliferation of gonadal cells by other means also blocks Sertoli cell differentiation (Schmahl et al., 2000), so this might explain the sex reversal in the triple knockout XY gonads. *Dhh* on the other hand has a downstream role in stimulating Leydig cell differentiation and this occurs later than sex determination of the supporting and GC lineages (Pierucci-Alves et al., 2001). *Dhh* knockout results in development of stunted testes and GC loss, but Sertoli cells still differentiate and testis cords still form (Bitgood et al., 1996).

**Effects of Genetic Background on Sex Determination**

The impact of spontaneous mutations or artificial knockouts of sex-determining genes on sex-reversal in mice depends upon the genetic background upon which it occurs. For example, the inbred C57BL/6J mouse strain is known to be much more susceptible to XY sex-reversal than outbred mouse strains. This phenomenon is typified by C57BL/6 mice carrying a *Mus domesticus poschiavinus* Y chromosome, whose gonads develop either as fully sex-reversed ovaries or ovotestes because of one or more C57BL/6 genetic determinants being incompatible with *poschiavinus Sry*-driven testis determination (Eckner et al., 1996). As such, sex reversal in these mice is prevented by transgenic insertion of *Mus musculus Sry* (Eicher et al., 1995). Variations of sex-reversal on these genetic backgrounds may be due to variations in expression levels of different *Sry* alleles, which is also affected by the genetic background it is found in due to upstream genetic determinants (Albrecht et al., 2003). Additionally, Sry proteins between species and genetic backgrounds differ and vary in both their ability to initiate testis development and to antagonise ovary development.

# 1.4. GC Development in the Gonad

## 1.4.1. Colonisation of the Gonads by GCs

The majority of GCs have colonised the genital ridges by E11.0 - E11.5 (Garcia-Castro et al., 1997; Gomperts et al., 1994), and become more rounded in shape as they form tighter aggregates (Molyneaux et al., 2001). Movements of the GCs once in the genital ridge slow significantly in both sexes, but the nature of their movements differs between male and female embryos (Molyneaux et al., 2001). with male GC movements being more directional and less random. On reaching the genital ridges GCs non-sex-specifically begin to express certain post-migratory GC markers. These include Germ cell nuclear antigen (GCNA) (Enders and May, 1994), *Mouse vasa homologue* (*Mvh*) (Fujiwara et al., 1994) and *Daz-like* (*Dazl*) (Seligman and Page, 1998).

There are approximately 3000 GCs at E11.5 as the GCs are colonising the genital ridges (Tam and Snow, 1981). Over the next 2 days the GCs proliferate with a doubling time of roughly 16 hours, similar to that of migratory GCs. Despite the sex-specific differentiation of the surrounding gonadal cells and their own sex-specific commitment events, proliferation rates of XY and XX GCs in E11.5-E13.5 gonads are remarkably similar, resulting in roughly 10'000 GCs per gonad at E13.5 (Schmahl et al., 2000; Tam and Snow, 1981). However, there are sex-specific differences in post-migratory GC requirements for mitogenic/survival factors. For example, XY GCs are responsive to GP130-mediated (Molyneaux et al., 2003) and FGF9 (DiNapoli et al., 2006) signaling, because knockouts of *Gp130* or *Fgf9* result in sex-specific deficiencies in XY GC numbers. However, it is not completely clear whether this is due to a direct effect on the GCs or some indirect effect due to somatic cell dysfunction, especially in the *Fgf9* knockout where Sertoli cell differentiation is perturbed (DiNapoli et al., 2006).

Both *Dazl* and *Mvh* are also required sex-specifically for maximal post-migratory male GC survival, for *Dazl* on an in bred C57BL/6 background (Lin and Page,

2005; Tanaka et al., 2000). In *Dazl* knockout gonads male GCs are sex-specifically lost due to apoptosis between E13.5-E15.5, and any surviving male GCs do not develop normally (Lin and Page, 2005). *Dazl* is expressed GC-specifically in the post-migratory gonad, indicating that *Dazl* provides some cell-autonomous survival effect for male GCs. However, widespread death of embryonic male GCs in *Dazl* knockout mice is specific to the C57BL/6 background, therefore it is the combined effect of C57BL/6 testes development and *Dazl* loss that is responsible for this male-specific GC death. *Mvh* is also expressed GC-specifically when GCs colonise the gonads (Fujiwara et al., 1994), and its knockout similarly results in a sex-specific defect in male GC development from E11.5-E12.5, on a mixed genetic background (Tanaka et al., 2000). A reduction in proliferation may be the cause of reduction in GC numbers in the *Mvh* knockout because the *Mvh* knockout GCs have less proliferative capacity *in vitro*. So *Mvh* and *Dazl*, both of which encode RNA-binding proteins, have sex-specific pro-survival and/or pro-proliferative role in embryonic male GCs *in vivo*.

### 1.4.2. Sex-Specific GC Differentiation

GCs remain bipotential until E12.5-E13.5, meaning they can commit to either spermatogenesis or oogenesis, and their choice depends upon the sex of the gonad in which they are in during a short time frame, rather than the chromosomal make-up of the GCs themselves (Ford et al., 1975; Palmer and Burgoyne, 1991). At ~E12.5 both XX and XY GCs enter a post-mitotic state that represents the end of the last mitotic division and the beginning of meiosis I (McLaren, 1984; McLaren, 2003). Concurrently with entry into this post-mitotic state, XY GCs commit to spermatogenesis between E11.5 and E12.5 and enter a reversible mitotic arrest in the $G_0$ phase of the cell cycle (Adams and McLaren, 2002; McLaren and Southee, 1997; Western et al., 2008) until just after birth, where they re-enter the cell cycle as spermatogenic stem cells (McLaren, 2003).

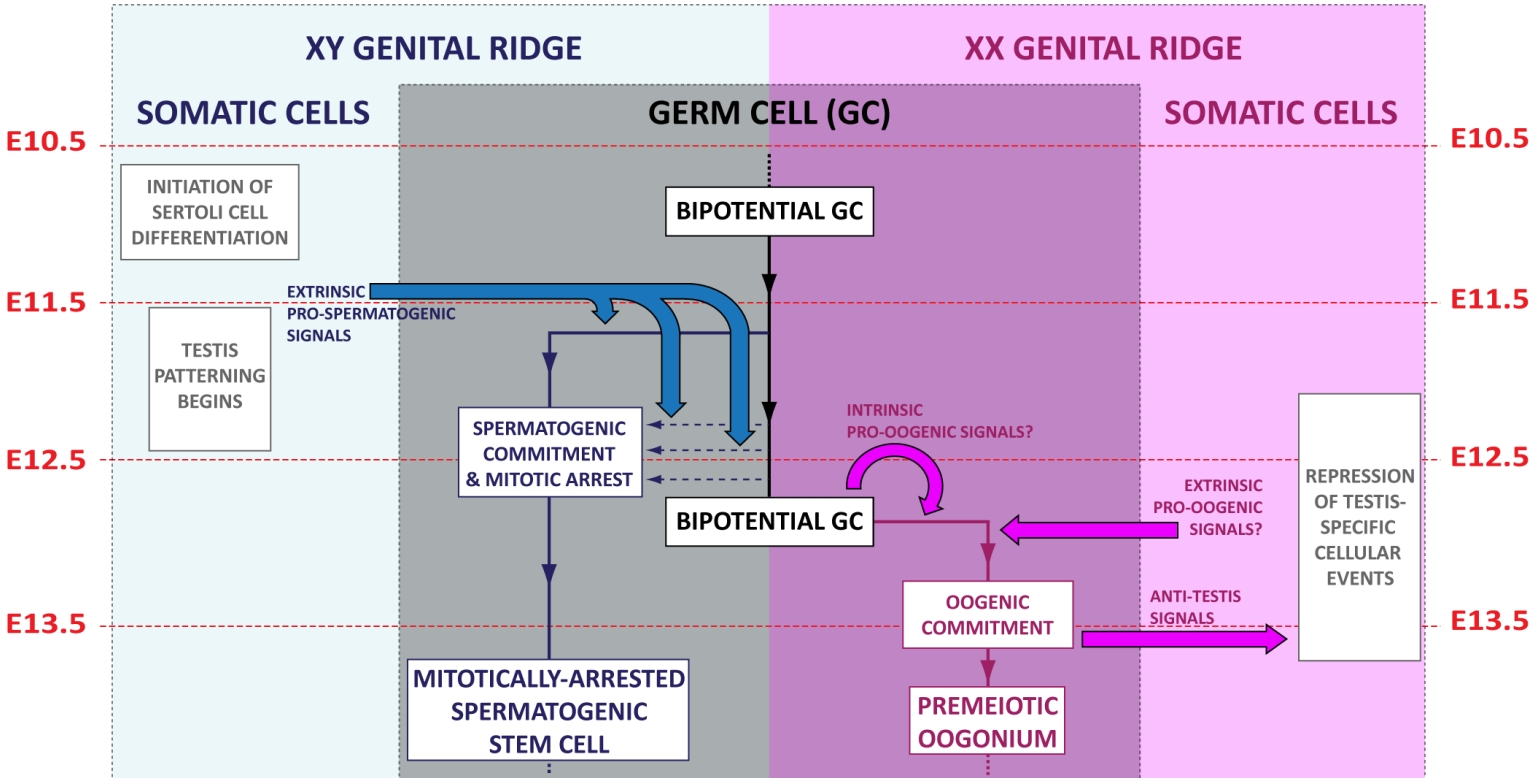


**Figure 1.4.1.** ***Scheme showing the timeline of sex-specific GC development*.** Before E11.5 XX and XY GCs are sexually bipotential, meaning they can commit to either spermatogenesis or oogenesis, depending upon the environment they find themselves in. Masculinising signals from the developing testes cause either XX or XY GCs to commit to spermatogenesis and enter mitotic arrest. *In vivo* this occurs between E11.5 and E12.5. In the absence of these pro-spermatogenic signals, which we as yet do not know the identity of, both XX and XY GCs commit to oogenesis between E12.5 and E13.5 and prepare to enter meiosis. Oogenic commitment might well be a latent ability of GCs that is triggered by intrinsic molecular events, or might be triggered by extrinsic signals from the ovary. A candidate for the latter is retinoic acid. Once committed, female GCs inhibit testis formation by as yet unidentified mechanisms. References can be found in the text.

The XY GCs begin their mitotic arrest from E12.5, and by E14.5 there are almost no XY GCs in S phase (Western et al., 2008). The masculinising environment of the embryonic testis is the developmental cue that causes the XY GCs to commit to spermatogenesis, and this must act on the GCs before E13.5 to cause them to commit to spermatogenesis (Adams and McLaren, 2002; McLaren and Southee, 1997). In the absence of exposure to these masculinising signals, either *in vivo* in the developing ovary or in re-aggregate culture with E12.5 XX genital ridges or embryonic lung cells, both XX and XY GCs commit to oogenesis between E12.5 and E13.5. Oogenically-committed GCs enter into prophase I of meiosis at E13.5-E14.5 (Adams and McLaren, 2002; McLaren and Southee, 1997), proceed through leptotene, zygotene and pachytene stages of meiosis I then finally arrest in the diplotene stage of meiosis around the time of birth until oocyte maturation in the adult (McLaren, 2003). Once XX or XY GCs are committed to oogenesis at E13.5, the GCs are refractory to masculinising signals (Adams and McLaren, 2002; McLaren and Southee, 1997). Additionally, meiotic XX GCs have a negative effect on testes development, because XX gonads placed in between an E11.5 XY gonad and a mesonephros blocks mesonephric cell migration from the mesonephros into the XY gonad, but only when the XX gonad contains meiotic XX GCs (Yao et al., 2003). It has not been shown whether this effect of oogenic female GCs is due to a direct effect of these oogenic GCs or an indirect effect of oogenic GCs on differentiation of the somatic cells of the gonad.

Both male and female GCs upregulate meiotic markers such as Scp1 and Scp3 at E12.5-E13.5 (Di Carlo et al., 2000), indicating that both populations prepare to enter meiosis. These markers are downregulated in the vast majority of spermatogenic XY GCs by E14.5 (Di Carlo et al., 2000; Yao et al., 2003), but remain expressed in leptotene and zygotene oocytes at E14.5-E15.5 (Di Carlo et al., 2000; Yao et al., 2003). Bipotential GCs appear morphologically identical prior to these commitment events (McLaren and Southee, 1997). However, the chromosomal conformations of spermatogenic and oogenic GCs differ markedly by E14.5 and provide an easy means of distinguishing the two fates after standard histological staining.

XX GCs that find themselves committed to spermatogenesis due to the masculinising effects of the developing testis are unable to form fully mature sperm (McLaren, 1981) presumably due to lack of spermatogenic genes found on the Y chromosome. On the other hand, a small proportion of XY GCs that commit to oogenesis in an ovary do form functional oocytes able to contribute to viable offspring (Burgoyne et al., 1988).

## 1.4.3. Control of Sex-Specific GC Differentiation

***Pro-Meiotic Signals or Cell-autonomous Meiotic Initiation?***

The fact that GCs commit to oogenesis and begin meiotic initiation outside of a masculinising environment, irrespective of their sex chromosome complement, suggests that commitment to the oogenic pathway and initiation of meiosis is the default pathway for GCs and is therefore under the control of some intrinsic mechanism. However, it is possible that one or more pro-meiotic signals operate in the E12.5-E13.5 XX gonad to cause GCs to commit to meiosis. These pro-meiotic signals would also be present *in vivo* in the adrenal gland (Zamboni and Upadhyay, 1983) and in the anterior region of wild-type embryonic testes (Yao et al., 2003); in cultures of re-aggregated E11.5 testes (McLaren and Southee, 1997), embryonic lung (McLaren and Southee, 1997) and $Sl^4$-m220 cells (Chuma and Nakatsuji, 2001); and in feeder-free cultures (Farini et al., 2005); because all these environments support initiation of meiosis in embryonic GCs as shown by robust expression of meiotic markers.

Intriguingly, the timing of meiotic entry of XX and XY GCs in these diverse conditions is very similar – within 1 day – of meiotic entry *in vivo* in the XX gonad at E13.5. This suggests that either the intrinsic pro-meiotic signal is expressed by GCs at E12.5-E13.5, or that GCs become receptive to ubiquitous extrinsic pro-meiotic signals at E12.5-E13.5.

Any extrinsic pro-meiotic signals might originate from the anterior part of the mesonephros and diffuse into the anterior part of the E12.5-E14.5 XX gonad *in vivo*, because the appearance of meiotic markers, and presumably entry of XX GCs into meiosis, occurs in an anterior to posterior wave at E13.5-E15.5 (Bullejos and Koopman, 2004; Menke et al., 2003; Yao et al., 2003). Additional evidence for a pro-meiotic signal originating from the anterior mesonephros is that a small number of GCs at the anterior end of the E13.5-E14.5 testis in close juxtaposition to the mesonephros appear to enter into meiosis, as shown by meiotic marker expression, before degenerating by E15.5 (Yao et al., 2003). These GCs may encounter the pro-meiotic signal before they commit to spermatogenesis, and this is compounded by the delay in testis formation at the poles of the XY gonad. However, this phenomenon and the observed pattern of meiotic entry in ovaries might instead be due to GCs colonising the anterior gonad first and therefore being more developmentally advanced.

Recent work suggests that one candidate for an extrinsic pro-meiotic signal is Retinoic Acid (RA) (Bowles et al., 2006; Koubova et al., 2006). However, the existence of an intrinsic pro-meiotic signal has not yet been disproven.

### *RA as a Pro-meiotic Signal Opposed by Cyp26b1*

Recently, some have theorised that RA is the pro-meiotic signal operating in ovaries to induce XX GCs to enter meiosis. The supporting evidence for this theory is as follows. *Aldh1a2*, a major RA-synthesising enzyme, is expressed in the mesonephroi of both XX and XY genital ridges between E11.5 and E13.5 (Bowles et al., 2006). Consequently, there is very high RA receptor activity in the mesonephroi non-sex-specifically and moderate RA receptor reporter activity female-specifically in the gonads at E13.5-E14.5, measured by an RA response element-lacZ transgene (Bowles et al., 2006). Lack of RA receptor activity in the male gonad at E13.5-E14.5 correlates with gonadal expression of *Cyp26b1*, an RA-metabolising enzyme, which becomes male-specific in gonads from E11.5/E12.5 onwards (Bowles et al., 2006; Koubova et al., 2006). So, *in*

*vivo* in the gonads, there are sex-specific differences in RA activity and some observations suggest that this could account for meiotic entry of XX GCs.

Treatment of cultured E12.5 XY gonads with RA or RA receptor agonists (Koubova et al., 2006) induces expression of *Stra8*, which is expressed female-specifically in GCs from E13.5 (Menke et al., 2003) and is required for entry of female and male GCs into meiosis (Baltus et al., 2006). In organotypic cultures, RA accelerates the entry of XX rat GCs into meiosis (Livera et al., 2000), while RA, RA receptor agonists or Am580, an artificial non-degradable retinoid, stimulate a proportion of mouse XY GCs to enter meiosis if treated before spermatogenic commitment at E12.5 (MacLean et al., 2007; Trautmann et al., 2008). All of this suggests that RA does have a pro-meiotic effect on some bipotential GCs, possibly by activating *Stra8* expression, a well-documented consequence of RA treatment (Oulad-Abdelghani et al., 1996).

Cyp26b1 appears to have a role in the male gonad in preventing excessive mesonephric RA, which is a potent mitogen for migratory and post-migratory GCs (Koshimizu et al., 1995), from interfering with mitotic arrest of the spermatogenic GCs. *Cyp26b1* knockout results in some of the GCs inside the cords entering meiosis (MacLean et al., 2007), probably due to widespread expression of *Stra8* of the GCs in the knockout testes (Bowles et al., 2006). Some have taken male-specific expression of *Cyp26b1* as the primary mechanism by which GCs in testes are prevented from entering meiosis and stimulated to enter mitotic arrest.

Despite this evidence, there are still major flaws in both the RA and Cyp26b1 aspects of this theory. Firstly, culture of E12.5 XY gonads with RA, or with the Cyp26b1 inhibitor ketaconazole, induces *Stra8* expression but does not induce meiotic entry of the GCs (Best et al., 2008; Koubova et al., 2006), indicating that although RA often stimulates meiotic gene expression, this does not always result in meiotic entry. One study has observed leptotene- and zygotene-like chromosome conformations in about ~20% of XY GCs when cultured with RA for 4 days (Trautmann et al., 2008). However, RA treatment in that study also

resulted in apoptosis of many of the GCs, and the pro-meiotic effect of RA in those gonads, and gonads in other studies (Livera et al., 2000), may have been an indirect effect on male somatic cell differentiation, because RA perturbs multiple aspects of testis development, including Sertoli cell differentiation (Cupp et al., 1999; Li and Kim, 2004). One other study also observed widespread apoptosis and increased mitosis of GCs in XY gonads cultured with Am580 (MacLean et al., 2007). Also in that study (MacLean et al., 2007), meiotic GCs were reported in testis cords of *Cyp26b1* knockout XY gonads. However, many of the GCs identified as meiotic in that paper appeared to be in fact apoptotic. This suggests that RA might simply act as a mitogenic stimulus for the XY GCs in these artificial situations, preventing masculinising signals from arresting them mitotically and allowing meiotic entry, which is a latent ability of XY GCs (McLaren 1997). Apoptosis of the majority of the GCs in the *Cyp26b1* knockout or in RA-treated XY gonads (MacLean et al., 2007), therefore, might occur due to the RA mitogenic stimulus conflicting with the as yet unidentified masculinising anti-meiotic/pro-mitotic arrest signal.

Most notable is the fact that XY GCs found in the XY mesonephros still enter mitotic arrest (McLaren, 1983), and so are still able to receive masculinising signals from the XY gonad and commit to spermatogenesis despite the high RA levels in the mesonephros (Bowles et al., 2006). Additionally, in some circumstances, such as in E11.5 cultured XY gonads transiently treated with brefeldin A, which reversibly inhibits secretion (Best et al., 2008), or *in vivo* in *Nanos2* knockout XY testes in which *Cyp26b1* expression levels are similar to wildtype (Suzuki and Saga, 2008), XY GCs are able to enter meiosis while they are still enclosed in the testis cords, which according to the Cyp26b1 theory would be sheltered from the effects of RA. All of this evidence suggests that treatment of bipotential GCs with RA allows the automatic meiotic entry of some GCs, but RA is not the primary *in vivo* pro-meiotic signal in XX gonads. Furthermore, Cyp26b1 prevents RA from interfering with other masculinising signals that induce mitotic arrest of GCs in the testes, but is not the primary anti-

meiotic signal inducing spermatogenic commitment and mitotic arrest of XY GCs *in vivo*.

### *The Anti-meiotic Effect of the Developing Testis*

Before committing to meiosis, both XX and XY GCs are receptive to the masculinising environment of the developing testis (Adams and McLaren, 2002), which causes them to commit to spermatogenesis. The identities of the signal or signals that mediate spermatogenic commitment are not currently known but some characteristics can be determined from experimental observations. Recently, some have hypothesised that instead of the developing testes providing a signal, the intact testis cords act as an epithelial barrier to diffusible pro-meiotic signals, such as RA (Koubova et al., 2006). This hypothesis is supported by experiments in which cord formation was perturbed by dis-aggregation and re-aggregation of E11.5 XY gonads, which resulted in meiotic entry of the XY GCs (McLaren and Southee, 1997). However, several other observations suggest testis cords are not required to either protect GCs from pro-meiotic signals or to transmit potential anti-meiotic signals. Spermatogenic GCs have been found in XY gonads in which cord formation was perturbed by cyclopamine treatment (Yao and Capel, 2002) or removal of the mesonephros (Buehr et al., 1993). Others have observed spermatogenic GCs outside of the cords in the interstitial areas of the testes and even in the mesonephroi (McLaren, 1983). Therefore, it appears that cord formation is not required for the anti-meiotic influence of the testis. Furthermore, assuming that they originate from the XY gonad, any such anti-meiotic signals are probably diffusible, because GCs found in the male mesonephros are able to receive it and develop as spermatogonia, whereas GCs found in the female mesonephros enter meiosis (McLaren, 1984). This fits nicely with the data indicating that masculinising signals from an XY gonad induce mesonephric cell migration, even when an XX gonad is placed in between (Tilmann and Capel, 1999).

Recent work suggests that the masculinisation signals causing GC spermatogenic commitment are secreted by Sertoli cells into adjacent GCs. Sertoli cells are specialised secretory cells that express secretory markers and contain secretory granules (Best et al., 2008), and are known to actively secrete proteins such as Ptgds (Samy et al., 2000). Re-aggregate culture of E11.5 XX genital ridges with a perinatal Sertoli cell line results in mitotic arrest of 75% of the observed GCs (Best et al., 2008), although this might be due to a detrimental effect of the Sertoli cell line on survival of meiotic GCs committed to oogenesis rather than sex-reversal of the GCs. More compelling was data showing transient treatment of E11.5 XY genital ridges with brefeldin A, a reversible inhibitor of secretion, which resulted in meiotic entry of a proportion of the XY GCs (Best et al., 2008), despite them still being enclosed in testis cords surrounded by Amh-expressing Sertoli cells. This work showed that secretion of masculinising factors in XY genital ridges at a specific time point is critical for mitotic arrest and spermatogenic commitment of bipotential GCs, and Sertoli cells, being specialised secretory cells and in direct contact with the GCs, are a likely source for it.

*In vitro* evidence suggests that the cytokine LIF is a potential anti-meiotic signaling molecule. *In vitro* treatment of E11.5 GCs with LIF or oncostatin M, another interleukin-6 cytokine, inhibits their expression of meiotic markers and progression through meiosis I (Chuma and Nakatsuji, 2001; Farini et al., 2005) and *Lif* mRNA is also expressed more highly in E13.5 male genital ridges compared to female genital ridges (Chuma and Nakatsuji, 2001). However, LIF- and oncostatin M- treatment enhanced the proliferation of GCs rather than triggering mitotic arrest (Chuma and Nakatsuji, 2001), so the observed anti-meiotic effect may simply be a consequence of a mitogenic effect of these growth factors. Additionally, LIF transforms cultured GCs into ESC-like embryonic germ cells (Matsui et al., 1992), which actively proliferate *in vitro*, indicating that the anti-meiotic of LIF is probably due to diversion of GCs towards some other developmental state rather than commitment to spermatogenesis. Whichever developmental pathways that are activated by LIF

in GCs are incompatible with meiotic entry, or it might be that the GCs do not enter meiosis because this IL-6 signaling does not allow them to enter a post-mitotic state. Whatever the case, *Lif* signaling is not required *in vivo* for male GC development, because *Lif* knockout male mice are fertile (Stewart et al., 1992). Additionally, knockout of *Gp130*, the shared interleukin-6 receptor, had no effect on fertility of male mice (Molyneaux et al., 2003). However, these knockouts did have reduced numbers of male, but not female, GCs at E13.5, indicating that Gp130 signaling sex-specifically enhances *in vivo* survival and/or proliferation of male GCs, shortly after or during their spermatogenic commitment.

### *Molecular Consequences of Sex-specific GC Differentiation*

Advances in molecular analysis techniques are now allowing us to probe in more detail what is occurring in mitotically arrested male GCs and early meiotic female GCs. These sex-specific molecular differences not only allow rapid identification of spermatogenic or oogenic commitment, but also give us insight into both the upstream events triggering sex-specific commitment and the downstream mechanisms mediating meiotic initiation or mitotic arrest.

Meiotic entry of XX GCs from E13.5 is followed by the expression of several meiotic markers. Immunostaining for Sycp3, a component of the synaptonemal complex, is seen in both XX and XY E13.5 GCs as clumps of expression in the nucleus (Di Carlo 2000). However, by E14.5, Sycp3 is expressed in XX GCs sex-specifically, as XY GCs downregulate Sycp3 (Di Carlo et al., 2000), and high level immunostaining for Sycp1, another synaptonemal complex protein, appears in an anterior to posterior wave (Yao et al., 2003). Sycp1 immunostaining at E14.5-E15.5 is seen as thread-like structures as the axial elements form along the condensed prophase chromosomes (Di Carlo et al., 2000; Yao et al., 2003). γ-H2AX, a marker for DNA double-strand breaks that occur in meiotic prophase I, is detected in a similar dynamic wave of expression from E14.5 in XX GCs (Yao et al., 2003).

*Stra8* and *Nanos2* are required for the initiation of meiosis or maintenance of mitotic arrest, respectively. *Stra8* is expressed specifically in pre-meiotic GCs, including embryonic XX GCs from E12.5 to E16.5, in an anterior-posterior wave similar to and slightly preceding the waves of upregulation of the meiotic marker *Dmc1* (Menke et al., 2003); and pre-meiotic and early prophase spermatogonia in postnatal testes (Oulad-Abdelghani et al., 1996). *Stra8* is required for meiotic initiation and/or progression into meiotic prophase for female GCs at E13.5-E15.5 (Baltus et al., 2006) and for meiotic prophase progression in male GCs in the adult (Mark et al., 2008), as displayed in *Stra8* knockout gonads. In the embryonic *Stra8* knockout ovary, XX GCs have pre-leptotene nuclear morphology similar to wildtype GCs. However, after E13.5 the GCs fail to progress through further stages of prophase I. At E14.5-E15.5 in the knockout ovaries, no GCs are seen with the typical leptotene or zygotene nuclear morphology that is seen after standard histological staining or Sycp3 or Rec8 immunostaining of wildtype GCs. Additionally, an absence of intense γ-H2AX immunostaining at E15.5 shows that DNA double-strand breaks do not occur in GCs in the knockout ovaries. Finally, it was also suggested that the GCs in the knockout ovaries do not undergo pre-meiotic DNA synthesis because at E13.5-E15.5 the knockout GCs have DAPI staining intensity consistent with 2n rather than 4n nuclei, which is seen in wildtype meiotic GCs at E15.5. RA is purported to be the upstream signal that stimulates *Stra8* expression in embryonic XX GCs (Bowles et al., 2006), because of RA's ability to stimulate *Stra8* transcription in GCs (Best et al., 2008; Bowles et al., 2006; Oulad-Abdelghani et al., 1996). However, it is still not clear whether it is RA, an unidentified external signal or an intrinsic cell-autonomous trigger that operates *in vivo* to activate *Stra8* expression and initiate meiosis in E12.5/E13.5 XX GCs.

Nanos is one of several RNA-binding proteins that have essential conserved roles in GC development. In mice there are 3 *Nanos* genes, and *Nanos2* is male-specifically upregulated in GCs at E12.5/E13.5 shortly following spermatogenic commitment (Tsuda et al., 2003). Adult *Nanos2* knockout male mice are viable

but devoid of GCs, whereas females are viable and fertile (Tsuda et al., 2003). Loss of GCs in the testes of knockout XY mice begins after E14.5 when an increase in apoptotic GCs is observed, and a complete loss of spermatogenic GCs in postnatal testes ensues. Apoptotic loss of GCs in the testes of *Nanos2* knockout mice prevented the analysis of the developmental state of these GCs. However, additional knockout of *Bax2* prevented this apoptotic loss (Suzuki and Saga, 2008). Molecular analysis of embryonic knockout testes in *Nanos2*/*Bax2* double knockout mice found that the GCs appeared to commit to spermatogenesis and did not enter meiosis, similar to wildtype XY GCs, at E12.5-E13.5. However, 2 days later they became positive for phospho-H3 immunostaining at E15.5, indicating their re-entry into the cell cycle. Furthermore, the GCs also upregulated the early meiotic markers *Stra8* and *Sycp3* at E15.5 and had zygotene and pachytene Sycp3 immunostaining by E17.5, indicating their entry and progression through prophase I of meiosis. Conversely, ectopic expression of *Nanos2* in XX GCs cell-autonomously prevented *Stra8* transcription, Stra8 protein expression and synaptonemal complex formation and instead resulted in positive immunostaining for the male-GC-specific markers H3K9me2, Tudor-domain containing 1 (Tdr1d) and Dnmt3L, without affecting neighbouring XX GCs (Suzuki and Saga, 2008). These experiments clearly show that *Nanos2* prevents meiotic entry and maintains mitotic arrest of spermatogenic GCs *in vivo*, possibly by inhibiting Stra8 expression. *Nanos2* must function downstream of any putative masculinising signals operating at E12.5 because the male GCs still appear to commit to spermatogenesis and arrest mitotically between E12.5 and E15.5 and because Nanos2 expression does not appear in wildtype XY GCs until after their spermatogenic commitment.

By E13.5, GCs in male and female gonads are entering very different stages of the cell cycle. One recent study looked at the expression patterns of certain cell-cycle genes and proteins in purified spermatogenic XY GCs and compared that with expression in XX GCs for some markers (Western et al., 2008). They found that at E12.5-E14.5, XY GCs downregulate Ki67, a marker for any stage of the

cell cycle except $G_0$, concomitantly with their entry into mitotic arrest, suggesting that the XY GCs complete any initiated cell cycles when they receive the masculinising signals at E11.5-E12.5, before exiting the cell cycle in $G_0$. At E12.5 XY GCs have hyperphosphorylated retinoblastoma protein (Rb), which when hyperphosphorylated stimulates cells to enter S phase, but between E12.5 and E13.5 Rb becomes dephosphorylated into its hypophosphorylated inactive form. This is not surprising given the fact that XY GCs arrest mitotically at this time, but provides one possible mechanism by which XY GCs are induced into mitotic arrest. In contrast XX GCs maintain their Rb in its hyperphosphorylated form. By E15.5 XY GCs do not express detectable levels of Rb protein, suggesting that the XY GCs enter a more quiescent state, although presence or absence of the p107 and p130 pocket proteins, which can stimulate cell cycle entry in place of Rb, is not known. XY GCs sex-specifically express the p21 and p27 cyclin-dependant kinase inhibitors at the protein level between E12.5 and E15.5, which might explain the rapid dephosphorylation of Rb and mitotic exit. The masculinising signals that cause XY GCs to commit to spermatogenesis would be expected to act upon these pathways to cause mitotic arrest.

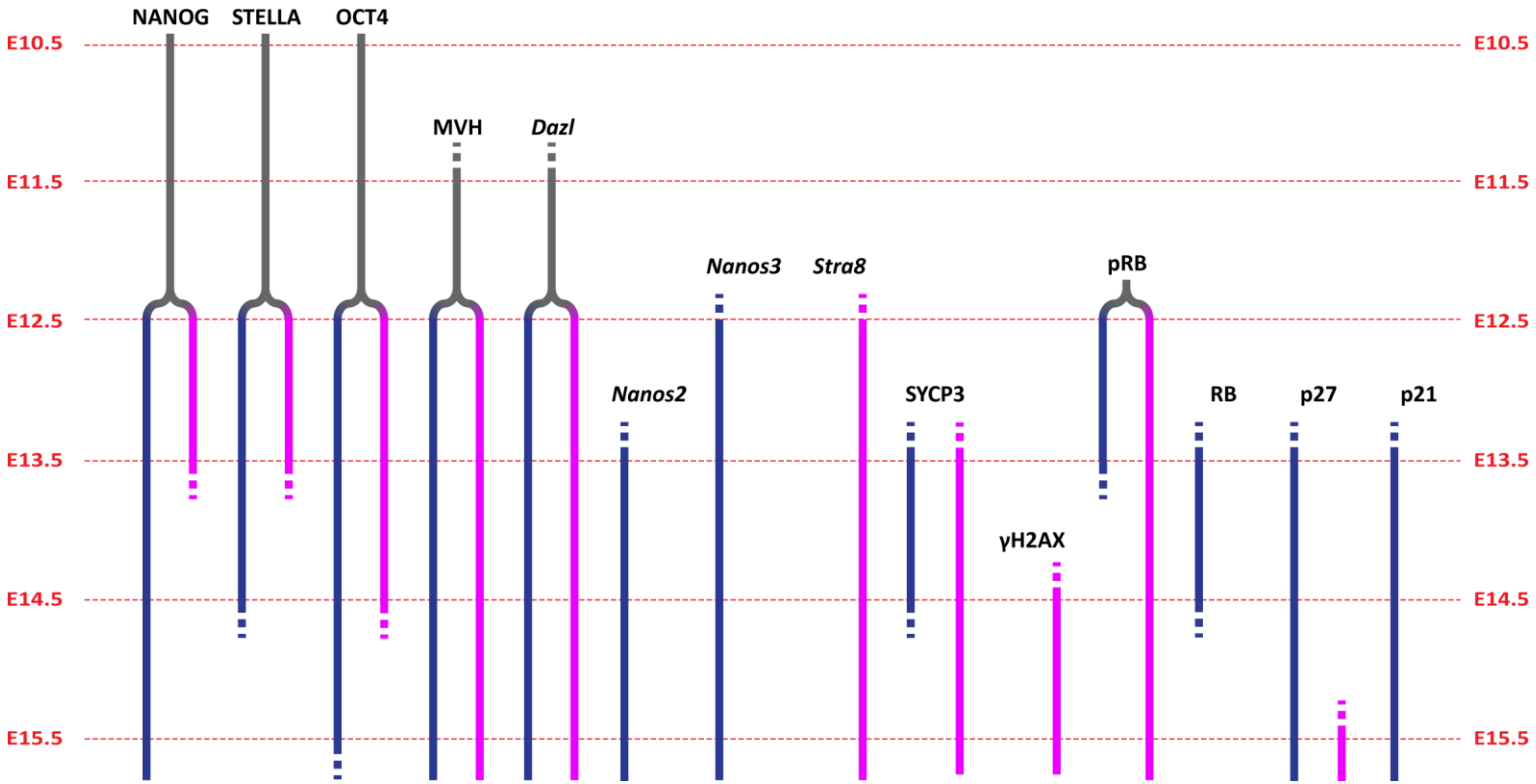


**Figure 1.4.2.** ***Summary of Expression of GC-expressed Genes Between E10.5 and E15.5.*** Solid grey lines represent expression by bipotential GCs. When male GCs commit to spermatogenesis at E12.5, the solid lines split into blue and pink, representing expression by male or female GCs, respectively. Where solid lines begin at the top with a dashed line, this indicates expression turning on, and expression has been shown to be undetected at the stage(s) prior to this switching on. Conversely, dashed ends at the bottom of a line represent expression turning off, and expression has been shown to be undetected at the stage(s) following this switching off. Where lines begin or end in a solid line, expression was either not studied for prior/following stage(s) or the data is not shown on this diagram. For example, pRB expression before E12.5 was not studied. Gene names in italics represent mRNA expression whereas gene names in capital letters represent protein expression.

| *Gene* | *Known Function (if any)* |
|---|---|
| ***Nanog*** | Maintains GC pluripotency |
| ***Stella*** | Maintains GC pluripotency |
| ***Oct4*** | Maintains GC pluripotency |
| ***Mvh*** | Maintains proliferation and differentiation of GCs during embryogenesis |
| ***Dazl*** | Survival factor for GCs and promotes differentiation |
| ***Nanos2*** | Spermatogenic GC survival and maintenance of mitotic arrest in embryonic spermatogonia |
| ***Nanos3*** | Unknown |
| ***Stra8*** | Meiotic induction of female GCs |
| ***Sycp3*** | Component of the synaptonemal complex in meiotic GCs |
| ***γH2ax*** | Marker for double-strand breaks in meiosis |
| ***Rb*** | Cell cycle control/unknown in GCs |
| ***p27*** | Inhibits the cell cycle/unknown in GCs |
| ***p21*** | Inhibits the cell cycle/unknown in GCs |

**Table 1.4.1 Functions of GC-expressed Genes (where known).**

### *Concluding Remarks On the Control of Sex-specific GC Differentiation*

Despite recent advances there are still many questions that remain to be answered when it comes to our understanding of the intracellular mechanisms controlling the commitment of E11.5-E13.5 GCs to spermatogenesis or oogenesis. Stra8 definitely appears to be required for the initiation of meiosis in female E13.5-E15.5 GCs (Baltus et al., 2006). Many now believe RA induces Stra8 expression and meiosis in this system, but critical interpretation of all the available data suggests that RA is not the in vivo factor stimulating Stra8 expression in E13.5-E14.5 female GCs. Therefore, what are the upstream

molecular events that do regulate sex-specific *Stra8* expression in female GCs? Examination of the *Stra8* promoter region and sex-specific expression analyses of transcription factors in E13.5 GCs may yield some candidates. Another very large question that remains to be answered is how does Stra8 initiate meiosis in female GCs? *Stra8* appears to be confined to vertebrate species (Baltus et al., 2006), contains a putative helix-loop-helix domain (Baltus et al., 2006), suggesting that it may be a transcription factor, and is a phosphoprotein (Oulad-Abdelghani et al., 1996). However, at present not much else is known in terms of the functional aspects of Stra8.

On the other side of the coin, progress has been made towards understanding the signals mediating spermatogenic commitment and mitotic arrest of male GCs by E12.5. The masculinising signals are likely to be secreted factors (Best et al., 2008), but the identity of those factors is not yet known. Additionally, we know the consequences of those signals – mitotic arrest associated with Rb hypophosphorylation and CDKI expression (Western et al., 2008), but what are the intracellular events mediating these effects? Much is known about the control of these cell cycle events in somatic cells (Satyanarayana and Kaldis, 2009), and one class of proteins known to be involved are the tissue-specific basic helix-loop-helix transcription factors (Zebedee and Hara, 2001), which are investigated in Chapter 3 of this thesis.

## 1.5. *Lipocalin-type Prostaglandin $D_2$ Synthase* (*Ptgds*)

One particular gene known to be expressed in the GCs in a sex-specific manner shortly after sex-specific commitment is *Ptgds*, which is expressed male-specifically in gonads from E11.5 in Sertoli cells and GCs (Adams and McLaren, 2002) Not only is *Ptgds* expressed sex-specifically, but *Ptgds* and its enzymatic product prostaglandin $D_2$ ($PgD_2$) have both been shown to have masculinising effects on bipotential gonad cells (Adams and McLaren, 2002; Moniot et al., 2009; Wilhelm et al., 2005), but its role in spermatogenically-committed GCs has not been explored.

### 1.5.1. Prostaglandin $D_2$ ($PgD_2$)

$PgD_2$ is an extracellular paracrine and autocrine signalling molecule with diverse roles in nociception (Eguchi et al., 1999), sleep control (Huang et al., 2007), inflammation (Harris et al., 2002), reproduction (Saito et al., 2002) and embryonic testis development (Adams and McLaren, 2002; Wilhelm et al., 2005). Prostaglandin $H_2$ is the general substrate for generation of prostaglandins, including $PgD_2$, and COX1 and COX2 catalyse its production from arachidonic acid (Kostenis and Ulven, 2006; Urade and Hayaishi, 2000). $PgD_2$ can itself be metabolised, both enzymatically and non-enzymatically, into various products (Kostenis and Ulven, 2006; Urade and Hayaishi, 2000), including the F and J prostaglandins, which have biological activity and possible *in vivo* roles (Urade and Hayaishi, 2000).

$PgD_2$ has 2 main receptors, both of which are G-protein-coupled (Kostenis and Ulven, 2006). The first and most well-studied, DP1, is linked to $G_s$ subunits, and therefore its activation results in the catalytic generation of cAMP and increases

in cellular cAMP levels, (Boie et al., 1995) which can activate PKA. The DP1 receptor is widely expressed in a variety of tissues (Kostenis and Ulven, 2006), and its *in vivo* roles include vasodilation and anti-inflammation effects (Kostenis and Ulven, 2006) as well as promoting Sertoli-cell differentiation in embryonic gonads (Adams and McLaren, 2002; Malki et al., 2005; Wilhelm et al., 2005). The second, less well-studied, receptor for $PgD_2$ is the CRTH2 receptor, the expression of which is restricted to hematopoietic cells (Kostenis and Ulven, 2006). CRTH2 is coupled to $G_i$ subunits and therefore CRTH2-mediated signalling results in decreased cellular cAMP and increased intracellular $Ca^{2+}$ levels. CRTH2-mediated signalling is heavily implicated in immune cell behaviour and is pro-inflammatory (Kostenis and Ulven, 2006).

### 1.5.2. *In Vivo* Roles of *Ptgds*

*Ptgds*, also known as Brain-type or glutathione-independent Prostaglandin $D_2$ Synthase or Beta-trace (human), is one of 2 enzymes that catalyses the production of $PgD_2$ from $PgH_2$. Hematopoietic Prostaglandin $D_2$ Synthase (Hpgds) is the other enzyme and is functionally and evolutionary diverse from Ptgds (Urade and Hayaishi, 2000). *Hpgds* will not be discussed further.

Ptgds is a bifunctional protein that binds to biologically active lipophilic molecules as well as catalyses the production of $PgD_2$. The catalytic functions of Ptgds require the presence of free sulfhydryl compounds such as glutathione, β-mercaptoethanol, dithiothreitol, cysteine or cysteamine (Urade and Hayaishi, 2000). The lipophilic molecules Ptgds can bind to include retinoic acid (RA), thyroid hormone, bile acids and testosterone (Beuckmann et al., 1999; Tanaka et al., 1997), all of which have important biological roles.

It is unclear, i.e. it has not been shown directly, when Ptgds functions as a $PgD_2$-producing enzyme and when it functions as a lipophilic molecule binding protein. However, some insight can be learned from its subcellular localisation

and the co-expression of certain genes. In certain cells, such as perivascular cells of the meninges, Ptgds is co-expressed with COX2 (Beuckmann et al., 1999), suggesting that in these cells Ptgds produce $PgD_2$. In arachnoid trabecular cells, Ptgds immunostaining localised to nuclear envelopes, Golgi and secretory vesicles, suggesting that these cells secrete Ptgds. Secretion of Ptgds protein has also been detected in a number of cell types (Urade and Hayaishi, 2000), including Sertoli cells (Samy et al., 2000). On the other hand, meningeal macrophages express Ptgds in lysosomes, so these cells may endocytose extracellular Ptgds.

What is known is that binding of lipophilic molecules by Ptgds results in inhibition of Ptgds catalytic activity in *in vitro* assays (Beuckmann et al., 1999; Tanaka et al., 1997), suggesting that Ptgds cannot simultaneously perform both functions.

*Ptgds* knockout mice are viable and fertile (Eguchi et al., 1999), but display a number of abnormal behavioural phenotypes, involved in sleep (Huang et al., 2007) and nociceptive (Eguchi et al., 1999) behaviours. $PgD_2$ is involved in these behaviours (Urade and Hayaishi, 2000), suggesting that these behavioural phenotypes are caused by loss of $PgD_2$-production by Ptgds. *Ptgds* also has a role in augmenting mouse embryonic testis development, which becomes apparent when *Ptgds* is knocked out on a C57BL/6 genetic background (Moniot et al., 2009). This role of Ptgds is also attributable to $PgD_2$-production by Ptgds, as shown by the masculinising effects of PgD2 on bipotential gonad somatic cells (Adams and McLaren, 2002; Wilhelm et al., 2005). Other reproductive and neuronal roles have been postulated for *Ptgds*, due to its high expression in certain tissues and fluids such as seminal plasma (Saito et al., 2002) and cerebro-spinal fluid (Hoffmann et al., 1993). There are several papers showing that the lipocalin function of Ptgds does have *in vivo* roles, although these are currently rare (Kanekiyo et al., 2007).

## 1.5.3. Role of *Ptgds* in Embryonic Testis Development

*Ptgds* is expressed in various parts of the mammalian male reproductive tract. The earliest observed expression in the mouse gonad occurs male-specifically in the early stages testis development at E11.5, shortly following the burst of *Sry* expression in the embryonic XY gonad (Adams and McLaren, 2002). *Ptgds* expression continues in the embryonic gonad, with mRNA expression being clearly restricted to the testis cords in E13.5 testis (Adams and McLaren, 2002), and Ptgds immunoreactivity present in Sertoli cells and some GCs in E12.5 testes (Moniot et al., 2009). This early male-specific *Ptgds* expression following *Sry* induction is also observed at the same developmental time point in the developing chicken testis (Moniot et al., 2008), and *Ptgds* mRNA is also detected in embryonic testis and epididymis of sheep (Fouchecourt et al., 2003), suggesting conserved functions for *Ptgds* in embryonic testis development.

Despite being expressed at high levels in embryonic testes from E11.5, *Ptgds* expression is limited to Sertoli cells and GCs (Adams and McLaren, 2002). Ptgds protein expression is also limited to these cell types in the E13.5 testes (Moniot et al., 2009), with the highest expression in Sertoli cells, and only some GCs expressing detectable Ptgds protein. Similarly, *Ptgds* mRNA expression is not always detected at high levels in GC cytoplasm (Wilhelm et al., 2007), and this suggests that mRNA expression levels in male GCs are lower than in Sertoli cells at E13.5. This mirrors the situation in 20-day-old juvenile rats, in which Sertoli cells express roughly 3-fold higher levels of Ptgds protein than GCs from the same animals (Samy et al., 2000).

Recent work by several groups has now more fully described the role *Ptgds* plays in embryonic testis development. Adams & McLaren first demonstrated a role for $PgD_2$ in embryonic gonad development when they partially masculinised XX bipotential gonads in organotypic culture with $PgD_2$ (Adams and McLaren, 2002). This partial masculinisation is characterised by Amh-expressing regions of XX gonads, which contained low numbers of

prospermatogonial germ cells and cells with Sertoli- and peritubular myoid-like characteristics arranged in disorganised testis cord-like structures (Adams and McLaren, 2002). Further work by other groups showed that inhibition of $PgD_2$ signalling through the DP1 receptor prevents the recruitment of a small population of E12-E13.5 XX non-*Sry*-expressing cells to a Sertoli cell fate when they are cultured with identically-staged XY embryonic gonadal cells (Wilhelm et al., 2005). A similar recruitment of non-*Sry*-expressing XX cells to Sertoli cell fate also occurs when XX embryonic gonadal cells are exposed to XY embryonic gonadal cells in embryonic XX-XY chimaeric gonads (Palmer and Burgoyne, 1991), suggesting that $PgD_2$ signalling through the DP1 receptor might be partly responsible for this *in vivo* phenomenon.

The ability of $PgD_2$/DP1 signalling to masculinise XX and probably XY non-*Sry*-expressing gonadal cells to a Sertoli cell fate is due to at least 2 downstream effects. Firstly, $PgD_2$/DP1 signalling stimulates *Sox9* mRNA and protein expression, and this has been shown for ovarian cancer cells (Malki et al., 2007), as well as cultured XX gonadal cells (Malki et al., 2005). Secondly, $PgD_2$/DP1 signalling induces nuclear import of Sox9 protein, possibly by activation of PKA-mediated Sox9 phosphorylation (Malki et al., 2005; Wilhelm et al., 2005). Increased expression and nuclear localisation of Sox9 protein in embryonic gonadal cells results in the differentiation of these cells as Sertoli cells, as shown by Amh expression (Adams and McLaren, 2002).

*Ptgds* expression in Sertoli cells of E11.5-E13.5 testes is due to transcriptional activation by direct recruitment of Sox9 to the *Ptgds* promoter (Wilhelm et al., 2007). In C57BL/6 mice, which are more sensitive to perturbations in testis determination due to a delay in testis development (Eicher and Washburn, 1986; Eicher et al., 1996), *Ptgds* knockout results in decreased Sox9 protein expression and nuclear localisation in E11.5-E13.5 testis (Moniot et al., 2009), identically to what occurs with DP1 antagonism of sex reversal of XX gonadal cells in organotypic cultures (Malki et al., 2005). This suggests that $PgD_2$, generated by Ptgds, induces a small proportion of Sertoli cells in embryonic testes that would not otherwise differentiate as Sertoli cells.

This Ptgds/$PgD_2$ masculinisation pathway is a secondary mechanism, at least in most, especially outbred, mouse strains (Moniot et al., 2009), and is conserved in non-mammalian chordates such as birds (Moniot et al., 2008). The main pathway of testis-determination in mammals is cell autonomous *Sox9* induction by Sry, which drives differentiation of the majority of Sertoli cells (Sekido et al., 2004; Wilhelm et al., 2007). Ptgds recruits a small number of non-Sry-expressing somatic cells to a Sertoli cell fate (Wilhelm et al., 2005), and this small population of cells may correspond to the ~10% of XX Sertoli cells in the testes of XX-XY chimaeric mice (Palmer and Burgoyne, 1991). This is why removal of *Ptgds* in C57BL/6 mice only results in a delay, rather than a complete block, in testis development (Moniot et al., 2009).

## 1.5.4. Control of *Ptgds* Gene Transcription

A variety of compounds and transcription factors positively or negatively regulate *Ptgds* expression in certain cell types. Dexamethasone and other glucocorticoid receptor agonists are reported to stimulate *Ptgds* mRNA and protein expression in mouse neuronal cells, rat cardiomyocytes and in rat heart *in vivo* (Garcia-Fernandez et al., 2000; Tokudome et al., 2009), while estrogen increased *Ptgds* mRNA and protein levels in hearts of treated rats (Otsuki et al., 2003). Several groups have shown that thyroid hormone treatment in rhabdomyosarcoma cells increases *Ptgds* expression (White et al., 1997), while Ptgds expression is reduced in brains of hypothyroid rats (Garcia-Fernandez et al., 1998). The actions of estrogen and thyroid hormone can be explained by the binding of activated estrogen (Otsuki et al., 2003) and thyroid hormone (White et al., 1997) receptors at specific response elements in the *Ptgds* promoter. The effects of dexamethasone and glucocorticoids may be indirect because direct receptor binding, or even the presence of a glucocorticoid response element, in the *Ptgds* promoter was not shown (Garcia-Fernandez et al., 2000; Tokudome et al., 2009).

TPA, an activator of PKC, has been shown to both negatively and positively regulate *Ptgds* expression, in conjunction with other factors. TPA negates the positive effects of dexamethasone on *Ptgds* expression in mouse neuronal cells by unknown mechanisms (Garcia-Fernandez et al., 2000). Conversely, PKC activation was shown to de-repress negative inhibition of *Ptgds* expression in human neuronal cells imposed by the Hes1 bHLH protein (Fujimori et al., 2005).

Fujimori *et al* showed that Hes1 binds at an N-box in the *Ptgds* promoter to inhibit transcription (Fujimori et al., 2005), while transcriptional activation of *Ptgds* requires binding of AP2beta to an *AP2* element in the Ptgds promoter (Fujimori et al., 2005; Fujimori and Urade, 2007). A number of other transcription factors have been shown to regulate *Ptgds* expression, have binding sites in the *Ptgds* promoter and/or have been shown to bind directly to *Ptgds* promoter elements. These include NF-κB (Fujimori et al., 2003) and Sox9 (Wilhelm et al., 2007) and as well as several bHLH transcription factors such as Mitf (Takeda et al., 2006), Srebf1 (Fujimori and Urade, 2007) and Usf1 (Fujimori et al., 2008; Fujimori and Urade, 2007).

Sox9 is believed to drive male-specific *Ptgds* expression in mouse embryonic gonads, because Sox9 binds to the *Ptgds* promoter *in vivo* in E11.5 male, but not female, gonads, while *Ptgds* expression begins at around E11.5 (Wilhelm et al., 2007). Because *Sox9* is expressed specifically by Sertoli cells in embryonic testes, this drives Sertoli-cell-specific expression of *Ptgds*. However, Ptgds mRNA is detectable in E13.5 male GC cytoplasm (Adams and McLaren, 2002) and Ptgds protein is also detected in GCs of embryonic male E12.5 gonads (Moniot et al., 2009). Sox9 is not expressed in GCs, therefore, Sox9-independent pathways are likely to drive Sox9 expression in GCs.

## 1.6. Aims of the Research

Until recently, sex-specific markers for GCs at the earliest stages of sex-specific differentiation (i.e. E12.5/E13.5) have been lacking. In the last 10 years or so, this has changed. We have discovered several sex-specific markers. Using these markers, we can now begin to discern the molecular events that control and achieve the very diverse sex-specific cellular fates occurring in male and female GCs at his early stage. It is likely that many more unidentified genes are also involved. In order to discover some of these unknown genes I carried out an RtPCR expression screen comparing male and female E13.5 GC cDNA.

I decided to analyse sex-specific gene expression at E13.5 for several reasons. Firstly, at E13.5, both male and female GCs are committed to their respective differentiation programs – spermatogenesis or oogenesis, respectively. Analysis of differences at E12.5 would only identify gene expression changes that occur in male GCs as a result of male commitment. I desired to identify bHLH genes involved in male and female commitment events, the latter of which would not likely be present at E12.5. In addition, the increased numbers of GCs at E13.5 make performing an expression screen much less problematic than analysis of E12.5 material. The most upstream gene expression changes associated with spermatogenic commitment of male GC are likely to first occur at E12.5. Therefore, a limitation of analysing sex-specific expression differences at E13.5 rather than at E12.5 is that some of these male-specific expression differences could be missed if they quickly decline by E13.5. However, for the reasons stated earlier in this paragraph, I chose E13.5 as the time-point to study, and it was hoped that at least some of the earliest male-specific changes in gene expression persist until at least E13.5 and could be identified in the screen.

Rather than carrying out a genome-wide screen, I decided to specifically analyse the 114 genes belonging to the bHLH family of transcription factors. There were two reasons for this. Firstly, previous studies have characterised the involvement of the bHLH proteins Figla and Ngn3 in later stages of sex-specific

GC development so it is possible that other bHLH proteins are involved in the earliest stages of sex-specific GC development. Secondly, we previously identified that female GCs sex-specifically express *Id1* mRNA at E13.5. Id1 is a dominant negative bHLH, so it was theorised that female GCs express Id1 protein to ensure negative regulation of one or more unknown bHLH proteins that promote male-specific GC development. Therefore, this screen might identify these bHLH proteins, if they are expressed male-specifically at the mRNA level in E13.5 GCs. Another limitation of this screen is that it could not identify Id1-supressed bHLH proteins whose mRNA is expressed equally in both male and female GCs at E13.5.

The screen identified a number of bHLH genes that were potentially sex-specifically expressed by E13.5 GCs. The second aim of the research was therefore to determine whether these potential genes, along with *Ptgds*, which was previously identified as being male-specifically expressed in E13.5 GCs, were in fact sex-specifically expressed by GCs, and not some other gonadal cell type contaminating the GC cDNAs used in the screen. I used two methods to accomplish this. Firstly, I carried out PCR on cDNA libraries prepared from single male and female GCs to identify whether *Id1*, *Id2* and *Id3 (female-specific)* and/or *Ptgds (male-specific)* mRNAs were expressed by E13.5 GCs. Secondly, I used immunofluorescence staining against Id1 (female-specific) and Mnt and Ptgds (male-specific) to identify whether E13.5 GCs expressed these proteins sex-specifically.

The third aim of the research was to use these sex-specific markers as a tool to discover potential upstream molecular events controlling the early stages of sex-specific GC development. Towards this aim, I identified signalling pathways that previous studies have shown to affect *Ptgds* expression, either positively or negatively. I then attempted to activate or repress *Ptgds* expression in female or male GCs, respectively, by treating genital ridges with compounds to activate these pathways. If one or more of these compounds successfully activated *Ptgds* expression, I could then examine the GCs in these genital ridges for evidence of

sex-reversal, thereby identifying potential signaling pathways controlling male/female GC fate commitment.

Mnt protein was found to be male-specifically enriched in E13.5 GCs in this study. Mnt belongs to the bHLH-ZIP class of bHLH proteins and suppresses Myc transcriptional activity. Due to Myc's involvement in activation of DNA synthesis, it was theorised that Myc could be acting in female GCs to activate genes for pre-meiotic S-phase and that male GCs expressed Mnt to suppress this activity and bring about mitotic arrest in male GCs. Therefore, a potential fourth aim of this research was to analyse by cross-linking immunoprecipitation whether Myc and/or Mnt occupy certain cell cycle gene promoters differently in E13.5 male and female GCs. Unfortunately, due to time constraints, the cross-linking immunoprecipitation protocol was not optimised and this aim was not realised.

# Chapter 2:
# Methods and Materials

## 2.1. Animals and Tissue Dissection

Outbred CD1 mouse embryos were used unless otherwise stated. CD1 mice were naturally mated with the day of appearance of a vaginal plug counted as E0.5 (0.5 days post coitum). Generation of Oct4-GFP transgenic mice was carried out by others (Yoshimizu et al., 1999). These mice possess a transgene consisting of an 18kb region of the *Oct4* locus (GOF-18) containing EGFP (Enhanced Green Fluorescent Protein) in place of the *Oct4* coding region and the critical upstream and downstream regulatory elements. Expression of the transgene closely mimics the expression pattern of the endogenous *Oct4* gene. Homozygous *Oct4-GFP* male studs of mixed genetic background were generated from embryos donated by Hans Scholer. To confirm the homozygosity of the transgene in the studs, the studs were crossed with wildtype CD1 female mice and transmission of the transgene identified by green fluorescent GCs in E13.5 genital ridges in the resultant heterozygous embryos. To generate embryos for experimentation, the studs were crossed with CD1 female mice to produce heterozygote Oct4-GFP embryos, which were treated identically to wildtype embryos. Wildtype and Oct4-GFP embryonic gonads were dissected into PB1 media on ice. E11.5 gonads were sexed by PCR as described below, while E12.5 and older gonads were sexed according to the gonad appearance.

XY$^{Tdym1}$ and XX$^{Sry}$ embryos were generated as described previously (Durcova-Hills et al., 2004). Males with an MF1 random-bred (NIMR stock) background carrying the *Sry* deletion *Tdy$^{m1}$* and complemented by an autosomally located *Sry* transgene were mated at the National Institute for Medical Research to MF1 or 129/SvEv-*Gpi1$^{c}$* to generate XX and XY$^{Tdym1}$ female and XX*Sry* and XY$^{Tdym1}$*Sry* male embryos, from which gonads were dissected at E13.5 and processed for *in situ* hybridisation.

## 2.2. Sexing of E11.5 Embryos

For dissected E11.5 genital ridges, the corresponding heads of the embryos were sexed using PCR against the *Uba1* and *Ube1y1* genes as used previously (Chuma and Nakatsuji, 2001). PCR against *Uba1* on the X chromosome and *Ube1y1* on the Y chromosome, using a common pair of primers, results in 2 products that differ in length by 19 nucleotides. The heads were boiled for 10mins in 0.5ml $dH_2O$, triturated and spun down at 13'000rpm in a microcentrifuge for 5mins to crudely isolate genomic DNA into the supernatant. 2µl of the supernatant was added to PCR reactions with the final concentrations: 1x PCR Buffer (Invitrogen), 2.0mM $MgCl_2$, 0.4mM dNTPs, 1.0µM Ube1XA (5'-TGGTCTGGACCCAAACGCTGTCCACA-3') and Ube1XB (5'-GGCAGCAGCCATCACATAATCCAGATG-3') primers. The samples were run on a PCR cycler with the following program: 95˚C for 2mins, followed by 30 cycles of 95˚C for 30s and 68˚C for 1min. Products were visualised by agarose gel electrophoresis.

## 2.3. Oct4-GFP Gonad Microscopy

E13.5 Oct4-GFP genital ridges were dissected the same as wildtype genital ridges. Microscopy was performed on a stereo microscope equipped with a CCD camera. Brightfield and GFP fluorescence image were taken of the same gonad. Images were combined in Photoshop.

## 2.4. Generation of Purified GC PolyA$^+$ mRNA

E13.5 Oct4-GFP genital ridges were trypsinised and triturated, spun down at 5'000rpm for 5mins in a microcentrifuge and the pellet resuspended in PB1 media containing 4mg/ml BSA. The cell suspensions were kept on ice until fluorescence-activated cell sorting using a FACSVantage SE Cytometer (BD Macrosort) operated by a PC running FACSDiva software (BD Macrosort). GCs were sorted using 2 gates: 1 gate measuring GFP fluorescence and another gate measuring size/shape by side/forward scattering of light. After sorting, small aliquots were processed for alkaline phosphatase staining and the remainder spun down at 5000rpm for 5mins, the supernatant aspirated and the pellet frozen on dry ice before storage at -20˚C.

PolyA$^+$ mRNA was prepared from the purified GC pellets using Dynabeads mRNA DIRECT™ Micro Kit (Invitrogen) as per the manufacturer's instructions except taking the beads through the protocol one more time after the first elution. The resulting mRNA was stored at -20˚C or reverse transcribed immediately. cDNA was prepared as described for gonad cDNA.

## 2.5. Alkaline Phosphatase Staining of Purified GCs

Aliquots of freshly-purified GCs were allowed to attach to slides for 5mins before fixing with 4% formaldehyde at room temperature for 2mins and washing 3 times with PBS. GCs were then equilibrated in NTMT (100mM NaCl, 100mM pH9.5 TrisHCl, 50mM $MgCl_2$, 1% Tween-20) for 10mins before addition of 4.5µl/ml of 50mg/ml 4-nitro blue tetrazolium chloride (NBT) and 3.5µl/ml of 50mg/ml 5-bromo-4-chloro-3-indolyl-phosphate (BCIP) stock solutions. Samples were then incubated at room temperature in the dark for 5-10mins,

washed several times with PBS once GCs showed obvious dark purple stain then incubated in PBS containing DAPI, washed with PBS and coverslips applied.

## 2.6. Whole-gonad and Whole-Embryo cDNA Preparation

E13.5 male and female gonads were trypsinised and triturated, spun down at 5'000rpm for 5mins in a microcentrifuge and the pellet resuspended in TRI Reagent (Sigma). Whole embryos were homogenised using a hand held electronic homogeniser, trypsinised and triturated then homogenised in TRI Reagent. RNA was extracted according to the TRI Reagent manufacturer's instructions (Sigma), resuspended in $dH_2O$ and RNA concentration measured using a spectrophotometer. cDNA was prepared using Superscript III (Invitrogen) according to the manufacturer's instructions.

## 2.7. Generation of Single-cell cDNA Libraries

Single-cell cDNA libraries were prepared as described previously (Brady and Iscove, 1993) with changes made to allow detection of expression by gene-specific PCR. E13.5 male and female gonads were dissected away from mesonephroi, trypsinised and triturated, spun down at 5'000rpm for 5mins in an Eppendorf microcentrifuge and the pellet resuspended in PB1 media containing 4mg/ml BSA. An aliquot of this initial cell suspension was diluted into a large droplet of PB1 media, and single GC-like cells were aspirated from this droplet by fine glass pipette into a fresh 1ul drop of PB1 media containing 4mg/ml Acetylated BSA (Sigma). The single cells were then transferred into 4µl cell lysis buffer (1x 1$^{st}$ Strand Buffer (Invitrogen), 11.8µM dNTPs, 25nM

oligod$T_{24}$, 0.5% Nonidet P-40 (Sigma), 300U/ml RNAguard (GE), 300U/ml Prime RNAse Inhibitor (Eppendorf)) in RNAse-free 0.2ml PCR tubes on ice. The samples were incubated at 65°C for 1min then placed at room temperature for 4mins before collecting to the bottom of the tube at 11'000rpm for 1min and placing on ice. 1.0ul Superscript III (Invitrogen) was added and samples incubated at 50°C for 15mins, placed on ice for 1min, then incubated at 70°C for 10mins. Samples were spun at 13'000rpm for 1min at 4°C then placed on ice.

For polyA tailing of the cDNAs, 5.5µl 2x tailing buffer (2x Tdt Buffer (Invitrogen), 1.4mM dATP, 850U/ml Terminal Deoxynucleotidyl Transferase (Invitrogen)) was added to each sample. Samples were then incubated at 37°C for 15mins and 65°C for 10mins, spun at 13'000rpm at 4°C for 2mins and placed on ice. General amplification of tailed cDNAs was accomplished as follows. 4ul of the tailed cDNA was added to 16ul PCR buffer (1.25x PCR Buffer without $MgCl_2$ (Invitrogen), 0.125µg/µl BSA (NEB), 1.25mN dNTPs, 0.125% Triton X-100, 6.25µM Oligo $dT_{24}$, 3.75µM $MgCl_2$, 156.25U/ml Taq (Invitrogen)) and samples underwent the following PCR program: 94°C 2mins, followed by 20 cycles of 94°C 1min, 42°C 1mins, 72°C 6mins, then a last step of 72°C for 5mins. Samples were then stored at -20°C.

## 2.8. Gene-specific PCR Analysis

PCR reactions were setup on ice as follows. 0.5µl of template cDNA was added into 19.5µl PCR buffer with final concentrations: 1x PCR Buffer without $MgCl_2$ (Invitrogen), 2mM dNTPs, 3.5mM $MgCl_2$, 0.3µM primers, 25U/ml Taq (Invitrogen). The following PCR program was used: 95°C 1min, followed by 95°C for 30s, 52-62°C (standard 62°C but optimised for each primer set where required) for 30s, 72°C for 1min 30s. Products were visualised by agarose gel electrophoresis.

## 2.9. Real-time PCR (RtPCR) Analysis

For analysis of initial GC cDNA 15µl Real-time PCR reactions were setup by hand as follows. 5.0µl of template cDNA was added to 10µl PCR mix (one PCR mix was made per gene analysed), to give final concentrations of 1x SYBR Green PCR Master Mix (Applied Biosystems) and 0.3µM primers. Reactions were prepared in 96-well plates that were then sealed, given a pulse spin to collect the liquid to the bottom of the wells and the reactions carried out on a Biorad CFX96 cycler (Bio-rad Laboratories) with the following program: 95°C 10mins, then 40 cycles of 95°C 15s, 60°C 1min. The detector was set to measure SYBR green fluorescence at the end of each cycle. After completion a melting curve program was carried out: 35°C for 30s then heating at 0.2°C/s to 85°C with continuous SYBR green fluorescence measurements. Biorad CFX software (Bio-rad Laboratories) was used to analyse the results using a standard curve of serially diluted positive control cDNA.

For the bHLH screen, one PCR mix was prepared per gene analysed, to give final reaction concentrations of 1x FastStart Taqman Probe Master Mix (Roche), 0.3µM primers and 250nM Universal ProbeLibrary Hydrolysis Probe (Roche). Diluted cDNA was also prepared. A Biomek 3000 (Beckman Coulter) automated pipetting robot was programmed to pipette first master mix then cDNA into 384-well plates, which were then sealed and given a pulse spin before carrying out the reactions on a 7900HT Fast Real-Time PCR System (Applied Biosystems) with the following program: 95°C 10mins, then 40 cycles of 95°C for 15s and 60°C for 1min. Representative male, female, positive control and $dH_2O$ control reactions per gene were analysed by gel electrophoresis to ensure the presence of only one product.

## 2.10. Data Analysis for bHLH Screen Part 2

Triplicate technical replicates were analysed for each gene in part 2 of the screen and for most of the genes another set of triplicates was analysed on a different biological sample. The data from these biological replicates was analysed separately. Data was collected and analysed using SDS V2.0 (Applied Biosystems). Standard curves were used only if they included triplicate reactions at 5 different dilutions. The data was imported into Microsoft Excel, which was used to normalise the data according to the relative *Gapdh* and *Tub1a1* levels in male and female GC cDNA. All standard errors associated with mean averages were propagated. The data was entered into Graphpad Prism 4.0, for statistical analysis, as separate male and female means (converted relatively so that the lower mean had a value of one) with the propagated standard errors of the means (also converted relatively) and the number of replicates. Unpaired 2-tailed t-tests were calculated from these figures to compare differences between male and female GC cDNA.

## 2.11. Immunofluorescence of Embryonic Genital Ridges

E11.5, E12.5 or E13.5 genital ridges were fixed for 1 hour in freshly-thawed 4% paraformaldehyde in PBS at 4°C with constant mixing. After fixation, the genital ridges were washed 3 times with PBS for 5mins then stored at 4°C for up to 5 days before wax embedding. For wax embedding, the genital ridges were washed twice for 5mins in 70% ethanol, once in 90% ethanol, 3 times in absolute ethanol, then one rinse and one 5 minute wash in xylene before 3 5min washes in wax at 58°C. Genital ridges were then embedded into blocks, which were then allowed to solidify overnight at room temperature then stored at 4°C.

Blocks were sectioned into 6μm sections onto frosted slides, which were dried and incubated at 50°C overnight. Sections were stored at 4°C until use.

Wax-embedded sections were deparaffinised before use by washing twice in xylene, twice in absolute ethanol, once in 90% ethanol, twice in 70% ethanol then 3 times in PBS. Antigen retrieval was accomplished by boiling for 20mins in a microwave oven on full power whilst immersed in 100mM pH6 sodium citrate buffer. Sections were washed once in PBS, blocked (5/10% serum, 0.1% Tween-20, 0.05% sodium azide, in PBS) for one hour, incubated with primary antibodies for one hour, secondary antibodies and DAPI for one hour, each at room temperature in the dark, washed in PBS 3 times and mounted with Vectashield (Vector Labs) and cover slips. Fluorescence staining was viewed using an Axioplan II fluorescence microscope (Carl Zeiss) outfitted with a Coolsnap digital camera (Photometrics) and operated by an Apple mac running IPLab software (BD Biosciences). For each field, identical exposure times were used to capture an image for each channel, and these images were then recombined in Photoshop (Adobe). Images of male, female and control sections were processed identically.

The α-Id1 antibody used (BCH-1/37-2 from Biocheck Inc.) is a rabbit monoclonal IgG generated against recombinant full-length mouse Id1, is specific to mouse Id1 (Perk et al., 2006), and was used at 0.05μg/ml. The α-Mnt antibody used (sc-769 from Santa Cruz Biotech.) is a rabbit polyclonal IgG generated against residues 226-361 of human Mnt, and was used at 0.4μg/ml. Generation of the Rat α-GCNA polyclonal antibodies was described previously (Enders and May, 1994) and these were used at 1:100, while mouse α-Dazl antibodies (kindly given by Howard Cooke) were used at 1:1000. The Ptgds antibody used is a rabbit polyclonal IgG antibody generated against full length human Ptgds protein (sc-30067), which was used at 0.2μg/ml concentration. The Amh antibody used was a mouse monoclonal IgG (Abcam) used at 1:40 final dilution. $Alexa_{594}$ α-rabbit IgG secondary antibodies were used for α-Id1, α-Ptgds and α-Mnt detection, $Alexa_{488}$ α-rat IgM secondary antibodies were used for α-GCNA detection, and $Alexa_{488}$ α-mouse secondary antibodies were used for

α-Dazl and α-Amh detection. All secondary antibodies were acquired from Molecular Probes (Invitrogen).

For quantitative immunofluorescence analysis, the "Measure Regions" script of Fovea Pro 4.0 plugin (Reindeer Graphics) for Adobe Photoshop was used to measure the mean pixel intensity in the relevant channel for manually-identified nuclei. GC nuclei were identified by manual inspection of the GC marker channel. Calculations were accomplished in Microsoft Excel and statistical analysis done using unpaired 2-tailed t-tests in Graphpad Prism.

## 2.12. Culture of Embryonic Genital Ridges

Sexed E11.5 genital ridges were placed on top of agar (2% agar in PBS) blocks in culture dishes containing PGC media (DMEM, 10% FCS, 2mM glutamine, 100units/ml penicillin, 0.05mg/ml streptomycin, 1.5mM Sodium Pyruvate, 0.1% Fungizone, 0.1μM β-mercaptoethanol, 1μg/ml Fungizone (Sigma)) with either a tested compound or equivalent vehicle added. Levels of media were supplemented each day of culture. After 2/3 days of culture, the genital ridges were washed in PBS then processed for *in situ* hybridisation.

## 2.13. Wholemount *In Situ* Hybridisation

Wholemount *in situ* hybridisation was accomplished using digoxigenin-labeled cRNA probes as previously described (Adams and McLaren, 2002). PCR was performed on male gonad cDNA using primers against nucleotides 1-637 of *Ptgds* (AB006361 Genbank) and blunt-end cloned into pBluescript II SK+ (Stratagene). The clones were checked by restriction digestion and sequencing and one clone selected for linearisation at either the 5' or 3' end of the *Ptgds*

insert. The linearised clones were then used as templates for generation of digoxigenin-labeled sense and antisense cRNA probes using the DIG Probe Synthesis Kit (Roche) according to the manufacturer's instructions. Probe length was checked by RNAse-free gel electrophoresis and probe concentration was checked using a UV spectrophotometer.

Wholemount *in situ* hybridisation was carried out as described previously (Henrique et al., 1995). Briefly, genital ridges were fixed in fresh 4% paraformaldehyde, washed in PBS/0.1% Tween-20 then dehydrated into methanol, and stored for up to one month at -20°C. Genital ridges were then rehydrated into PBS/Tween-20, treated with 10µg/ml proteinase K for 13mins, refixed in 4% paraformaldehyde and 0.1% gluteraldehyde, washed then equilibrated in hybridisation buffer (50% formamide, 1.3x SSC, 5mM pH8 EDTA, 50µg/ml yeast RNA, 0.2% Tween-20, 0.5% CHAPS, 100µg/ml Heparin) at 70°C with constant mixing. After equilibration, 1µg/ml of the cRNA probe was added and the genital ridges incubated overnight at 70°C with constant mixing. After hybridisation, genital ridges were washed in hybridisation buffer at 70°C, transferred gradually to MABT (100mM maleic acid, 150mM NaCl, pH7.5, 0.5% Tween-20) at 70°C then washed several times in MABT at room temperature, before blocking with Blocking Reagent (Roche) and 20% serum and incubating overnight at 4°C with 1/2000 Anti-digoxigenin-AP, Fab fragments (Roche). Excess antibody was washed away with several rinses and long washes in MABT, before NBT/BCIP staining as described for alkaline phosphatase staining of purified GCs.

# Chapter 3:
# Real-time PCR Screen to Identify Candidate bHLH Genes Involved in Early Sex-specific Germ Cell Differentiation

# 3.1. Chapter Introduction and Aims

This screen was prompted by the finding that *Id1*, which belongs to the basic helix-loop-helix (bHLH) family of transcription factors, is sex-specifically upregulated in E13.5 female GC cDNA (I. Adams unpublished data). This finding was corroborated by real-time PCR (RtPCR) against *Id1*, which found a robust 40-fold sex-specific enrichment of *Id1* mRNA in E13.5 female GC cDNA (L. Lewis unpublished data). *Id1* itself is one of four Id proteins that make up a sub-class of bHLH proteins that are involved in the stimulation of the cell cycle and inhibition of differentiation (Yokota, 2001; Zebedee and Hara, 2001).

The *Id* genes are upregulated in culture cells in response to stimulation by serum (Barone et al., 1994; Hara et al., 1994) or BMP (Hollnagel et al., 1999; Nakashima et al., 2001), and are required for efficient S-phase entry of various cultured cells in response to those signals, as shown by knockdown of Ids by antisense techniques, which results in delayed S-phase entry (Barone et al., 1994; Swarbrick et al., 2005). As well as stimulating the cell cycle, *Ids* inhibit the differentiation of cell types *in vivo* and *in vitro*. *Id1* expression is downregulated when cells differentiate, and forced expression of *Id1* prevents differentiation (Desprez et al., 1995). Similarly, ectopic expression of *Id1* prevents neuronal differentiation of embryonic stem cells in the absence of BMPs (Ying et al., 2003). Expression patterns of *Id1*, *Id2* and *Id3* are overlapping (Yokota, 2001), and these genes have redundant roles in embryonic development (Fraidenraich et al., 2004). However, double knockouts of *Id* genes are embryonic lethal (Fraidenraich et al., 2004; Lyden et al., 1999). In *Id1*/*Id3* double knockout embryos, many cells differentiate precociously, as shown by increased expression of differentiation markers, and some progenitor populations prematurely exit the cell cycle, resulting in a reduction in numbers of some cell types.

The bHLH transcription factors comprise at least 114 genes in the mouse (Ensembl Genome Browser [online], Release 47. Available from:

http://www.ensembl.org/index.html [Accessed 15/11/2007]). Tissue-specific bHLHs promote cell-type-specific gene transcription and differentiation during embryonic development of many tissues (Massari and Murre, 2000). bHLHs must dimerise to become transcriptionally active, and most tissue-specific bHLHs must heterodimerise with a ubiquitously-expressed Class A bHLH to form an active heterodimer. Most tissue-specific bHLHs, therefore, rely on Class A bHLHs to affect transcription of their target genes. The Id proteins possess a dimerisation domain but do not possess a DNA-binding domain and, therefore, they form inactive heterodimers with other bHLHs. The Ids have particularly high affinity for Class A bHLHs (Yokota, 2001), and because of this the Id proteins sequester Class A bHLHs away from tissue-specific bHLHs, resulting in reduction of cell-type-specific gene expression and inhibition of differentiation.

Several bHLHs have suspected or proven roles in various postnatal and late embryonic stages of GC development. *Sohlh1* and *Sohlh2* have germ-cell-specific expression profiles and their knockout results in defects in the mitosis-meiosis transition of spermatogonia in adult testis (Ballow et al., 2006; Hao et al., 2008; Toyoda et al., 2009), as well as defects in oogenesis (Choi et al., 2008; Pangas et al., 2006; Toyoda et al., 2009). *Figla* is expressed sex-specifically in female GCs undergoing oogenesis, and its knockout results in a female-specific defect in folliculogenesis shortly after birth (Soyal et al., 2000). *Ngn3* also has a suspected role in spermatogenesis, primarily because it is expressed in all spermatogonial stem cells that give rise to subsequent, more mature spermatogenic cells (Yoshida et al., 2004). In addition, *Tcfl5* has a GC-restricted expression pattern and is primarily expressed in spermatocytes and spermatids (Siep et al., 2004).

Because bHLH genes are involved in later stages of sex-specific GC development, and the dominant negative bHLH *Id1* is sex-specifically enriched in female GC cDNA between E11.5 and E13.5, it was theorised that bHLHs could have a role in the decision of embryonic GCs to commit to spermatogenesis or oogenesis, which occurs just before E13.5. One plausible mechanism would be that female GCs express Id1 to ensure the negative regulation of a male-GC-expressed bHLH

that initiates mitotic arrest in male GCs. In fact, many bHLHs have the effect of promoting cell cycle exit at the same time as triggering cell-type-specific differentiation programs (Zebedee and Hara, 2001).

An expression screen was carried out to find candidate bHLH genes that might be involved in this developmental decision. The aim of the screen was to find candidate genes whose expression was consistently and significantly higher in one sex compared to the other in E13.5 GCs. In the course of the screen, 21 out of 114 bHLH genes were found to be sex-specifically enriched in E13.5 GC cDNA. Experiments were then carried out on a number of these sex-specifically enriched genes to confirm that it is specifically GCs and not another contaminating cell types that express them. Single-cell RT-PCR confirmed that *Id1* and *Id3* mRNA were expressed by female GCs. Immunofluorescence staining for Id1 and Mnt confirmed that female and male GCs, respectively, sex-specifically express higher levels of Id1 and Mnt at the protein level. Further Id1 and Mnt immunofluorescence analysis of E11.5 and E12.5 tissue was carried out in order to discover temporal changes in protein expression between E11.5 and E13.5 in male and female GCs.

## 3.2. Characterisation of FACS-purified E13.5 GCs

In order sex-specific differences in E13.5 GC gene expression, E13.5 GC cDNA was prepared from male and female GCs. Firstly, the GCs were purified by FACS of E13.5 male and female genital ridges from *Oct4-GFP* mice that contain a transgene consisting of *Oct4* genomic sequences with *GFP* in place of *Oct4*. The *GFP* transgene is expressed GC-specifically from E8.0 and this continues in male and female post-migratory GCs, resulting in GCs with fluorescent green signal (Yoshimizu et al., 1999). Brightfield and green fluorescent images of E11.5, E12.5 and E13.5 transgenic male and female genital ridges were overlaid (E13.5 tissue shown in Figure 3.2.1, A and B). The pattern of GFP positive cells was consistent with GC expression. For each FACS experiment, 3 litters-worth of male and female genital ridges (30-40 genital ridges per sex) were pooled and GCs were purified based on green fluorescence and shape and size. This generally resulted in the collection of 100'000 to 200'000 GCs per sex, which was 3.5-4% of the parent population. A $GFP^-$ cell fraction was also collected.

To check the purity of these GC preparations, aliquots were fixed onto slides and stained by alkaline phosphatase (AP) staining and DAPI (Figure 3.2.1, C). The number of $AP^+$ nuclei was scored in 3 separate experiments and the percentage of $AP^+$ nuclei calculated. Both male and female GC preparations were very pure – males roughly 97% and females roughly 98.5%.

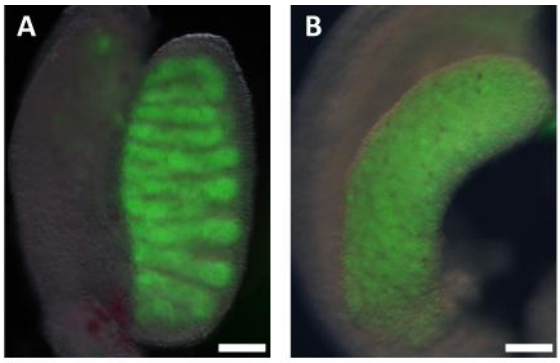


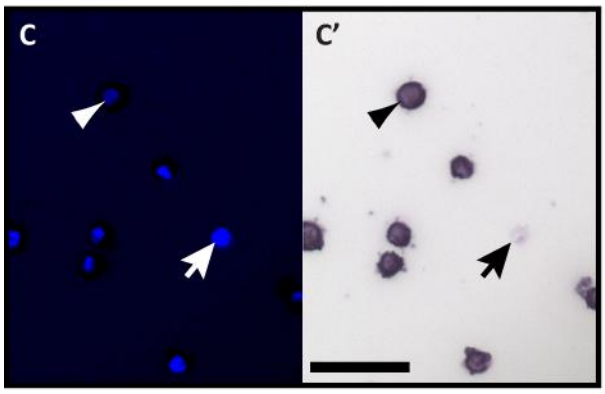


(D)

| | APase Positive | |
|---|---|---|
| | ♂ | ♀ |
| Count 1 | 122/126 | 119/122 |
| Count 2 | 105/109 | 109/111 |
| Count 3 | 111/113 | 130/131 |
| Sum | **338/348** | **358/364** |
| % Positive | **97.1%** | **98.4%** |

**Figure 3.2.1. Characterisation of FACS-purified E13.5 GC Populations by Alkaline Phosphatase Staining.** GCs from E13.5 Testes, (A), and Ovaries, (B), from Oct4-GFP mice were purified by FACS using GC-specific expression of GFP. Images (A) and (B) are a composite of brightfield images overlaid with green fluorescent signals of freshly-dissected E13.5 Oct4-GFP genital ridges. Scales in (A) and (B) are 100µm. After sorting, fresh cells were fixed and stained for alkaline phosphatase to identify GCs and DAPI to identify all cells, then blue fluorescence, (C), and brightfield, (C'), images taken to visualize DAPI and alkaline phosphatase staining, respectively. Scale in (C') is 50µm. Each $DAPI^{+}$ cell was counted and classified as either a GC or non-GC based on alkaline phosphatase staining from 3 separate cell-sorting experiments, (D), and the percentage of GCs calculated.

## 3.3. bHLH Screen Part 1

The bHLH screen was split into 2 parts. In the first part, all 114 bHLHs genes were assayed non-quantitatively for sex-specific expression in E13.5 male and female GC cDNAs. 26 genes that had the highest sex-specific expression differences according to the results of the first part of the screen were quantitatively analysed in the second part of the screen.

### 3.3.1. cDNA Normalisation

This section describes the strategies employed to check and normalise the GC cDNAs for use in the first part of the bHLH expression screen.

Male and female E13.5 GCs were purified as described in the previous section (section 3.2). PolyA$^+$ mRNA was extracted and GC cDNA prepared as described in Chapter 2. An initial real-time PCR (RtPCR) experiment was carried out to quantitatively check the relative expression of the housekeeping genes *Glyceraldehyde-3-phosphate Dehydrogenase* (*Gapdh*) and *α-tubulin* (*Tubala*) in each fresh batch of male and female GC cDNA, and to allow pre-normalisation of the cDNA by dilution for this, the first part of the screen. An example of one of these analyses is shown in Figure 3.3.1 (A-D) for *Tuba1a*. All primers used in this screen for housekeeping and bHLH gene expression analysis are listed in appendix i.

The purpose of the first part of the screen was to quickly identify which bHLH genes might be expressed differently in male and female GCs. To do this quickly, non-quantitative RtPCR was used to measure and compare the mean threshold cycles ($C_{(t)}$s) for male and female cDNAs, each in triplicate, for each gene. To

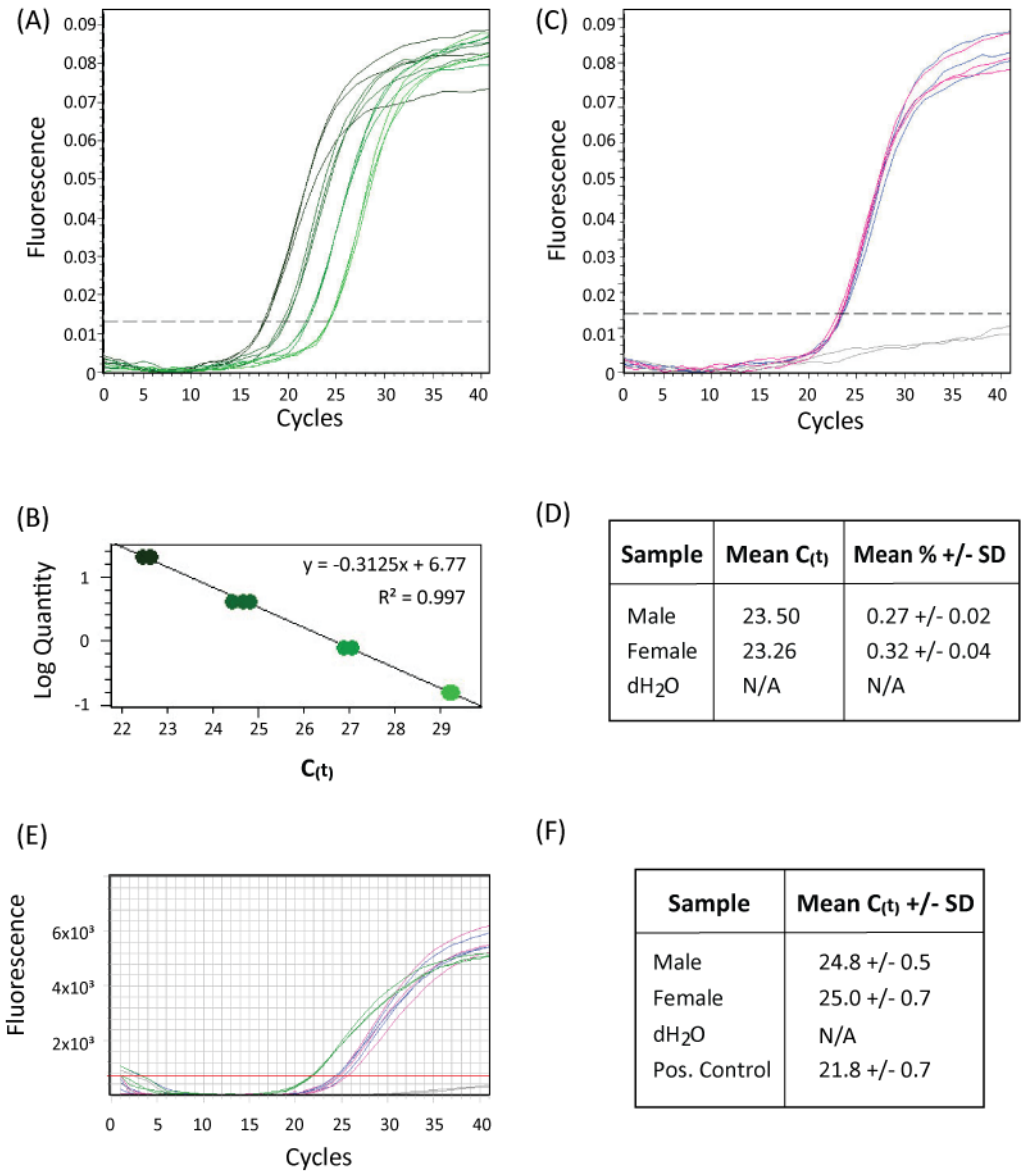


| Sample | Mean $C_{(t)}$ | Mean % +/- SD |
|---|---|---|
| Male | 23. 50 | 0.27 +/- 0.02 |
| Female | 23.26 | 0.32 +/- 0.04 |
| $dH_2O$ | N/A | N/A |

| Sample | Mean $C_{(t)}$ +/- SD |
|---|---|
| Male | 24.8 +/- 0.5 |
| Female | 25.0 +/- 0.7 |
| $dH_2O$ | N/A |
| Pos. Control | 21.8 +/- 0.7 |

**Figure 3.3.1. *α-tubulin* (*Tuba1a*) Expression Analysis in GC cDNAs for the 1st Part of the Screen.** Real-time PCR (RtPCR) using primers for *Tuba1a* was used to measure the threshold cycles ($C_{(t)}$) of serially-diluted standard cDNAs (green traces), in triplicate, (A), which were then used to produce a standard curve, (B). Parallel RtPCR reactions of male GC (blue traces) and female GC (pink traces) cDNAs, in triplicate, were also carried out, (C), and the mean male and female $C_{(t)}$ values calculated along with standard deviations ("+/- SD"), (D). Parallel $dH_2O$ negative control reactions (grey traces), in duplicate, were also carried out. A "%" value, which was the % of starting quantity according to the standard curve (100% being the highest dilution of standard cDNA), was calculated for each male and female reaction. "Mean %" was then calculated along with standard deviations, (D). These Mean % values were used to calculate the relative male:female *Tuba1a* levels, which were used in conjunction with relative *Gapdh* levels to dilute the cDNAs to equivalence. RtPCR reactions, (E), were run after each freeze-thaw of the GC cDNA, along with diluted positive control cDNA (green traces), and used to check the equivalence of the GC cDNAs, (F).

remove the need for retrospective normalisation by quantitative analysis of housekeeping gene expression, the male and female GC cDNAs were diluted to equivalence before the experiments with respect to their *Gapdh* and *Tuba1a* levels. Relative bHLH gene expression was then analysed in the male and female cDNAs after storage at -20˚C.

Each subsequent experiment in the first part of the screen, after freeze-thaw of the GC cDNA, included analyses of $C_{(t)}$s for both *Gapdh* and *Tuba1a* to ensure that the GC cDNAs were still equivalent (Figure 3.3.1E and F).

## 3.3.2. bHLH Screen Part 1 Results

In order to do identify which genes might be enriched sex-specifically in E13.5 GC cDNA, each gene was analysed by comparing the mean $C_{(t)}$ of triplicate male and female GC cDNAs, and were analysed quantitatively in the second part of the screen if the mean $C_{(t)}$s for male and female cDNAs differed by 2.0 cycles or more. 114 bHLH genes, as listed in Ensembl Genome Browser as having a bHLH domain (Ensembl Genome Browser [online], Release 47. Available from: http://www.ensembl.org/index.html [Accessed 15/11/2007]), were tested in total. 82 bHLH genes were either undetected in GC cDNA or had a mean $C_{(t)}$ difference between male and female GC cDNA of less than 2.0 cycles. The mean male and female $C_{(t)}$s for the remaining 32 genes differed by 2.0 cycles or more, and 26 of these genes, along with 1 other selected gene, were analysed quantitatively in the second part of the screen (Section 3.4).

Each analysis in this first part of the screen included 11 Real-time PCR reactions per gene – 3 replicates each containing male GC cDNA, female GC cDNA and positive control cDNA, and 2 replicates containing $dH_2O$. The positive control cDNA consisted of diluted cDNA generated from various embryonic tissues from E11.5, E13.5, E14.5 and E17.5 embryos. As described in the previous section, male and female GC cDNAs were diluted to equivalence based on the results of

an initial quantitative analysis of *Tuba1a* and *Gapdh* prior to analysis of bHLH genes. During analyses of bHLH genes in this part of the screen, parallel reactions were also included for *Tuba1a* and *Gapdh*. For both housekeeping genes, the male and female GC cDNAs consistently amplified within 0.3 cycles of one another, while the positive control cDNA amplified 3.0 +/- 0.6 cycles before male and female GC cDNAs. The primers used for analysis of bHLH and housekeeping genes in this screen are listed in appendix i.

A valid result for each cDNA (male GC cDNA, female GC cDNA and positive control cDNA) consisted of at least 2 out of the 3 reactions having $C_{(t)}$s within ±2.0 cycles. Such replicates were deemed to concur and the mean of the concurring replicates was calculated and used as the result for that cDNA for that gene. 10.3% of the reactions did not concur in this way, and were disregarded. A valid result for each gene consisted of valid mean $C_{(t)}$s for each cDNA and no meaningful amplification in the $dH_2O$ reactions. Two exceptions to these parameters are the analyses for *Tcfeb* and *Tcfl5*, which are explained below. The decision to accept only 2 rather than all 3 concurring replicates was made to allow this part of the screen to progress in a timely fashion.

3.5% of the reactions amplified with an abnormal, non-sigmoidal shape and/or were markedly different in appearance compared to the other 2 triplicates. These reactions were deemed anomalous and the data from them disregarded. The cause of these anomalous reactions is unknown. For genes where replicate reactions showed similar non-sigmoidal reaction kinetics, different primers that did result in reliable sigmoidal reactions were used.

For 30 out of the total 114 bHLH genes, no amplification was detected before the end of the reaction (40 cycles) in both male and female GC cDNAs (appendix v). The positive control of embryonic tissue cDNA ensured that the primers were able to reliably detect transcript of known splice variants for these 30 genes, with the exception of *MycS*, for which amplifications were detected in genomic DNA. *MycS* has a very restricted expression pattern (Asai et al., 1994;

Sugiyama et al., 1989), and was undetected in positive control cDNA, as well as in GC cDNAs.

Of the bHLH genes for which a PCR product was detected in GC cDNAs, 52 genes showed a sex-specific difference in mean $C_{(t)}$ of less than 2 cycles, and were not looked into further. Figure 3.3.2 displays the data for these genes.

No reaction was detected in positive control cDNA for *Tcfeb* or *Tcfl5*, whereas robust amplifications were detected in male and female GC cDNAs for these genes. The amplification detected in the male and female GC cDNAs was considered acceptable for a valid result. Previous studies found that both *Tcfl5* and *Tcfeb* have very restricted expression patterns, which would explain why amplification failed in positive control cDNAs. Interestingly, *Tcfl5* expression is spermatocyte-specific in adult mice with limited expression in embryonic tissues (Siep et al., 2004), while a testis-specific splice variant of *Tcfeb* is detected in adult tissues and high level embryonic *Tcfeb* expression is limited to specific trophoblastic cells (Steingrimsson et al., 1998).

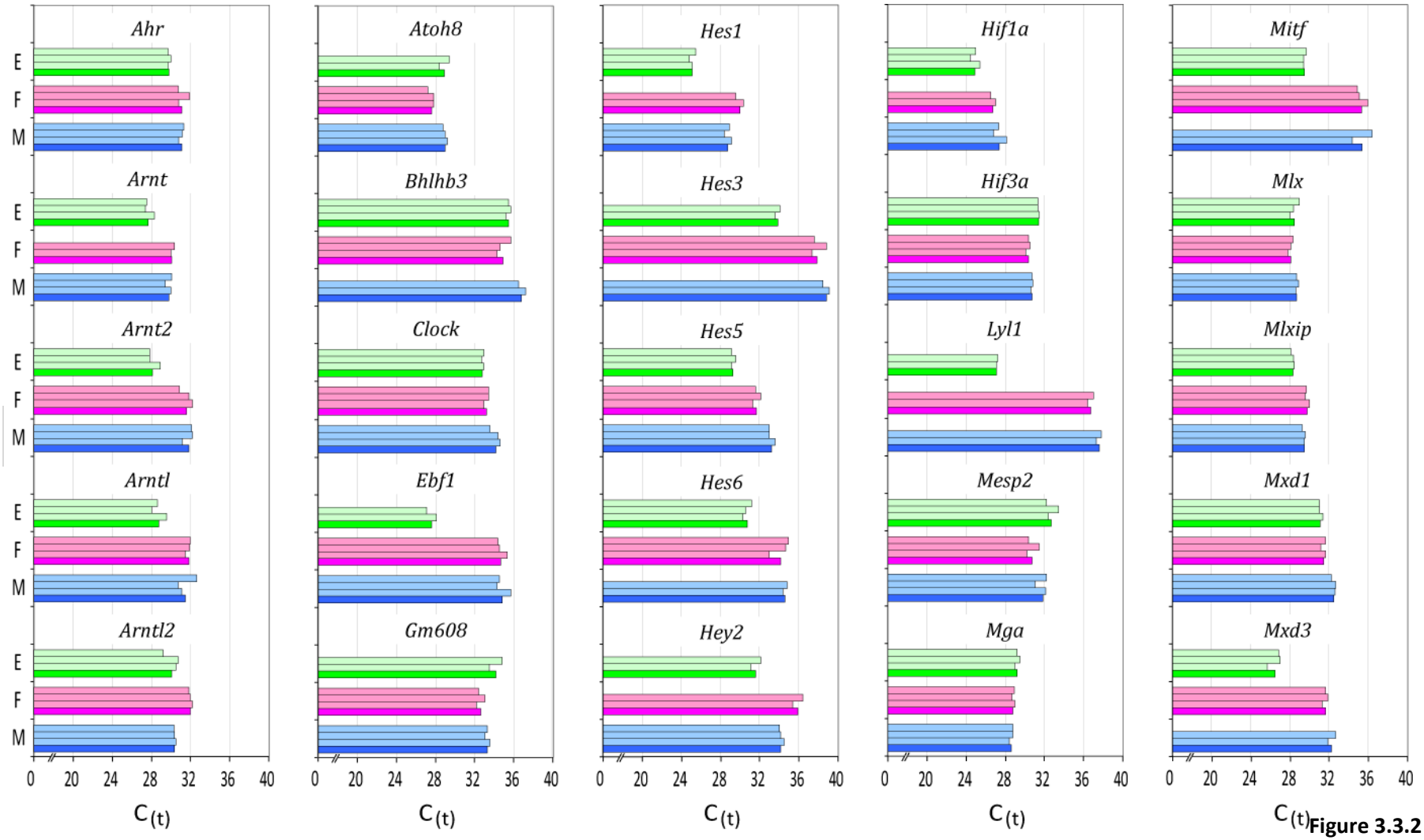
Ahr
Arnt
Arnt2
Arntl
Arntl2
Atoh8
Bhlhb3
Clock
Ebf1
Gm608
Hes1
Hes3
Hes5
Hes6
Hey2
Hif1a
Hif3a
Lyl1
Mesp2
Mga
Mitf
Mlx
Mlxip
Mxd1
Mxd3
E
F
M
0 20 24 28 32 36 40
C(t)

**Figure 3.3.2**

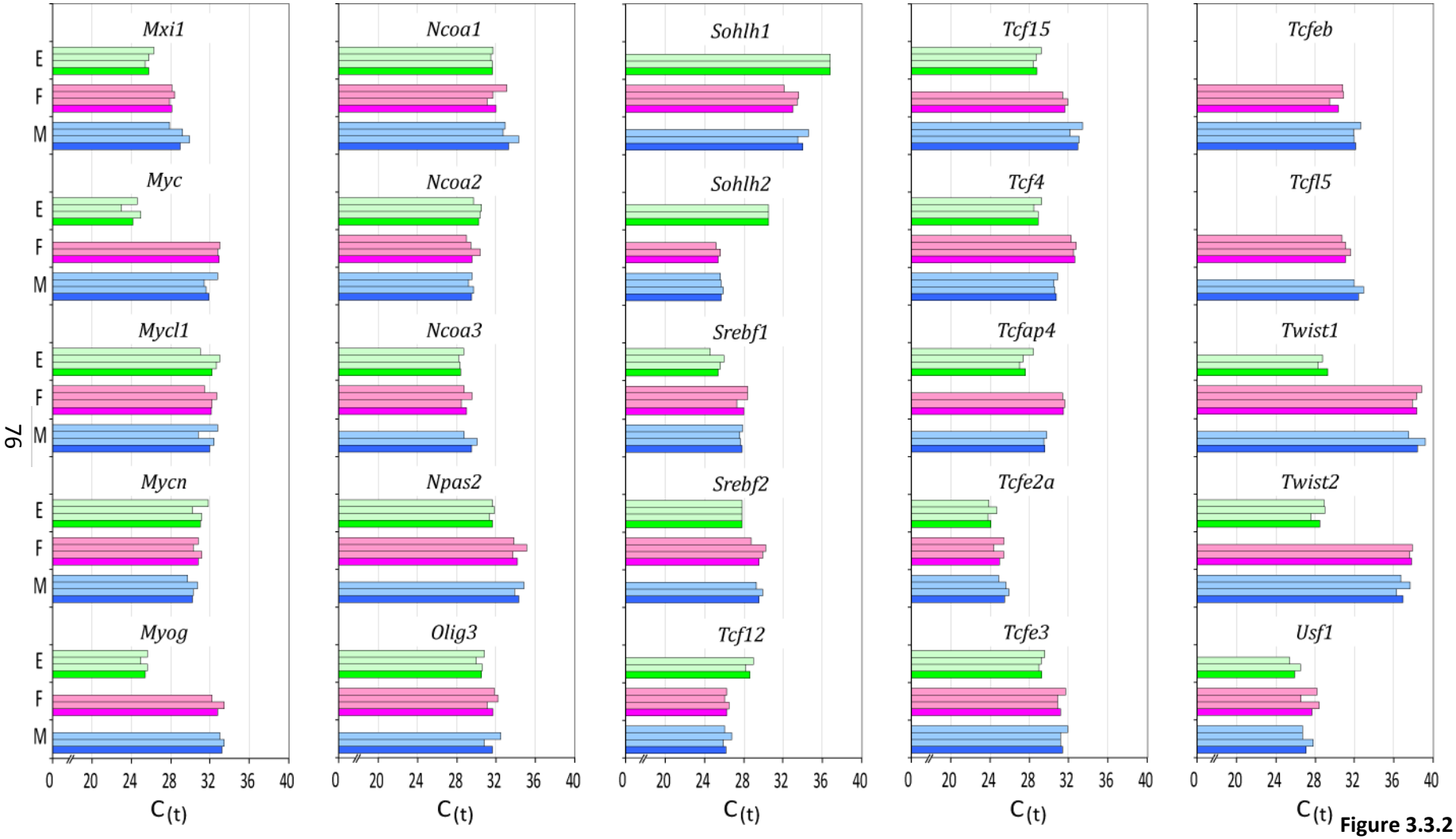
Mxi1
Myc
Mycl1
Mycn
Myog
Ncoa1
Ncoa2
Ncoa3
Npas2
Olig3
Sohlh1
Sohlh2
Srebf1
Srebf2
Tcf12
Tcf15
Tcf4
Tcfap4
Tcfe2a
Tcfe3
Tcfeb
Tcfl5
Twist1
Twist2
Usf1
E
F
M
0 20 24 28 32 36 40
C(t)

**Figure 3.3.2**

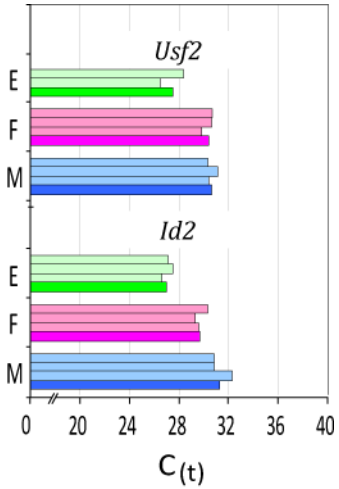


**Figure 3.3.2. bHLH Genes with Less Than 2.0 Cycle Sex-specific Difference in E13.5 GC cDNA**. Triplicate Real-time PCR reactions were carried out containing male GC cDNA, female GC cDNA and positive control cDNA. $C_{(t)}$s for concurring reactions (within ±2.0 cycles) are shown for male GC cDNA (light blue bars), female GC cDNA (light pink bars) and positive control cDNA (light green bars) along with the calculated mean $C_{(t)}$ of the concurring reactions (bars in corresponding colours except dark). "M" = male GC cDNA reactions, "F" = female GC cDNA reactions and "E" = Embryo (positive control) cDNA reactions, Note the break in the x-axis in the first 20 cycles for clarity.

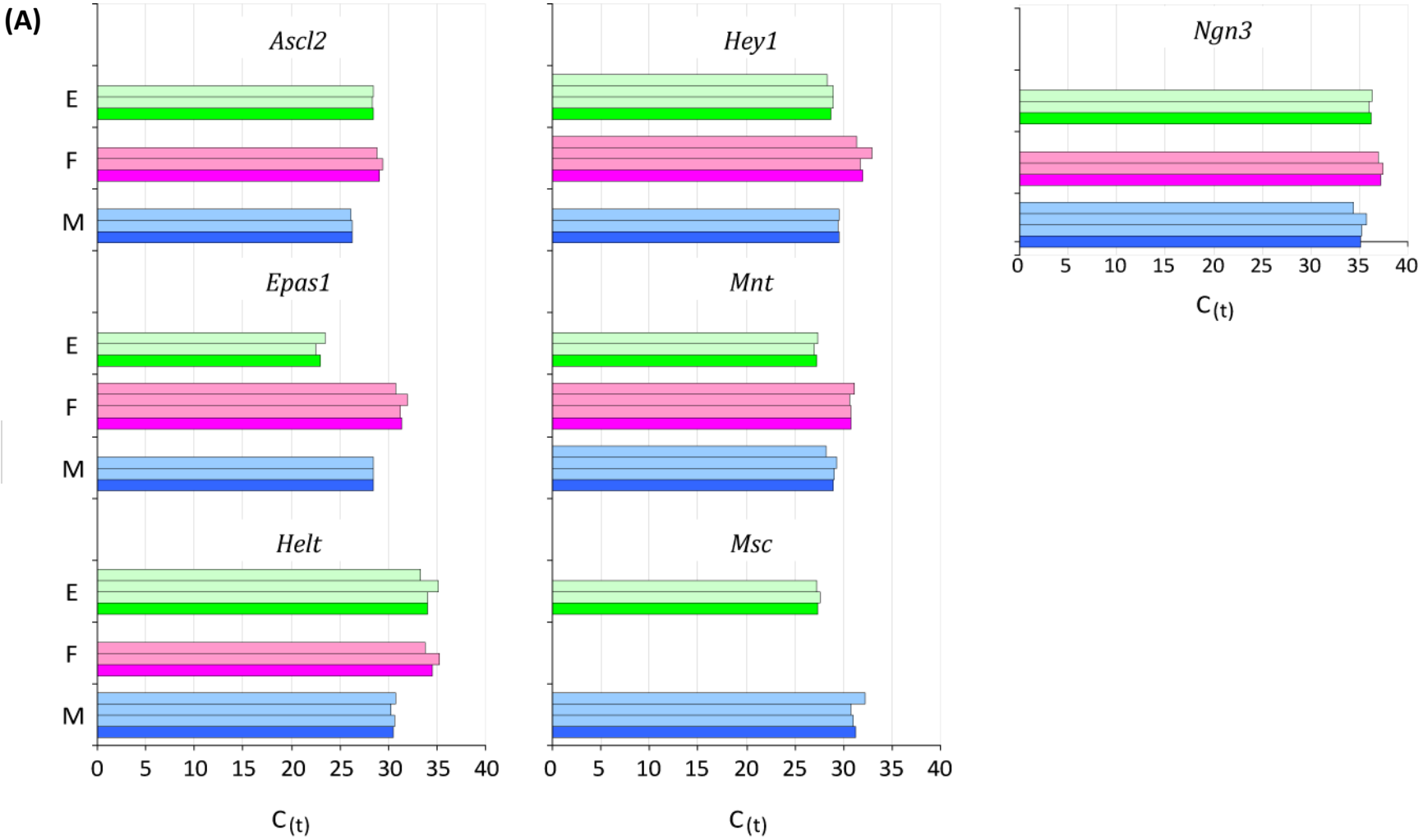
(A)
Ascl2
Hey1
Ngn3
Epas1
Mnt
Helt
Msc
E
F
M
0 5 10 15 20 25 30 35 40
C(t)

**Figure 3.3.3**

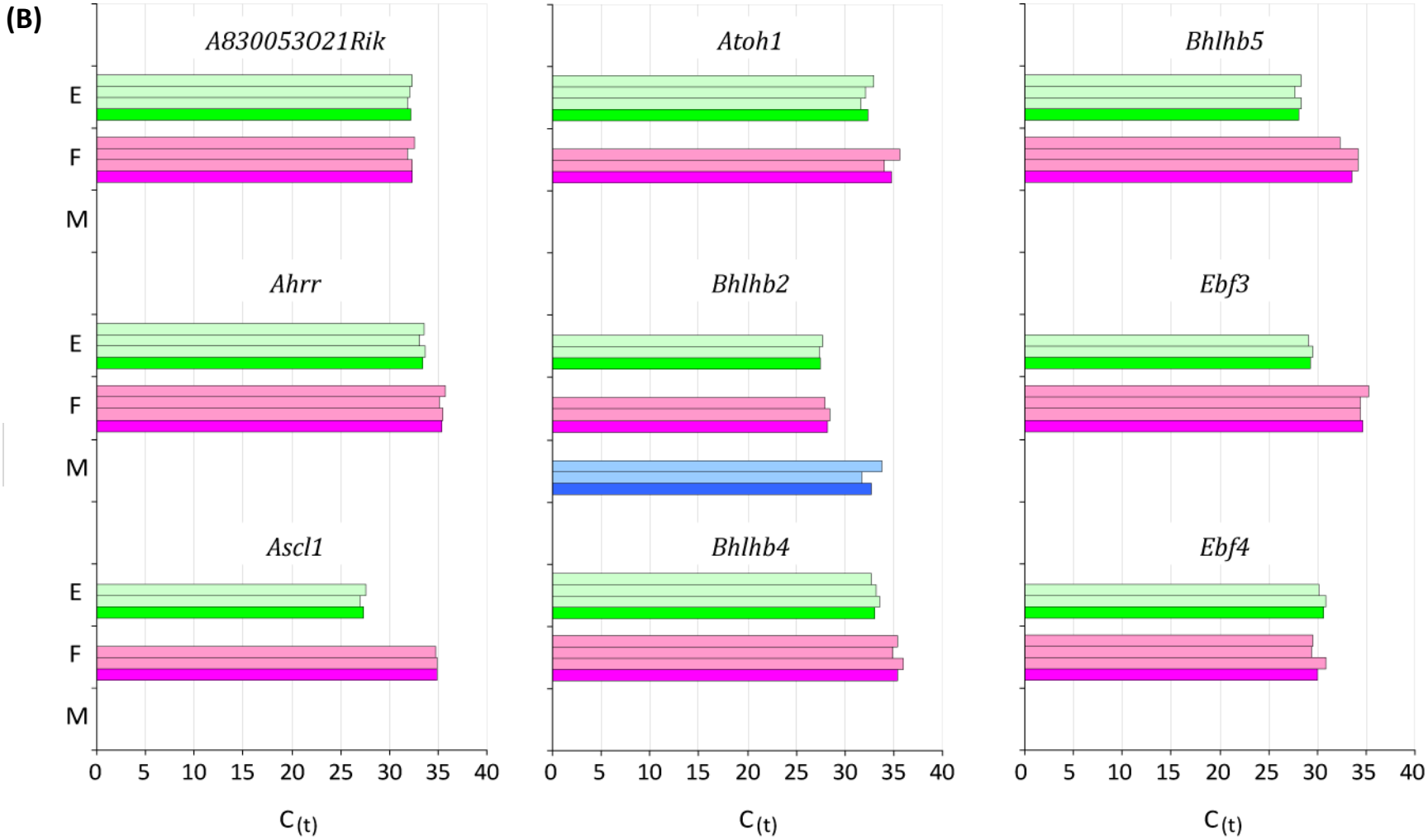
(B)
A830053O21Rik
Atoh1
Bhlhb5
Ahrr
Bhlhb2
Ebf3
Ascl1
Bhlhb4
Ebf4
E
F
M
0 5 10 15 20 25 30 35 40
C(t)

Figure 3.3.3

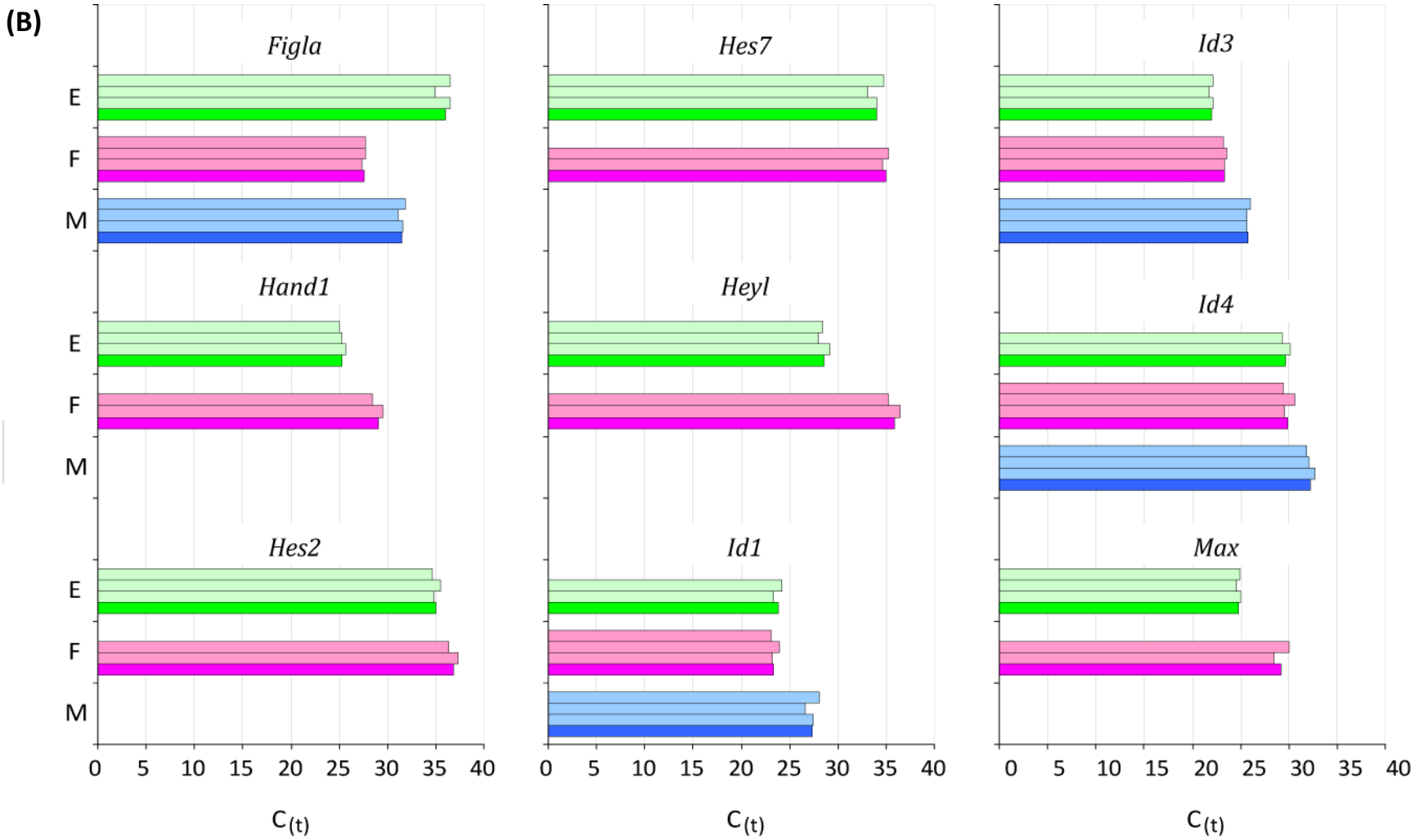
(B)
Figla
Hes7
Id3
Hand1
Heyl
Id4
Hes2
Id1
Max
E
F
M
0 5 10 15 20 25 30 35 40
C(t)

**Figure 3.3.3**

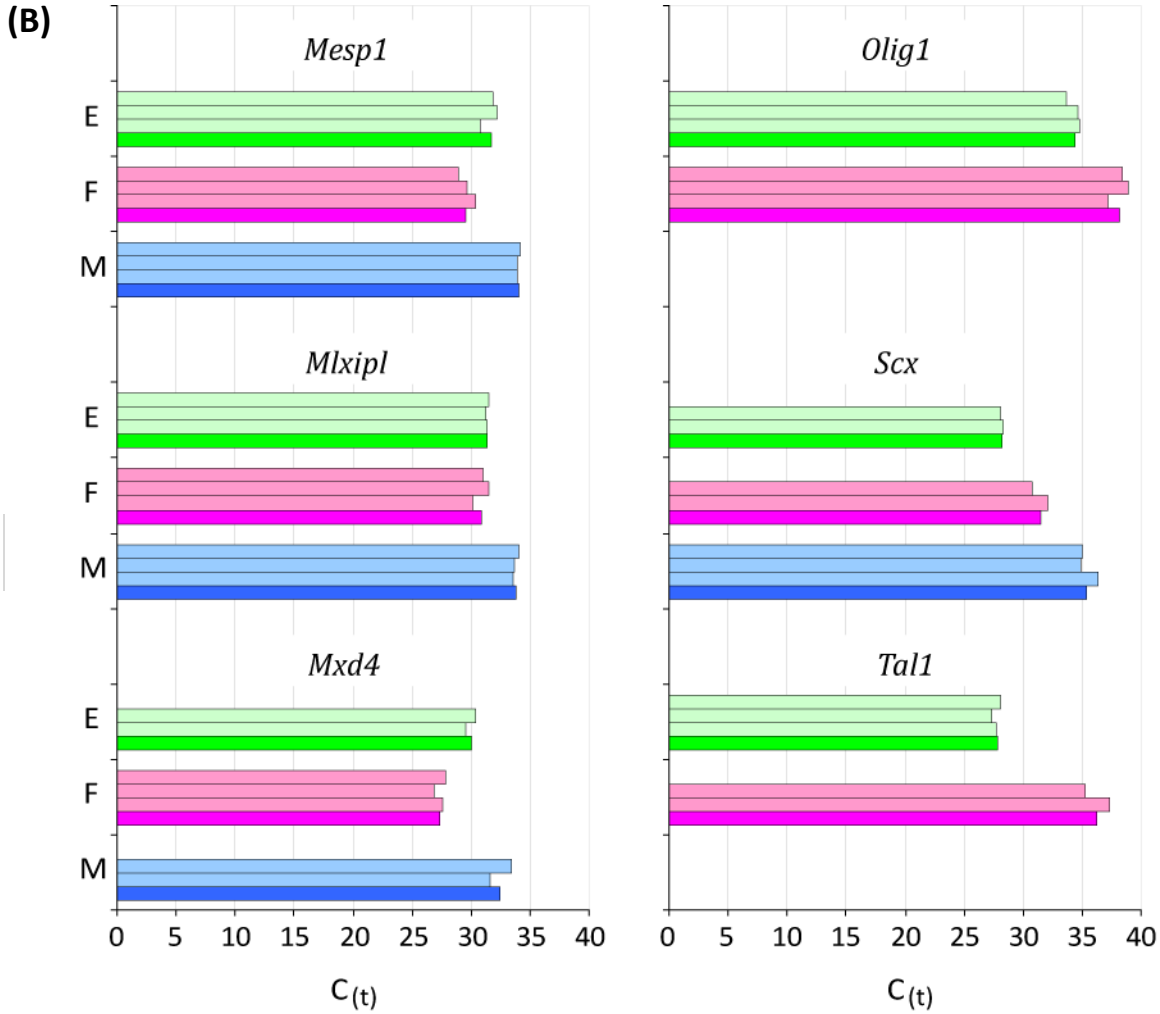


**Figure 3.3.3. bHLH Genes with 2.0 cycles or Greater Sex-specific Difference in E13.5 GC cDNA**. RtPCR reactions were carried out as explained in the legend for Figure 3.3.2 and in the text. $C_{(t)}$s for concurring reactions are shown for male GC cDNA (light blue bars), female GC cDNA (light pink bars) and positive control cDNA (light green bars) along with the mean $C_{(t)}$s of the concurring reactions (bars in corresponding colours except dark), for the 7 genes with a lower mean $C_{(t)}$ in male GC cDNA, (A), and the 25 genes with a lower mean $C_{(t)}$ in female GC cDNA, (B). "M" = male GC cDNA reactions, "F" = female GC cDNA reactions and "E" = Embryo (positive control) cDNA reactions.

For the 32 remaining bHLH genes, mean $C_{(t)}$s for the male and female GC cDNAs were 2 or more cycles different from each other. Figures 3.3.3 and 3.3.4 display the results for these genes.

Interestingly, 25 out of 32 of the genes with a 2.0 cycles or greater sex-specific mean $C_{(t)}$ difference had a lower mean $C_{(t)}$ in female GC cDNA compared to male GC cDNA, and therefore are potentially enriched in female GC cDNA. Furthermore, no amplification was detected at all in male GC cDNA for 15 of these 25. Conversely, 7 genes had a lower mean $C_{(t)}$ in male GC cDNA, and no amplification detected in female GC cDNA for only one of these (*Msc*). Therefore, potentially many more bHLH genes are enriched in female GC cDNA compared to male GC cDNA. This is interesting because most sex-specific expression screens in embryonic genital ridges find considerably more genes enriched in male genital ridges (McClive et al., 2003).

26 of these 32 genes were assessed quantitatively in the second part of the screen, whereas the remaining 6 (*Ascl1*, *Bhlhb5*, *Ebf3*, *Heyl*, *Tal1* and *Tcf21*) were not. Although these 6 genes showed a sex-specific mean $C_{(t)}$ difference of 2.0 cycles or greater, the lower mean $C_{(t)}$ of the GC cDNAs was also at least 5 cycles higher (i.e. occurred at least 5 cycles later) than the mean $C_{(t)}$ of the positive control cDNA. This $C_{(t)}$ difference of at least 5 cycles make these genes less interesting candidates for several reasons. Firstly, if the detected transcripts originate from GCs, rather than contaminating somatic cells, then the amount of transcript in the GCs is potentially very low. Low amounts of transcript in the GCs make accurate quantification more problematic (especially here where GC cDNA was scarce) and could indicate a lack of significant sex-specific function in GCs. Alternatively, this low-level amplification could originate from somatic cells transcripts contaminating the GC preparations, and therefore these genes are negligible for the main aim of this screen. It must be remembered that one or more of these genes might still have important sex-specific functions specifically in GCs. And, more likely, it is also possible that some of these genes are enriched sex-specifically in E13.5 gonads. However, due to the large

number of potentials derived from the first part of the screen, an astute decision was made to concentrate on the more easily detectable genes.

*Epas1* is another gene having a greater than 2.0 cycle sex-specific difference in mean $C_{(t)}$, but with a very late mean $C_{(t)}$, so would ordinarily be removed from quantitative analysis in the second part of the screen. However, *Epas1* was previously shown to be expressed in E15.5 testis, but in somatic cells of the interstitium rather than in the testis cords where the GCs are located (Tian et al., 1998). As such, the lower relative mean $C_{(t)}$ observed with male cDNA compared to female cDNA is suspected to originate from transcripts of contaminating somatic cells. It was therefore decided to include *Epas1* in the second part of the screen, in order to observe how such a gene might behave in this analysis.

*Id2* was also specifically chosen for accurate quantification in the second part of the screen, even though the sex-specific mean $C_{(t)}$ difference was less than 2 cycles. *Id2* was included because the closely related genes *Id1*, *Id3* and *Id4* did show differences larger than 2.0 cycles in mean $C_{(t)}$ between male and female GC cDNA.

# 3.4. bHLH Screen Part 2

## 3.4.1. cDNA Normalisation

This section describes the strategies employed to check and normalise the GC cDNAs for use in the second part bHLH expression screen. The second part of the screen accurately quantified the relative levels of the potentially-sex-enriched bHLH genes in male versus female GC cDNA. The GC cDNAs were not diluted to equivalence for these experiments. Instead, normalisation was accomplished after analysis using the quantified relative male:female *Gapdh* or *Tuba1a* levels, which were analysed and calculated independently for each experiment, along with the bHLH genes.

Relative male:female levels for each gene were quantified using a standard curve consisting of 5 concentrations of standard cDNA, and were then normalised using the relative male:female levels of *Gapdh* or *Tuba1a*, which were measured in identical fashion. Therefore, the results of the second part of the screen are normalised to *Gapdh* or *Tuba1a*. The *Tuba1a*-normalised data is shown in the following section, section 3.4.2. Figure 3.4.1 shows a representative example of *Tuba1a* quantification data for an experiment from the second part of the screen.

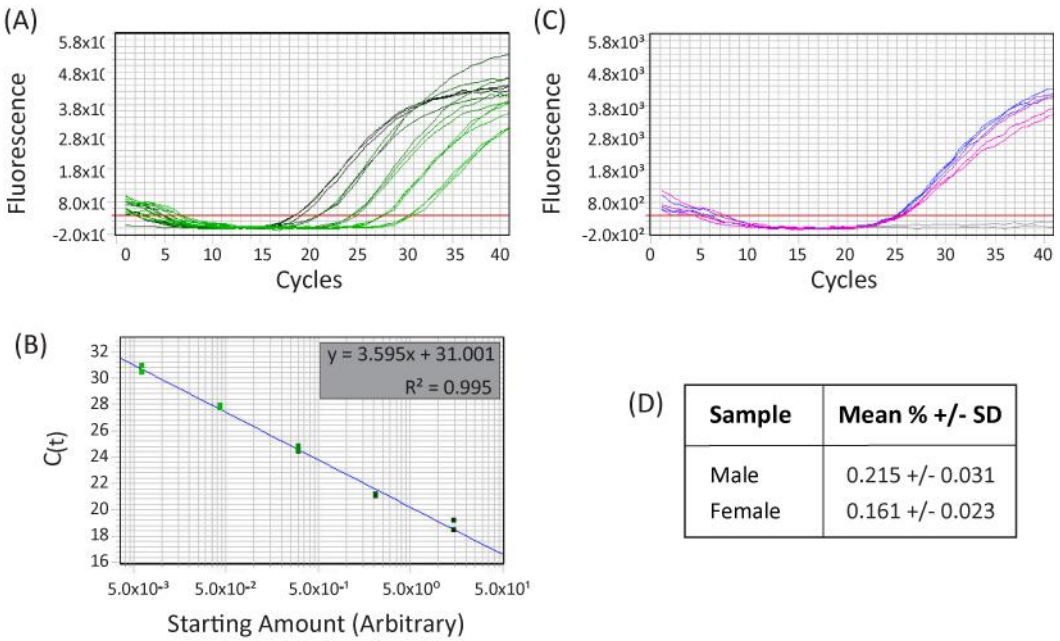


(D)

| Sample | Mean % +/- SD |
|---|---|
| Male | 0.215 +/- 0.031 |
| Female | 0.161 +/- 0.023 |

**Figure 3.4.1. *α-tubulin* (*Tuba1a*) Expression Analysis in E13.5 GC cDNAs for the 2nd Part of the Screen.** Relative *Tuba1a* levels in male and female GC cDNA were measured by RtPCR using a standard curve, (B), generated using 5 concentrations of standard cDNA, (A). Triplicate male (blue traces) and female (pink traces) were analysed in parallel, along with duplicate negative controls, (C), and the percentage of starting cDNA relative to the standard cDNA recorded and averaged ("Mean %"), (D). This data was then used to normalise the relative bHLH gene levels for genes measured in the same experiment (Section 3.4.2).

## 3.4.2. bHLH Screen Part 2 Data

The results of the first part of the screen identified 32 genes with 2.0 cycles or greater sex-specific difference in mean $C_{(t)}$ in E13.5 GC cDNA. This second part of the screen aimed to accurately quantify the differences of 26 of those genes, along with Id2, by Quantitative RtPCR. The remaining 6 genes were not analysed in this part of the screen due to their high $C_{(t)}$ values compared to positive control cDNA. The primer sets used for this analysis are listed in appendix iv and were designed using the Roche UPL Assay Designer (Universal ProbeLibrary [online]. Available from: http://www.roche-applied-science.com/sis/rtpcr/upl/ezhome.html [Accessed 04/03/2008]). All primers were manufactured by Sigma and the sequences were checked against the mRNA sequence(s) of the relevant genes obtained from Ensembl (Ensembl Genome Browser [online], Release 47. Available from: http://www.ensembl.org/index.html [Accessed 15/11/2007 - 04/03/2008]) to ensure that they targeted the correct sequences. The data was normalised to both *Tuba1a* and *Gapdh*. However, the data shown in the tables and figures in this section are normalised to *Tuba1a*, which differs by only up to 25% compared to the *Gapdh*-normalised data (shown in appendix vi). Therefore, statistical significance was retained across both sets of normalised data, and the analysis below does not differentiate between them, except where specified.

A total of 15 genes were found to be significantly enriched sex-specifically – 4 (*Epas1*, *Helt*, *Mnt* and *Ngn3*) male-enriched, and 11 female-enriched (*A830053O21Rik*, *Bhlhb2*, *Ebf4*, *Figla*, *Id1*, *Id2*, *Id3*, *Mesp1*, *Mlxipl*, *Mxd4* and *Scx*) - in E13.5 GC cDNA (Tables 3.4.1 and 3.4.2, and Figures 3.4.2 and 3.4.3). A further 7 genes – one male-specific (*Msc*) and 6 female-specific (*Ahrr*, *Atoh1*, *Bhlhb4*, *Hand1*, *Hes2* and *Hes7*) - were detected sex-specifically, with no amplification at all detected in the other sex (Table 3.4.3). For all of these genes except *A830053O21Rik* and *Hes2*, the fact that statistically-significant fold enrichments or sex-specific amplifications were replicated on separate biological samples

makes these genes very good candidates for sex-specific expression in E13.5 GCs. The 5 remaining genes (*Ascl2*, *Hey1*, *Id4*, *Max* and *Olig1*) showed negligible, non-significant and/or non-replicated sex-specific differences (Table 3.4.4).

In addition to the standards consisting of serially-diluted positive control cDNA, (mixed embryonic tissue cDNA for all except *Figla*, for which E15.5 female genital ridge cDNA was used), 9 reactions per gene were setup and analysed: 3 sets of triplicate samples containing male GC cDNA, female GC cDNA or $dH_2O$. Each set of triplicate samples consisted of 3 technical replicates containing an aliquot of the same cDNA sample. The data from each experiment was used only if all three negative control reactions failed to show meaningful amounts of fluorescence. The data from the standards was used to generate a standard curve, which was used to calculate the relative starting amounts of bHLH transcript per sample. Reactions were run out on agarose gels to ensure that only one product was generated, the length of which corresponded to the gene under study.

The reactions in this second part of the screen were only excluded if their overall reaction kinetics were not sigmoidal in shape, as would be expected of a normal PCR reaction. 4 reactions were excluded for this reason (one each from *Helt*, *Ngn3*, *Id1* and *Id4*). The assumed cause of these abnormal reactions kinetics are unwanted contaminations in the reaction or some other anomalous phenomenon or technical error, and as such do not represent normal variations in PCR reactions. In the first part of the screen, a replicate was excluded if it disagreed from the other 2 replicates by a certain amount. This approach is appropriate for an initial screening for potential target genes, but is inappropriate for quantitative measurement of expression levels. Thus all replicates were included regardless of how much they disagreed. A number of reactions were repeated with optimisations to reduce variation between replicates.

| Gene | Total ♂ Reps. | Total ♀ Reps. | Fold Enrichment (♂/♀) | |
|---|---|---|---|---|
| | | | Biological Rep. 1 | Biological Rep. 2 |
| ***Epas1*** | 6 | 6 | 3.5 +/- 0.6 (**) | 5.2 +/- 0.4 (***) |
| ***Helt*** | 6 | 5 | 3.3 +/- 1.1 (**) | 3.8 +/- 0.4 (**) |
| ***Mnt*** | 6 | 6 | 2.6 +/- 0.4 (**) | 3.8 +/- 0.8 (**) |
| ***Ngn3*** | 6 | 5 | 11.8 +/- 4.9 (**) | 5.4 +/- 1.5 (*) |

**Table 3.4.1. bHLH Screen Part 2: Male-Enriched Genes (normalised to *Tuba1a*).** Each of the 2 biological replicate consisted of triplicate RtPCR reactions containing male or female GC cDNA. The total number of technical replicates across both biological replicates is shown ("Total ♂/♀ Reps."). In parallel, relative *Tuba1a* levels were also measured and used to normalise the relative bHLH levels, resulting in the mean fold-enrichments shown. The "+/-" values shown here are the standard errors of the calculated and normalised means, which incorporates errors from both the bHLH and *Tuba1a* reactions by error propagation. Statistical significances were calculated using unpaired 2-tailed t-tests and are displayed by bracketed asterisks ("ns" = not significant, "*" = P<0.05, "**" = P<0.005, "***" = P<0.0005).

| Gene | Total ♂ Reps. | Total ♀ Reps. | Fold Enrichment (♀/♂) | |
|---|---|---|---|---|
| | | | Biological Rep. 1 | Biological Rep. 2 |
| ***A830053O21Rik*** | 3 | 4 | 58.5 +/- 4.1 (***) | - |
| ***Bhlhb2*** | 6 | 6 | 16.5 +/- 3.8 (**) | 14.4 +/- 8.6 (*) |
| ***Ebf4*** | 6 | 6 | 123.0 +/- 51.5 (*) | 107.4 +/- 13.0 (***) |
| ***Figla*** | 6 | 6 | 84.1 +/- 21.8 (***) | 79.3 +/- 12.9 (***) |
| ***Id1*** | 6 | 5 | 42.0 +/- 6.2 (***) | 39.0 +/- 3.0 (***) |
| ***Id2*** | 6 | 6 | 32.0 +/- 10.9 (*) | 34.6 +/- 3.5 (***) |
| ***Id3*** | 6 | 6 | 18.4 +/- 6.8 (*) | 13.4 +/- 1.6 (**) |
| ***Mesp1*** | 6 | 6 | 15.2 +/- 4.0 (*) | 10.7 +/- 1.4 (**) |
| ***Mlxipl*** | 6 | 6 | 12.9 +/- 4.5 (**) | 26.4 +/- 10.4 (*) |
| ***Mxd4*** | 6 | 6 | 6.7 +/- 0.4 (***) | 3.9 +/- 0.5 (**) |
| ***Scx*** | 6 | 6 | 31.0 +/- 9.4 (*) | 32.6 +/- 12.4 (**) |

**Table 3.4.2. bHLH Screen Part 2: Female-Enriched Genes (normalised to *Tuba1a*).** See legend for Table 3.4.1. 2 biological replicates were carried out for all genes except *A830053O21Rik*, for which only one was carried out.

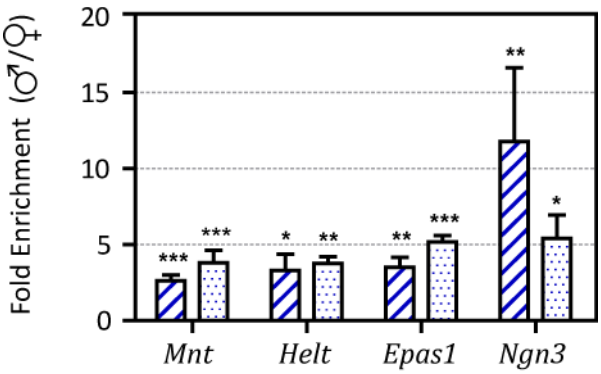


**Figure 3.4.2. Male-enriched bHLH Genes (normalised to *Tuba1a*).** The data shown in Table 3.4.1 represented as a bar chart. The mean ♂/ ♀ fold enrichments for both biological replicate 1 (blue diagonal hatched bars) and biological replicate 2 (blue dotted bars) are shown. Standard Errors are shown as solid lines and statistical significance as asterisks above each bar.

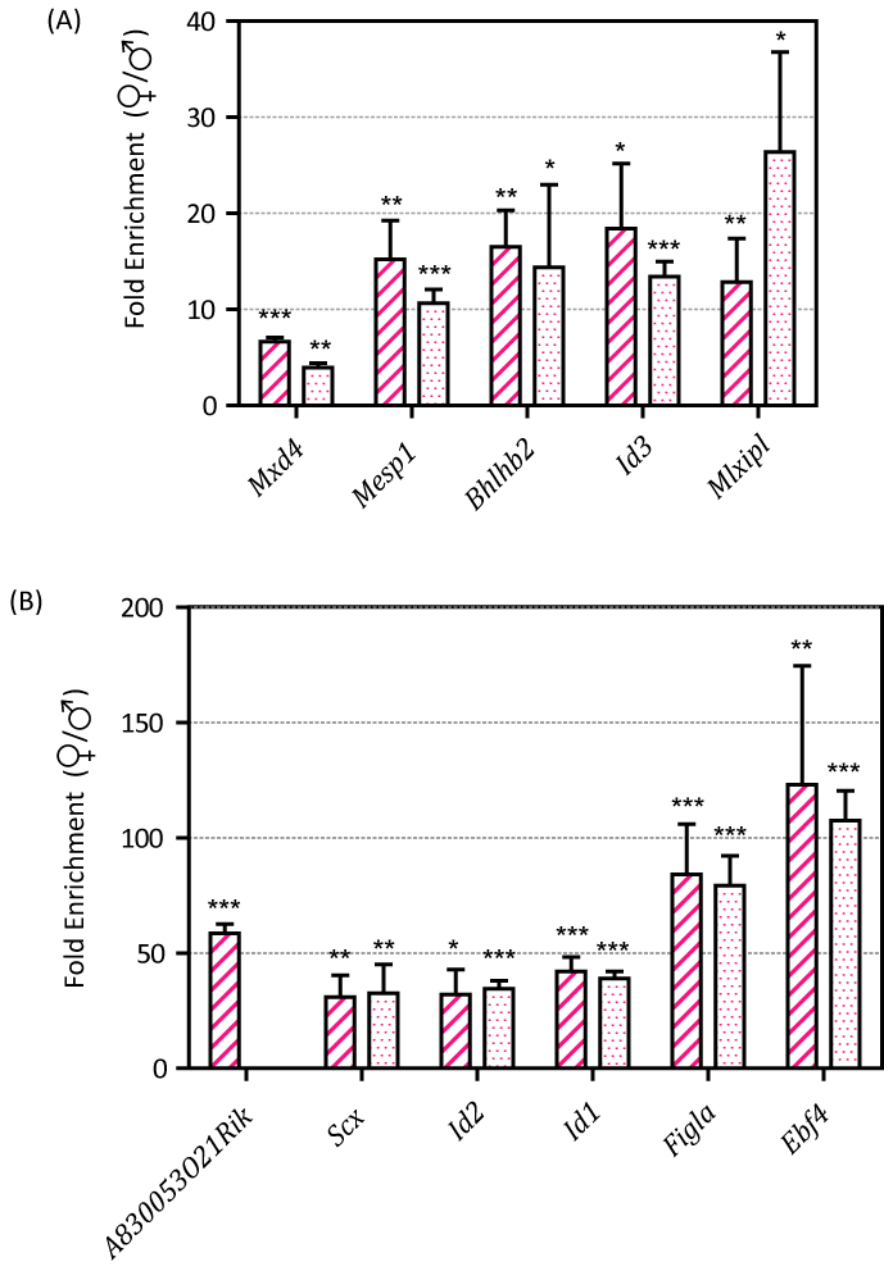


**Figure 3.4.3. Female-enriched bHLH Genes (normalised to *Tuba1a*).** The data shown in Table 3.4.2 represented as a bar chart. The mean ♀/♂ fold enrichments for both biological replicate 1 (pink diagonal hatched bars) and biological replicate 2 (pink dotted bars) are shown. Standard Errors are shown as solid lines and statistical significance as asterisks above each bar. For clarity, genes with less than 30-fold enrichment are shown in (A), and those with greater than 30-fold enrichment are shown in (B).

As can be seen in Tables 3.4.1 and 3.4.2 and Figures 3.4.2 and 3.4.3, the 2 biological replicates of some of the sex-specifically-enriched genes differ greatly, and it was decided to keep the data for the biological replicates separate because of this. These biological replicate variations are most notable for *Ngn3*, *Mlxipl*, and *Mxd4*. This puts some doubt upon the precision of the fold-enrichments for these genes. Despite the difference in magnitude for the fold-enrichments between the biological replicates, statistical significance is retained. However, a third biological replicate for these genes would more accurately ascertain the true magnitude of the sex-specific enrichments.

There are a number of possible causes of these variations between biological replicates. It must be remembered that the purified GC preparations did contain a fraction of contaminating somatic cells, and the proportion of contaminating cells varied between different GC preparations by as much as 1-3%. If the enrichment seen for these genes originated as high expression in one population of the contaminating somatic fraction as opposed to expression in GCs, then variations in the proportion of the expressing cell populations in the contaminating somatic fraction could drastically alter the overall enrichment seen. For example, *Epas1* expression is enriched in male GC cDNA over female GC cDNA in the second part of this screen, although to differing degrees in the two biological replicates (3.52-fold and 5.18-fold for biological replicate 1 and 2, respectively). Somatic cells of the E15.5 mouse testis were previously shown to express *Epas1* (Tian et al., 1998). If the expression seen in this screen originates solely in somatic cells then an increase in the contaminating population from 1% to 2% could cause as much as a two-fold difference between the two biological replicates. In the reverse situation, a contaminating population of somatic cells in one GC cDNA that express the gene in question highly could mask or reduce an enrichment in the cDNA of the opposite sex that in fact does originate from GC expression. These explanations would not hold true for GC-specific genes, and *Ngn3* is a likely male-GC-specific candidate gene (Yoshida et al., 2004).

Another possible explanation for the observed differences in biological replicates of the same gene could be that one replicate is invalid due to anomalous replicates. Replicates were included in the analysis regardless of their variation from each other. For the most part experiments were repeated if the replicates varied too greatly. However, this was not possible for all genes, owing to the large number of genes analysed and the scarcity of GC cDNA. This can be seen in the first biological replicate of *Ngn3*. The magnitude of male/female enrichment may be overestimated in this biological replicate because of the large variations in the female replicates, the lowest of which had a value of 0.06, much lower than the other 2 female replicates that had values of 0.24 and 0.36. Once again, further biological replicates would help to more precisely measure the true magnitude of the sex-specific enrichments for these genes.

Table 3.4.3 shows those genes that were detected in one sex only. This sex-specific amplification was observed over two biological replicates for male-specific *Msc*, and for female-specific *Ahrr*, *Atoh1*, *Bhlhb4*, *Hand1* and Hes7 and over one replicate for female-specific *Hes2*. For the sex these genes were detected in, the reactions of both biological replicates amplified robustly and, apart from the second biological replicate of *Hes7*, all within 2.0 cycles of one another. Conversely, all samples in the other sex completely failed to amplify before the end of the assay, and this was not due to poor quality male cDNA, as robust *Gapdh* and *Tuba1a* expression was detected in those cDNAs. For *Ahrr* and *Hes2*, the female samples amplified quite late (~36 cycles), and it is possible that further optimisation of the RtPCR assays would result in robust detection in the male GC cDNA. Therefore, *Hes2* and *Ahrr* are at the very least female-specifically enriched, while *Msc*, *Atoh1*, *Bhlhb4*, *Hand1* and *Hes7* are either very sex-specifically enriched or expressed sex-specifically, and are very interesting candidates for sex-specific functions in embryonic GCs.

| Gene | Total ♂ Reps. | Total ♀ Reps. | No. of Biological Reps. | Sex Detected In |
|---|---|---|---|---|
| ***Msc*** | 6 | 6 | 2 | ♂ |
| ***Ahrr*** | 8 | 8 | 2 | ♀ |
| ***Atoh1*** | 6 | 6 | 2 | ♀ |
| ***Bhlhb4*** | 6 | 6 | 2 | ♀ |
| ***Hand1*** | 6 | 6 | 2 | ♀ |
| ***Hes7*** | 6 | 6 | 2 | ♀ |
| ***Hes2*** | 4 | 4 | 1 | ♀ |

**Table 3.4.3. bHLH Screen Part 2: Genes Detected Sex-Specifically.** RtPCR was carried out as described in the legend for Table 3.4.1. The number of biological replicates carried out ("No. of Biological Reps.") and the number of technical replicates over both biological replicates ("Total ♂/♀ Reps.") is shown for each gene.

| Gene | Total ♂ Reps. | Total ♀ Reps. | Fold Enrichment (Male/Female) | |
|---|---|---|---|---|
| | | | Biological Rep. 1 | Biological Rep. 2 |
| ***Ascl2*** | 6 | 6 | 0.5 +/- 0.1 | 0.8 +/- 0.3 |
| ***Hey1*** | 6 | 6 | 1. 8 +/- 0.2 | 2.0 +/- 0.2 |
| ***Id4*** | 5 | 6 | 0.3 +/- 0.1 | 0.9 +/- 0.0 |
| ***Max*** | 6 | 6 | 1.0 +/- 0.1 | 1.4 +/- 0.1 |
| ***Olig1*** | 3 | 3 | 0.7 +/- 0.1 | - |

**Table 3.4.4. bHLH Screen Part 2: Genes With Negligible or No Sex-Specific Enrichment.** RtPCR was carried out as described in the legend for Table 3.4.1. The calculated and normalised mean enrichments as well as the standard error ("+/-") is shown for each biological replicate, and the total number of technical replicates over both biological replicates ("Total ♂/♀ Reps.") is shown for each gene.

For the remaining 5 genes, no convincing sex-specific enrichments that were sustained over 2 biological replicates were observed (Table 3.4.4). The lack of robust sex-specific difference was very surprising for *Max*. In the first part of the screen, *Max* transcripts were completely undetected in all triplicates of male GC cDNA (Figure 3.3.3), suggesting female-GC-specific expression. To ensure this disparity was not caused by the different sets of primers used in the 2 parts

of the screen, a quantitative RtPCR using the primers from the first part of the screen was carried out, and this resulted in similar normalised amounts of correctly-sized product in both male and female GC cDNA (data not shown). Additionally, a semi-quantitative PCR using a third primer set detected roughly equal amounts of both splice forms of *Max* (data not shown). Therefore, it is likely that the lack of amplification in the male GC cDNA reactions in the first part of the screen was anomalous, and *Max* is not enriched sex-specifically in E13.5 GC cDNA.

The data for *Id4* and *Ascl2*, do suggest that these genes may be enriched in female GCs at E13.5. However, more replicates are required to arrive at definite conclusions for these genes. *Hey1* is consistently enriched male-specifically in this screen, but these enrichments were lower than 2-fold.

Why were the sex-specific differences seen in the first part of the screen not reliably replicated in the second part of the screen for *Ascl2*, *Id4*, *Max* and *Olig1*? The situation with Max suggests that the first set of data for *Max* is incorrect, and for the remaining 3 genes, there may be sex-specific differences, but these are probably not large or robust enough to result in a reliable result from more precise quantitative assays, as in the second part of the screen. As such, these 5 genes (including *Hey1*) are not as promising candidate sex-specific genes as the other 22 genes.

In summary, 20 bHLH genes were found to be either sex-specifically enriched or sex-specifically expressed in E13.5 GC cDNA over 2 biological replicates, with another 2 bHLH genes over one biological replicate. However, as suggested by *Epas1*, the enrichments may or may not be due to GC-specific expression The remaining sections of this chapter aim to confirm GC-specific and sex-specific expression for the female-enriched *Id1*, *Id2* and *Id3* and for the male-enriched *Mnt*. hint at

## 3.5. Verification of Sex-Specific Germ Cell Expression of *Id* and *Mnt*

### 3.5.1. Characterisation of cDNA Libraries Prepared From Single E13.5 Gonadal Cells

The technique used was adapted from Brady and Iscove (Brady and Iscove, 1993). Only one round, rather than 2 rounds as stated in the original protocol, of PCR was carried out in the current study to amplify the tailed cDNAs non-specifically and this change to the original protocol was made to enable subsequent expression analysis by gene-specific PCR. This adaption may have changed the representivity of the final cDNA libraries compared to the original protocol. Briefly, single cells were picked, their PolyA$^+$ mRNA reverse transcribed and the resultant cDNA non-specifically amplified to generate a cDNA library of the original cell that was then analysed for the presence of multiple target genes. Brady and Iscove suggest, and others have employed (Saitou et al., 2002), the use of Southern Hybridisation, while others have used quantitative methods (Yabuta et al., 2006), to assess the presence of genes of interest in the single-cell cDNA libraries. In this study end-point PCR was used to assess gene expression using the amplified cDNA libraries as substrate.

Male and Female samples were collected in 3 separate biological experiments per sex, with controls included in all biological replicates. For the male analysis, 38 RT$^+$/cell$^+$ libraries, which had a cell and reverse transcriptase (RT) added into them, 8 no-RT controls (i.e. had a cell but no RT added to them) and 11 no-cell controls (i.e. had media instead of a cell, and RT, added to them) were generated. For the female analysis, 49 RT$^+$ cell$^+$ libraries, 9 no-RT controls and 8 no-cell controls were generated. To increase the chance of only one cell being collected into each sample, the cell was collected first into a fresh drop of media, and then a fresh glass pipette used to transfer the cell into the sample tube.

Exactly the same procedure was used for no-cell controls, except media instead of the cell was transferred into the tube for the second transfer.

The amplified cDNAs were first tested for *Glyceraldehyde 3-phosphate Dehydrogenase* (*Gapdh*) expression by PCR in order to determine which cDNA libraries had amplified properly and had detectable transcripts. All male and female no-RT and no-cell controls were negative for *Gapdh* expression, and cell-type-specific expression as described below, with the primers and conditions used, indicating that products detected in the samples are likely dependent upon RT and represent mRNA expression of the cells added. The absence of detected *Gapdh* expression in the no-cell controls implies that product detected in the $RT^+/cell^+$ libraries originates from RT expression of the added cell rather than from some contamination from the RT enzyme.

Of the 38 male $RT^+/cell^+$ libraries, 27 were positive and 11 were negative for *Gapdh* expression and of the 49 female $RT^+/cell^+$ libraries, 21 were positive and 28 negative for *Gapdh* expression. Presuming that a cell was successfully placed into each sample, then the fact that *Gapdh* was not detected in some libraries suggests that reverse transcription or amplification failed to amplify the mRNA from these single cells. Therefore, these libraries were not used in subsequent analyses.

Those libraries that tested positive for *Gapdh* were then tested, along with the control samples, for expression of markers to identify the cell type of each library (Figures 3.5.1 and 3.5.2 and Table 3.5.1). There are several bipotential cell lineages in the gonad, including GCs and at least 3 somatic cell lineages: supporting cells, steroidogenic cells and connective tissue cells (Swain and Lovell-Badge, 1999). *Dazl* (Seligman and Page, 1998) and *Stella* (Bowles et al., 2006) are GC-specific genes expressed by migratory and post-migratory GCs, including male and female E13.5 GCs. Therefore, analysis of *Dazl* and *Stella* expression was used to identify GC libraries. Primers against *Sox9* and *SF-1* were used in order to identify male somatic cells. *Sox9* expression is restricted to Sertoli cells (Sekido and Lovell-Badge, 2009), the supporting cells of the

testis, whereas *SF-1* is expressed by various somatic cell types in the testis shortly after sex determination (Hatano et al., 1994), including Sertoli cells, Leydig cells and peritubular myoid cells. Importantly, neither *Sox9* nor *SF-1* are expressed in GCs. *Gata4* and *SF-1*, which are also not expressed by GCs, were used for the identification of female somatic cell libraries. *SF-1* is expressed in multiple somatic cell lineages in the embryonic ovary (Hatano et al., 1994), including granulosa cells and theca cells, the supporting and steroidogenic cells, respectively, of the mouse ovary. *Gata4* is expressed only at low levels in embryonic mouse ovary but highly in various somatic cells in the adult ovary, including theca and granulosa cells (Heikinheimo et al., 1997). In this study, *Gata4* transcripts were detected in 4 out of 6 libraries testing negative for GC markers, indicating that *Gata4* is expressed in E13.5 female somatic cells at levels detectable by this single-cell PCR analysis.

2 technical replicates of the cell-type-specific marker analysis PCR were carried out, and the same result obtained for each. Assuming that only one cell was placed into each sample during the picking, each sample should test negative for both sets of markers or positive for either GC or somatic markers, but no sample should test positive for both somatic and GC markers.

| | **No. of Positive Libraries** | |
|---|---|---|
| | ♂ | ♀ |
| $GC^{-/-}/SOM^{-/-}$ | 4 | 1 |
| $GC^{+/+}/SOM^{-/-}$ | 18 | 9 |
| $GC^{+/-}/SOM^{-/-}$ | 0 | 6 |
| $GC^{-/-}/SOM^{+/+}$ | 2 | 1 |
| $GC^{-/-}/SOM^{+/-}$ | 3 | 3 |
| $GC^{+/-}/SOM^{+/+}$ | 0 | 1 |
| **TOTAL** | **27** | **21** |

**Table 3.5.1 Cell-type-Specific Expression Analysis of Single E13.5 Gonadal Cell cDNA Libraries.** Summary of data from Figures 3.5.1 and 3.5.2.

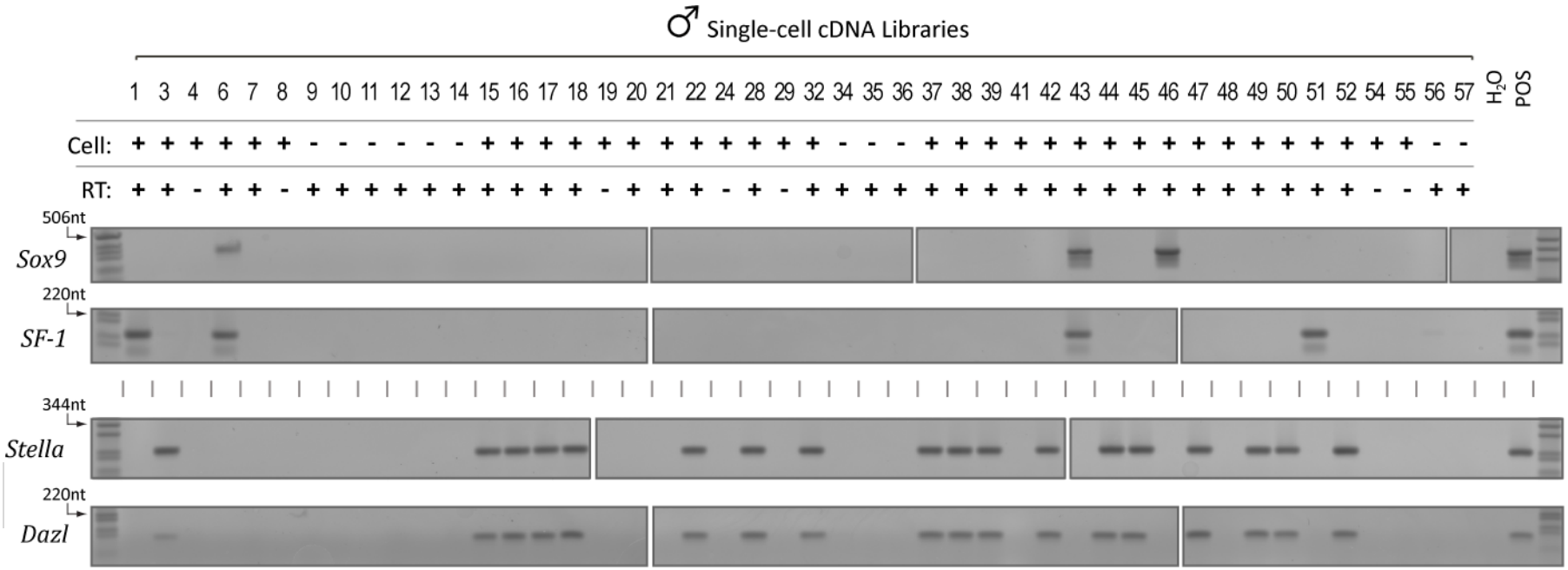




**Figure 3.5.1. Cell-type Specific PCR Analysis of Male *Gapdh*$^+$ Single-cell cDNA Libraries.** Single cells from E13.5 male gonads or blank media ("±Cell") were reverse transcribed ("±RT") and the cDNA amplified non-specifically to produce cDNA libraries. The libraries were produced in 3 separate experiments (Batch 1 = samples 1 to 14, Batch 2 = samples 15 to 36, Batch 3 = samples 37 to 57), each of which included actual samples (Cell$^+$/RT$^+$), no-cell controls (Cell$^-$/RT$^+$) and no-RT controls (Cell$^+$/RT$^-$). PCR was carried out on *Gapdh*$^+$ samples, no-RT controls and no-cell controls using primers to somatic markers (*Sox9* and *SF-1*) and GC markers (*Stella* and *Dazl*), along with a PCR negative control ("$H_2O$") and positive control ("POS") consisting of mixed E13.5 male and female gonad cDNA. For each marker analysed, all samples were run in the same PCR experiment, except for *Sox9*, for which the samples were run in 2 separate experiments (Experiment 1 = samples 1 to 36, Experiment 2 = sample 37 to 57). The products from each PCR experiment were run out on multiple agarose gels (as denoted in separate boxes) and the gels shown above are from one of 2 replicates per gene that both gave the same result. 1kb ladder (Invitrogen) was run alongside reactions and the arrows and numbers to the left of the gels indicate the size of the fragments in the 1kb ladder in nucleotides (nt).

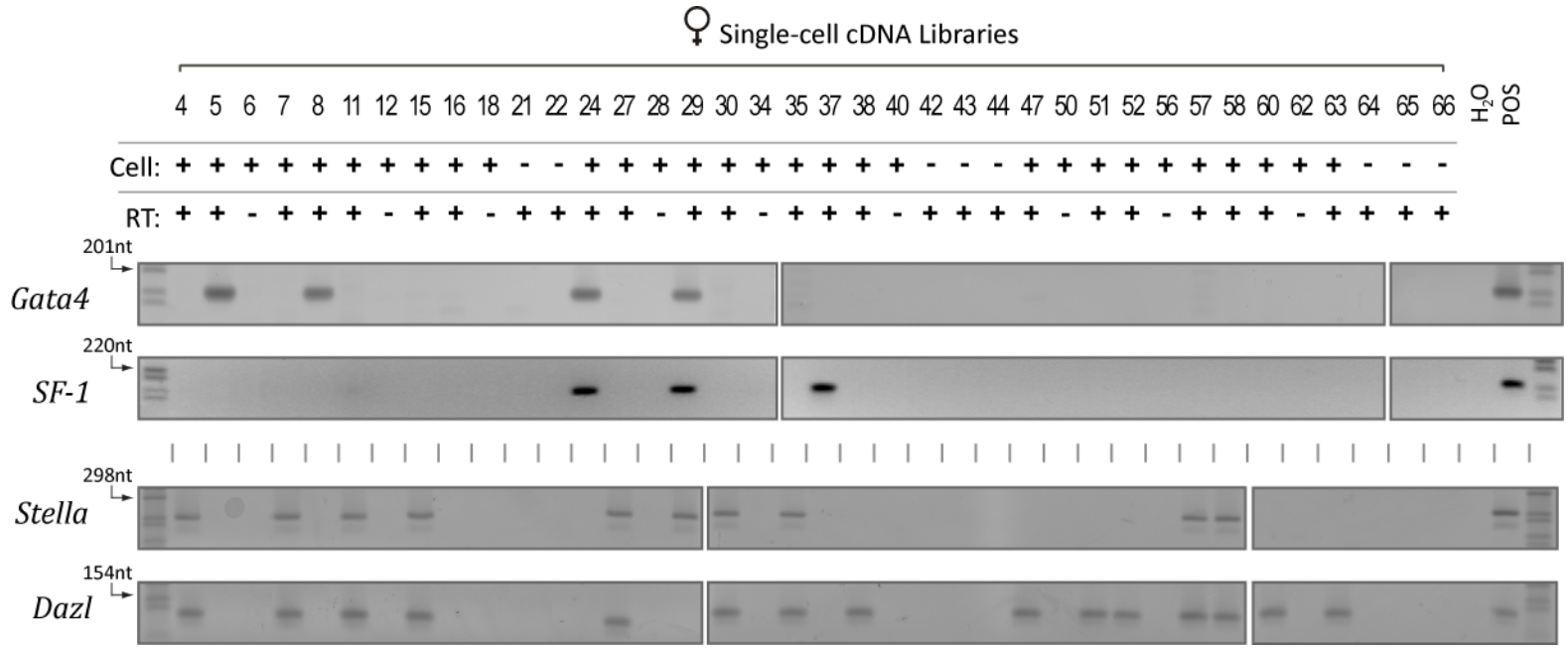


**Figure 3.5.2. Cell-type Specific PCR Analysis of Female *Gapdh*$^+$ Single-cell cDNA Libraries.** Single cells from E13.5 female gonads or blank media ("±Cell") were reverse transcribed ("±RT") and the cDNA amplified non-specifically to produce cDNA libraries. The libraries were produced in 3 separate experiments (Batch 1 = samples 1 to 22, Batch 2 = samples 23 to 44, Batch 3 = samples 45 to 66), each of which included actual samples (Cell$^+$/RT$^+$), no-cell controls (Cell$^-$/RT$^+$) and no-RT controls (Cell$^+$/RT$^-$). PCR was carried out on *Gapdh*$^+$ samples, no-RT controls and no-cell controls using primers to somatic markers (*Gata4* and *SF-1*) and GC markers (*Stella* and *Dazl*), along with a PCR negative control ("$H_2O$") and positive control ("POS") consisting of mixed E13.5 male and female gonad cDNA. For each marker analysed, all samples were run in the same PCR experiment. The products were run out on multiple agarose gels (as denoted in separate boxes) and the gels shown above are from one of 2 replicates per gene that both gave the same result. 1kb ladder (Invitrogen) was run alongside reactions and the arrows and numbers to the left of the gels indicate the size of the fragments in the 1kb ladder in nucleotides (nt).

Of the male libraries, 18 were positive for GC markers and negative for somatic cell markers, and were therefore male GC libraries. Of those 18, all were positive for both GC markers ($GC^{+/+}/SOM^{-/-}$). 5 other male libraries were somatic cell libraries because they were negative for GC markers and positive for somatic markers. Of the 5 male somatic cell libraries, 2 were positive for both somatic cell markers ($GC^{-/-}/SOM^{+/+}$) and the other 3 were positive for one somatic cell marker only ($GC^{-/-}/SOM^{+/-}$). The 3 *Sox9* positive male somatic cell libraries are likely to be Sertoli cells, because *Sox9* expression is restricted to Sertoli cells (Sekido and Lovell-Badge, 2009). 4 libraries were negative for both GC and somatic cell markers ($GC^{-/-}/SOM^{-/-}$), and these libraries may have been generated from male gonadal cell types other than GC, Leydig, Sertoli or peritubular myoid cells. Alternatively, the single-cell PCR procedure may not have been able to detect low level expression of cell-type-specific genes by GC, Leydig, Sertoli or peritubular myoid cells. Finally, none of the male samples were positive for both somatic cell and GC markers, suggesting that it is likely that only GCs, or somatic cells, but not both were added into each male sample.

Of the female libraries, 15 were positive for GC markers and negative for somatic cell markers, identifying these as female GC libraries. Of those 15, 9 were positive for both GC markers ($GC^{+/+}/SOM^{-/-}$) and 6 positive for only one GC marker ($GC^{+/-}/SOM^{-/-}$), which was *Dazl* in all 6 cases. Another 4 female samples were GC marker negative and somatic marker positive, identifying these as female somatic cell libraries. Of those 4, 1 was positive for both somatic markers ($GC^{-/-}/SOM^{+/+}$) and the other 3 were positive for one somatic marker only ($GC^{-/-}/SOM^{+/-}$). One female library, library 29, was positive for both somatic markers and one GC marker, which was *Dazl* ($GC^{+/-}/SOM^{+/+}$). The fact that none of the 19 male or female no-cell controls was positive for any gene tested suggests that it is unlikely multiple cells were added together into any one sample, including library 29. Therefore, the presence of somatic cell and GC markers in the female library 29 is likely due to cross-contamination after cell picking. 2 female libraries were negative for both GC and somatic markers ($GC^{-/-}/SOM^{-/-}$). The lack of cell-type-specific gene expression in these libraries might

be due to insufficient RT and/or amplification of those cells during the procedure, or because those cells do not express detectable levels of these genes, in which case they could be cells other than germ, granulosa or theca cells.

Only 9 of 15 female GC libraries were positive for both GC markers. The remaining 6 libraries were *Dazl*$^{+}$/*Stella*$^{-}$. The difference in detection between *Dazl* and *Stella* in the female libraries might be due to the fact that *Dazl* remains expressed in female GCs past E13.5/E14.5 (Seligman and Page, 1998), whereas *Stella* expression is downregulated at E13.5-E14.5 in female GCs (Sato et al., 2002; Yamaguchi et al., 2005) or might be due to differences in the efficiency of *Dazl*/*Stella* amplification during the protocol. The fact that 18/18 male GC libraries were positive for both GC markers suggests that the differences detected in female GC libraries may be the result of true differences in *Dazl* and *Stella* expression by E13.5 female GCs. A Fischer's exact statistical test result of 0.0045 indicates that this sex-specific difference is statistically significant. However, biological replicate variation was not tested here and might have resulted in this apparent 'sex-specific' difference, especially because 4 out of 6 of these *Dazl*$^{+}$/*Stella*$^{-}$ libraries were collected in biological replicate 2 while the other 2 were collected in biological replicate 3, with none collected in biological replicate 1.

18/27 (67%) male and 14/21 (67%) female libraries were GC libraries. This is high compared to the proportion of GCs identified in the total cell population during FACS (Chapter 4, Section 4.2.1), which was less than 5%, even when taking into account that mesonephric cells were removed before single cells were picked in these single cell assays. The reason that the proportion of GCs identified in the male (and female) libraries was so high was that there was a bias towards GC-like cells during the picking. Therefore, the proportion of GC compared to somatic cell libraries here does not represent the true proportions of these cells *in vivo*.

The 15 female GC libraries and 15 of the male GC libraries were analysed for expression of genes of interest in this Chapter and in Chapter 4 (Section 4.2.2).

## 3.5.2. Analysis of *Id1*, *Id2* and *Id3* Expression in Single E13.5 GC cDNA Libraries

The results from the bHLH screen indicate that a number of genes are enriched in a sex-specific manner in E13.5 GC cDNA. However, because there was 1-3% contaminating cells in the GC preparations (Figure 3.2.1), it is unclear whether this sex-specific enrichment originates from GC or contaminating somatic cell expression. In order to ascertain which gonadal cells might be expressing the genes, single-cell reverse transcription PCR was performed on individual gonadal cells. The analysis assessed the expression of *Id1*, *Id2* and *Id3*, which were sex-specifically enriched in female E13.5 GC cDNA. These were chosen for further confirmation because of their involvement in the cell cycle and are therefore might be involved in initiating meiosis in female GCs. The analysis suggests that *Id1* and *Id3* could be expressed female-specifically in E13.5 GCs. However, due to the low number of GCs analysed (15 per sex spread over 3 biological replicates), the results are only slightly significant and firm conclusions cannot be drawn.

cDNA libraries were generated from single E13.5 gonadal cells and analysed for GC and somatic cell markers to identify the cell type, as detailed in section 3.5.1. For each sex, 15 GC cDNA libraries, 3 no-RT control samples, 2 somatic cell libraries and 1 $dH_2O$ negative control, were analysed for *Id1*, *Id2* and *Id3* expression. At least one of the 15 GC libraries and one of the 3 no-RT controls originated from each of the 3 separate collection experiments.

The first 5 GC libraries of the 15 from each sex are shown in Figure 3.5.3 below, together with control samples. The results from all 15 GC libraries are shown in Figure 3.5.3B. These results were verified by a technical repeat of each PCR, which produced the same results.

(A)

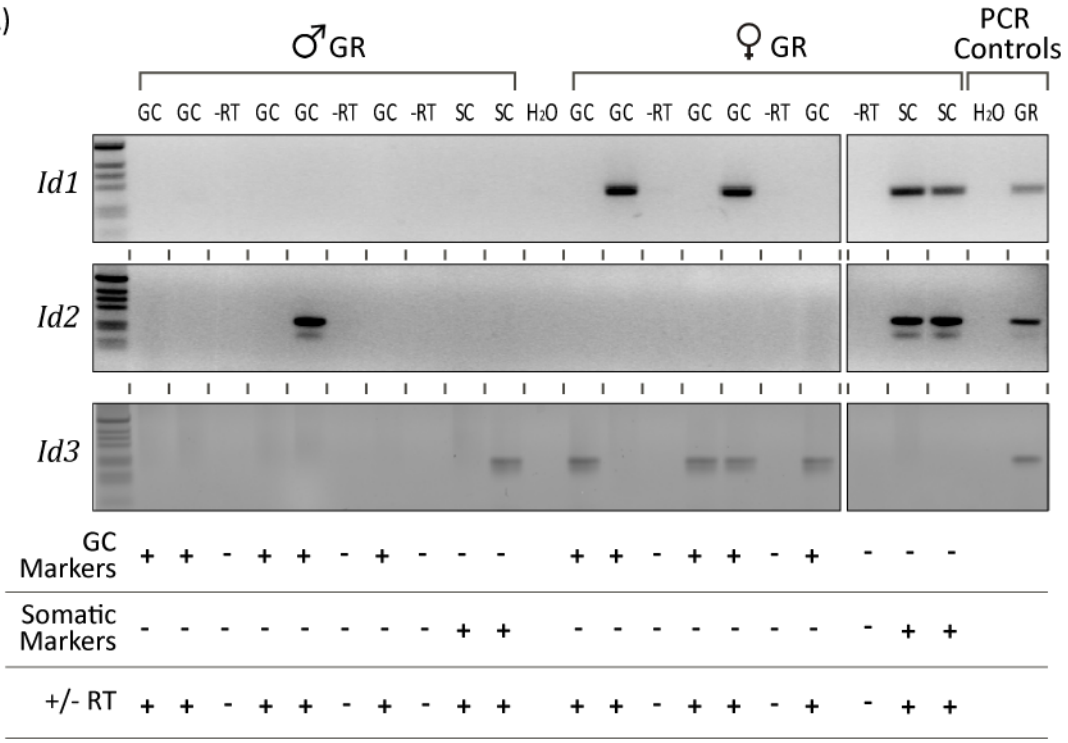


(B)

| Gene | % Positive ♂ | % Positive ♀ | P (Fisher's) |
|---|---|---|---|
| ***Id1*** | 6.7 | 46.7 | 0.0352 |
| ***Id2*** | 6.7 | 0.0 | - |
| ***Id3*** | 13.3 | 60.0 | 0.0209 |

(C)

| Expression | ♂ | ♀ |
|---|---|---|
| $Id1^-/Id3^-$ | 12 | 4 |
| $Id1^+/Id3^-$ | 1 | 2 |
| $Id1^-/Id3^+$ | 2 | 4 |
| $Id1^+/Id3^+$ | 0 | 5 |

**Figure 3.5.3. Single-cell reverse transcription PCR of *Id* Genes in E13.5 GCs**. Single-cell cDNA libraries were generated from single male or female E13.5 gonad cells and tested for expression of the GC markers *Dazl* and *Stella* and the somatic cell markers *SF1* and *Sox9* for male libraries, and *SF1* and *Gata4* for female libraries, to ascertain the original cell type (See Figures 3.5.1 and 3.5.2). 15 $GC^+$/$somatic^-$ libraries (labeled as "GC" above the gel), the analysis for 5 of which is shown here, along with no reverse transcriptase (-RT) controls, $H_2O$ negative controls, genital ridge (GR) cDNA positive controls, and 2 $GC^-$/$somatic^+$ (SC) libraries per sex, were tested for *Id1*, *Id2* and *Id3* expression analysis by PCR and gel electrophoresis, (A). A summary of the results from all 15 $GC^+$/$somatic^-$ libraries for *Id1*, *Id2* and *Id3* is shown, (B). Fisher's tests were carried out to ascertain the statistical significance of the results. The number of libraries showing different combinations of *Id1* and *Id3* detection, (C), was used to calculate (using a *Phi* analysis) a correlation efficient of 0.2182 for coincident detection of *Id1* and *Id3* in female GCs.

Only 1 out of 15 male GC$^+$/somatic$^-$ samples were positive for *Id1*, compared with 6 out of 15 female GC$^+$/somatic$^-$ samples. A Fisher's Test result of 0.0352 shows this difference to be significant. For *Id3*, 2 out of 15 male GC$^+$/somatic$^-$ samples were positive whereas 9 out of 15 female GC$^+$/somatic$^-$ samples were positive. A Fisher's Test result of 0.0209 shows this difference to be significant also. For *Id2*, the story is different - 1 out of 15 male GC$^+$/somatic$^-$ samples were positive whereas 0 out of 15 female GC$^+$/somatic$^-$ samples were positive for *Id2*. Once more, this result was verified by a replicate PCR that obtained the same results. This difference was not significant using a Fisher's Test. Of the 15 GC$^+$/somatic$^-$ female cDNA libraries, 5 were positive, while 4 were negative for both *Id1* and *Id3*. Using a *Phi* test, a correlation coefficient of 0.2182 was calculated, indicating weak or no correlation between *Id1* and *Id3* detection in GC$^+$/somatic$^-$ female GC libraries.

These single-cell PCR analyses are not very robust due to the small number of GCs tested from each biological replicate. More thorough analyses that test a larger number of GCs per biological replicate would yield more useful data. However, what can be said from these analyses is that firstly, both *Id1* and *Id3* transcripts were readily detectable in multiple cDNAs derived from single cells that are very likely to be GCs due to the combined detection of GC markers *Dazl* and *Stella*, and the absence of somatic marker detection. This suggests that female GCs do express both *Id1* and *Id3*, lending weight to the argument that the female-specific enrichments seen in the bHLH screen indicate higher expression of *Id1* and *Id3* in female GCs compared to male GCs. Furthermore, significantly more female than male GC cDNA libraries expressed detectable levels of both genes.

The primers used in the *Id2* single-cell PCR are able to detect transcripts, as shown by robust products in the positive control (female genital ridge cDNA) and the 2 female GC$^-$/somatic$^+$ samples. The failure of the single-cell PCR to detect a sex-specific difference of *Id2*, and furthermore, that transcript was detected in only 1 out of all 30 GCs, is at odds with the bHLH screen data showing robust 30-fold female-specific enrichment in E13.5 GC cDNA. Somatic

cell contamination in the purified GC preparations used in the screen could account for this disparity. Alternatively, owing to the large magnitude (30-fold) and reliability of the screen result, a more likely explanation is that the different primers sets used in the screen and this single-cell analysis detect alternative splice forms of *Id2*. *Id2* splice variants are postulated (Mantani et al., 1998), but have not been detected. Unfortunately, primers to detect alternative splice forms of *Id2* would not be suitable for this single-cell analysis, but it should be possible to test the single-cell primers in a quantitative RtPCR on E13.5 GC cDNA.

## 3.5.3. Id1 Protein Expression in E11.5-E13.5 Gonads

The results of the bHLH screen suggest that *Id1* mRNA is enriched sex-specifically in E13.5 female GC cDNA. The current section describes the result of immunofluorescence experiments to ascertain sex-specific enrichment of Id1 protein in E13.5 GCs. E11.5 and E12.5 tissue was also examined by immunofluorescence to discover when sex-specific differences in GC Id1 protein expression arise.

For all embryonic stages studied (except the quantitative study at E13.5), at least 2 separate experiments were carried out on separately processed tissue and a similar result obtained. The data from one of these experiments is shown in each of the figures below. For each experiment, tissue sections were stained with Id1 antibodies (Perk et al., 2006), along with DAPI and anti-GC-marker antibodies – against cytoplasmic Dazl for E13.5 tissue and predominantly-nuclear GCNA for E11.5 and E12.5 tissue - to identify GC nuclei. For E12.5 and E13.5 experiments, consecutive sections from the same genital ridges were processed in identical fashion in parallel using IgG instead of Id1 antibodies as negative controls for Id1 staining. For the E11.5 experiments, sections from different genital ridges were processed in parallel as negative controls. At least 3 genital ridges from different embryos were examined in each experiment, and representative images recorded.

The monoclonal mouse IgG α-Id1 antibody (37-2) used here was developed using recombinant full-length mouse Id1 and produces a single clear band at 17kDa by Western Blot, which corresponds to Id1 and does not appear in Western Blots of *Id1* null HeLa cell extract (Perk et al., 2006). In addition, one very faint non-specific band is seen by Western Blot at 34kDa using this antibody. The monoclonal rat IgM α-GCNA antibody was developed previously more than 15 years ago (Enders and May, 1994), is reactive to an unknown GC antigen and has since been used in many research papers to specifically identify GCs (e.g. Lin and Page, 2005). The mouse α-Dazl polyclonal antibody was also

developed previously, against the C-terminal 22 residues of mouse Dazl (Ruggiu et al., 1997) and produces a clear band on a Western blot that is absent from *Dazl* null cell extracts (Ruggiu et al., 2000).

Background fluorescence was evident in the negative controls, and consisted of 2 types. Firstly, low-level homogenous staining was evident in cytoplasm and nucleus of all cells, and was of much lower fluorescence than the Id1-antibody-associated staining. Secondly, particular cells that were possibly red blood cells exhibited uniformly high-level fluorescence in red, green and blue channels throughout each cell (see asterisk-marked cells in low power images in Figures 3.5.4A, 3.5.7A and 3.5.8A). This high-level fluorescence was found in both IgG- and antibody-stained tissue, and was visible immediately following processing, before application of antibodies. Therefore, this auto-fluorescence was ignored with respect to analysis of antibody-associated fluorescence. Additionally, these cells were avoided when selecting regions of tissue for high power images. In comparison to both these types of background fluorescence, Id1-associated fluorescence was nearly always nuclear and punctate.

Figure 3.5.4 shows immunofluorescence images from Id1- and IgG-stained E13.5 tissue. A clear difference is visible in the Id1 fluorescence intensity between male and female GC nuclei that is evident even in low power images. Male GC nuclei have consistently very low intensity or undetectable levels of Id1 fluorescence, and staining of the testes is mostly restricted to the interstitial region. Conversely, female GCs have heterogeneous levels of Id1 fluorescence.

A closer look at the E13.5 Id1-stained male tissue (high power images in Figure 3.5.4B) shows that the only cells located in the testicular cords with detectable Id1 levels have $Dazl^-$ cytoplasm, whose shape and location at the perimeter of the testis cords suggests they are Sertoli Cells. A very minor fraction of the GCs in E13.5 male tissue appear to have detectable levels of punctate Id1 fluorescence that is higher than background IgG levels. Interstitial cells, on the other hand, have heterogeneous nuclear Id1 fluorescence, ranging from

background levels comparable to male GC nuclei to higher Id1 fluorescence that is punctate.

High power images of E13.5 female Id1-stained tissue confirm that female GC nuclei have heterogeneous Id1 fluorescence levels, and, where this staining is higher than background, is punctate. An interesting pattern to the heterogeneous Id1 staining of E13.5 female GCs is evident. Female GC nuclei with no Id1 fluorescence are usually grouped together, such as the group of female GCs in Figure 3.5.4.B pointed out by the white arrowhead, away from nuclei showing detectable levels of Id1 fluorescence.

In summary then, nearly all $Dazl^+$ GCs in male E13.5 gonads had undetectable or almost undetectable nuclear Id1 fluorescence while, conversely, $Dazl^+$ GCs in female E13.5 gonads had heterogeneous levels of nuclear Id1 fluorescence that tended to be more uniform in physically-linked clusters of GCs.

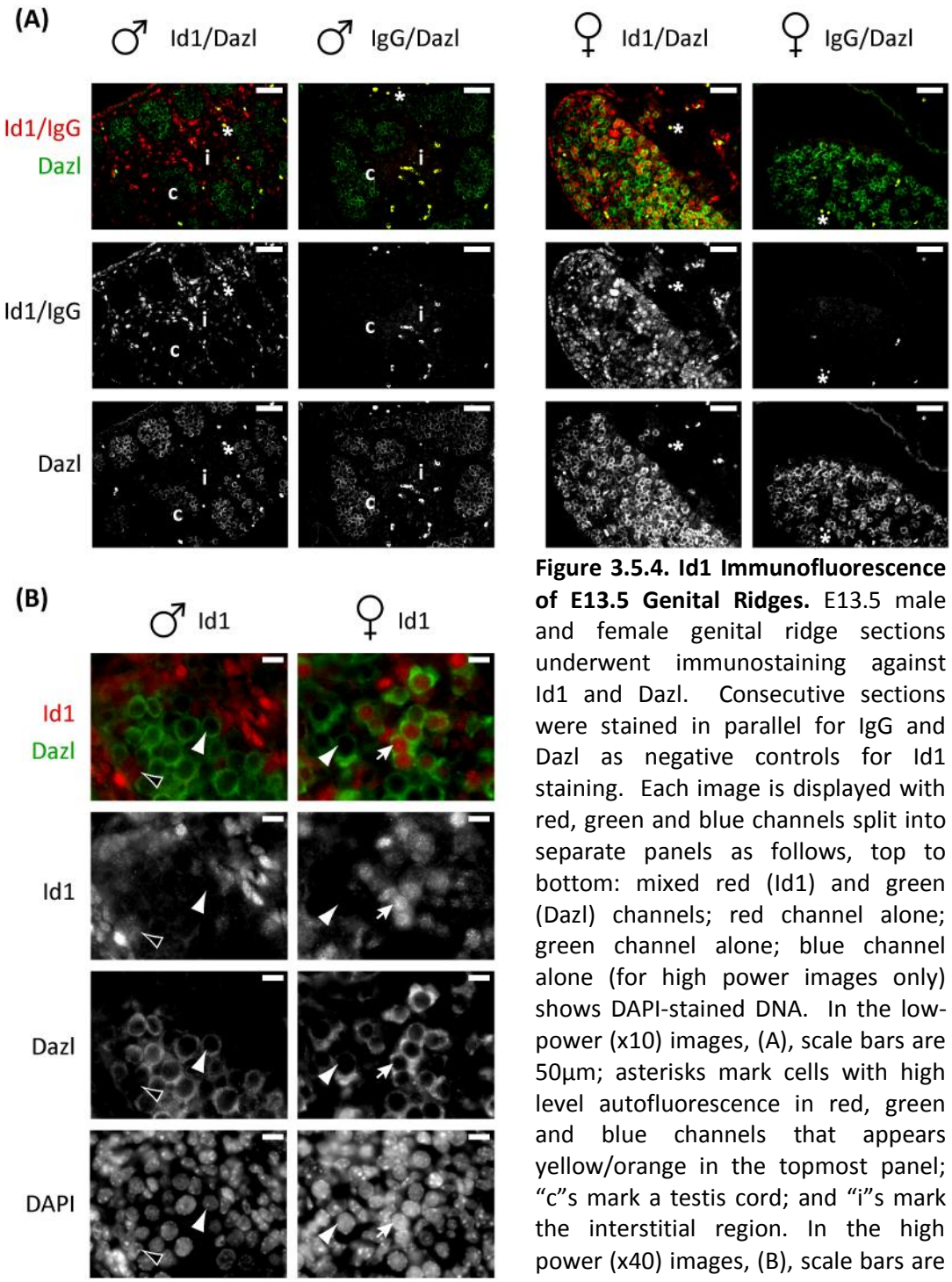


**Figure 3.5.4. Id1 Immunofluorescence of E13.5 Genital Ridges.** E13.5 male and female genital ridge sections underwent immunostaining against Id1 and Dazl. Consecutive sections were stained in parallel for IgG and Dazl as negative controls for Id1 staining. Each image is displayed with red, green and blue channels split into separate panels as follows, top to bottom: mixed red (Id1) and green (Dazl) channels; red channel alone; green channel alone; blue channel alone (for high power images only) shows DAPI-stained DNA. In the low-power (x10) images, (A), scale bars are 50µm; asterisks mark cells with high level autofluorescence in red, green and blue channels that appears yellow/orange in the topmost panel; "c"s mark a testis cord; and "i"s mark the interstitial region. In the high power (x40) images, (B), scale bars are 10µm; white arrows mark a representative female GC nucleus with high Id1 fluorescence; white arrowheads mark representative male and female GC nuclei with undetectable Id1 fluorescence; and black arrows with white outline mark a Sertoli-like cell with intermediate Id1 fluorescence.

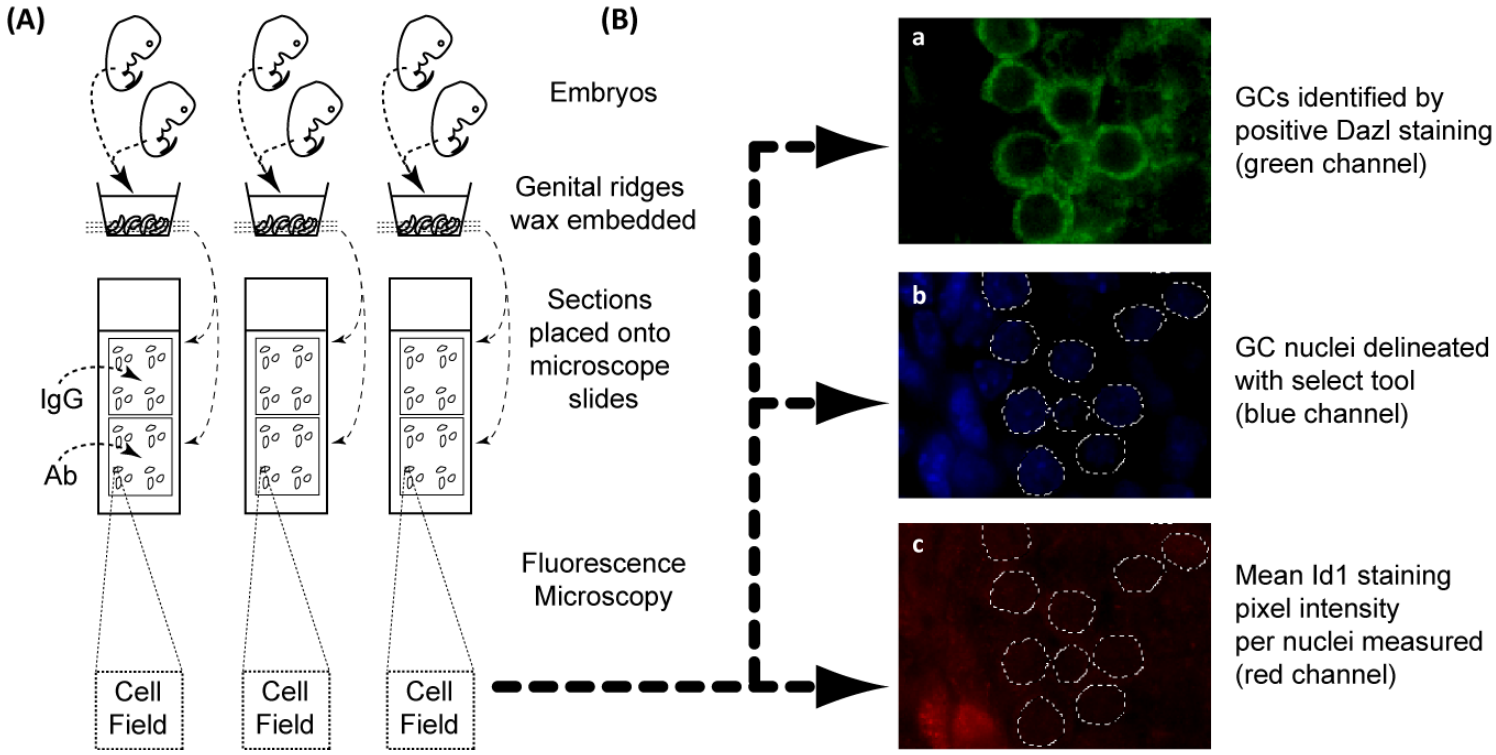


**Figure 3.5.5. Outline of Quantitative Immunostaining Protocol.** Embryonic genital ridges were dissected and wax embedded and sectioned onto three slides. Half of the sections on each slide were stained with antibody (Ab) and the other half with IgG as negative control. One Image of a representative antibody-stained cell field and one of a representative IgG-stained cell field were recorded from each slide, (A). Average Id1 staining for each nuclei in these images was analysed in Adobe Photoshop CS in the following way, as in (B). For each image recorded, GCs (germ cells) were first identified by cytoplasmic Dazl immunostaining in the green channel, (a), and all GC nuclei delineated with the select tool in the DAPI/blue channel, (b). The Id1 staining level for each nuclei was then calculated by taking the mean red channel pixel intensity inside the selected area for each nuclei, (c). The mean red pixel intensities of all GC nuclei in each cell field were themselves meaned to give the mean Id1 fluorescence for each image.

In order to quantify these sex-specific differences in Id1-antibody staining of E13.5 GCs and to quantifiably define the heterogeneous Id1 fluorescence levels in E13.5 female GCs, nuclear Id1 fluorescence levels were quantified in several images of male and female E13.5 gonads, as shown in Figure 3.5.5 and 3.5.6. Sections from genital ridges on 3 separate slides were processed for immunostaining. Half of the sections on each slide were stained with Id1 and the other half with IgG as a negative control. One high power image of a representative cell field from each slide was recorded. The mean nuclear Id1 (red channel) pixel intensity of nuclei of $Dazl^+$ (green channel) cells was recorded and the mean of all $Dazl^+$ nuclei from each image calculated. The 3 means were combined and the standard errors propagated to obtain the results shown in Figure 3.5.6A (Male Id1 = 20.8 ± 3.4; Male IgG = 27.3 ± 4.9; Female Id1 = 43.2 ± 8.3; Female IgG = 21.5 ± 2.9; n = 3 for each). The mean Id1 fluorescence levels for female GC nuclei were ~200% that of male GC nuclei. This sex-specific difference is statistically significant (P=0.0117). 256 out of 400, or 64%, of female E13.5 GC nuclei had Id1 fluorescence levels that were higher than background levels in IgG-stained female nuclei. Therefore, this 64% of female GC nuclei expressed detectable levels of Id1 protein. The mean Id1 fluorescence in male GC nuclei was similar to that of background-level fluorescence in IgG-stained male GC nuclei, and 0 out of 354 male GC nuclei had higher Id1 levels than IgG stained male GC nuclei. Therefore, E13.5 male GC nuclei express undetectable levels of Id1 protein.

It is surprising to find that female GCs on average have only 2-fold more Id1 fluorescence than male GCs, considering that female GCs express 40-fold more *Id1* transcripts than male GCs according to the results from the bHLH screen. This discrepancy is unlikely to be due to low-level translation of abundant transcripts in female GCs. A more likely explanation for this discrepancy is that the Id1 fluorescence levels shown here are not corrected for background. Therefore, background levels of fluorescence, which are only 2-fold lower than the mean Id1 fluorescence of female GCs according to IgG-stained tissue, are

probably masking the true extent of the difference in Id1 protein levels between male and female GCs.

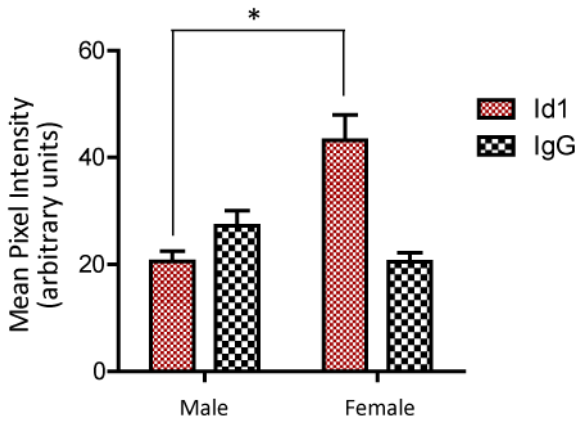


**Figure 3.5.6. Quantification of Id1 Immunofluorescence Intensity of E13.5 GCs.** Sections from 3 separate genital ridges per sex were analysed quantitatively for anti-Id1 immunostaining. Consecutive sections from the same genital ridges were analysed in parallel for IgG as negative controls. 1 representative image per gonad was recorded and the mean red (Id1/IgG) pixel intensity for each GC nuclei measured. GCs were identified by manual inspection of the cytoplasmic Dazl staining of each nucleus, and nuclei of GCs were manually delineated with reference to the DAPI staining signal. The mean intensity from the 3 images was averaged to obtain the results represented by the bars in the chart, and the error bars represent the SD of these means, which was propagated throughout. Data from Id1-stained sections is represented as a small red-and-white-checked bar, while data from IgG-stained sections is represented as large black-and-white-checked bars. An unpaired, two-tailed t-test was calculated and the result displayed as an asterisk: "*", $P<0.05$.

In order to determine when the sex-specific difference in Id1 expression arises, Id1/IgG immunostaining was carried out on E11.5 and E12.5 genital ridge sections. E11.5 embryos were sexed by PCR before processing for immunostaining. Both male and female E11.5 GC nuclei have heterogeneous Id1 fluorescence levels (Figure 3.5.7). Some GCs have low Id1 fluorescence at or close to background levels, such as the GCs indicated by white arrowheads in the high power images in Figure 3.5.7B. The majority have noticeably higher punctate Id1 fluorescence, like the GCs indicated by white arrows in Figure

3.5.7B. Some somatic nuclei have very high Id1 fluorescence and are the most highly-stained cells.

At E12.5, there is a clear sex-specific difference in GC Id1 fluorescence (Figure 3.5.8). E12.5 male GC nuclei have undetectable levels of Id1 fluorescence. Female GCs, on the other hand, have heterogeneous levels of punctate Id1 fluorescence that is higher than background IgG levels in the vast majority of GC nuclei. Heterogeneous levels of punctate Id1 fluorescence are also seen in female somatic cells and in male somatic cells in the interstitial regions of the gonads. The Id1 fluorescence of E12.5 female GC nuclei is generally high and it is difficult to find female GCs with comparatively low Id1 fluorescence. This is in contrast to the Id1 fluorescence staining of E13.5 female GCs, which is more heterogeneous.

Qualitative inspection of the data suggests that the ratio of high/low-level Id1 fluorescent female GC nuclei decreases between E12.5 and E13.5, when female GCs commit to meiosis. However, the lack of quantitative analyses of the Id1 fluorescence levels of E12.5 female GC nuclei here makes this impossible to confirm.

So, in summary, male and female E11.5 GCs have heterogeneous levels of punctate Id1 fluorescence in their nuclei, proportionally more of which have higher fluorescence levels. No sex-specific difference is obvious at E11.5. This suggests that, at E11.5, male and female GCs express similar levels of Id1 protein. Between E11.5 and E12.5 a change occurs in male GCs, whose nucleic Id1 fluorescence drop to undetectable levels, whereas female GCs continue to have heterogeneous Id1 fluorescence. According to this, male GCs sex-specifically stop expressing Id1 protein, at a time when they also commit to spermatogenesis and enter mitotic arrest. At E13.5, this pattern is continued: male GCs still do not express Id1, while female GCs continue to express heterogeneous levels of Id1.

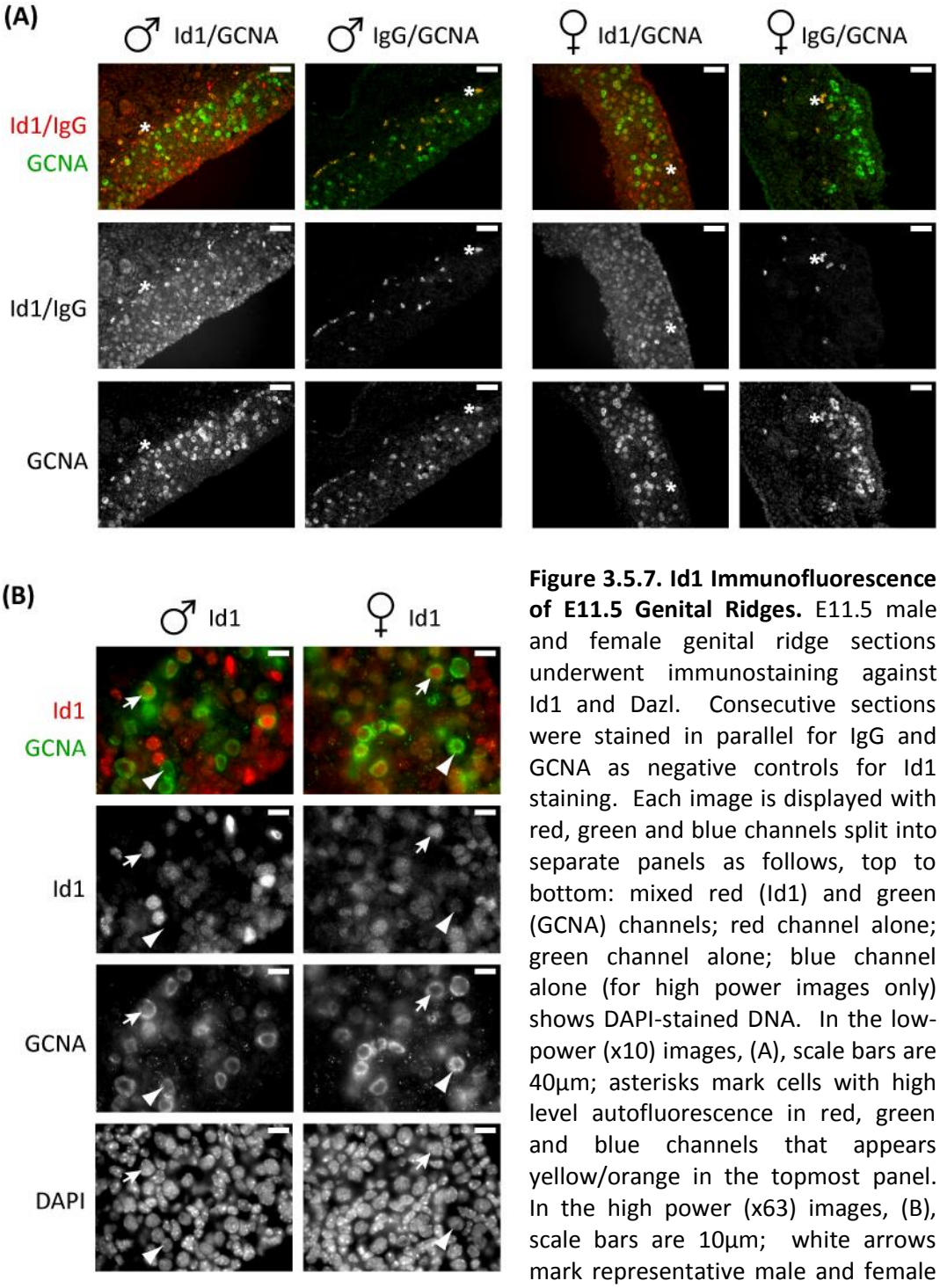


**Figure 3.5.7. Id1 Immunofluorescence of E11.5 Genital Ridges.** E11.5 male and female genital ridge sections underwent immunostaining against Id1 and Dazl. Consecutive sections were stained in parallel for IgG and GCNA as negative controls for Id1 staining. Each image is displayed with red, green and blue channels split into separate panels as follows, top to bottom: mixed red (Id1) and green (GCNA) channels; red channel alone; green channel alone; blue channel alone (for high power images only) shows DAPI-stained DNA. In the low-power (x10) images, (A), scale bars are 40µm; asterisks mark cells with high level autofluorescence in red, green and blue channels that appears yellow/orange in the topmost panel. In the high power (x63) images, (B), scale bars are 10µm; white arrows mark representative male and female GC nuclei with high Id1 fluorescence; and white arrowheads mark representative male and female GC nuclei with low/undetectable Id1 fluorescence.

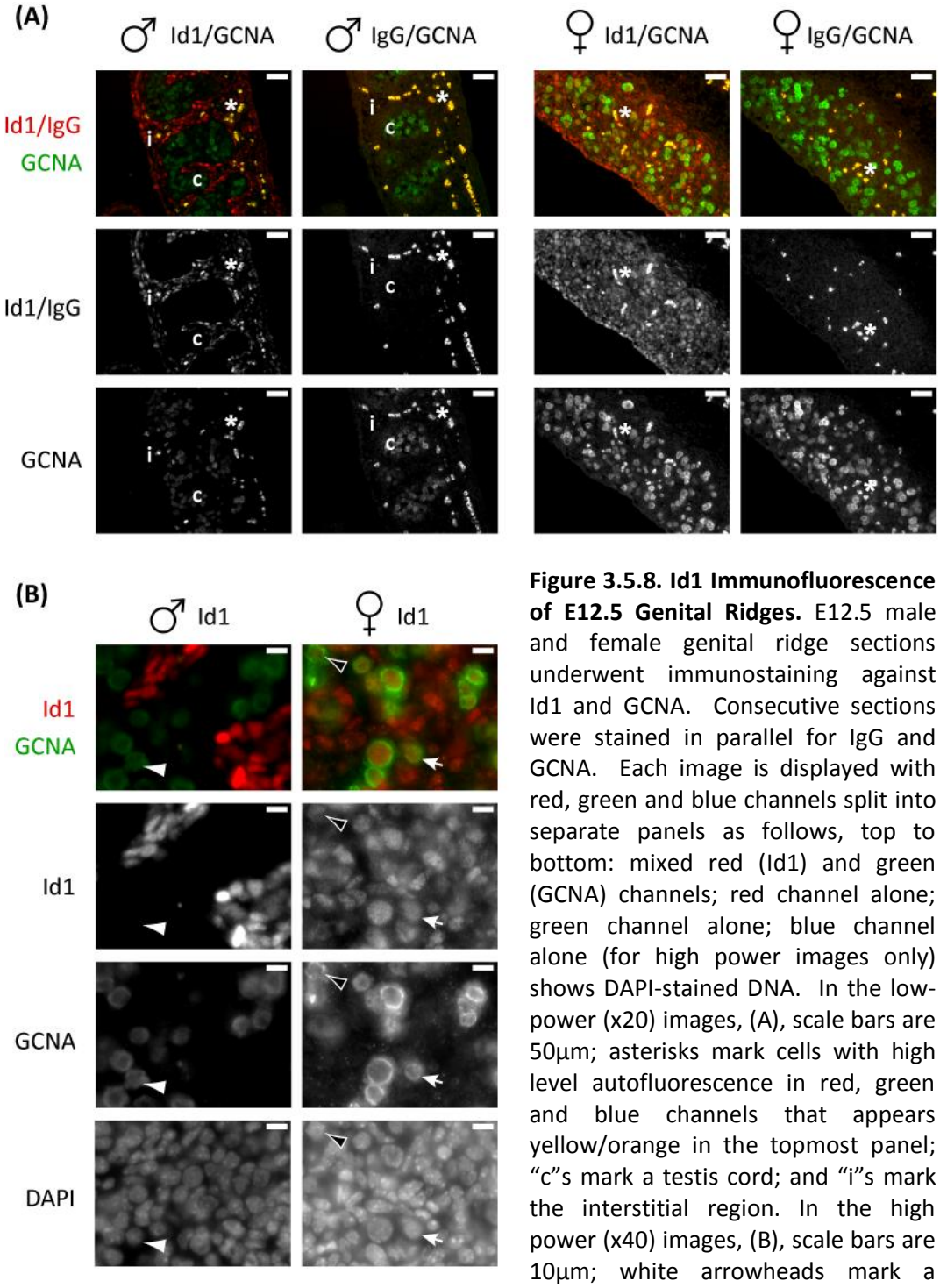


**Figure 3.5.8. Id1 Immunofluorescence of E12.5 Genital Ridges.** E12.5 male and female genital ridge sections underwent immunostaining against Id1 and GCNA. Consecutive sections were stained in parallel for IgG and GCNA. Each image is displayed with red, green and blue channels split into separate panels as follows, top to bottom: mixed red (Id1) and green (GCNA) channels; red channel alone; green channel alone; blue channel alone (for high power images only) shows DAPI-stained DNA. In the low-power (x20) images, (A), scale bars are 50µm; asterisks mark cells with high level autofluorescence in red, green and blue channels that appears yellow/orange in the topmost panel; "c"s mark a testis cord; and "i"s mark the interstitial region. In the high power (x40) images, (B), scale bars are 10µm; white arrowheads mark a representative male GC nucleus with very low Id1 fluorescence; white arrows mark a representative female GC nucleus with high Id1 fluorescence; and black arrowheads with white outline mark a representative female GC nucleus with intermediate Id1 fluorescence.

## 3.5.4. Mnt Protein Expression in E11.5-E13.5 Gonads

The results of the screen in Section 3.4.4 show that *Mnt* mRNA is sex-specifically enriched in E13.5 male GC cDNA. In order to support this result and to see whether male and female E13.5 GCs specifically express different levels of Mnt protein, fluorescence immunostaining was carried out on paraffin-embedded E13.5 male and female gonad sections. In addition, E12.5 and E11.5 gonad sections were also examined by fluorescence immunostaining in order to determine when sex-specific differences in GC Mnt staining first arise.

For all embryonic stages studied (except the quantitative study at E13.5), at least 2 separate experiments were carried out and a similar result obtained. For each experiment, tissue sections were stained with GCNA antibodies and DAPI, in addition to Mnt antibodies, to identify GC nuclei. Consecutive sections from the same gonads and fixed onto the same slides were stained in parallel with IgG instead of Mnt as negative controls for Mnt staining. At least 3 separate gonads were examined in each experiment, and representative images recorded.

The rabbit α-Mnt polyclonal antibodies used for these immunofluorescence experiments was obtained from Santa Cruz Biotechnology, developed against residues 226-361 of human Mnt and produces a clear band on a Western of mouse cell extract that disappears when *Mnt* is knocked down by antisense RNA (Popov et al., 2005). Verification and source of the GCNA antibodies was described at the beginning of Section 3.5.3.

The majority of cells in the IgG controls, as shown in the figures below, had low, background levels of fluorescence in nuclei and cytoplasm. A minority of cells in E12.5 and E13.5 tissue, believed to be red blood cells, had consistently highly intense autofluorescence in red, green and blue channels (see asterisk-marked cells in IgG controls in Figure 3.5.9A and Figure 3.5.12A). The fluorescence in these cells appeared after processing of the tissue prior to addition of antibodies, and was therefore ignored for the purposes of analysis of Mnt

staining patterns. Also, when fields for high power images were chosen, these cells were avoided.

Throughout all embryonic stages examined, Mnt fluorescence overlapped strongly with DAPI and was therefore predominantly nuclear. Figure 3.5.9 shows representative images of Mnt immunostaining on E13.5 gonad sections. As shown in the low power images in part (A) of the figure, a difference in the pattern of Mnt immunofluorescence between male and female gonads is evident. $GCNA^+$ GC nuclei in the male gonad have relatively similar fluorescence levels to that of the majority of $GCNA^-$ somatic cells[1]. Mnt fluorescence between GCs and non-GCs in the female gonad is more heterogeneous: regions of $GCNA^+$ GC nuclei have low Mnt fluorescence in comparison to surrounding $GCNA^-$ nuclei.

High-power images of E13.5 gonad tissue (Figure 3.5.9B) confirm this sex-specific difference in staining patterns, and suggest that male GC nuclei have higher Mnt fluorescence than female GC nuclei. For example, compare the male and female GCs marked by white arrows in Figure 3.5.9B. Female somatic cells also have higher Mnt fluorescence than female GCs – compare the $GCNA^-$ somatic nucleus (black arrowhead with white outline) with the $GCNA^+$ GC nucleus (white arrow).

[1] There were also some unidentified $GCNA^-$ interstitial cells that had very high Mnt fluorescence levels but these are not discussed further. Some of these can be seen in the male low power Mnt image in Figure 3.5.9A.

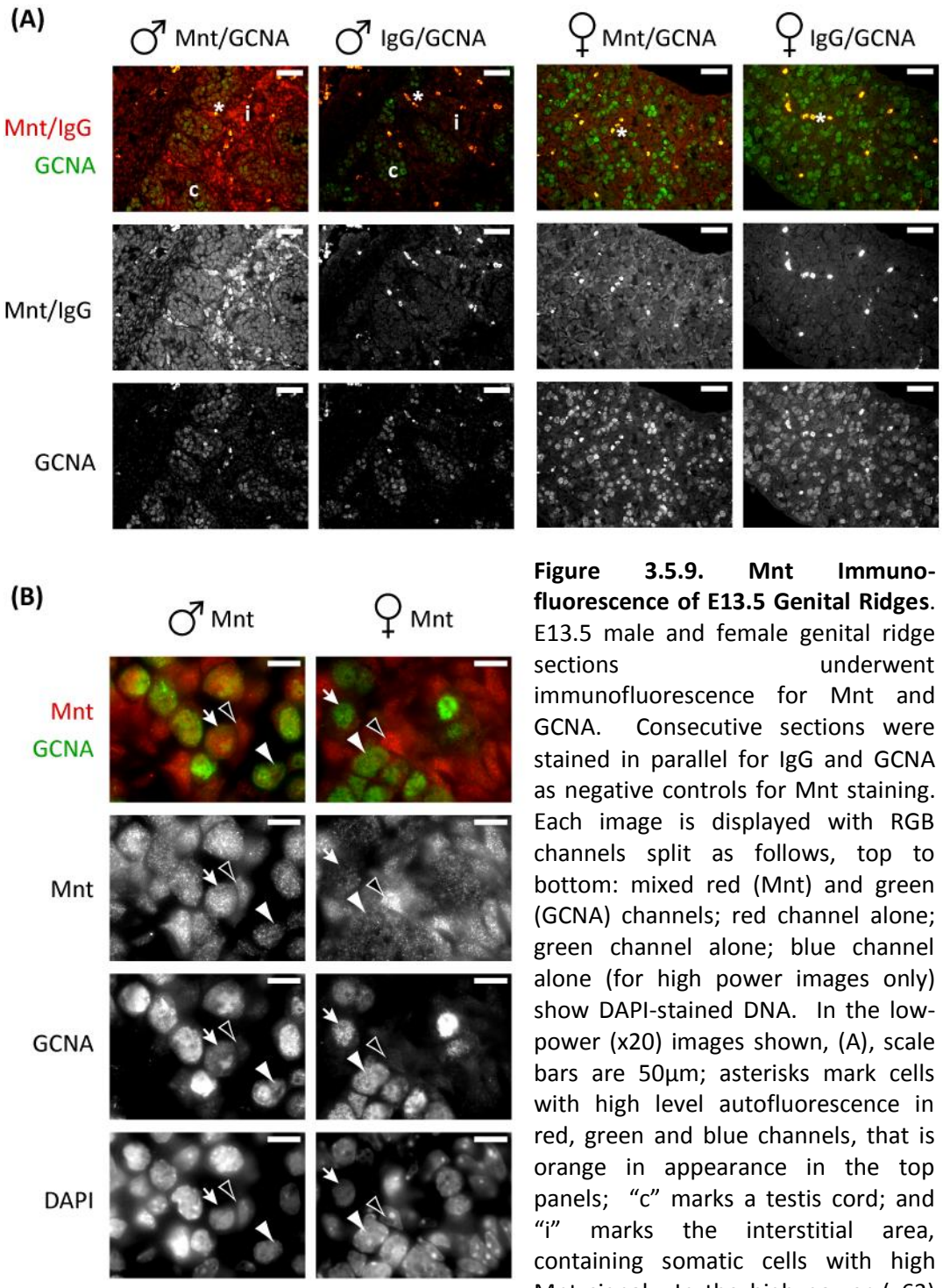


**Figure 3.5.9. Mnt Immuno-fluorescence of E13.5 Genital Ridges**. E13.5 male and female genital ridge sections underwent immunofluorescence for Mnt and GCNA. Consecutive sections were stained in parallel for IgG and GCNA as negative controls for Mnt staining. Each image is displayed with RGB channels split as follows, top to bottom: mixed red (Mnt) and green (GCNA) channels; red channel alone; green channel alone; blue channel alone (for high power images only) show DAPI-stained DNA. In the low-power (x20) images shown, (A), scale bars are 50µm; asterisks mark cells with high level autofluorescence in red, green and blue channels, that is orange in appearance in the top panels; "c" marks a testis cord; and "i" marks the interstitial area, containing somatic cells with high Mnt signal. In the high power (x63) images, (B), scale bars are 10µm. White arrows mark representative GC nuclei and black arrowheads with white outlines mark GCNA$^-$ somatic nuclei with high Mnt fluorescence.

To ascertain the robustness of these observed differences, the staining intensities of Mnt-stained and GCNA-stained E13.5 tissue were analysed quantitatively (Figure 3.5.10). The analysis was accomplished identically to the Id1 quantitative immunofluorescence (Figure 3.5.5), except two instead of three slides were analysed. Therefore, the Mnt pixel intensities quoted below and in Figure 3.5.10 are the mean of two cell fields of GC nuclei. Half the sections on each slide were stained for Mnt and GCNA, while the other half were stained for IgG and GCNA as negative controls. Another difference between this analysis and the Id1 quantitative immunofluorescence is that both Mnt (red channel) and GCNA (green channel) pixel intensities were recorded (as opposed to Mnt alone) for both $GCNA^+$ GCs and $GCNA^-$ somatic cells (as opposed to GCs alone). $GCNA^+$ GC nuclei were identified by manual inspection of the GCNA staining pattern. $GCNA^-$ cell nuclei were identified by definite absence of GCNA staining.

The mean Mnt pixel intensity of male $GCNA^+$ GCs was significantly higher than that of female $GCNA^+$ GCs, with a P value of 0.0061 calculated using an unpaired 2-tailed t-test (male GC Mnt = 120.1 ± 3.06, n = 2, female GC Mnt = 77.85 ± 1.27, n = 2). Background fluorescence of IgG-stained nuclei was much lower than the Mnt fluorescence of the tissue sections from the same gonads, which were handled in parallel, and these differences were also significant. A P value of 0.0020 (male GC Mnt = 120.1 ± 3.06, n = 2, male GC IgG = 24.46 ± 2.93, n = 2) was calculated comparing male Mnt-stained with male IgG-stained GCs, and a P value of 0.0035 (female GC Mnt = 77.85 ± 1.27, n = 2, female GC IgG = 25.22 ± 2.85, n = 2) was calculated comparing female Mnt-stained with female IgG-stained GCs. Therefore, male GC nuclei have significantly higher Mnt staining levels than female GC nuclei at E13.5. Also, the levels of Mnt staining in male and female GC nuclei were significantly higher than background staining due to IgG.

Additionally, a P value of 0.0271 was calculated (female GC Mnt = 77.85 ± 1.27, n = 2, female somatic Mnt = 92.77 ± 2.16, n = 2) when comparing Mnt fluorescence levels of female GC nuclei and female somatic nuclei. Conversely, no significant difference was seen between Mnt staining intensities of male GC

nuclei and male somatic cell nuclei. Therefore, Mnt staining levels of female GCs are significantly lower than those of female somatic cells, while male GCs and somatic cells have the same levels of Mnt immunostaining.

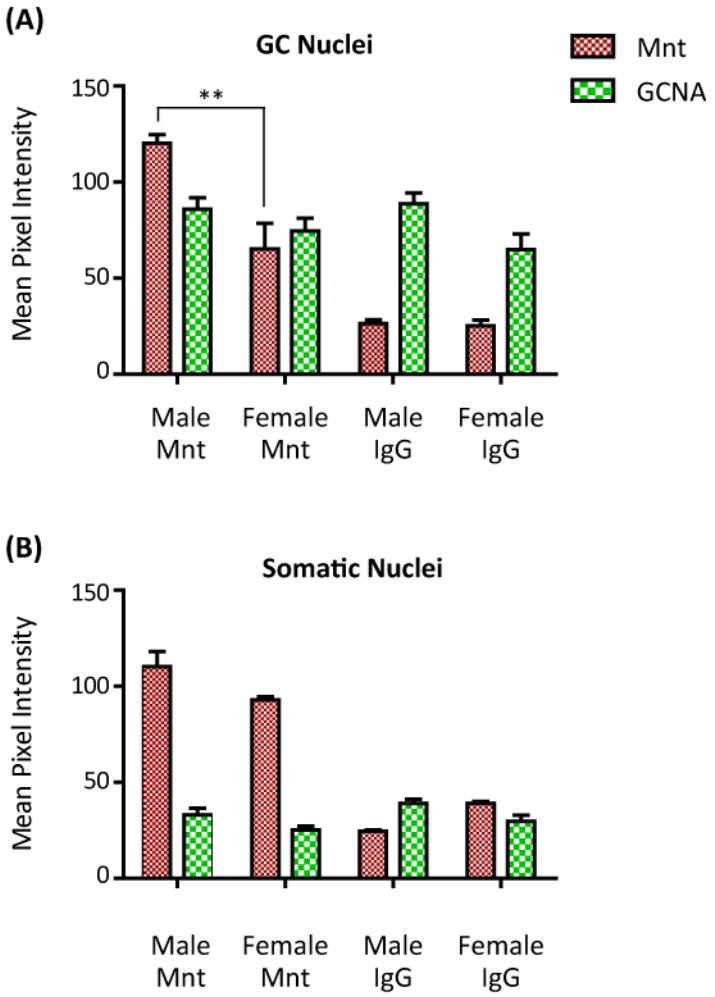


**Figure 3.5.10. Quantification of Mnt Immunofluorescence Intensity of E13.5 Gonadal Cells.** Sections from 2 separate gonads per sex were analysed by quantitative immunofluorescence for Mnt and GCNA. Consecutive sections from the same gonads were analysed in parallel for IgG and GCNA as negative controls. 2 images per gonad (a total of 4 images per condition: Male Mnt/Female Mnt/Male IgG/Female IgG) were recorded and the mean red (Mnt/IgG) and green (GCNA) pixel intensity for each nuclei (demarcated by DAPI staining) measured. The mean intensity from the 4 images was averaged to obtain the results represented by the bars in the chart and the error bars represent the SEM of these means. Red (Mnt/IgG) pixel intensity is represented by small red and white checked bars; green (GCNA) pixel intensity is represented by large green and white checked bars. $GCNA^{+}$ nuclei (A) were identified manually by inspection of the GCNA staining pattern of each nuclei. All other nuclei, which include true somatic cells and GCs with very low GCNA staining were classed as $GCNA^{-}$ (B). An unpaired, two-tailed t-test was calculated and the result displayed as an asterisk in (A): "**", $P<0.005$.

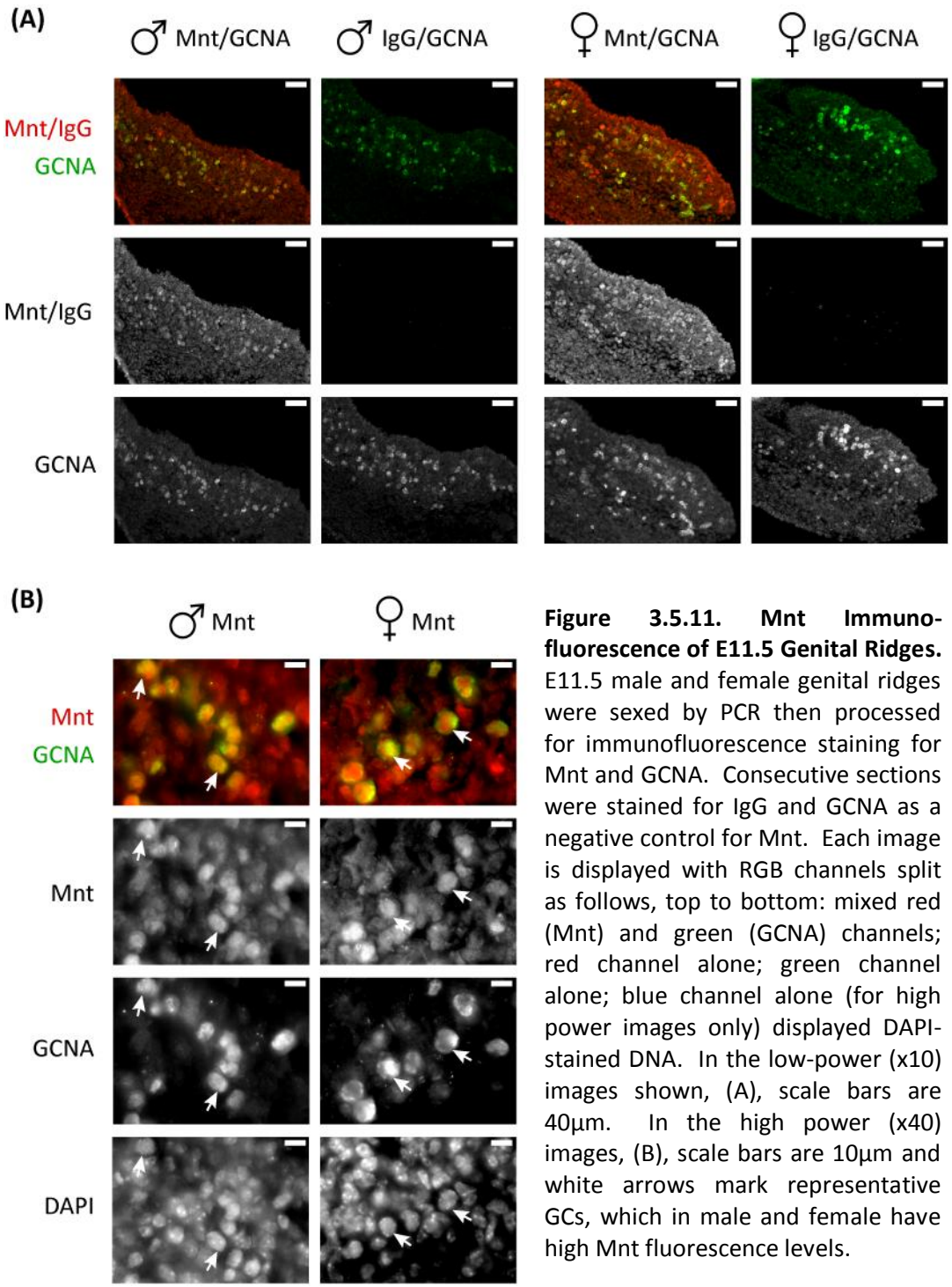


**Figure 3.5.11. Mnt Immuno-fluorescence of E11.5 Genital Ridges.** E11.5 male and female genital ridges were sexed by PCR then processed for immunofluorescence staining for Mnt and GCNA. Consecutive sections were stained for IgG and GCNA as a negative control for Mnt. Each image is displayed with RGB channels split as follows, top to bottom: mixed red (Mnt) and green (GCNA) channels; red channel alone; green channel alone; blue channel alone (for high power images only) displayed DAPI-stained DNA. In the low-power (x10) images shown, (A), scale bars are 40µm. In the high power (x40) images, (B), scale bars are 10µm and white arrows mark representative GCs, which in male and female have high Mnt fluorescence levels.

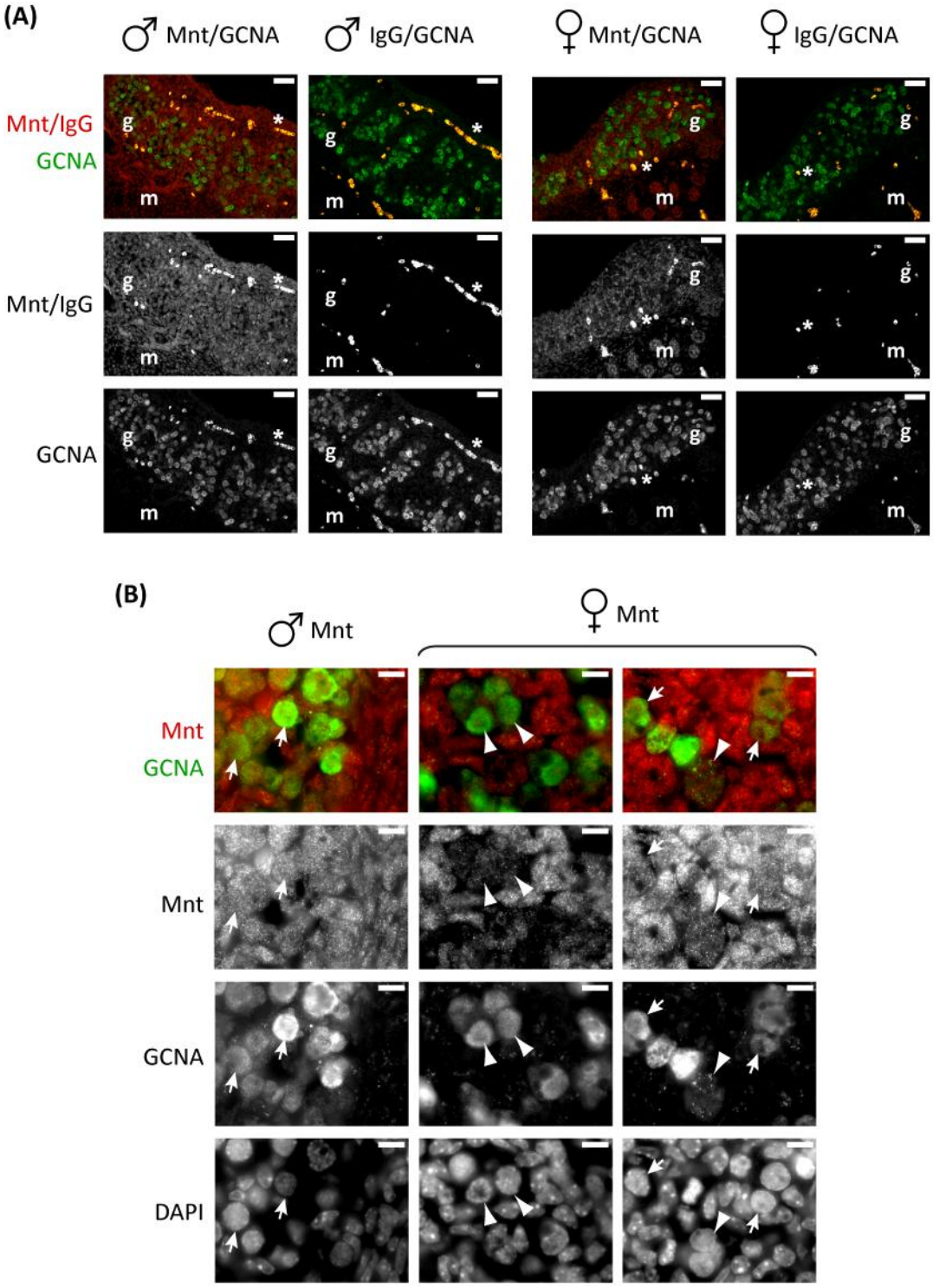
(A)
♂ Mnt/GCNA
♂ IgG/GCNA
♀ Mnt/GCNA
♀ IgG/GCNA
Mnt/IgG
GCNA
Mnt/IgG
GCNA
g
m
*
(B)
♂ Mnt
♀ Mnt
Mnt
GCNA
Mnt
GCNA
DAPI

In conclusion, these Mnt fluorescence patterns suggest that E13.5 male GCs express higher levels of Mnt protein than E13.5 female GCs, at a stage when male GCs have committed to spermatogenesis and are entering mitotic arrest. To ascertain when this sex-specific difference in Mnt protein levels arises, immunofluorescence experiments were performed on E11.5 (Figure 3.5.11) and E12.5 (Figure 3.5.12) genital ridges.

Gonads from several E11.5 embryos were sexed by PCR and processed for and analysed by Mnt or IgG immunofluorescence staining. This analysis was repeated on one separate occasion, with similar results. Figure 3.5.11 shows representative images from these analyses. All $GCNA^+$ GC nuclei in both male and female gonads stained strongly for Mnt, and were among the most strongly Mnt-stained nuclei.

To conclude, male and female E11.5 GC nuclei had very similar levels of Mnt fluorescence, and these staining intensities were higher than the Mnt staining of the surrounding somatic nuclei.

At E12.5, Mnt immunostaining in male and female GC nuclei is much more heterogeneous than that at E11.5 (Figure 3.5.12). The general pattern and sex-specific intensity differences of Mnt staining are similar to that observed at E13.5. As shown in the high power images in Figure 3.5.12B, $GCNA^+$ GC nuclei in the E12.5 female gonad have generally less intense Mnt staining than their surrounding $GCNA^-$ somatic nuclei, and furthermore appear to have less intense

---

**Figure 3.5.12. Mnt Immunofluorescence of E12.5 Genital Ridges.** E12.5 male and female genital ridge sections underwent immunofluorescence for Mnt and GCNA. Consecutive sections were stained for IgG and GCNA as a negative control for Mnt. Each image is displayed with RGB channels split as follows, top to bottom: mixed red (Mnt) and green (GCNA) channels; red channel alone; green channel alone; blue channel alone (for high power images only) displayed DAPI-stained DNA. In the low-power (x20) images (A) shown, scale bars are 40µm; asterisks mark cells with high level autofluorescence in red, green and blue channels; "g" marks the gonad; and "m" marks the mesonephroi. In the high power (x63) images, (B), scale bars are 10µm. White arrows mark representative GC nuclei with relatively intermediate Mnt staining levels, while white arrowheads mark female GC nuclei with lower Mnt staining intensities.

Mnt staining compared to GCNA$^+$ E12.5 male GC nuclei. For example, compare the 2 male GCs indicated by white arrows with the 2 female GCs in the left female panel and the female GC in the right female panel indicated by white arrowheads. Other female E12.5 GC nuclei, however, have Mnt fluorescence intensity similar to that seen in the majority of male GC nuclei and the surrounding female somatic nuclei. 2 such female GCs are indicated by white arrows in the right female panel in Figure 3.5.12B.

Qualitatively therefore, Mnt staining of E12.5 tissue was similar to, but not as sexually different as that in E13.5 tissue. Mnt levels were not quantified in E12.5 tissue.

In conclusion to this section, at E11.5, both male and female GC nuclei have high Mnt immunofluorescence intensities and no sex-specific difference is seen at this early stage when GCs are sexually bipotential. At E12.5, a time when male GCs have just committed to spermatogenesis, sex-specific differences in Mnt staining intensities arise. GC nuclei no longer have such predominant Mnt staining intensity compared to the surrounding somatic cells, and this is most obvious for female GC nuclei, which have heterogeneous Mnt staining intensities that are in general noticeably lower than male GC nuclei. By E13.5, when male GCs are entering a mitotic arrest and female GCs are entering meiosis, male GC nuclei have significantly higher levels of Mnt immunofluorescence than female GC nuclei.

## 3.6. bHLH Screen Discussion

Previous studies have identified several bHLH genes as having functions at different stages of GC differentiation. Both *Sohlh1* and *Sohlh2* are required for mitosis-meiosis transition of spermatogonia in testis (Ballow et al., 2006; Hao et al., 2008; Toyoda et al., 2009), while ablation of either gene results in sterility of female mice due to defects in oogenesis (Choi et al., 2008; Pangas et al., 2006; Toyoda et al., 2009). *Figla* is also required for successful oogenesis, because *Figla* knockout results in defective folliculogenesis that begins perinatally and is associated with deficient oogenic expression (Soyal et al., 2000). Additionally, both *Ngn3* and *Tcfl5* are believed to be involved in spermatogenesis – *Ngn3* is expressed in both spermatogonial stem cells and undifferentiated spermatogonial stem cells (Yoshida et al., 2004), whereas *Tcfl5* has been shown to bind to the promoter of *Calmegin*, a gene first expressed in meiotic prophase, stimulate *Calmegin* transcription, and is expressed in primary spermatocytes and spermatids (Siep et al., 2004). So bHLHs are known to have roles in postnatal stages of GC development. The dominant negative bHLH *Id1* was previously identified as being sex-specifically enriched in E13.5 female GC cDNA (Adams, I.R., unpublished data). *Id1* maintains cells such as embryonic stem cells (Ying et al., 2003) and myoblasts (Jen et al., 1992) in an undifferentiated state by preventing bHLH-mediated differentiation (Ruzinova and Benezra, 2003). Therefore, it was hypothesised that differential expression of *Id1* and other bHLHs might be involved in sex-specific differentiation of E13.5 GCs. This screen was carried out to find out which bHLHs are sex-specifically expressed in E13.5 GCs.

### *Diverse Sex-specific Differences in bHLH Expression of E13.5 GCs*

The findings of this screen are very positive, in that 20 out of 114 genes were enriched or detected sex-specifically in E13.5 GC cDNA, over 2 biological

replicates. 14 genes were found to be enriched sex-specifically, while another 6 genes were expressed sex-specifically over 2 biological replicates, suggesting that there may be striking differences in bHLH-mediated transcription between male and female GCs at E13.5. Interestingly, 15 of those genes were enriched/specifically-expressed in female cDNA, while only 5 were in male cDNA, and additionally the fold-enrichments for female-enriched genes were generally much higher than those of the male-enriched genes. This suggests that female GCs express higher levels of a variety of bHLH genes at a time when they are initiating meiosis (McLaren, 1984).

*Figla* and *Ngn3* were here found to be enriched in female, or male GC cDNA, respectively. Previous studies show that both *Figla* (Soyal et al., 2000) and *Ngn3* (Yoshida et al., 2004) are involved in sex-specific GC development, albeit at postnatal rather than embryonic stages. *Figla* expression was first detected female-specifically at E13.0 by RNAse protection of whole gonads (Soyal et al., 2000), confirming the female-specific expression detected in this screen in E13.5 GCs. Defects in female GC development in *Figla* knockout mice are first seen at 1 or 2 days post partum, which is the same time that *Figla* expression peaks at roughly 30-fold of the levels detected at E13.0. Therefore, the sex-specific expression detected in this screen in E13.5 female GCs does not appear to be required for meiotic initiation and embryonic development of female GCs. Germline expression of *Ngn3* was previously not detected at either E13.5 or E18.5 by *in situ* hybridisation, Northern hybridisation or reverse transcription PCR (Yoshida et al., 2004), although the results of these assays were not shown, and this is in disagreement with male-specific detection in this study at E13.5. The discrepancy of these previous findings with the current screen could be due to the use of more sensitive RtPCR assays using purified GC cDNA in this screen.

*Epas1*, *Helt*, *Mnt*, *Msc* and *Ngn3* were enriched sex-specifically in male E13.5 GC cDNA. *Helt* expression in the adult is restricted to testis (Guimera et al., 2006a). However, GC expression of *Helt* has not yet been shown and the expression seen in purified GCs in this study could originate from GC or somatic cell expression. *Helt* (Guimera et al., 2006a) and *Ngn3* (Gradwohl et al., 2000) knockout mice die

postnatally, and analysis of GC development in these mice has not yet been published. *Msc* was detected sex-specifically in male GC cDNA, and could therefore be an interesting candidate gene. *Msc* knockout results in only mild facial muscle defects and no fertility defect of male or female mice was reported (Lu et al., 2002) so a vital role for *Msc* in male-specific GC development is ruled out.

The bHLHs enriched/detected sex-specifically in female E13.5 GC cDNA are spread across all bHLH classes except Class A. Of those genes, *Mesp1* (Saga et al., 1999), *Scx* (Brown et al., 1999) and *Hand1* (Riley et al., 1998) knockouts die embryonically before sex-specific GC differentiation, precluding straightforward examination of roles for these genes in sex-specific GC differentiation. *Math1* (Ben-Arie et al., 1997) and *Hes7* (Bessho et al., 2001) knockouts die postnatally before fertility could be assessed, while no knockouts have been carried out for *Ebf4* and *Mxd4*. *Bhlhb2* (Sun et al., 2001), *Mlxipl* (Iizuka et al., 2004), *Ahrr* (Hosoya et al., 2008) and *Bhlhb4* (Bramblett et al., 2004) knockouts are viable and fertile, which rules out critical roles for these genes in sex-specific differentiation of GCs.

### *The Myc Antagonist Mnt is Enriched in Male E13.5 GCs*

The bHLH-Zip *Mnt* was enriched 3-fold in male GC cDNA. Because of its role in suppressing the cell cycle by antagonising Myc activity (Hooker and Hurlin, 2006), it was decided to look into GC expression of *Mnt* more closely and ask the question of whether *Mnt* could be involved in the developmental decision of male GCs to enter mitotic arrest at E12.5. This male-specific *Mnt* mRNA enrichment was confirmed at the protein level by Mnt immunofluorescence, which found 2-fold higher Mnt immunofluorescence levels in E13.5 male GC nuclei compared to female GC nuclei. According to this, male GCs express higher Mnt protein than female GCs at E13.5, but the actual sex-specific fold-enrichment of male Mnt levels would be higher than 2-fold if corrected for background. Mnt antagonises Myc-induced S-phase entry via 2 mechanisms

(Hooker and Hurlin, 2006). Firstly, Mnt competes with Myc for binding to Max, which is required for Myc function. Secondly, Mnt-Max heterodimers compete with Myc-Max heterodimers for binding to the same promoter target sequences, and inhibits their expression. Some of these Myc targets are *Cyclins A1*, *B*, *D1*, *D2* and *E1*, *Cdk4* and *E2F2* (Walker et al., 2005), expression of which stimulates progression through various cell cycle transitions for example by phosphorylating retinoblastoma protein (Rb) and removing Rb-mediated inhibition of S-phase entry (Trimarchi and Lees, 2002). Acute removal of c-Myc from murine embryonic fibroblasts by Cre-mediated recombination results in almost complete loss of S phase entry (Walker et al., 2005). In these cells, simultaneous removal of Mnt restores S-phase entry to nearly wild-type levels, indicating that in the absence of c-Myc, Mnt prevents cell cycle entry. A possible mechanism for this is hypophosphorylation of Rb, because acute removal of Mnt results in hyperphosphorylation of Rb. Between E12.5 and E13.5, Rb in male GCs is completely converted from a hyperphosphorylated form into a hypophosphorylated form (Western et al., 2008) and this might contribute to mitotic arrest of male GCs. Is higher Mnt protein in male GCs responsible for this?

Mnt levels in male E13.5 GCs are not consistently high, and furthermore, Mnt immunostaining levels are very high at E11.5, when GCs are actively proliferating. Therefore, it seems unlikely that a change in Mnt levels can account for mitotic arrest of male GCs at E13.5. Instead, a theoretical role for Mnt in stimulating or augmenting mitotic arrest of male GCs would be that a drop in active Myc activity in E12.5-E13.5 male GCs allows cell cycle suppression by Mnt, among other mechanisms. This is supported by data indicating that Mnt suppresses cell-cycle re-entry and proliferation of cells in which *c-Myc* is removed, because subsequent removal of *Mnt* rescues these cell cycle defects ((Nilsson et al., 2004; Walker et al., 2005). Furthermore, many of the hallmarks of *c-Myc* or *N-Myc* gene removal, including delay of cell-cycle re-entry and embryonic lethality, are phenocopied by *Mnt* overexpression (Hurlin et al., 1997; Walker et al., 2005). Another conclusion from the current data

could be that Mnt is not required for mitotic arrest of E13.5 male GCs and the sex-specific difference in Mnt levels is simply a consequence, rather than a cause, of sex-specific differentiation of GCs. Similarly, high Mnt protein expression in E11.5 GCs might be a result of high Myc activity in E11.5 GCs, because Mnt levels are responsive to acute changes *c-Myc* expression (Walker et al., 2005).

One interesting finding is that E11.5 GCs, both in male and female genital ridges, have very high nuclear Mnt immunofluorescence and are potentially the highest Mnt-expressing cells in the genital ridges at that stage. This is surprising because E11.5 GCs are actively proliferating, and may indicate that proliferation of GCs at this developmental stage occurs through Myc-independent pathways. Alternatively, these high Mnt levels are insufficient to completely block GC proliferation, which is supported by the fact that ectopic expression of Mnt in fibroblasts slows but does not completely block cell cycle progression (Walker et al., 2005) and also that both migratory and post-migratory GCs have a doubling time of roughly 16 hours, which is slower than their proliferation before specification (Lawson and Hage, 1994; Tam and Snow, 1981). Comparing the consistently high Mnt levels at E11.5 with the low Mnt levels at E13.5 suggests that female GCs downregulate Mnt between E11.5 and E13.5 as they prepare for meiosis. This might be a mechanism to prevent Mnt from interfering with meiotic entry.

### *Multiple Id Genes are Enriched in Female E13.5 GCs*

The *Id* genes have very well-documented roles in stimulating S-phase and proliferation, which is why knockout of the *Ids*, especially *Id1*, *Id3* and *Id4*, results in decreased proliferation of various stem cell populations *in vivo*. In this screen, *Id1* and *Id3* were female-specifically enriched in E13.5 GC cDNA, by roughly 40-fold and 15-fold, respectively. *Id1* and *Id3* expression was also detected in E13.5 female GC cDNA libraries by single-cell reverse transcription PCR, indicating that *Id1* and *Id3* are expressed by female GCs and partially

validating the female-specific *Id1* and *Id3* enrichments detected in the bHLH screen. Immunofluorescence experiments also showed that female GCs express significantly higher levels of Id1 protein at E13.5 and probably E12.5 also. Could the Ids have roles in promoting meiotic entry of female GCs?

Ids stimulate the cell cycle in a variety of ways, but in particular by inhibiting transcriptional activation of Cyclin-dependent kinase inhibitor (CDKI) genes mediated by Class A/B bHLHs (Garrett-Engele et al., 2007; Liu et al., 2004; Prabhu et al., 1997; Rothschild et al., 2006) and by increasing expression of *Cyclins D1* and *E1* (Jeon et al., 2008; Swarbrick et al., 2005), leading to increased CyclinD/E-Cdk activity (Swarbrick et al., 2005). Meiotic defects in knockout animals of Cdk2 (Berthet et al., 2003; Ortega et al., 2003) and Cyclin A1 and expression of Cyclin A2 in E13.5-E15.5 female GCs (Persson et al., 2005) suggests that Id1 could affect the later stages of prophase I by stimulating expression of these genes. However, no role has yet been shown for Cyclins or Cdks in meiotic initiation of mouse GCs (Satyanarayana and Kaldis, 2009), and the expression of Id1 was not assessed at later meiotic stages.

Data from several studies suggests that *Id1* and/or *Id3* are dispensable for the initiation or progression meiosis. Nuclear Id1 and Id3 immunostaining is absent in spermatogonial stem cells, differentiating spermatogonia and early spermatocytes in the adult testis (Sablitzky et al., 1998). Additionally and more importantly, are the findings of one study that rescued the embryonic lethality of *Id1*/*Id3* double knockout mice (Fraidenraich et al., 2004). Double knockout of Id1 and Id3 results in embryonic lethality due to defects in cardiac development. However, the cardiac defects were rescued by injection of wildtype embryonic stem cells into the knockout blastocysts and the resultant chimaeric females were fertile and transmitted $Id1^{-}/Id3^{-}$ alleles to offspring when mated with $Id1^{-/-}/Id3^{+/-}$ male mice. This indicates that neither *Id1* nor *Id3* are required cell-autonomously for female GCs to initiate and successfully proceed through meiosis.

*Id2* was upregulated 30-fold in female GC cDNA but was not detected in female GC cDNA libraries by single-cell reverse transcription PCR, possibly due to a splice form not detected by the single-cell primers or because the single-cell PCR method was unable to detect *Id2* transcripts from single cells. GC expression of *Id2* splice variants was not explored in this study, but should be investigated. A role for *Id2* in GC cell cycle control – either mitotic or meiotic – is attractive because of Id2's unique ability to directly inhibit Rb (Lasorella et al., 2000), in addition to the general mitogenic abilities of the Ids (Liu et al., 2004). However, *Id2* knockout female mice are fertile and able to produce offspring, although are unable to wean them due to a lactation defect (Mori et al., 2000). Therefore, *Id2* does not have a non-redundant role in female GC development. However, it is possible that only one of *Id1*, *Id2* and *Id3* is needed for any non-redundant role of these three genes in triggering meiosis.

### *Lack of Id Protein in Male GCs Could Facilitate Mitotic Arrest*

This study shows that the sex-specific difference of Id1 protein levels first appears between E11.5 and E12.5. At E11.5, at a time when male GCs are actively proliferating at a high rate as shown by high BrdU incorporation (Western et al., 2008), male GCs express heterogeneous levels of Id1 protein, and this expression may relate to the phase of the cell cycle the GCs are in. To show this would require a quantitative analysis of Id1 protein expression in male E11.5 GCs, which was not carried out in this study. At E12.5 male GCs are committed to spermatogenesis and begin to enter mitotic arrest (Adams and McLaren, 2002; McLaren and Southee, 1997), and this coincides with almost a complete loss of detectable levels of Id1 protein in E12.5 male GCs. The marked disappearance of Id1 protein in male GCs between E11.5 and E12.5 will serve as a useful marker for GCs committed to spermatogenesis, but also provides a plausible mechanism for augmentation of mitotic arrest of male GCs at E12.5.

Loss of Id protein in male GCs would facilitate mitotic arrest of male GCs by at least 2 mechanisms – decreased Cyclin expression and increased CDKI

expression, both of which would lead to Rb hypophosphorylation and inhibition of S-phase entry. Previous characterisation of cell cycle components in male GCs shows that Rb is present and hyperphosphorylated at E12.5, but by E13.5 becomes hypophosphorylated, concomitantly with downregulation of *Cyclin E* (Western et al., 2008). Downregulation of Id1 by siRNA expression in breast epithelial cells has previously been shown to result in reduced Cyclin E-Cdk2 activity and pRB hypophosphorylation, and this was associated with decreased expression of *Cyclin E* and *Cyclin D1* (Swarbrick et al., 2005).

Western and colleagues found that male GCs express higher p21 and p27 protein than female GCs at E13.5, and found that p27 protein levels increased between E12.5 and E13.5 in male GCs, concomitantly with Rb dephosphorylation (Western et al., 2008). Previous studies utilising Id-knockdown or knockout strategies have demonstrated that Id proteins reduce proliferation and prevent differentiation by inhibiting expression of *p21* in endothelial progenitors *in vivo* (Ciarrocchi et al., 2007) and fibroblasts *in vitro* (Li et al., 2005a), *p27* in cultured fibroblasts (Chassot et al., 2007) and human lymphomas (Garrett-Engele et al., 2007), and *p16* in cultured human fibroblasts (Zheng et al., 2004). Therefore, decreased *Id1* in E12.5-E13.5 male GCs expression could result in increase *p21* and *p27* expression and this could translate into sex-specific increases in p21 and p27 protein expression, which could contribute to male GC mitotic arrest.

Ids suppress CDKI expression by inhibiting the activity of various transcription factors, including ELK1 (Chassot et al., 2007), Ets1/2 (Ohtani et al., 2001; Stinson et al., 2003), Polycistins (Li et al., 2005b) and positively acting bHLHs (Garrett-Engele et al., 2007; Liu et al., 2004; Prabhu et al., 1997), all of which contribute to cell cycle arrest in cells in which they are expressed. All 3 Class A bHLHs (*E2A*/*Tcfe2a*, *E2-2*/*Tcf4* and *HEB*/*Tcf12*), were detected non-sex-specifically in E13.5 GC cDNA, and *Helt* and *Ngn3* were detected male-specifically in the current study and, if they are expressed in male GCs, are therefore potential targets for Id-mediated repression of mitotic arrest.

Other bHLHs were detected non-sex-specifically but much more readily in E13.5 GC cDNA than positive control cDNA, and are therefore promising candidates for GC-specific Class A bHLH heterodimer partners susceptible to Id1 inhibition. These include *Sohlh1* and *Sohlh2*, which are required for male and female GC differentiation (Choi et al., 2008; Hao et al., 2008; Pangas et al., 2006; Toyoda et al., 2009). Additionally, *Tcfeb*, which has a testis-specific splice form (Steingrimsson et al., 1998), and *Tcfl5* (Siep et al., 2004), which is expressed in spermatocytes and controls Calmegin gene transcription, may have roles in GC development and might serve as targets for inhibition by Id1. The male-enriched Mnt would not be expected to interact with Id proteins as it belongs to the Max-network of bHLH-Zips, which generally do not interact with Ids and other non-bHLH-Zip bHLHs (Loveys et al., 1996; Murre et al., 1989).

### *Sex-specific Signaling Could Affect GC Id Expression*

A variety of different signaling pathways stimulate Id expression. Most notably, exposure of cells to serum (Barone et al., 1994; Hara et al., 1994) and BMPs (Hollnagel et al., 1999; Nakashima et al., 2001; Ying et al., 2003) results in increased Id gene activation. BMPs are involved in multiple stages of GC development, such as primordial germ cell specification (Lawson et al., 1999; Ying et al., 2000; Ying and Zhao, 2001) and spermatogenesis (Zhao and Hogan, 1996). Knockout of *Bmp7* results in reduced levels of proliferation of E10.5-E11.5 mouse GCs according to phospho-Histone H3 staining, and the magnitude of the effect is more severe for GCs in male genital ridges (Ross et al., 2007), suggesting that there are sex-specific compensatory mechanisms in operation. The female genital ridge at E11.5 and E12.5 has higher *Bmp2* and *Bmp4* expression (Ross et al., 2007; Yao et al., 2004), and this could compensate for *Bmp7* knockout in female E11.5-E12.5 genital ridges. The effect of lower BMP dosage on GC proliferation in the *Bmp7* knockout might be mediated by a decrease in *Id* expression, because BMP stimulation of proliferation in other systems requires *Id* expression (Hua et al., 2006). Similarly, sex-specifically

lower *Bmp2* and *Bmp4* expression in male gonads at E11.5-E13.5 could cause the lower *Id* expression seen in this screen and Id1 immunostaining in E12.5 and E13.5 male gonads.

Interestingly, a number of studies report that FGF signaling has a negative impact on *Id* expression. FGF signaling through its receptors, such as Fgfr3, inhibits *Id1* expression and induces mitotic arrest in chondrocytes (Rozenblatt-Rosen et al., 2002), and also induces mitotic arrest of neuroblastoma cells that is associated with changes in Id1, Id2 and Id3 cellular localisation and enhanced *p21* expression (Higgins et al., 2009). FGF9 signaling serves as an essential reinforcement mechanism to ensure Sertoli Cell differentiation during the first stages of sex-specific testis development at E11.0-E12.5 (Colvin et al., 2001; Kim et al., 2006). In *Fgf9* knockout gonads, a direct effect of *Fgf9* removal on GCs was not analysed, but E11.5-E13.5 GCs express multiple FGF receptors (Resnick et al., 1998; Schmahl et al., 2004) and are receptive to FGF signals (Resnick et al., 1998), so it is possible that FGF9 signaling in the differentiating male gonad could block *Id* expression in E12.5-E13.5 GCs.

# Chapter 4:
# Investigation of Sex-specific *Ptgds* Expression in E13.5 Male GCs

# 4.1. Chapter Introduction and Aims

Ptgds, a Prostaglandin $D_2$ ($PgD_2$) producing enzyme that is also a lipophilic molecule binding protein (Urade and Hayaishi, 2000), is sex-specifically upregulated in male gonads from E11.5 (Adams and McLaren, 2002). In embryonic gonad development, Ptgds has a role in augmenting testis development, because *Ptgds* knockout in C57BL/6 mice results in a delay in testis development (Moniot 2009).

This phenotype of C57BL/6 *Ptgds* knockout mice is probably due to the $PgD_2$-producing, rather than the lipocalin, function of Ptgds, for several reasons. $PgD_2$ partially masculinises cultured bipotential XX gonads (Adams and McLaren, 2002). This masculinising effect of $PgD_2$ is due to sex-reversal of XX supporting cells to a Sertoli cell fate via $PgD_2$-mediated activation of intracellular cAMP and upregulation of *Sox9* mRNA and protein expression in these cells (Malki et al., 2005; Wilhelm et al., 2005). $PgD_2$ is also able to recruit non-Sry-expressing XY somatic cells to a Sertoli cell fate by an identical mechanism (Wilhelm et al., 2005), and loss of this supplementary masculinising pathway probably accounts for the delay caused by *Ptgds* knockout in C57BL/6 mice.

*Ptgds* mRNA has been detected in the cytoplasm of both Sertoli cells and GCs by in situ hybridisation (Adams and McLaren, 2002). However, others dispute whether GCs express *Ptgds* mRNA (Wilhelm et al., 2007), even though Ptgds protein expression is detectable in GCs by immunostaining (Wilhelm et al., 2007).

The aim of the experiments in this chapter is to clarify whether E13.5 male GCs, which are committed to spermatogenesis, express *Ptgds*, whether they express any GC-specific isoforms of *Ptgds*, and whether they express Ptgds protein. In a second set of experiments, this study aims to identify candidate signaling pathways controlling sex-specific commitment of GCs to spermatogenesis using Ptgds expression as a marker for spermatogenically-committed GCs.

## 4.2. Characterisation of Male-Specific Expression of Ptgds

### 4.2.1. *Ptgds* PCR Analysis of E13.5 GC cDNAs

PolyA$^+$ mRNA was prepared from purified E13.5 male and female GCs and GFP$^-$ cells, which were purified and collected as described in the previous section, alongside E13.5 male and female genital ridge cells. The GC, GFP$^-$ and genital ridge mRNAs were reverse transcribed, resulting in GC RT$^+$, GFP$^-$ RT$^+$ and GR RT$^+$ cDNAs respectively. Mock reverse transcribed GC mRNAs were generated simultaneously resulting in GC RT$^-$ cDNAs.

GC RT$^+$, GC RT$^-$ and GFP$^-$ RT$^+$ cDNAs were checked by 30 cycles of end-point PCR for GC and somatic markers. The GC marker *Mvh* was detected in GC RT$^+$ cDNAs, but not in GC RT$^-$ cDNA or GFP$^-$ cDNAs. Conversely, the somatic markers *Gata4* and *Lhx9* were detected in GFP$^-$ cDNAs but not in GC RT$^+$ cDNAs (Figure 4.2.1A). Therefore, the patterns of GC and somatic cell expression are preserved in the generated GC RT$^+$ and GFP$^-$ cDNAs, and the lack of detection in GC RT$^-$ samples suggests that the detected products in the GC RT$^+$ samples is RT-dependent and originates from GC mRNA expression. In order to gauge the relative amounts of cDNA in the male and female GC RT$^+$ cDNAs, these cDNAs were checked by semi-quantitative PCR against the housekeeping genes *Glyceraldehyde 3-phosphate Dehydrogenase* (*Gapdh*) and *β-actin* (*Actb*) (Figure 4.2.1B). *Gapdh* and *Actb* expression was always similar for the male and female GC cDNAs.

Expression of somatic cell markers *Amh* and *SF-1* was tested for male and female, respectively, GC RT$^+$, GC RT$^-$ and GR RT$^+$ cDNAs by semi-quantitative PCR at 25, 30, 35 and 40 cycles of PCR. Detection of the somatic markers *Amh* in male GC cDNA and *SF-1* in female GC cDNA after 35/40 cycles (Figure 4.2.1C)

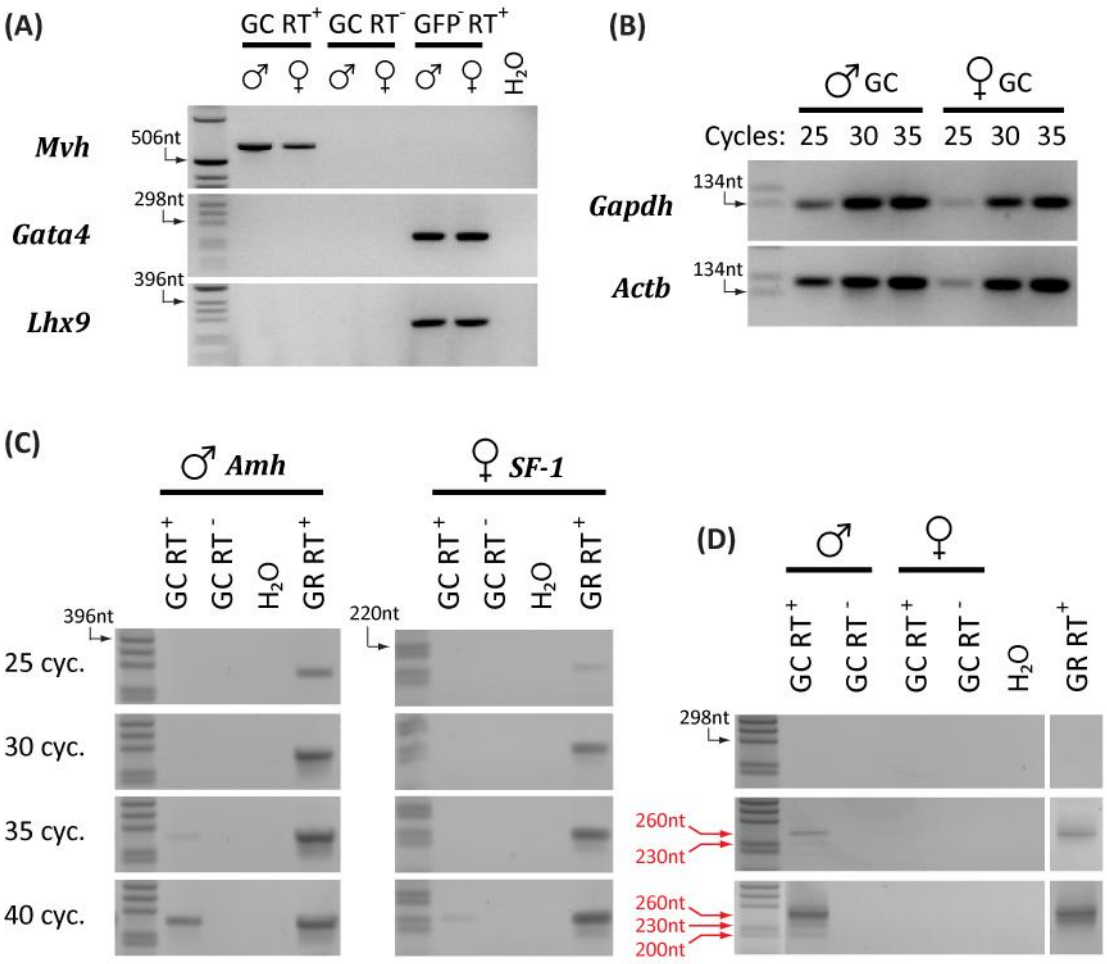


**Figure 4.2.1. Characterisation of FACS-purified E13.5 GC Populations by Reverse Transcription PCR.** E13.5 male and female GCs were purified as described in Section 3.2 (Figure 3.2.1). PolyA$^+$ mRNA was purified and reverse transcribed to make GC RT$^+$ cDNAs. Mock reverse transcribed samples (RT$^-$) were generated in parallel. male and female GC RT$^+$ and RT$^-$ samples, together with cDNA generated from the GFP- cell fraction obtained from FACS (GFP$^-$ RT$^+$), were checked for expression of the GC marker *Mvh*, and the somatic cell markers *Gata4* and *Lhx9*, by end-point PCR (30 cycles), (A). Semi-quantitative PCR, with aliquots removed for analysis at 25, 30, 35 and/or 40 cycles (as labeled above the gel in (B) and to the left of the gel in (C), was carried out on the male and female E13.5 GC RT$^+$ samples for analysis of the housekeeping genes *Gapdh* and *Actb*, (B), and the somatic cell markers *Amh* for male cDNAs and *SF-1* for female cDNAs, (C). E13.5 genital ridge cDNA samples (GR RT$^+$) were run alongside GC cDNAs for somatic cell marker expression in (C). *Ptgds* expression of GC RT$^+$, GC RT$^-$ and male GR RT$^+$ cDNAs was also assessed semi-quantitatively, (D), at 30, 35 and 40 cycles, as labeled to the left of the gel in (C). All these analyses were carried out on the same batch of GC cDNAs, and were replicated on 1 other batch of GC cDNA, with similar results. PCR products were analysed by gel electrophoresis with 1kb ladder (Invitrogen) run in the left-most lane of all gels. In all gels, black arrows with numbers indicate length of 1kb fragment, in nucleotides (nt). Red arrows with numbers in (D) represent approximate lengths of *Ptgds* PCR products according to the 1kb ladder.

shows that somatic cell gene expression is detectable in the GC cDNAs and likely originates from contaminating somatic cells in the purified GCs.

Equivalent amounts of cDNA according to housekeeping gene semi-quantitative PCR were analysed by PCR using primers against part of the *Ptgds* coding region that are able to detect both known *Ptgds* splice variants, which differ by only 33 nucleotides (nt) (Adams and McLaren, 2002). Various products were detected in male cDNAs, but not in female cDNAs throughout the *Ptgds* expression analysis. 2 products were detected in male GC cDNA after 35 cycles of PCR (Figure 4.2.1D). The larger product of roughly 260nt, which was more abundant than the smaller product of roughly 230nt, was also detected in male GR cDNA. This 260nt product corresponds to the larger splice form detected previously (Baker and O'Shaughnessy, 2001) and should give a product of 252nt using the current primers. The 230nt product was not detected in male GR cDNA, and was therefore specific to male GC cDNA after 35 cycles. The 230nt product corresponds to the shorter known splice form detected previously, which should give a product of 219nt with the current primers. At 40 cycles, the 260 and 230nt *Ptgds* products were more abundant in male GC cDNA, and a third product of roughly 200nt also appeared in male GC cDNA. The 230nt product was also detected in GR cDNA after 40 cycles.

A lack of detected product in the $RT^-$ samples suggests that the products detected in male GC cDNA originate from mRNA expression. Additionally, *Mvh* and housekeeping gene transcripts were readily detected in the female GC cDNAs, indicating that RT of the female samples occurred as expected and female GC expression is detectable. In summary, these data imply that detectable levels of *Ptgds* transcripts are expressed by cells in the male GC preparations, but not expressed by cells in the female GC preparations. The longer splice form detected here at 260nt in male GC cDNA could be originate from GC expression of the longer *Ptgds* splice form, or might originate from expression by somatic cell contamination in the male GC preparations. However, detection of *Amh*, which is expressed highly by E13.5 Sertoli cells, in the male GC cDNA occurred 10-15 cycles later than detection in male GR cDNA,

which is consistent with expression by a small contaminating population of cells. On the other hand, expression of the 260nt splice form of *Ptgds* appeared at the same time (after 35 cycles) in male GC cDNA and male GR cDNA, albeit at a lower level in male GC cDNA, and this is consistent with low level expression by GCs rather than the contaminating somatic cells. Therefore, the data do suggest that male GCs express the longer splice form of *Ptgds*.

Similarly, the 230nt product appeared first in male GC cDNA at 35 cycles but did not appear in GR cDNA until 40 cycles, indicating that the shorter known *Ptgds* splice form might be expressed GC-specifically in E13.5 male genital ridges. However, although the same amount of RNA was input into the male GC and GR cDNAs, housekeeping gene expression of these cDNAs was not compared directly, putting this conclusion in doubt. A more quantitative comparison of male GR cDNA with GC cDNA is required to make this a firm conclusion. The 200nt product detected only in male GC cDNA does not correspond to any previously identified splice form and could also represent a GC-specific splice form. In summary therefore, the presence of multiple *Ptgds* splice forms that were not detected in male GR cDNA, and of *Ptgds* amplification consistent with expression by the majority of cells, in FACS-purified GC cDNA indicates that GCs express multiple splice forms of *Ptgds*.

### 4.2.2. *Ptgds* Expression in E13.5 Single Gonadal Cell cDNA Libraries

15 E13.5 GC cDNA libraries from each sex that were generated and tested as described in the Section 3.5.1 (Figure 3.5.1 and 3.5.2 and Table 3.5.1) were selected for analysis of *Ptgds* expression, using different primers than those used for the *Ptgds* expression analysis of FACS-purified GC cDNAs in the previous section (Figure 4.2.1D). The primers used here recognise both splice forms of *Ptgds*, which differ by 33 nucleotides (nt) in the 3' un-translated region of the mRNA (Baker and O'Shaughnessy, 2001). *Ptgds* expression analyses of the first 5 of the 15 GC cDNA libraries are shown in Figure 4.2.2, together with no-RT control samples and somatic cell libraries. The male somatic cell libraries were *Sox9* positive and therefore probable Sertoli cell libraries. *Ptgds* transcripts were not detected in any of the 15 GC libraries of either sex. However, *Ptgds* transcripts were detected in male somatic cell libraries, indicating that *Ptgds* expression is detectable in the single-cell libraries. A major product of roughly 175nt was detected in both male somatic cell libraries, and this corresponds to the longer known *Ptgds* splice form (Baker and O'Shaughnessy, 2001). A minor product of roughly 150nt was also detected in one of the 2 male somatic libraries, and this corresponds to the shorter known splice variant. Detection of the shorter splice form in this male Sertoli cell library suggests that Sertoli cells may express the shorter splice form in addition to the longer *Ptgds* splice form at detectable levels. A second primer set, using primers designed specifically to recognise the longer *Ptgds* splice variant gave similar results – with products detected only in the male somatic cell libraries.

This lack of *Ptgds* detection in E13.5 male GC cDNA libraries is in direct contradiction to the results of the previous section that detected 3 *Ptgds* splice forms after 40 cycles of PCR in FACS-purified E13.5 male, but not female, GCs (Figure 4.2.1). The primer set used in this single-cell analysis should be able to

detect the same *Ptgds* splice forms as the set used in the FACS analysis because they are designed to the same region of the *Ptgds* gene. The results from the previous section attribute the detected *Ptgds* products to GC-specific expression; therefore, the most likely explanation for the lack of detection in the male GC libraries is because the *Ptgds* expression level in male GCs is below the detection limit of this single-cell assay.

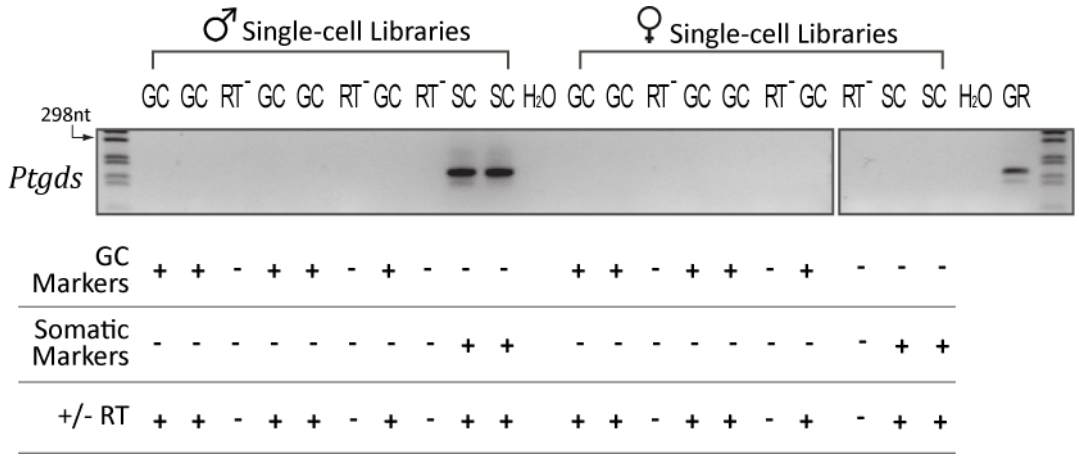


**Figure 4.2.2. *Ptgds* PCR of Male and Female Single-Cell cDNA Libraries.** Germ cell ("GC") and somatic cell ("SC") cDNA libraries were generated, alongside no RT ("RT$^-$") control libraries, from single E13.5 male and female gonadal cells as described in Section 3.5.1, and were positive or negative for GC and somatic markers, as labeled ("+" or "-"), when tested by PCR. 5 of these libraries from each sex were analysed for expression of *Ptgds*, along with 3 no–RT controls, 2 SC libraries and negative and positive PCR controls that consisted of $H_2O$ or mixed E13.5 male and female genital ridge cDNA (GR), respectively. Products were run on agarose gels with 1kb DNA ladders run in the right- and left-most lanes. The arrow shows the size of the fragment in the 1kb ladder in nucleotides (nt).

## 4.2.3. Ptgds Immunostaining of E13.5 Testes

In the previous sections, it was shown that male GCs sex-specifically express Ptgds *mRNA*. To see whether male GCs express Ptgds protein, E13.5 testis sections were treated with Ptgds antibodies (Figure 4.2.3). E13.5 testes were wax-embedded, sectioned then processed for immunostaining using antibodies against Ptgds and Amh to mark Sertoli cell cytoplasm. Ptgds immunostaining was highest in cells in the testis cords, which agrees with *in situ* hybridisation *Ptgds* signal that is restricted to the cords in embryonic testis (Adams and McLaren, 2002). In the cords, both $Amh^+$ Sertoli cells and large, spherical $Amh^-$ GCs had roughly the same amount of Ptgds immunostaining signal, and that signal was higher in non-DAPI-stained cytoplasmic areas of stained cells. No IgG negative control was carried out in this experiment, so it is impossible to say with certainty that the Ptgds immunostaining observed is different from background staining.

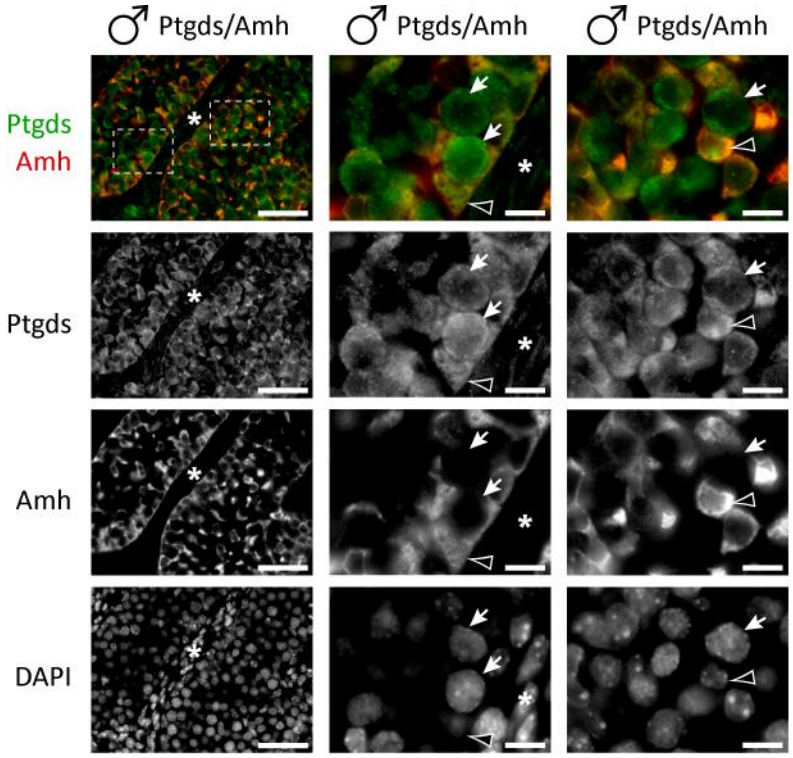


**Figure 4.2.3. Ptgds Immunofluorescence staining of E13.5 Testes.** E13.5 testes were embedded in wax, sectioned then processed for immunostaining after antigen retrieval. Sections were stained with Ptgds antibodies, along with Amh antibodies to mark Sertoli cell cytoplasm and DAPI to mark cell nuclei. Separate images were recorded for green fluorescence (Ptgds), red fluorescence (Amh) and blue fluorescence (DAPI) channels for representative areas of the gonad sections. Channels from the same area are shown as stacked vertical images, in the order: Red/green combined, green, red then blue, top to bottom. Images in the left column are x40 images of a gonadal section that intersects 2 cords, scale bar 50µm. Asterisks mark the interstitial area and white dashed boxes mark areas zoomed to in the images in the middle and right columns. In the middle and right columns, scale bars are 10µm, white arrows mark GCs, black arrows with white outlines mark Sertoli cell nuclei, and asterisks mark the interstitial area.

## 4.2.4. *Ptgds* Expression in XX*Sry* and XY$^{Tdym1}$ Gonads

The results from the previous sections in this chapter suggest that GCs do express *Ptgds*, but at a lower level than do Sertoli cells, which is in keeping with previous data showing that *Ptgds* mRNA expression is detected more readily in Sertoli cell cytoplasm (Wilhelm et al., 2007). Recent data describes that Ptgds expression in E12.0-E14.5 XY gonads is dependent upon Sox9 expression, because *Ptgds* expression is heavily downregulated in XY gonads in which Sox9 is conditionally knocked out (Moniot et al., 2009). That study went on to show that Sox9 directly activates Sertoli cell Ptgds expression in XY gonads. Because *Sox9* expression in the embryonic gonad is dependent upon *Sry* expression (Sekido and Lovell-Badge, 2009), it is logical to assume that Sertoli cell Ptgds expression is also dependent upon Sry expression.

In the current study, wholemount *in situ* hybridisation was carried out on XX*Sry* transgenic and XY*Sry* knockout gonads to find out whether *Ptgds* expression is in fact dependent upon *Sry*. Gonads from XY$^{Tdym1}$ embryos develop as ovaries because of *Sry* deletion, while insertion of an autosomally located *Sry* transgene causes gonads from XX*Sry* embryos to develop as testes (Durcova-Hills et al., 2004). Gonads from these mice were removed at E13.5 and *Ptgds* expression analysed by *in situ* hybridisation (Figure 4.2.4). 3/3 wildtype E13.5 XY testes were positive for *Ptgds* staining in the testis cords, while 4/4 E13.5 XY$^{Tdym1}$ ovaries were negative for *Ptgds* staining. Conversely, 4/4 wildtype E13.5 XX ovaries were negative for *Ptgds* staining, while 3/3 E13.5 XX*Sry* testes were positive for *Ptgds* in the testes cords, identical to wildtype E13.5 testes. These results indicate that *Ptgds* expression in the developing gonad is dependent upon the presence of *Sry*.

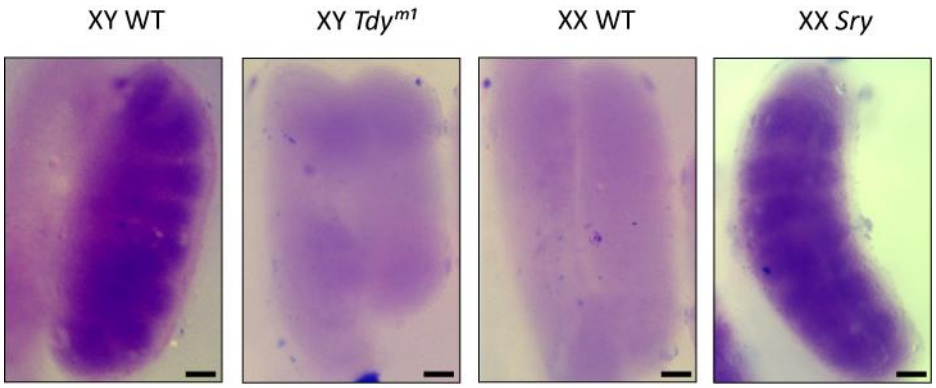


**Figure 4.2.4. Ptgds Expression in E13.5 XY$^{Tdym1}$ and XX*Sry* Transgenic Gonads.** E13.5 testes were dissected, processed for *in situ* hybridisation against *Ptgds* and images captured by stereo microscopy. Representative images are shown. Positive *in situ* signal appears as purple stain, as seen in the WT testis, and is not to be confused with blue precipitate on the surface of all GRs. Scale bars are 10µm.

## 4.3. Inducing/Suppressing *Ptgds* Expression in Cultured Genital Ridges (GRs)

The previous sections in this chapter displayed that male GCs sex-specifically express *Ptgds* at E13.5. Therefore, *Ptgds* expression is a marker for male-specific differentiation of GCs. The purpose of this study was to attempt to activate or repress *Ptgds* expression in E13.5 female or male GCs, respectively, in order to identify upstream pathways contributing to the sex-specific differentiation of GCs *in vivo*. Previous studies show that treatment of cells with 12-O-Tetradecanoylphorbol-13-acetate (TPA) can either activate (Fujimori et al., 2005) or repress (Garcia-Fernandez et al., 2000) *Ptgds* expression. TPA treatment in these studies was shown to activate PKC to affect *Ptgds* gene transcription. Dexamethasone (Garcia-Fernandez et al., 2000) and T3 (Garcia-Fernandez et al., 1998; White et al., 1997) have also been characterised for their ability to activate *Ptgds* expression via glucocorticoid receptor activation and thyroid hormone receptor activation, respectively. Therefore, TPA, Dexamethasone and Thyroid Hormone (T3) were tested for their ability to activate or repress *Ptgds* expression in embryonic female or male GCs, respectively. ionomycin, a calcium ionophore that activates PKC in treated cells (Webb and Miller, 2003), was also tested for its ability to affect *Ptgds* transcription in embryonic GCs.

E11.5 genital ridges (GRs) were sexed by PCR before being cultured for 48 hours in their respective compounds or vehicles. After this time, the genital ridges were processed for wholemount *in situ* hybridisation (WISH) against *Ptgds* to check for changes in expression of *Ptgds*. In separate experiments, the cultured GRs were processed for immunostaining against GCNA to check that GCs had survived in the gonads.

In total, 5 female GRs were cultured in TPA, 5 were cultured in ionomycin, 12 were cultured in T3 and 11 were cultured in Dexamethasone. All GRs were

negative for *Ptgds* detection by WISH (Figure 4.3.1A and C, and 4.3.1A and C), while simultaneously-processed E13.5 wildtype testis were positive for *Ptgds.*

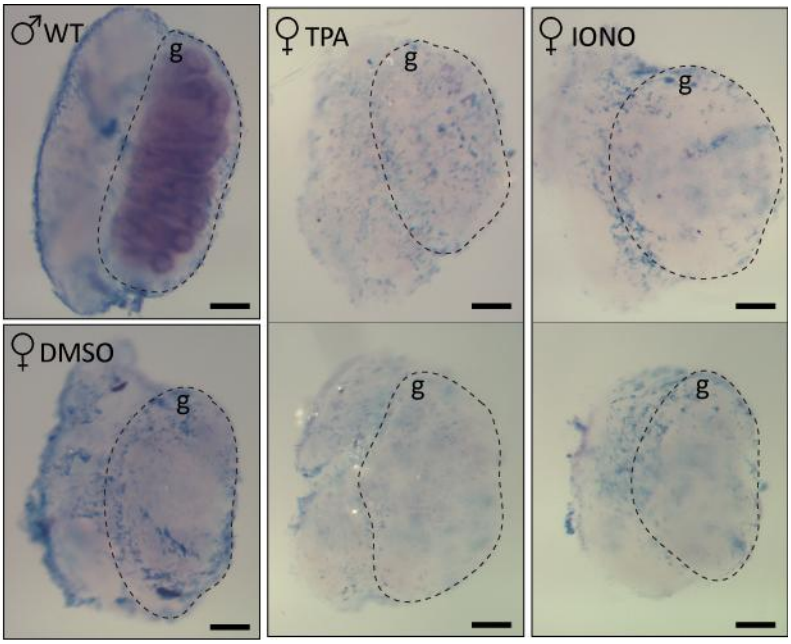


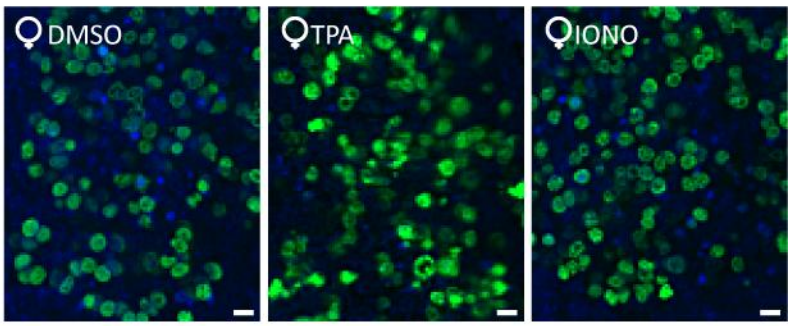


(C)

| Treatment | *Ptgds* WISH | | GCNA immuno | |
|---|---|---|---|---|
| | GRs Negative | Bio. Reps. | GRs Positive | Bio. Reps. |
| *DMSO* | 3/3 | 1 | 9/10 | 3 |
| *TPA* | 5/5 | 1 | 7/9 | 2 |
| *IONO* | 5/5 | 1 | 3/3 | 1 |

**Figure 4.3.1. *Ptgds* Expression in Female GRs Cultured With TPA and Ionomycin.** Female E11.5 GRs were cultured for 2 days with 160nM 12-O-Tetradecanoylphorbol-13-acetate (TPA), 1µM ionomycin or vehicle (DMSO), as labeled. After culturing, GRs were processed for wholemount in situ hybridisation, alongside E13.5 wildtype (WT) testes, using a probe against Ptgds, (A). Scale bars in (A) are 100µm and the areas of the GRs enclosed by dashed lines, marked with "g" are the gonads. Positive in situ signal appears as purple stain, as seen in the WT testis, and is not to be confused with blue precipitate on the surface of all GRs. In separate experiments, identically cultured GRs were processed for immunostaining against GCNA (green signal) to assess GC survival, (B). DAPI was included to stain all nuclei (blue signal). Representative images were recorded and are shown here, scale bars are 10µm. The total number of GRs having negative Ptgds in situ signal or positive GCNA immunostaining, out of the number tested, is shown in (C), along with the number of biological replicates carried out ("Bio. Reps.").

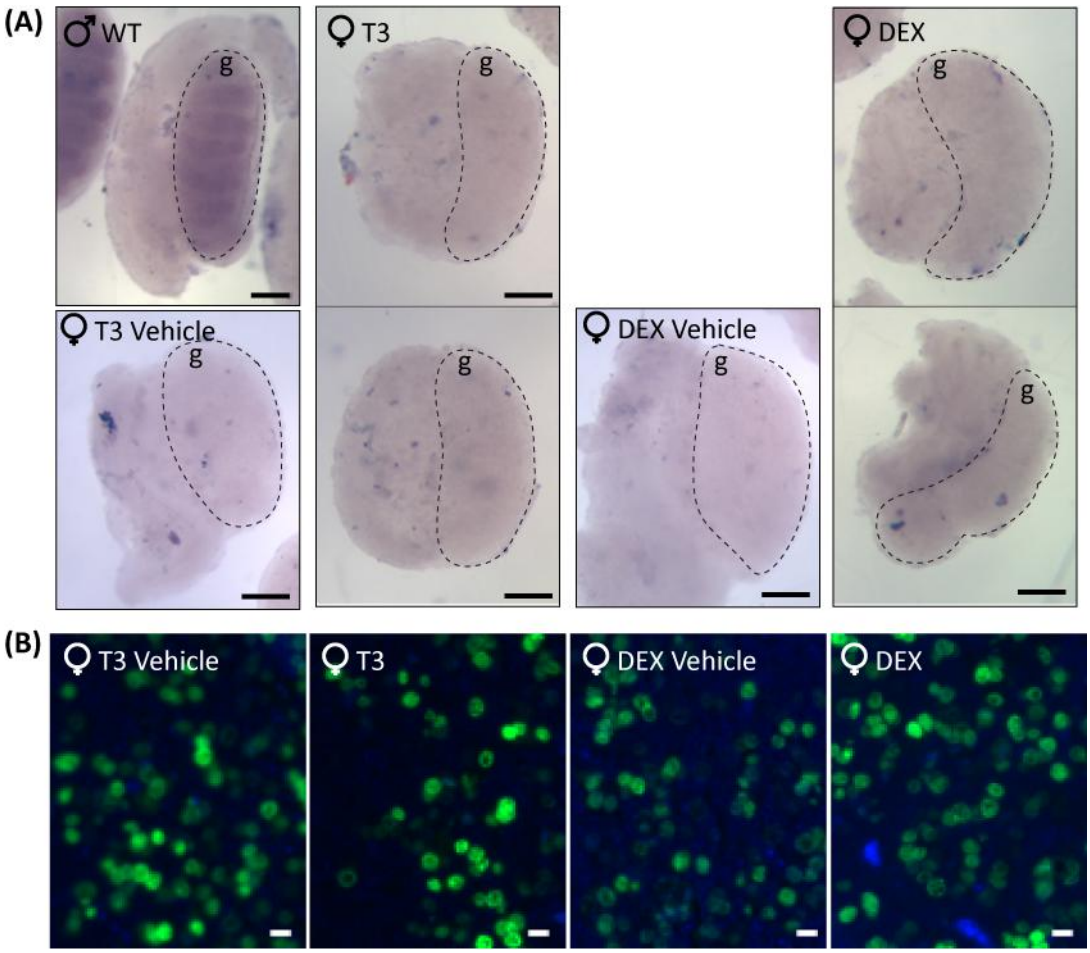


(C)

| Treatment | *Ptgds* WISH | | GCNA immuno | |
|---|---|---|---|---|
| | GRs Negative | Bio. Reps. | GRs Positive | Bio. Reps. |
| ***T3 Vehicle*** | 13/13 | 3 | 3/3 | 1 |
| ***T3*** | 12/12 | 3 | 4/4 | 1 |
| ***DEX Vehicle*** | 10/10 | 3 | 4/4 | 1 |
| ***DEX*** | 11/11 | 3 | 5/5 | 1 |

**Figure 4.3.2. *Ptgds* Expression in Female GRs Cultured With T3 and DEX.** Female E11.5 GRs were cultured for 2 days with 100nM 3,3′,5-Triiodo-L-thyronine (Thyroid Hormone, T3), 100nM Dexamethasone (DEX) or their respective vehicles, NaOH or Ethanol, as labeled. After culturing, GRs were processed for wholemount *in situ* hybridisation, alongside E13.5 wildtype (WT) testes, using a probe against *Ptgds*, (A). Scale bars in (A) are 100µm and the areas of the GRs enclosed by dashed lines, marked with "g" are the gonads. Positive *in situ* signal appears as purple stain, as seen in the WT testis, and is not to be confused with blue precipitate on the surface of all GRs. In separate experiments, identically cultured GRs were processed for immunostaining against GCNA (green signal) to assess GC survival, (B). DAPI was included to stain all nuclei (blue signal). Representative images were recorded and are shown here, scale bars are 10µm. The total number of GRs having negative *Ptgds in situ* signal or positive GCNA immunostaining, out of the number tested, is shown in (C), along with the number of biological replicates carried out ("Bio. Reps.").

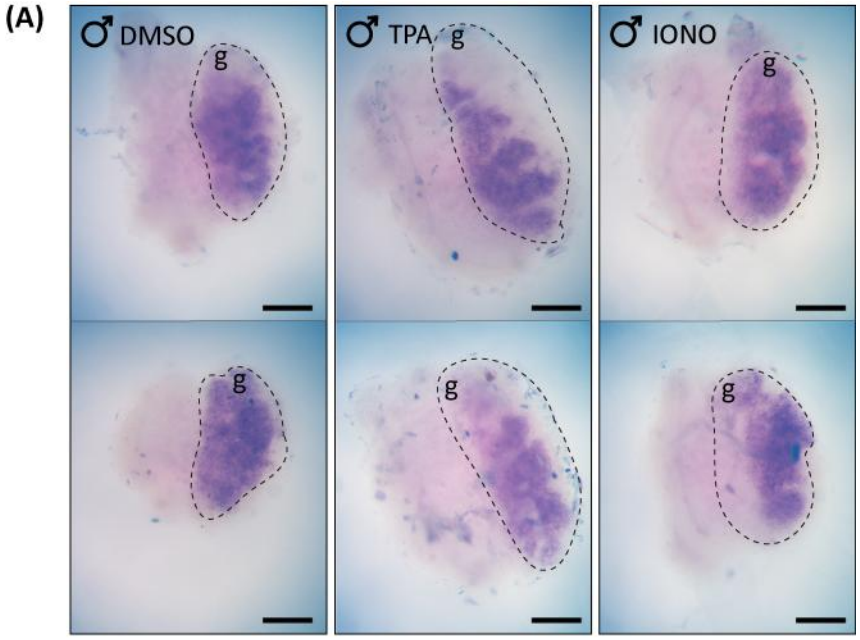


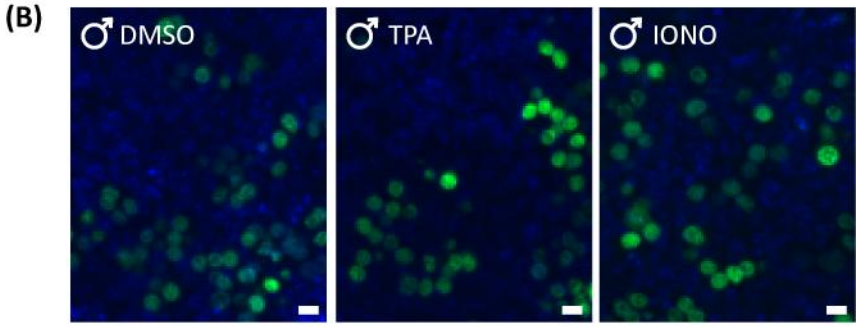


(C)

| Treatment | *Ptgds* WISH | | GCNA immuno | |
|---|---|---|---|---|
| | GRs Positive | Bio. Reps. | GRs Positive | Bio. Reps. |
| ***DMSO*** | 9/9 | 2 | 8/10 | 2 |
| ***TPA*** | 10/10 | 2 | 5/5 | 1 |
| ***IONO*** | 9/9 | 2 | 4/6 | 1 |

**Figure 4.3.3. *Ptgds* Expression in Male GRs Cultured With TPA and Ionomycin.** Male E11.5 GRs were cultured for 2 days with 160nM 12-O-Tetradecanoylphorbol-13-acetate (TPA), 1µM ionomycin or vehicle (DMSO), as labeled. After culturing, GRs were processed for wholemount *in situ* hybridisation using a probe against *Ptgds*, (A). Scale bars in (A) are 100µm and the areas of the GRs enclosed by dashed lines, marked with "g" are the gonads. Positive *in situ* signal appears as purple stain, as seen in the cultured male gonads, and is not to be confused with blue precipitate on the surface of some GRs. In separate experiments, identically cultured GRs were processed for immunostaining against GCNA (green signal) to assess GC survival, (B). DAPI was included to stain all nuclei (blue signal). Representative images were recorded and are shown here, scale bars are 10µm. The total number of GRs having negative *Ptgds in situ* signal or positive GCNA immunostaining, out of the number tested, is shown in (C), along with the number of biological replicates carried out ("Bio. Reps.").

WISH staining, showing that the probe and protocol were able to detect *Ptgds* transcripts. Therefore, under the culture conditions used, the concentrations of TPA, ionomycin, T3 and Dexamethasone tested failed to induce detectable levels of *Ptgds* expression in female GRs.

It is possible that one or more of the compounds did in fact induce *Ptgds* expression in GCs, but the treatments caused the GCs to die, resulting in loss of detection of the induced *Ptgds* expression. To rule this possibility out, GCNA immunostaining of identically cultured GRs showed that, in a vast majority of cases (7/9 for TPA, 3/3 for ionomycin, 4/4 for T3 and 5/5 for dexamethasone), treated GRs contained many GCNA$^+$ GCs, comparable in number to that in vehicle-cultured GRs (Figure 4.3.1B and C, and 4.3.2B and C). 2/9 GRs cultured in TPA contained very few GCNA$^+$ GCs after culturing (0-5 per 6μm section). However, GC loss also occurred in 1/10 cultured in DMSO vehicle, indicating that these occurrences were probably not due to addition of TPA. The absence of *Ptgds* expression in the treated female GRs also indicates that these compounds were unable to stimulate *Ptgds* expression in female somatic cells in the gonads. In summary, this data suggests that, at the concentrations tested, TPA, ionomycin, T3 and dexamethasone were unable stimulate detectable levels of *Ptgds* expression in surviving female GCs or somatic cells.

Because PKC activation has also been shown to inhibit *Ptgds* gene induction (Garcia-Fernandez et al., 2000), E11.5 male GRs were similarly cultured in TPA, ionomycin or vehicle DMSO, to see if these treatments could inhibit *Ptgds* expression in male GCs. The results from this analysis are shown in Figure 4.3.3. All 10/10 and 9/9 male GRs cultured in TPA and ionomycin, respectively, were positive for *Ptgds* WISH staining and had similar levels of *Ptgds* WISH staining as male GRs cultured in vehicle. 5/5 and 4/6 of the TPA- and ionomycin-cultured GRs were also positive for GCNA immunostaining showing that numerous GCs survived, similar to 8/10 DMSO-cultured GRs that also had numerous GCNA$^+$ GCs. The nature of this WISH protocol means that WISH signals are not quantifiable and/or not accurately representative of expression

levels. Therefore, quantification could not be carried out, and it cannot be ruled out that *Ptgds* expression dropped in one particular cell type, e.g. GCs. However, the data do suggest that culture of male GRs with TPA or ionomycin, at the concentrations tested here, does not overtly affect *Ptgds* expression of male GRs as measured by WISH.

# 4.4. Chapter Discussion

***Male GCs Sex-specifically Express Ptgds***

A role for *Ptgds* in embryonic testis development was first shown when Adams & McLaren (Adams and McLaren, 2002) found that *Ptgds* is enriched sex-specifically in male GC cDNA, and that exogenous $PgD_2$, Ptgds's catalytic product, partially sex-reverses cultured female gonads. Since then, further studies have shown that Ptgds augments male-specific gonad development by reinforcing Sertoli cell differentiation. Ptgds accomplishes this by increasing *Sox9* transcription (Moniot et al., 2009; Wilhelm et al., 2005) and enhancing nuclear localisation of Sox9 protein (Malki et al., 2005; Moniot et al., 2009), at least partially via $PgD_2$/cAMP/PKA signaling (Malki et al., 2005).

*Ptgds* expression in E13.5 testes is restricted to the testis cords (Adams and McLaren, 2002; Wilhelm et al., 2007). There are conflicting data with respect to which cell type in embryonic testis cords - GCs or Sertoli cells, or both - express *Ptgds*. *Ptgds* transcript has been detected by *in situ* hybridisation in apparent Sertoli cell and GC cytoplasm (Adams and McLaren, 2002). Others describe *Ptgds in situ* hybridisation signal, using probe generated from the same cDNA sequence as Adams & McLaren (Adams and McLaren, 2002), as having an opposite pattern to *Oct4* expression in E13.5 testes (Wilhelm et al., 2007), and therefore conclude that Sertoli cells but not GCs express *Ptgds*. However, in the Wilhelm paper, *Ptgds* in situ hybridisation signal that is slightly higher than background can be seen in GC cytoplasm in the images in that paper, albeit at a lower level than in Sertoli cell cytoplasm.

The current study aimed to clarify whether E13.5 male GCs express *Ptgds*. *Ptgds* transcripts were sex-specifically detected in purified male E13.5 GC cDNA by end-point PCR after 35 cycles of PCR, which was the same number of cycles after which *Ptgds* expression was detected in male genital ridge cDNA that was generated from the same amount of mRNA (Figure 4.2.1). Another previous

study similarly detected *Ptgds* transcripts in cDNA generated from SSEA-1-purified E13.5 male GCs, but to a lesser degree than in the somatic fractions (Tanaka et al., 2002). The male GC cDNA used in the previous study (Tanaka et al., 2002) and the current study (Figure 3.2.1) contained roughly 5% and 3%, respectively, of contaminating somatic cells. This raises the question of whether the *Ptgds* expression detected in male GC cDNA originates from Sertoli cell or GC mRNA expression. *Amh* expression was also detected in the male GC cDNA in the current study (Figure 4.2.1), indicating that somatic cell transcripts are represented in the male GC cDNA. However, *Amh* expression was detected 10-15 cycles later in male GC cDNA than in male genital ridge cDNA that was prepared from the same amount of mRNA, and this late appearance of PCR product is consistent with expression by a small contaminating population of cells. On the other hand, *Ptgds* expression was detected at the same time – after 35 cycles of PCR – but with a lower amount of product. This is consistent with expression by the majority of cells in the male GC cDNA at a lower level than that of Sertoli cells in the genital ridge cDNA. Therefore, this PCR data suggests that *Ptgds* mRNA is expressed by GCs.

PCR was also used in the current study to see whether *Ptgds* transcripts were detectable in cDNA libraries prepared from single E13.5 male GCs, which do not contain contaminating somatic cell transcripts. However, *Ptgds* was not detected in 15 out of 15 E13.5 male GC single-cell cDNA libraries, whereas it was robustly detected in Sertoli cell cDNA libraries (Figure 4.2.2). This lack of *Ptgds* detection contradicts the detection of GC *Ptgds* expression in male GC cDNA, as described in the previous paragraph. There are several possible explanations for this discrepancy. Firstly, it is possible that Sertoli cells and GCs express different splice forms of *Ptgds* that were not detected by a particular primer set. However, this cannot explain the discrepancy because the primer sets used in the single-cell library analysis and the FACS GC cDNA analysis, although different, were designed to the same region of the *Ptgds* 3' untranslated region and are therefore able to detect all known *Ptgds* splice forms. The theory that the *Ptgds* expression detected in the FACS GC cDNA

originated as contaminating Sertoli cell expression does not hold up due to the conclusions made in the previous paragraph. A third explanation for the discrepancy would be that E13.5 male GCs do express *Ptgds*, but the level of expression is below the detection limit of the single-cell procedure, and that is why *Ptgds* was not detected in the male GC cDNA libraries.

Previous studies have detected 2 splice forms of *Ptgds* (Baker and O'Shaughnessy, 2001), and both were detected in male FACS-purified GC and male genital ridge cDNA. However, the shorter known splice form was more abundant in the male GC cDNA, with the 230nt product appearing first in male GC cDNA. Additionally, an even shorter 200nt product was also detected in male GC cDNA. This product does not correspond to any known *Ptgds* splice form and was not detected in male genital ridge cDNA, suggesting that E13.5 male GCs may express a GC-specific splice form of *Ptgds*.

Ptgds immunostaining was also carried out on E13.5 testes sections and Ptgds protein was readily detected in male E13.5 GC cytoplasm (Figure 4.2.3). Unfortunately, no negative control was carried out for this immunostaining, so the detected immunostaining might signify background staining only. On the other hand, the immunostaining levels were only slightly less intense than high level staining in Sertoli cell cytoplasm, and much higher than in the interstitial area, which is in agreement with previous detection of *Ptgds* mRNA that is restricted to the testis cords as shown in previous studies (Adams and McLaren, 2002; Wilhelm et al., 2007) and in the current study (*Ptgds-in situ*-stained E13.5 wildtype testes in Figures 4.3.1 and 4.3.2). Therefore, the immunostaining might represent the actual presence of Ptgds protein in E13.5 GC cytoplasm, and this is confirmed by a recent study detecting Ptgds immunostaining in the cytoplasm of some, but not all, $Mvh^+$ E12.5 male GCs (Moniot et al., 2009).

To conclude the Ptgds GC expression analysis, Ptgds was detected sex-specifically in male E13.5 GC cDNA, suggesting that male GCs sex-specifically express *Ptgds* mRNA. Expression was not detected in cDNA libraries generated from single E13.5 male GCs, suggesting that Ptgds expression in E13.5 male GCs

is lower than the detection limit of the single-cell analysis. Immunostaining experiments confirmed that GCs also express Ptgds protein, which was predominantly cytoplasmic.

### *Possible functions for Ptgds Expression in Male GCs*

What could be the function of Ptgds protein in E13.5 male GCs? *Ptgds* knockout C57BL/6 mice are fertile but show a delay in Sertoli cell differentiation and testis cord formation due to a delay in *Sox9* transcription and Sox9 protein mislocalisation (Moniot et al., 2009). Ptgds is a multifunctional protein, being a lipocalin able to bind to small lipophilic molecules such as retinoic acid (RA) with high affinity (Tanaka et al., 1997), and a $PgD_2$-producing enzyme. The $PgD_2$-producing function of Ptgds is relevant to gonad development because $PgD_2$ partially masculinises cultured XX genital ridges (Adams and McLaren, 2002) by recruiting Sertoli cells non-cell-autonomously (Wilhelm 2005).

Could $PgD_2$ signaling cause bipotential GCs to commit to spermatogenesis? The answer to this is probably no, because the vast majority of GCs in $PgD_2$-treated XX gonads develop as oocytes so are not sex-reversed (Adams and McLaren, 2002). However, $PgD_2$ production by Ptgds expressed in male GCs would endow committed male GCs with potential to masculinise the surrounding somatic cells, via augmentation of Sertoli cell differentiation. This might contribute to the enhanced masculinisation due to the presence of GCs in gonads with 'weak' *Sry* alleles, as opposed to reduced masculinisation in the absence of GCs due to concurrent *Kitl* knockout or *Kit* mutation in these same gonads (Nagamine and Carlisle, 1996). This means that once embryonic GCs are committed to spermatogenesis, they express *Ptgds* and produce $PgD_2$ to help ensure that the surrounding tissue is also masculinised. Ingenious experiments will be required to assess whether this is the case.

Ptgds can bind to lipophilic molecules, such as RA, with affinity similar to other retinoic acid binding proteins like retinol binding protein (Tanaka et al., 1997),

and this is of interest because RA promotes meiosis, as well as apoptosis and mitosis, in embryonic GCs (Koubova et al., 2006; MacLean et al., 2007; Trautmann et al., 2008). RA is produced in the mesonephros of both male and female genital ridges. However, sex-specific expression of Cyp26b1, an RA-metabolising enzyme, in the E11.5-E14.5 gonad prevents RA signaling in the male gonad at that time (Bowles et al., 2006), thereby preventing RA from interfering with mitotic arrest and spermatogenic commitment of male GCs. Ptgds expression in male GCs, and in Sertoli cells, could be another mechanism to ensure that RA does not interfere with GC spermatogenic commitment.

***TPA, Ionomycin, Dexamethasone and T3 failed to Affect GC Ptgds Expression***

Experiments were also carried out in this study to identify signaling pathways that might affect Ptgds expression in bipotential GCs. A recent study found that Sox9 is able to bind to the *Ptgds* promoter and activate its transcription (Wilhelm et al., 2007), while another study showed that the majority of *Ptgds* expression in developing embryonic testes depends on *Sox9* (Moniot et al., 2009). Therefore, it is likely that Sox9 activates *Ptgds* transcription in Sertoli cells during Sertoli cell differentiation. However, other pathways may activate *Ptgds* transcription in male E13.5 GCs. The pathways that activate GC *Ptgds* transcription also may overlap with the pathways that ensure commitment of GCs to spermatogenesis. Therefore, experiments were carried out in the current study to try to activate or repress *Ptgds* expression in female or male GCs, respectively, in the hope of identifying pathways contributing to sex-specific differentiation of GCs.

Active PKC (Fujimori et al., 2005), glucocorticoid signaling (Garcia-Fernandez et al., 2000; Tokudome et al., 2009) and thyroid hormone signaling (Garcia-Fernandez et al., 1998; White et al., 1997) can all stimulate *Ptgds* transcription in various cell types. In this study, organotypic culture of female GRs from E11.5 to E13.5 with TPA or Ionomycin, Dexamethasone or T3, which activate PKC, Glucocorticoid receptor and Thyroid hormone receptor, respectively, did not

activate detectable *Ptgds* expression in GCs, despite survival of most of the GCs. The concentrations of the compounds used were similar to those used to elicit *Ptgds* expression in other studies, but may not have been sufficient for activation of the pathways in the GCs in this organotypic culture system. Alternatively, the GCs themselves, or *Ptgds* transcription, may simply not have been receptive to those particular signals.

PKC activation has also been reported to repress *Ptgds* expression (Garcia-Fernandez et al., 2000), so TPA and Ionomycin were tested for their ability to inhibit *Ptgds* expression in E13.5 male GCs. Neither TPA nor Ionomycin treatment noticeably affected *Ptgds* expression in male GRs cultured from E11.5 to E13.5, indicating that *Ptgds* expression in the majority of expressing cells was unaffected. GC *Ptgds* expression was not looked at specifically, so it is possible that the treatments may have reduced male GC *Ptgds* expression, and this reduction was masked by continued expression in Sertoli cells. In summary then, no changes in GC Ptgds expression were identified due to treatment of cultured male or female gonads with any of the compounds tested. Therefore, the effects of activation of these pathways on spermatogenic commitment were not investigated.

# Chapter 5:
# General Discussion

The first part of this study – the bHLH expression screen – was successful. In total, 22 bHLH genes are now potential candidate genes for controlling the developmental decision of mouse GCs to commit to spermatogenesis or oogenesis, and enter mitotic arrest or meiosis, respectively. Further work is needed to corroborate which of these candidate genes are in fact sex-specifically expressed by GCs, rather than some other contaminating gonadal cell population.

In most screens studying sex-specific expression differences in E12.5-E14.5 gonadal cells, many more genes are discovered as being enriched in male gonads compared to female gonads (e.g. Bouma et al., 2004). This might be due to the fact that masculinisation of the gonad, which is more morphologically complex than ovary development at this early stage of gonad development, requires expression of more genes. Conversely, this study found many more bHLH genes sex-specifically enriched or expressed in E13.5 female GC cDNA. What is the significance of this? This finding could indicate that a number of bHLHs are actively involved in promoting meiosis-specific differentiation programs in female GCs. A survey of temporal changes in the expression of these bHLHs during spermatogonial development, as male GCs enter meiosis, could indicate a corresponding role for these bHLHs in promoting meiotic entry of male GCs. Alternatively, or additionally, the higher number of female-enriched bHLHs might indicate that male GCs at E13.5, as they are beginning mitotic arrest, generally reduce their transcriptional activity. This could easily be corroborated by a genome-wide microarray analysis of male and female E13.5 GCs.

Previous studies indicate that *Epas1* is expressed in E15.5 embryonic testis, but in somatic cells not GCs (Tian et al., 1998), suggesting that the male-specific enrichment detected in this screen might also be due to somatic cell, not GC, expression. Similarly, some of the bHLHs found to be enriched in female GC cDNA here might also represent bHLHs expressed by somatic cells rather than GCs, due to the small fraction of contaminating somatic cells. Any such bHLHs

might be involved in early ovarian somatic cell differentiation, an area that has recently been shown to be an active process (Nef et al., 2005), but is currently vastly under-researched. To confirm which of these bHLHs might have such biological functions will require more detailed expression analysis of all the candidate bHLH genes to determine precisely which cell types are expressing them, further highlighting the need for this type of analysis.

One of the rationales of the screen was to find a male-specific bHLH that acts within committed male GCs to promote mitotic arrest. This is a well-documented and common function for differentiation-inducing bHLHs (Zebedee and Hara, 2001). In this study five male-enriched/specific bHLHs were identified. Due to reasons discussed in the Chapter 3 discussion, *Epas1*, *Msc* and *Ngn3* are the most unlikely to have this biological activity. Of the remaining two, Mnt was confirmed as being male-specifically enriched at the protein level in E13.5 GCs and might contribute to, but is probably not the primary mechanism for, mitotic arrest of male GCs. *Helt* was not corroborated beyond the screen data, but interestingly in the adult its expression is restricted to the testis (Guimera et al., 2006a), indicating that *Helt* might be involved in adult spermatogonial differentiation. This identifies *Helt* as a very promising candidate for involvement in spermatogonial differentiation and its expression and biological functions should be studied further. Knockout of *Helt* has been accomplished (Guimera et al., 2006b) and results in post-natal death, so an analysis of the testis of knockout embryos could well shed light upon this.

*Helt* belongs to the bHLH-O class of bHLHs, which includes the *Hes* genes. The *Hes* genes are well-established as downstream effectors of Notch signaling (Kageyama et al., 2005). The bHLH-O class bHLHs are generally negative transcriptional regulators and have complex dimerisation and functional properties (Fischer and Gessler, 2007), being able to dimerise with, augment and repress various classes of bHLH, such as the Id proteins. The *Hey* genes also belong to the bHLH-O class. Interestingly, this study found that *Hey1* was slightly male-enriched in E13.5 GCs (~1.9-fold), and additionally that both male

and female GC *Hey1* expression was very high compared to control cDNA comprised of mixed embryo tissue. Furthermore, *Hey1* is expressed during multiple stages of adult spermatogenesis (Van Wayenbergh et al., 2003). This evidence, together with the fact that Notch signaling is a key regulator of the meiosis/mitosis switch in *C. elegans* GCs (Kimble and Crittenden, 2005), indicates that *Hey1* and other bHLH-O genes such as *Helt* are interesting candidates for controlling aspects of GC development, including mitotic arrest of spermatogenically-committed GCs. Because the dimerisation properties of bHLH-O proteins are so complex, and the functional properties of Helt are mostly unknown, it would be prudent to discover Helt's dimerisation properties, especially with the ubiquitous E-protein class A bHLHs, Hey1, the Id proteins and other candidate genes identified in the current screen. This might shed light upon the functional role, if any, of *Helt* in GC development.

*Mnt* belongs to the bHLH-Zip class of bHLH genes and interacts specifically with the bHLH-Zip Max, but not with other bHLHs, including Ids, E-proteins and bHLH-Zips other than Max (Hooker and Hurlin, 2006). Mnt counteracts Myc transcriptional activity by competing for Myc's obligatory partner Max, and by binding as repressive Mnt-Max heterodimers to Myc transcription targets. Knowing that E13.5 male GCs express greater Mnt protein than E13.5 female GCs prompts the theory that the purpose of this higher Mnt expression could be to counteract a potential pro-meiotic activity of Myc. Phase 1 of the screen identified *N-Myc* as being the only one out of three *Myc* genes to be expressed in E13.5 GCs. However, *N-Myc* PCR amplification occurred at roughly equal times for both female and male GC cDNA, and therefore *N-Myc* was not studied further in this study. A closer examination of *N-Myc*, for example by immunostaining in E13.5-E15.5 gonadal tissue might reveal a role for N-Myc in promoting meiosis in female GCs. Greater Myc activity in female GCs could also explain greater *Id* gene expression in female GCs, because previous studies have noted that *Id1* expression is responsive to Myc activity (Swarbrick et al., 2005), and that *Id2* is a direct downstream target of Myc (Lasorella et al., 2000).

Induction of a meiotic pathway in female GCs by Myc activity would be a novel role for Myc, but its expression has been noted before in type B spermatogonia and primary spermatocytes undergoing prophase I (Wolfes et al., 1989). In another previous study, investigators ectopically-expressed a *c-myc* transgene in rats under the regulatory influence of the metallothionein IIA promoter, which the authors claim results in *c-myc* expression in primary spermatocytes through to spermatid stages in adult spermatogenesis (Kodaira et al., 1996). In rats that expressed the transgene in their testes, spermatogenesis failed at prophase I and the spermatocytes underwent apoptosis. Thus, ectopic *c-myc* prevented successful meiotic entry of the spermatocytes and this may have been caused by deleterious effects of excessive Myc activity. Another way to study the possible effects of Myc activity on meiotic initiation would be to knockdown *c-myc*/*N-myc* expression in female GCs at E12.5/E13.5 and see whether this would prevent meiotic entry of female GCs.

*Ptgds* was previously identified as being male-enriched in E13.5 gonads (Adams and McLaren, 2002), but some have disputed whether GCs contribute to this enrichment (Wilhelm et al., 2007). Experiments in this study were also able to confirm that male E13.5 GCs probably express *Ptgds* mRNA at low levels, and have Ptgds immunostaining. A recent study also found that male GCs express Ptgds protein by immunostaining (Moniot et al., 2009). Now that we know that GCs express *Ptgds*, we can ask the question of whether this GC-specific *Ptgds* expression has biological significance. Any study of this will be complicated by the fact that Sertoli cells express higher levels of *Ptgds* mRNA and protein than male GCs. However, it should be possible to answer this question. For example by comparing the ability of committed male GCs from wild-type and *Ptgds* knockout embryos to sex-reverse female somatic cells. It is very likely that sex-reversal of female somatic cells due to GC-expressed Ptgds will be due to Prostaglandin $D_2$ ($PgD_2$) production, owing to the well-documented ability of $PgD_2$ to partially masculinise female gonads (Adams and McLaren, 2002; Wilhelm et al., 2005). In mice, this is a minor testis determination pathway, because *Ptgds* knockout results only in a delay in testis formation in C57Bl/6

mice (Moniot et al., 2009). However, this pathway might be more important in other species because the ability of $PgD_2$ to partially masculinise embryonic gonads is conserved in other animals such as chickens (Moniot et al., 2008).

Ptgds is a bifunctional protein that can also bind to lipophilic molecules, such as retinoic acid (RA), with high affinity (Tanaka et al., 1997). Owing to RA's ability to induce meiosis in some GCs (Livera et al., 2000; MacLean et al., 2007; Trautmann et al., 2008), we can also ask whether the ability of Ptgds to bind to lipophilic molecules is of biological relevance to this system. Ptgds in spermatogenically-committed GCs might act to scavenge free RA to prevent RA from interfering with mitotic arrest. Because binding of lipophilic molecules inhibits the catalytic activity of Ptgds (Tanaka et al., 1997), the presence of RA would counteract $PgD_2$ production and thus could be another mechanism whereby RA interferes with testis development and spermatogenesis. A biochemical analysis of Ptgds extracted from spermatogenically-committed GCs, in particular whether it is bound by lipophilic molecules like RA, would be a good way to test this hypothesis.

To conclude, this study has made excellent progress in identifying candidate bHLHs involved in the spermatogenesis/oogenesis switch and some progress in corroborating the GC-specific expression of some of these genes and also *Ptgds*. Further corroboration is needed for most of the candidate bHLHs identified, and once this is completed we can begin to study their functional relevance to early sex-specific GC differentiation.

# Appendices

# Appendix i:
## Primers used for analysis of FACS-purified GC cDNAs

| Gene | Forward Primer (5' – 3') | Reverse Primer (5' – 3') |
|---|---|---|
| ***Mvh*** | AGGAGCTTGCAGAGATGTTCAGCAGAC | CAACTGGATTGGGAGCTTGTGAAGAAG |
| ***Gata4*** | ATGCGCCCCATCAAAACAGAG | TGCAGTGATTATGTCCCCGTGA |
| ***Lhx9*** | CCAAGGACCTCAAACAGCTTGC | CCAAGGACCTCAAACAGCTTGC |
| ***Gapdh*** | CCTGCGACTTCAACAGCAACTCCCAC | TGAGGTCCACCACCCTGTTGCTGTA |
| ***Actb*** | CTGGTGGTACCACCATGTACCCAGG | AGTGAGGCCAGGATGGAGCCAC |
| ***Amh*** | CACCCTGAGCATCGATCAGCTGCAAG | ACCTCTGACCCAGGCTTCGAACACG |
| ***SF-1*** | TCCCTCGCCACTACCCTTGAAGCTG | GGAGACAGCCTTGTCCAGTTGGGTG |
| ***Ptgds*** | ACAGCAGAACCCAGACTCTGAAGGAC | GCAAAGCTGGAGGGTGTAGAGGTACT |

# Appendix ii:

## Primers used for analysis of Single-cell cDNA Libraries

| Gene | Forward Primer (5' – 3') | Reverse Primer (5' – 3') |
|---|---|---|
| ***Gapdh*** | CCTGCGACTTCAACAGCAACTCCCAC | TGAGGTCCACCACCCTGTTGCTGTA |
| ***Sox9*** | CTTACTCACTGCTGTGGCTGGAGAGT | AAGAAAGGCAGGGTGCACAAAGAAGG |
| ***SF-1*** | CTTTCCTGCTTTCGCGTCAGAT | GCACTTCTTGTCTTGGGGCTGT |
| ***Gata4*** | TTCCTTGTCCTCATCACCCACA | CCTTGAGGGAGAAACAGCGAAA |
| ***Stella*** | AAAAAAGGCTCGAAGGAAATGAG | AGTTAAGATTTCCCAGCACCAG |
| ***Dazl*** | CAGACAGTGGTCTCTTGTCTGTTT | TTAAGCACTGCCCGACTTCT |
| ***Id1*** | AGGGGATCTCTGGGAAAGAC | ATTTTCAGCCAGTGATCATTGTAA |
| ***Id2*** | TGATCGTCTTGCCCAGGTGTCGTTCT | TGGGTCCTTCTGGTATTCACGCTCCA |
| ***Id3*** | GCCTGAGGGCATGGATGAGCTTCG | GCTGACCAGCGTGTGCTAGCTCTTCA |
| ***Ptgds*** | GACATTGTTTTCCTGCCCCAAC | GGCAAAGCTGGAGGGTGTAGAG |

# Appendix iii:
## Genes, Primers and UPL Probes for bHLH Screen Part 1

| Ensembl Code | MGI Symbol | UPL No. | Forward Primer | Reverse Primer |
|---|---|---|---|---|
| ENSMUSG00000044243 | ***A830053O21Rik*** | 073 | GAGGCTGGCAGGAATTTTG | TGCCTCTTCTGCCTCGTC |
| ENSMUSG00000019256 | ***Ahr*** | 027 | GCACAAGGAGTGGACGAAG | AGGAAGCTGGTCTGGGGTAT |
| ENSMUSG00000021575 | ***Ahrr*** | 101 | ACCCCAAGGGGACTTCAG | GGGGATCTCCTTAGTATGTGCTT |
| ENSMUSG00000015522 | ***Arnt*** | 049 | TCCACTGCACAGGCTACATC | TCATCATCTGGGAGGGAGAC |
| ENSMUSG00000015709 | ***Arnt2*** | 040 | CACCAACACCAATGTCAAGC | CTCGCTGATGTACCTCCAGTT |
| ENSMUSG00000055116 | ***Arntl*** | 074 | TCAGATGACGAACTGAAACACC | CGGTCACATCCTACGACAAA |
| ENSMUSG00000040187 | ***Arntl2*** | 084 | AAGGAACTCAGTCACTTAATCCTCA | GCATCCAACCACAAACAGG |
| ENSMUSG00000020052 | ***Ascl1*** | 038 | GCTCTCCTGGGAATGGACT | CGTTGGCGAGAAACACTAAAG |
| ENSMUSG00000035951 | ***Ascl3*** | 060 | GAACAATTACGGGGATCCATAC | CAGCGCCTGTAGTTGGTGTA |
| ENSMUSG00000073043 | ***Atoh1*** | 069 | TGCGATCTCCGAGTGAGAG | CTCTTCTGCAAGGTCTGATTTTT |
| ENSMUSG00000037621 | ***Atoh8*** | 038 | CAAAGCCCTGCAGCAGAC | AGAGCTTCTGCCCATAGGAGT |
| ENSMUSG00000030103 | ***Bhlhb2*** | 050 | TCTCCTACCCGAACATCTCAA | AATGCTTTCACGTGCTTCAA |
| ENSMUSG00000030256 | ***Bhlhb3*** | 070 | CCTGCCCTTCTATCTGCTGT | TCTTGTCTAGCCAGGGCTGT |
| ENSMUSG00000045493 | ***Bhlhb4*** | 081 | CGCTTGGTAGCATACCTCAAC | CCGAGAACGGGTAAATCG |
| ENSMUSG00000025128 | ***Bhlhb5*** | 034 | ACACTTGCAGGGCAAACAA | GAATGTCCGGTTTGTCTCTGA |
| ENSMUSG00000052271 | ***Bhlhb8*** | 110 | GGCTAAAGCTACGTGTCCTTG | GGTGAGGCCCTTCCAACT |
| ENSMUST00000016399 | ***Btub*** | 055 | GGGACGTCTGCTCTCCAG | GCGGCACATACTTCTTACCG |
| ENSMUST00000016399 | ***Btub*** | 055 | GGGACGTCTGCTCTCCAG | GCGGCACATACTTCTTACCG |
| ENSMUSG00000029238 | ***Clock*** | 069 | TCATCTCACACCGCAGTCTC | GGAGGAGTGCTAGTATCAGTAGGG |
| ENSMUSG00000024140 | ***Epas1*** | 003 | GGAGCTCAAAAGGTGTCAGG | CAGGTAAGGCTCGAACGATG |
| ENSMUSG00000030001 | ***Figla*** | 068 | CTGGAAGAAGCGAAGGTCTC | GGACACATGAGGGTCAGAGG |
| ENSMUSG00000068284 | ***Gm608*** | 020 | TCAGCCAAACGTCAGAAGC | TCAGGGGCATACTTTCAAGC |
| ENSMUSG00000037335 | ***Hand1*** | 051 | CAAGCGGAAAAGGGAGTTG | GTGCGCCCTTTAATCCTCTT |

**Table iii.1. Genes, Primers and Probes used in Part 1 of the bHLH Screen**

| Ensembl Code | MGI Symbol | UPL No. | Forward Primer | Reverse Primer |
|---|---|---|---|---|
| ENSMUSG00000038193 | ***Hand2*** | 055 | CTTCAAGGGCCCAAGATTC | TCAGCGCATCCATTTTCTAA |
| ENSMUSG00000047171 | ***Helt*** | 080 | GTTCCGGGAAACTGGAGAA | TTGGCAAATTCTGCTAAAAGC |
| ENSMUSG00000022528 | ***Hes1*** | 099 | ACACCGGACAAACCAAAGAC | CGCCTCTTCTCCATGATAGG |
| ENSMUSG00000028940 | ***Hes2*** | 067 | AGCTGCGCAAGAACCTAAAG | TTCGAAGAGCGGGAAGTCT |
| ENSMUSG00000028946 | ***Hes3*** | 078 | TGGAGAGACACTACTCACATCAGA | TGTACTTAACACTCAGCTCCAGGATA |
| ENSMUSG00000048001 | ***Hes5*** | 022 | CCAAGGAGAAAAACCGACTG | TGCTCTATGCTGCTGTTGATG |
| ENSMUSG00000067071 | ***Hes6*** | 066 | ACGGATCAACGAGAGTCTTCA | TTCTCTAGCTTGGCCTGCAC |
| ENSMUSG00000023781 | ***Hes7*** | 078 | GAGAGGACCAGGGACCAGA | TTCGCTCCCTCAAGTAGCC |
| ENSMUSG00000040289 | ***Hey1*** | 017 | CATGAAGAGAGCTCACCCAGA | CGCCGAACTCAAGTTTCC |
| ENSMUSG00000019789 | ***Hey2*** | 001 | ATTGCAAATGACAGTGGATCAT | AGCATGGGCATCAAAGTAGC |
| ENSMUSG00000032744 | ***Heyl*** | 025 | CTGAATTGCGACGATTGGT | GCAAGACCTCAGCTTTCTCC |
| ENSMUSG00000021109 | ***Hif1a*** | 018 | CATGATGGCTCCCTTTTTCA | GTCACCTGGTTGCTGCAATA |
| ENSMUSG00000042745 | ***Id1*** | 093 | GCGAGATCAGTGCCTTGG | CTCCTGAAGGGCTGGAGTC |
| ENSMUSG00000020644 | ***Id2*** | 089 | ACAGAACCAGGCGTCCAG | AGCTCAGAAGGGAATTCAGATG |
| ENSMUSG00000007872 | ***Id3*** | 019 | GAGGAGCTTTTGCCACTGAC | GCTCATCCATGCCCTCAG |
| ENSMUSG00000021379 | ***Id4*** | 092 | AGGGTGACAGCATTCTCTGC | CCGGTGGCTTGTTTCTCTTA |
| ENSMUSG00000034041 | ***Lyl1*** | 041 | GCAGGACCCTTCAGCATCT | CCACCTTCTGGGGTTGGT |
| ENSMUSG00000059436 | ***Max*** | 050 | ACCTCAAGCGGCAGAATG | AGTTGGGCACTTGATCTTGC |
| ENSMUSG00000030544 | ***Mesp1*** | 089 | CCCATCGTTCCTGTACGC | TCTAGAAGAGCCAGCATGTCG |

**Table iii.1. Genes, Primers and Probes used in Part 1 of the bHLH Screen**

| Ensembl Code | MGI Symbol | UPL No. | Forward Primer | Reverse Primer |
|---|---|---|---|---|
| ENSMUSG00000030543 | ***Mesp2*** | 047 | CCCAGAGCCTAGGAACAAGAC | GGTTCTGGAGACACAGAAAGACTC |
| ENSMUSG00000033943 | ***Mga*** | 083 | CTACATCTGGGCTTATCCAGGT | AACAGGGTGCGTGGTTTC |
| ENSMUSG00000035158 | ***Mitf*** | 062 | AAGCTGGAGCATGCGAAC | GCGCTCTAGCCTGCATCT |
| ENSMUSG00000017801 | ***Mlx*** | 100 | GTGTCTTCAGCTGGATTGAGG | GATGAAGGACACCGATCACA |
| ENSMUSG00000038342 | ***Mlxip*** | 020 | GCCCAACCCACGAGAAATA | GGGTTGCAAAGGGATCAG |
| ENSMUSG00000005373 | ***Mlxipl*** | 069 | TGGAGAGCCTGGTACATTCA | GGTCACGAAACCACACACTG |
| ENSMUSG00000000282 | ***Mnt*** | 001 | AAGCGCAGCAACAACAGAG | CTCCTGCTCTCTCTCACGTTC |
| ENSMUSG00000025930 | ***Msc*** | 011 | AGCTTTCCAAACTGGACACG | GTCCAGAGACCACGAATGG |
| ENSMUSG00000047002 | ***Msgn1*** | 106 | AATTACCTGCCGCCTGTCT | TGAGTGTCTGGATCTTGGTGA |
| ENSMUSG00000001156 | ***Mxd1*** | 098 | ACAATGAAATGGAAAAGAACAGG | GCGGTACCAATCCCTTTAGC |
| ENSMUSG00000021485 | ***Mxd3*** | 025 | CCAGGGTGCATATCCAGAA | TGCGAAGCTTTTCCTTGAG |
| ENSMUSG00000037235 | ***Mxd4*** | 015 | GAAGCGTGCTAAGATGCACA | CGCTGAAGCTGTTCCTTGAT |
| ENSMUSG00000025025 | ***Mxi1*** | 055 | AGCCAAAGCACACATCAAGA | GCCGCTTTAAAAACCTCTGTT |
| ENSMUSG00000022346 | ***Myc*** | 077 | CCTAGTGCTGCATGAGGAGA | TCCACAGACACCACATCAATTT |
| ENSMUSG00000028654 | ***Mycl1*** | 045 | ACGGCACTCCTAGTCTGGAA | CCACGTCAATCTCTTCACCTT |
| ENSMUSG00000037169 | ***Mycn*** | 069 | CCTCCGGAGAGGATACCTTG | TCTCTACGGTGACCACATCG |
| ENSMUSG00000044597 | ***Mycs*** | 031 | CAGGCTGATGAGTCCAAGC | AGCAACTGCTGTTGTCTTTCAT |
| ENSMUSG00000000435 | ***Myf5*** | 010 | CTGCTCTGAGCCCACCAG | GACAGGGCTGTTACATTCAGG |
| ENSMUSG00000035923 | ***Myf6*** | 012 | GGGCCTCGTGATAACTGCT | AAGAAAGGCGCTGAAGACTG |
| ENSMUSG00000009471 | ***Myod1*** | 042 | AGCACTACAGTGGCGACTCA | GGCCGCTGTAATCCATCA |
| ENSMUSG00000026459 | ***Myog*** | 063 | CCTTGCTCAGCTCCCTCA | TGGGAGTTGCATTCACTGG |

**Table iii.1. Genes, Primers and Probes used in Part 1 of the bHLH Screen**

| Ensembl Code | MGI Symbol | UPL No. | Forward Primer | Reverse Primer |
|---|---|---|---|---|
| ENSMUSG00000020647 | ***Ncoa1*** | 084 | TGGCATGAACATGAGGTCAG | GCCAACATCTGAGCATTCAA |
| ENSMUSG00000005886 | ***Ncoa2*** | 002 | GAATGTCCCGACCAGCTC | TCGGCCAGCTCCTCTATGTA |
| ENSMUSG00000027678 | ***Ncoa3*** | 110 | GCAGCTGAGAATGCAGCTT | CCTGCCGGCTCTGATTTA |
| ENSMUSG00000034701 | ***Neurod1*** | 001 | CGCAGAAGGCAAGGTGTC | TTTGGTCATGTTTCCACTTCC |
| ENSMUSG00000038255 | ***Neurod2*** | 027 | ACAGCCCACCACGAATCT | TCCGTGAGGAAGTTACGAGAG |
| ENSMUSG00000048015 | ***Neurod4*** | 022 | ACTACTCGCGGGAGCTGAC | CCATCCAGGATTGTGTGTTG |
| ENSMUSG00000037984 | ***Neurod6*** | 080 | TCCTTCGAGGAAAGAGCATT | TCCTCCTCTTCTTTCTCGGTTT |
| ENSMUSG00000048904 | ***Neurog1*** | 101 | GACCTGTCCAGCTTCCTCAC | TGGAGGCTAGGGGCTGTAG |
| ENSMUSG00000027967 | ***Neurog2*** | 069 | ACATCTGGAGCCGCGTAG | CCCAGCAGCATCAGTACCTC |
| ENSMUSG00000044312 | ***Neurog3*** | 108 | ACTGCTGCTTGTCACTGACTG | ATGGTGAGCGCATCCAAG |
| ENSMUSG00000051251 | ***Nhlh1*** | 001 | GATCCCTTGGCAGAGTCCTT | CTTCAAAGTTCCATGGTCAAGA |
| ENSMUSG00000048540 | ***Nhlh2*** | 063 | AATATTGGCTGCTTTTAATATTTGC | GGACTCAGCATCATTTTGGAG |
| ENSMUSG00000070623 | ***NOVEL1*** | 010 | AGTGCGTGAATGAGGGCTAC | TGAGCCGCTTCTCAGTCAG |
| ENSMUSG00000057741 | ***NOVEL2*** | 017 | GCCATCAGCTACATCAAGCA | TGCTTTGGACTCGCCATC |
| ENSMUSG00000075157 | ***NOVEL3*** | 032 | GAGCCGGCACAGAAACAT | GTGTAGATCTGTTGGCAGTGCT |
| ENSMUSG00000001988 | ***Npas1*** | 074 | TCTACCTGGGTCTCTCACAGG | TCCCCAGGATGGATGTAGTC |
| ENSMUSG00000026077 | ***Npas2*** | 076 | GGAGTTCCCACAAGTCCTCA | ATCAGCTTGGTTGGAGTGGA |
| ENSMUSG00000021010 | ***Npas3*** | 107 | GGGCATCACCTCCTACCAG | ATTCTGATTGGTTGGGCAGA |
| ENSMUSG00000046160 | ***Olig1*** | 020 | GGCCCAGTTCTCCAAGTG | GGGAAGATTGGCTGAGGTC |
| ENSMUSG00000039830 | ***Olig2*** | 021 | AGACCGAGCCAACACCAG | AAGCTCTCGAATGATCCTTCTTT |
| ENSMUSG00000045591 | ***Olig3*** | 025 | CAGGAGAGTCGTCTGAACTCG | TGGCATCTTCTGGACCATATC |

**Table iii.1. Genes, Primers and Probes used in Part 1 of the bHLH Screen**

| Ensembl Code | MGI Symbol | UPL No. | Forward Primer | Reverse Primer |
|---|---|---|---|---|
| ENSMUST00000090749 | ***Ppia*** | 046 | GACGCCACTGTCGCTTTT | CTGCAAACAGCTCGAAGGA |
| ENSMUST00000090749 | ***Ppia*** | 046 | GACGCCACTGTCGCTTTT | CTGCAAACAGCTCGAAGGA |
| ENSMUSG00000026735 | ***Ptf1a*** | 073 | GGGACGAGCAAGCAGAAGTA | CGCGGTAGCAGTATTCGTG |
| ENSMUSG00000030259 | ***Rassf8*** | 079 | CTGTGGCGTCACGGAAGT | GGGTGTACCTTCCAGTTCGAC |
| ENSMUSG00000034161 | ***Scx*** | 029 | ACACCCAGCCCAAACAGAT | TCTGTCACGGTCTTTGCTCA |
| ENSMUSG00000019913 | ***Sim1*** | 049 | CGGCTCTCATCTACTCCAGAC | TGAAATGTACATGATCTTCCCATC |
| ENSMUSG00000062713 | ***Sim2*** | 109 | CCAGCCTTGACCTGAAGC | CATAGCCCGTAAGCTCTGTCA |
| ENSMUSG00000059625 | ***Sohlh1*** | 011 | GAGCGCGTTGTCATTCAGT | CTGGCTGCCATGAGTGAG |
| ENSMUSG00000027794 | ***Sohlh2*** | 005 | CATCGAGCTGTTCCTTCCAT | CTGGTCAGCATGGCATCTT |
| ENSMUSG00000020538 | ***Srebf1*** | 077 | ACAAGATTGTGGAGCTCAAAGAC | GCGCAAGACAGCAGATTTATT |
| ENSMUSG00000022463 | ***Srebf2*** | 074 | ACCTAGACCTCGCCAAAGGT | GCACGGATAAGCAGGTTTGT |
| ENSMUSG00000030255 | ***Sspn*** | 026 | AGCCCCTCCCTGCTAGTC | AGTCCAAGGTAAGCCACCAC |
| ENSMUSG00000028717 | ***Tal1*** | 060 | CGCCTCACTAGGCAGTGG | CTCTTCACCCGGTTGTTGTT |
| ENSMUSG00000028417 | ***Tal2*** | 017 | TGCGACAGCTACCTTGACTG | GCTCCCTGGTATTTGTGAAGA |
| ENSMUSG00000032228 | ***Tcf12*** | 100 | AACCAGAGGGAATGCTGCT | TTGTGTGGTCAGGGGAATAAA |
| ENSMUSG00000068079 | ***Tcf15*** | 080 | GTGTAAGGACCGGAGGACAA | GATGGCTAGATGGGTCCTTG |
| ENSMUSG00000045680 | ***Tcf21*** | 049 | CATTCACCCAGTCAACCTGA | CCACTTCCTTCAGGTCATTCTC |
| ENSMUSG00000006642 | ***Tcf23*** | 051 | CCAGAGCTAGGGGAACAGC | CTTCACCCGAGTCCGTTC |
| ENSMUSG00000053477 | ***Tcf4*** | 002 | TAGGGAAAGCCCTAGCTTCG | TGAAGGATTGGAGGAAAAGC |
| ENSMUSG00000005718 | ***Tcfap4*** | 016 | CGGGAACAGCAGCACCTA | CGATCACTGTGGGGTGGT |
| ENSMUSG00000020167 | ***Tcfe2a*** | 079 | GTGGGCTCTGACAAGGAACT | ACAGGTAGCGGGAACATCA |

**Table iii.1. Genes, Primers and Probes used in Part 1 of the bHLH Screen**

| Ensembl Code | MGI Symbol | UPL No. | Forward Primer | Reverse Primer |
|---|---|---|---|---|
| ENSMUSG00000000134 | ***Tcfe3*** | 080 | GGAACAGCAACGCTCCAA | GGGCCTGCAGTTCTAGCTC |
| ENSMUSG00000023990 | ***Tcfeb*** | 085 | GAGCTGGGAATGCTGATCC | CTTGAGGATGGTGCCTTTGT |
| ENSMUSG00000029553 | ***Tcfec*** | 009 | AGCTTAGGCTCCGGATTCA | TTCCTCTCAGGATGGGTCTG |
| ENSMUSG00000038932 | ***Tcfl5*** | 002 | CTTCACGACCACCGACCT | TGCAGCTGCGTGTACTCC |
| ENSMUSG00000035799 | ***Twist1*** | 058 | AGCTACGCCTTCTCCGTCT | TCCTTCTCTGGAAACAATGACA |
| ENSMUSG00000007805 | ***Twist2*** | 010 | CATGTCCGCCTCCCACTA | GGTGCCGAAAGTCACAGC |
| ENSMUSG00000026641 | ***Usf1*** | 074 | CCCCCTCACAGAGAGATGAA | CACTGTTCCCTCTTCGGTTT |
| ENSMUSG00000058239 | ***Usf2*** | 070 | GTCTGGATCCCGCTTCCT | GCCTTCCTGCAGCTCAAC |

**Table iii.1. Genes, Primers and Probes used in Part 1 of the bHLH Screen**

# Appendix iv:
## Genes, Primers and UPL Probes for bHLH Screen Part 2

| MGI Symbol | UPL No. | Forward Primer | Reverse Primer |
|---|---|---|---|
| ***Epas1*** | 3 | GGAGCTCAAAAGGTGTCAGG | CAGGTAAGGCTCGAACGATG |
| ***Helt*** | 81 | CGAGCTGGGCAAGACAGT | ATCTCCGCCTTCTCCAGTTT |
| ***Mnt*** | 72 | ACCATCGAGGTGGAAAAGG | CTTCTCGATGATGCCTCTCC |
| ***Msc*** | 1 | AAGCGCAGCAACAACAGAG | CTCCTGCTCTCTCTCACGTTC |
| ***Ngn3*** | 12 | GCAGCTTGTTTATGGGGTCT | AGCACATGTCCCCAAATAGG |
| ***A83005 3O21Rik*** | 73 | GAGGCTGGCAGGAATTTTG | TGCCTCTTCTGCCTCGTC |
| ***Bhlhb2*** | 50 | TCTCCTACCCGAACATCTCAA | AATGCTTTCACGTGCTTCAA |
| ***Ebf4*** | 70 | CCTCACCTTTCGCCATCA | AGGAGAAGACGCTGGTGGT |
| ***Figla*** | 68 | CTGGAAGAAGCGAAGGTCTC | GGACACATGAGGGTCAGAGG |
| ***Id1*** | 93 | GCGAGATCAGTGCCTTGG | CTCCTGAAGGGCTGGAGTC |
| ***Id2*** | 89 | ACAGAACCAGGCGTCCAG | AGCTCAGAAGGGAATTCAGATG |
| ***Id3*** | 19 | GAGGAGCTTTTGCCACTGAC | GCTCATCCATGCCCTCAG |
| ***Mesp1*** | 12 | CCAGACTGTACCATTCCAACC | TGCCTGCTTCATCTTTAGAGC |
| ***Mlxipl*** | 69 | TGGAGAGCCTGGTACATTCA | GGTCACGAAACCACACACTG |
| ***Mxd4*** | 15 | GAAGCGTGCTAAGATGCACA | CGCTGAAGCTGTTCCTTGAT |
| ***Scx*** | 66 | GCCTCAGCAACCAGAGAAAG | CCTTCACTAGTGGCATCACCT |
| ***Ahrr*** | 101 | ACCCCAAGGGGACTTCAG | GGGGATCTCCTTAGTATGTGCTT |
| ***Atoh1*** | 24 | TCTGATGAGGCCAGTTAGGAA | AGGGCATTTGGTTGTCTCAG |
| ***Bhlhb4*** | 16 | AAAATTACGCCGAGGTCCTT | TCACCTCCTGGGATCTTCC |
| ***Bhlhb5*** | 34 | ACACTTGCAGGGCAAACAA | GAATGTCCGGTTTGTCTCTGA |
| ***Hand1*** | 51 | CAAGCGGAAAAGGGAGTTG | GTGCGCCCTTTAATCCTCTT |
| ***Hes7*** | 78 | GAGAGGACCAGGGACCAGA | TTCGCTCCCTCAAGTAGCC |
| ***Hes2*** | 68 | GAAATGACTGTGCGCTTCC | ACCCTCGAGGTAGCTATTCAAA |
| ***Max*** | 52 | AGGACGCCTGCTCTACCA | TCACAAAGTCCACCAAACAGA |
| ***Ascl2*** | 71 | AAAGTGTGGACCGGTTGG | GCCAAACATCAGCGTCAGTA |
| ***Id4*** | 92 | AGGGTGACAGCATTCTCTGC | CCGGTGGCTTGTTTCTCTTA |
| ***Olig1*** | 20 | GGCCCAGTTCTCCAAGTG | GGGAAGATTGGCTGAGGTC |
| ***Hey1*** | 25 | CTGAATTGCGACGATTGGT | GCAAGACCTCAGCTTTCTCC |

**Table iv.1. Genes, Primers and Probes used in Part 2 of the bHLH Screen**

# Appendix v:
## Additional Results for bHLH Screen Part 1

| Gene | Positive Control | | ♂ N | ♀ N |
|---|---|---|---|---|
| | N | $C_t$ | | |
| ***Ascl3*** | 3 | 32.1 +/- 1.9 | 3 | 3 |
| ***Ascl4*** | 2 | 35.8 +/- 0.9 | 2 | 3 |
| ***Atoh7*** | 3 | 32.7 +/- 1.3 | 2 | 3 |
| ***Bhlhb8*** | 3 | 32.2 +/- 0.7 | 2 | 2 |
| ***Ebf2*** | 2 | 33.9 +/- 1.8 | 3 | 3 |
| ***Ferd3l*** | 2 | 35.5 +/- 0.8 | 3 | 2 |
| ***Hand2*** | 3 | 28.1 +/- 1.9 | 2 | 3 |
| ***Msgn1*** | 3 | 33.2 +/- 0.5 | 3 | 3 |
| ***Mycs (A)*** | 2 | 23.7 +/- 1.3 | 3 | 3 |
| ***Mycs (B)*** | 3 | 24.7 +/- 0.2 | 3 | 3 |
| ***Myf5*** | 2 | 27.7 +/- 0.6 | 2 | 3 |
| ***Myf6*** | 2 | 30.1 +/- 0.2 | 3 | 3 |
| ***Myod1*** | 3 | 30.9 +/- 1.2 | 3 | 3 |
| ***Neurod1*** | 2 | 28.2 +/- 0.4 | 3 | 3 |
| ***Neurod2*** | 2 | 28.8 +/- 0.0 | 3 | 3 |
| ***Neurod4*** | 3 | 35.0 +/- 1.4 | 3 | 3 |
| ***Neurod6*** | 2 | 28.5 +/- 0.3 | 3 | 2 |
| ***Neurog1*** | 2 | 34.0 +/- 0.3 | 2 | 2 |
| ***Neurog2*** | 3 | 31.2 +/- 0.8 | 3 | 3 |
| ***Nhlh1*** | 2 | 34.4 +/- 0.1 | 3 | 3 |
| ***Nhlh2*** | 3 | 28.3 +/- 0.7 | 3 | 2 |
| ***Npas1*** | 3 | 36.1 +/- 1.9 | 3 | 3 |
| ***Npas3*** | 2 | 36.2 +/- 0.4 | 3 | 3 |
| ***Npas4*** | 3 | 33.2 +/- 1.3 | 2 | 2 |
| ***Olig2*** | 3 | 31.4 +/- 0.5 | 3 | 3 |
| ***Ptf1a*** | 2 | 37.3 +/- 0.2 | 3 | 3 |
| ***Sim1*** | 3 | 35.3 +/- 0.5 | 3 | 3 |
| ***Sim2*** | 2 | 31.6 +/- 0.3 | 2 | 3 |
| ***Tal2*** | 3 | 31.7 +/- 1.4 | 2 | 2 |
| ***Tcf23*** | 3 | 28.6 +/- 0.6 | 3 | 3 |
| ***Tcfec*** | 2 | 31.5 +/- 0.6 | 3 | 3 |

**Table v.1. Genes that were not detected in male or female E13.5 GC cDNA in bHLH Screen Phase 1**

| Gene | Positive Control | | Male | | Female | | $\Delta C_t$ |
|---|---|---|---|---|---|---|---|
| | N | $C_t$ | N | $C_t$ | N | $C_t$ | |
| ***Ahr*** | 3/3 | 29.9 +/- 0.4 | 3/3 | 31.2 +/- 0.5 | 3/3 | 31.2 +/- 1.2 | **0.0** |
| ***Arnt*** | 3/3 | 27.8 +/- 0.9 | 3/3 | 29.9 +/- 0.7 | 2/3 | 30.2 +/- 0.3 | **-0.3** |
| ***Arnt2*** | 3/3 | 28.2 +/- 1.1 | 3/3 | 31.9 +/- 1.0 | 3/3 | 31.7 +/- 1.3 | **0.2** |
| ***Arntl*** | 3/3 | 28.8 +/- 1.6 | 3/3 | 31.5 +/- 2.0 | 3/3 | 31.9 +/- 0.5 | **-0.4** |
| ***Arntl2*** | 3/3 | 30.2 +/- 1.5 | 3/3 | 30.4 +/- 0.1 | 3/3 | 32.0 +/- 0.5 | **-1.6** |
| ***Bhlhb3*** | 3/3 | 35.5 +/- 0.5 | 2/3 | 36.9 +/- 0.6 | 3/3 | 34.9 +/- 1.5 | **1.9** |
| ***Clock*** | 3/3 | 32.9 +/- 0.3 | 3/3 | 34.3 +/- 1.0 | 3/3 | 33.3 +/- 0.5 | **1.0** |
| ***Ebf1*** | 2/3 | 27.7 +/- 1.0 | 3/3 | 34.8 +/- 1.4 | 3/3 | 34.8 +/- 0.8 | **0.1** |
| ***Gm608*** | 2/3 | 34.2 +/- 1.4 | 3/3 | 33.4 +/- 0.5 | 3/3 | 32.6 +/- 0.9 | **0.7** |
| ***Hes3*** | 2/3 | 33.9 +/- 0.4 | 2/3 | 38.8 +/- 0.6 | 3/3 | 38.0 +/- 1.4 | **0.9** |
| ***Hes5*** | 3/3 | 29.3 +/- 0.5 | 3/3 | 33.2 +/- 0.6 | 3/3 | 31.7 +/- 0.8 | **1.5** |
| ***Hes6*** | 3/3 | 30.8 +/- 0.9 | 2/3 | 34.7 +/- 0.4 | 3/3 | 34.3 +/- 2.0 | **0.4** |
| ***Hey2*** | 2/3 | 31.6 +/- 1.0 | 3/3 | 34.3 +/- 0.6 | 2/3 | 36.0 +/- 1.0 | **-1.7** |
| ***Hif1a*** | 3/3 | 25.0 +/- 1.0 | 3/3 | 27.4 +/- 1.2 | 2/3 | 26.8 +/- 0.6 | **0.7** |
| ***Lyl1*** | 2/3 | 27.2 +/- 0.0 | 2/3 | 37.6 +/- 0.5 | 2/3 | 36.8 +/- 0.6 | **0.8** |
| ***Mesp2*** | 3/3 | 32.7 +/- 1.2 | 3/3 | 31.8 +/- 1.2 | 3/3 | 30.7 +/- 1.2 | **1.1** |
| ***Mitf*** | 3/3 | 29.6 +/- 0.4 | 2/3 | 35.5 +/- 2.0 | 3/3 | 35.4 +/- 1.1 | **0.1** |
| ***Mlx*** | 3/3 | 28.5 +/- 1.0 | 3/3 | 28.8 +/- 0.3 | 3/3 | 28.1 +/- 0.5 | **0.7** |
| ***Mlxip*** | 3/3 | 28.4 +/- 0.4 | 3/3 | 29.5 +/- 0.3 | 3/3 | 29.8 +/- 0.4 | **-0.3** |
| ***Mxd1*** | 3/3 | 31.2 +/- 0.4 | 3/3 | 32.6 +/- 0.4 | 3/3 | 31.6 +/- 0.5 | **1.0** |
| ***Mxd3*** | 3/3 | 26.6 +/- 1.3 | 2/3 | 32.4 +/- 0.8 | 3/3 | 31.7 +/- 0.7 | **0.7** |
| ***Mxi1*** | 3/3 | 25.9 +/- 0.9 | 3/3 | 29.0 +/- 2.0 | 3/3 | 28.2 +/- 0.5 | **0.9** |
| ***Myc*** | 3/3 | 24.3 +/- 2.0 | 3/3 | 32.0 +/- 1.4 | 2/3 | 33.0 +/- 0.2 | **-1.0** |
| ***Mycl1*** | 3/3 | 32.2 +/- 2.0 | 3/3 | 32.1 +/- 2.0 | 3/3 | 32.2 +/- 1.2 | **-0.1** |
| ***Mycn*** | 3/3 | 31.1 +/- 1.6 | 3/3 | 30.3 +/- 1.0 | 3/3 | 30.8 +/- 0.8 | **-0.6** |
| ***Myog*** | 3/3 | 25.5 +/- 0.7 | 2/3 | 33.2 +/- 0.4 | 2/3 | 32.8 +/- 1.2 | **0.4** |
| ***Ncoa1*** | 3/3 | 31.7 +/- 0.2 | 3/3 | 33.3 +/- 1.7 | 3/3 | 32.0 +/- 2.0 | **1.3** |
| ***Ncoa2*** | 3/3 | 30.3 +/- 0.8 | 3/3 | 29.6 +/- 0.4 | 3/3 | 29.7 +/- 1.4 | **-0.1** |
| ***Ncoa3*** | 3/3 | 28.5 +/- 0.5 | 2/3 | 29.5 +/- 1.2 | 3/3 | 29.0 +/- 1.2 | **0.5** |
| ***Npas2*** | 3/3 | 31.7 +/- 0.5 | 2/3 | 34.4 +/- 0.8 | 3/3 | 34.3 +/- 1.4 | **0.1** |
| ***Olig3*** | 3/3 | 30.5 +/- 0.9 | 2/3 | 31.7 +/- 1.7 | 3/3 | 31.7 +/- 1.1 | **-0.1** |
| ***Sohlh1*** | 2/3 | 36.9 +/- 0.0 | 2/3 | 34.1 +/- 1.0 | 3/3 | 33.1 +/- 1.5 | **1.0** |
| ***Sohlh2*** | 2/3 | 30.6 +/- 0.0 | 3/3 | 25.8 +/- 0.3 | 2/3 | 25.5 +/- 0.4 | **0.3** |
| ***Srebf1*** | 3/3 | 25.4 +/- 1.4 | 3/3 | 27.8 +/- 0.3 | 3/3 | 28.1 +/- 1.1 | **-0.3** |
| ***Srebf2*** | 3/3 | 27.8 +/- 0.0 | 2/3 | 29.6 +/- 0.6 | 3/3 | 29.7 +/- 1.4 | **0.0** |
| ***Tcf15*** | 3/3 | 28.8 +/- 0.7 | 3/3 | 32.9 +/- 1.3 | 2/3 | 31.7 +/- 0.4 | **1.2** |
| ***Tcf4*** | 3/3 | 28.9 +/- 0.8 | 3/3 | 30.7 +/- 0.4 | 3/3 | 32.6 +/- 0.4 | **-1.9** |

**Table v.2. Genes with <2.0 cycles difference between male and female E13.5 GC cDNA in bHLH Screen Phase 1**

| Gene | Positive Control | | Male | | Female | | $\Delta C_t$ |
|---|---|---|---|---|---|---|---|
| | N | $C_t$ | N | $C_t$ | N | $C_t$ | |
| ***Tcfap4*** | 3/3 | 27.7 +/- 1.3 | 2/3 | 29.7 +/- 0.3 | 2/3 | 31.5 +/- 0.3 | **-1.9** |
| ***Tcfe2a*** | 3/3 | 24.2 +/- 0.9 | 3/3 | 25.5 +/- 1.0 | 3/3 | 25.1 +/- 1.0 | **0.4** |
| ***Tcfe3*** | 3/3 | 29.3 +/- 0.6 | 3/3 | 31.5 +/- 0.7 | 3/3 | 31.2 +/- 0.8 | **0.3** |
| ***Twist1*** | 2/3 | 29.4 +/- 0.6 | 2/3 | 38.4 +/- 1.7 | 3/3 | 38.4 +/- 0.9 | **0.1** |
| ***Twist2*** | 3/3 | 28.5 +/- 1.5 | 3/3 | 37.0 +/- 1.4 | 2/3 | 37.8 +/- 0.3 | **-0.9** |
| ***Usf2*** | 2/3 | 27.5 +/- 1.9 | 3/3 | 30.7 +/- 0.8 | 3/3 | 30.4 +/- 0.8 | **0.2** |

**Table v.2. Genes with <2.0 cycles difference between male and female E13.5 GC cDNA in bHLH Screen Phase 1**

| Gene | Positive Control | | Male | | Female | | $\Delta C_t$ (M-F) |
|---|---|---|---|---|---|---|---|
| | N | $C_t$ | N | $C_t$ | N | $C_t$ | |
| ***Ascl2*** | 2/3 | 28.4 +/- 0.1 | 2/3 | 26.3 +/- 0.1 | 2/3 | 29.1 +/- 0.5 | 2.8 |
| ***Epas1*** | 2/3 | 23.0 +/- 1.0 | 2/3 | 28.5 +/- 0.0 | 3/3 | 31.4 +/- 1.2 | 2.9 |
| ***Helt*** | 3/3 | 34.1 +/- 1.8 | 3/3 | 30.5 +/- 0.4 | 2/3 | 34.5 +/- 1.5 | 4.0 |
| ***Hey1*** | 3/3 | 28.7 +/- 0.5 | 2/3 | 29.5 +/- 0.2 | 3/3 | 32.0 +/- 1.5 | 2.5 |
| ***Mnt*** | 2/3 | 27.2 +/- 0.3 | 3/3 | 28.9 +/- 1.0 | 3/3 | 30.8 +/- 0.5 | 2.0 |
| ***Msc*** | 2/3 | 27.4 +/- 0.3 | 3/3 | 31.3 +/- 1.3 | 3/3 | 0.0 +/- 0.0 | M |
| ***Ngn3*** | 2/3 | 36.2 +/- 0.3 | 3/3 | 35.1 +/- 1.3 | 2/3 | 37.2 +/- 0.5 | 2.1 |
| ***A830053 O21Rik*** | 3/3 | 32.2 +/- 0.4 | 3/3 | 0.0 +/- 0.0 | 3/3 | 32.3 +/- 0.8 | F |
| ***Ahrr*** | 3/3 | 33.4 +/- 0.5 | 3/3 | 0.0 +/- 0.0 | 3/3 | 35.4 +/- 0.7 | F |
| ***Ascl1*** | 2/3 | 27.3 +/- 0.6 | 3/3 | 0.0 +/- 0.0 | 2/3 | 34.9 +/- 0.1 | F |
| ***Atoh1*** | 3/3 | 32.3 +/- 1.3 | 3/3 | 0.0 +/- 0.0 | 2/3 | 34.8 +/- 1.6 | F |
| ***Bhlhb2*** | 2/3 | 27.5 +/- 0.3 | 2/3 | 32.7 +/- 2.0 | 2/3 | 28.2 +/- 0.3 | 4.6 |
| ***Bhlhb4*** | 3/3 | 33.1 +/- 0.7 | 2/2 | 0.0 +/- 0.0 | 3/3 | 35.4 +/- 1.1 | F |
| ***Bhlhb5*** | 3/3 | 28.1 +/- 0.5 | 2/3 | 0.0 +/- 0.0 | 3/3 | 33.6 +/- 1.8 | F |
| ***Ebf3*** | 2/3 | 29.3 +/- 0.5 | 2/3 | 0.0 +/- 0.0 | 3/3 | 34.7 +/- 0.8 | F |
| ***Ebf4*** | 2/3 | 30.6 +/- 0.7 | 2/3 | 0.0 +/- 0.0 | 3/3 | 30.0 +/- 1.4 | F |
| ***Figla*** | 3/3 | 36.0 +/- 1.5 | 3/3 | 31.5 +/- 0.7 | 3/3 | 27.6 +/- 0.2 | 3.9 |
| ***Hand1*** | 3/3 | 25.3 +/- 0.6 | 2/3 | 0.0 +/- 0.0 | 2/3 | 29.0 +/- 1.1 | F |
| ***Hes2*** | 3/3 | 35.0 +/- 0.7 | 2/2 | 0.0 +/- 0.0 | 2/3 | 36.8 +/- 0.9 | F |
| ***Hes7*** | 3/3 | 34.0 +/- 1.6 | 3/3 | 0.0 +/- 0.0 | 2/3 | 35.0 +/- 0.7 | F |
| ***Heyl*** | 3/3 | 28.6 +/- 1.2 | 2/3 | 0.0 +/- 0.0 | 2/3 | 35.9 +/- 1.1 | F |
| ***Id1*** | 2/3 | 23.8 +/- 0.8 | 3/3 | 27.4 +/- 1.5 | 3/3 | 23.4 +/- 0.7 | 4.0 |
| ***Id3*** | 3/3 | 22.0 +/- 0.3 | 3/3 | 25.8 +/- 0.2 | 3/3 | 23.3 +/- 0.4 | 2.5 |
| ***Id4*** | 2/3 | 29.7 +/- 0.8 | 3/3 | 32.2 +/- 0.8 | 3/3 | 29.9 +/- 1.1 | 2.4 |
| ***Max*** | 3/3 | 24.8 +/- 0.5 | 3/3 | 0.0 +/- 0.0 | 2/3 | 29.2 +/- 1.6 | F |
| ***Mesp1*** | 3/3 | 31.7 +/- 1.4 | 3/3 | 34.0 +/- 0.3 | 3/3 | 29.6 +/- 1.5 | 4.3 |
| ***Mlxipl*** | 3/3 | 31.4 +/- 0.3 | 3/3 | 33.8 +/- 0.6 | 3/3 | 30.9 +/- 1.2 | 2.9 |
| ***Mxd4*** | 2/3 | 30.0 +/- 0.7 | 2/3 | 32.5 +/- 1.8 | 3/3 | 27.4 +/- 0.9 | 5.1 |
| ***Olig1*** | 3/3 | 34.4 +/- 1.0 | 2/3 | 0.0 +/- 0.0 | 3/3 | 38.2 +/- 1.6 | F |
| ***Scx*** | 2/3 | 28.2 +/- 0.1 | 3/3 | 35.4 +/- 1.3 | 2/3 | 31.5 +/- 1.2 | 3.9 |
| ***Tal1*** | 3/3 | 27.8 +/- 0.6 | 2/3 | 0.0 +/- 0.0 | 2/3 | 36.2 +/- 2.0 | F |
| ***Tcf21*** | 3/3 | 27.2 +/- 1.4 | 3/3 | 35.6 +/- 0.5 | 2/3 | 33.2 +/- 0.1 | 2.4 |

**Table v.3. Genes that had ≥2.0 cycles difference between male and female E13.5 GC cDNA in bHLH Screen Phase 1**

# Appendix vi:
## Additional Results for bHLH Screen Part 2

| Gene | Total ♂ Reps. | Total ♀ Reps. | Fold Enrichment (♂/♀) | |
|---|---|---|---|---|
| | | | Biological Rep. 1 | Biological Rep. 2 |
| ***Epas1*** | 6 | 6 | **4.1** +/- 1.2 (*) | **4.3** +/- 0.8 (*) |
| ***Helt*** | 6 | 6 | **4.9** +/- 2.8 (*) | **3.6** +/- 1.1 (*) |
| ***Mnt*** | 6 | 6 | **3.0** +/- 0.8 (*) | **3.6** +/- 1.3 (*) |
| ***Ngn3*** | 6 | 5 | **11.7** +/- 4.9 (*) | **5.9** +/- 1.2 (*) |

**Table vi.1. bHLH Screen Part 2: Male-Enriched Genes (normalised to *Gapdh*).** See legend for Table 3.4.1 (Chapter 3).

| Gene | Total ♂ Reps. | Total ♀ Reps. | Fold Enrichment (♀/♂) | |
|---|---|---|---|---|
| | | | Biological Rep. 1 | Biological Rep. 2 |
| ***A83000Rik*** | 3 | 4 | **16.9** +/- 5.3 (*) | **15.2** +/- 10.1 (ns) |
| ***Bhlhb2*** | 6 | 6 | **123.6** +/- 52.5 (*) | **130.8** +/- 25.9 (**) |
| ***Ebf4*** | 6 | 6 | **84.5** +/- 22.8 (***) | **73.3** +/- 13.1 (ns) |
| ***Figla*** | 7 | 6 | **36.4** +/- 8.4 (**) | **47.5** +/- 8.3 (**) |
| ***Id1*** | 6 | 5 | **31.9** +/- 11.2 (*) | **42.1** +/- 7.8 (**) |
| ***Id2*** | 6 | 6 | **18.8** +/- 6.9 (*) | **16.3** +/- 3.2 (**) |
| ***Id3*** | 6 | 6 | **15.3** +/- 4.2 (*) | **9.9** +/- 1.5 (**) |
| ***Mesp1*** | 6 | 6 | **11.0** +/- 4.5 (*) | **32.1** +/- 10.2 (*) |
| ***Mlxipl*** | 6 | 6 | **6.6** +/- 0.7 (**) | **4.2** +/- 1.3 (*) |
| ***Mxd4*** | 6 | 6 | **31.1** +/- 9.7 (*) | **39.7** +/- 15.7 (**) |
| ***Scx*** | 6 | 6 | **16.9** +/- 5.3 (*) | **15.2** +/- 10.1 (ns) |

**Table vi.2. bHLH Screen Part 2: Female-Enriched Genes (normalised to *Gapdh*).** See legend for Table 3.4.2 (Chapter 3).

| Gene | Total ♂ Reps. | Total ♀ Reps. | Fold Enrichment (♂/♀) | |
|---|---|---|---|---|
| | | | Biological Rep. 1 | Biological Rep. 2 |
| ***Ascl2*** | 6 | 6 | **0.5** +/- 0.1 | **0.9** +/- 0.4 |
| ***Hey1*** | 6 | 6 | **2.1** +/- 0.5(*) | **2.1** +/- 0.3(**) |
| ***Id4*** | 6 | 6 | **0.3** +/- 0.1 | **0.7** +/- 0.1 |
| ***Max*** | 6 | 6 | **1.0** +/- 0.1 | **1.2** +/- 0.2 |
| ***Olig1*** | 3 | 3 | **0.6** +/- 0.1 | - |

**Table vi.2. bHLH Screen Part 2: Female-Enriched Genes (normalised to *Gapdh*).** See legend for Table 3.4.4 (Chapter 3).

# References


**Adams, I. R. and McLaren, A.** (2002). Sexually dimorphic development of mouse primordial germ cells: switching from oogenesis to spermatogenesis. *Development* **129**, 1155-64.

**Albrecht, K. H. and Eicher, E. M.** (2001). Evidence that Sry is expressed in pre-Sertoli cells and Sertoli and granulosa cells have a common precursor. *Dev Biol* **240**, 92-107.

**Albrecht, K. H., Young, M., Washburn, L. L. and Eicher, E. M.** (2003). Sry expression level and protein isoform differences play a role in abnormal testis development in C57BL/6J mice carrying certain Sry alleles. *Genetics* **164**, 277-88.

**Allegrucci, C., Thurston, A., Lucas, E. and Young, L.** (2005). Epigenetics and the germline. *Reproduction* **129**, 137-49.

**Ancelin, K., Lange, U. C., Hajkova, P., Schneider, R., Bannister, A. J., Kouzarides, T. and Surani, M. A.** (2006). Blimp1 associates with Prmt5 and directs histone arginine methylation in mouse germ cells. *Nat Cell Biol* **8**, 623-30.

**Anderson, R., Fassler, R., Georges-Labouesse, E., Hynes, R. O., Bader, B. L., Kreidberg, J. A., Schaible, K., Heasman, J. and Wylie, C.** (1999). Mouse primordial germ cells lacking beta1 integrins enter the germline but fail to migrate normally to the gonads. *Development* **126**, 1655-64.

**Arango, N. A., Lovell-Badge, R. and Behringer, R. R.** (1999). Targeted mutagenesis of the endogenous mouse Mis gene promoter: in vivo definition of genetic pathways of vertebrate sexual development. *Cell* **99**, 409-19.

**Asai, A., Miyagi, Y., Sugiyama, A., Nagashima, Y., Kanemitsu, H., Obinata, M., Mishima, K. and Kuchino, Y.** (1994). The s-Myc protein having the ability to induce apoptosis is selectively expressed in rat embryo chondrocytes. *Oncogene* **9**, 2345-2352.

**Bagheri-Fam, S., Sim, H., Bernard, P., Jayakody, I., Taketo, M. M., Scherer, G. and Harley, V. R.** (2008). Loss of Fgfr2 leads to partial XY sex reversal. *Dev Biol* **314**, 71-83.

**Baker, P. J. and O'Shaughnessy, P. J.** (2001). Expression of prostaglandin D synthetase during development in the mouse testis. *Reproduction* **122**, 553-9.

**Ballow, D., Meistrich, M. L., Matzuk, M. and Rajkovic, A.** (2006). Sohlh1 is essential for spermatogonial differentiation. *Dev Biol* **294**, 161-7.

**Baltus, A. E., Menke, D. B., Hu, Y. C., Goodheart, M. L., Carpenter, A. E., de Rooij, D. G. and Page, D. C.** (2006). In germ cells of mouse embryonic ovaries, the decision to enter meiosis precedes premeiotic DNA replication. *Nat Genet* **38**, 1430-4.

**Barone, M. V., Pepperkok, R., Peverali, F. A. and Philipson, L.** (1994). Id proteins control growth induction in mammalian cells. *Proc Natl Acad Sci U S A* **91**, 4985-8.

**Barrionuevo, F., Bagheri-Fam, S., Klattig, J., Kist, R., Taketo, M. M., Englert, C. and Scherer, G.** (2006). Homozygous inactivation of Sox9 causes complete XY sex reversal in mice. *Biol Reprod* **74**, 195-201.

**Ben-Arie, N., Bellen, H. J., Armstrong, D. L., McCall, A. E., Gordadze, P. R., Guo, Q., Matzuk, M. M. and Zoghbi, H. Y.** (1997). Math1 is essential for genesis of cerebellar granule neurons. *Nature* **390**, 169-72.

**Berthet, C., Aleem, E., Coppola, V., Tessarollo, L. and Kaldis, P.** (2003). Cdk2 knockout mice are viable. *Curr Biol* **13**, 1775-85.

**Bessho, Y., Sakata, R., Komatsu, S., Shiota, K., Yamada, S. and Kageyama, R.** (2001). Dynamic expression and essential functions of Hes7 in somite segmentation. *Genes Dev.* **15**, 2642-2647.

**Best, D., Sahlender, D. A., Walther, N., Peden, A. A. and Adams, I. R.** (2008). Sdmg1 is a conserved transmembrane protein associated with germ cell sex determination and germline-soma interactions in mice. *Development* **135**, 1415-25.

**Beuckmann, C. T., Aoyagi, M., Okazaki, I., Hiroike, T., Toh, H., Hayaishi, O. and Urade, Y.** (1999). Binding of biliverdin, bilirubin, and thyroid hormones to lipocalin-type prostaglandin D synthase. *Biochemistry* **38**, 8006-13.

**Bishop, C. E., Whitworth, D. J., Qin, Y., Agoulnik, A. I., Agoulnik, I. U., Harrison, W. R., Behringer, R. R. and Overbeek, P. A.** (2000). A transgenic insertion upstream of sox9 is associated with dominant XX sex reversal in the mouse. *Nat Genet* **26**, 490-4.

**Bitgood, M. J., Shen, L. and McMahon, A. P.** (1996). Sertoli cell signaling by Desert hedgehog regulates the male germline. *Curr Biol* **6**, 298-304.

**Boie, Y., Sawyer, N., Slipetz, D. M., Metters, K. M. and Abramovitz, M.** (1995). Molecular cloning and characterization of the human prostanoid DP receptor. *J Biol Chem* **270**, 18910-6.

**Bortvin, A., Goodheart, M., Liao, M. and Page, D. C.** (2004). Dppa3 / Pgc7 / stella is a maternal factor and is not required for germ cell specification in mice. *BMC Dev Biol* **4**, 2.

**Bouma, G. J., Albrecht, K. H., Washburn, L. L., Recknagel, A. K., Churchill, G. A. and Eicher, E. M.** (2005). Gonadal sex reversal in mutant Dax1 XY mice: a failure to upregulate Sox9 in pre-Sertoli cells. *Development* **132**, 3045-54.

**Bouma, G. J., Hart, G. T., Washburn, L. L., Recknagel, A. K. and Eicher, E. M.** (2004). Using real time RT-PCR analysis to determine multiple gene expression patterns during XX and XY mouse fetal gonad development. *Gene Expr Patterns* **5**, 141-9.

**Bowles, J., Knight, D., Smith, C., Wilhelm, D., Richman, J., Mamiya, S., Yashiro, K., Chawengsaksophak, K., Wilson, M. J., Rossant, J. et al.** (2006). Retinoid signaling determines germ cell fate in mice. *Science* **312**, 596-600.

**Bowles, J., Teasdale, R. P., James, K. and Koopman, P.** (2003). Dppa3 is a marker of pluripotency and has a human homologue that is expressed in germ cell tumours. *Cytogenet Genome Res* **101**, 261-5.

**Brady, G. and Iscove, N. N.** (1993). Construction of cDNA libraries from single cells. *Methods Enzymol* **225**, 611-23.

**Bramblett, D. E., Pennesi, M. E., Wu, S. M. and Tsai, M. J.** (2004). The transcription factor Bhlhb4 is required for rod bipolar cell maturation. *Neuron* **43**, 779-93.

**Brown, D., Wagner, D., Li, X., Richardson, J. A. and Olson, E. N.** (1999). Dual role of the basic helix-loop-helix transcription factor scleraxis in mesoderm formation and chondrogenesis during mouse embryogenesis. *Development* **126**, 4317-29.

**Buehr, M., Gu, S. and McLaren, A.** (1993). Mesonephric contribution to testis differentiation in the fetal mouse. *Development* **117**, 273-81.

**Bullejos, M. and Koopman, P.** (2001). Spatially dynamic expression of Sry in mouse genital ridges. *Dev Dyn* **221**, 201-5.

**Bullejos, M. and Koopman, P.** (2004). Germ cells enter meiosis in a rostro-caudal wave during development of the mouse ovary. *Mol Reprod Dev* **68**, 422-8.

**Burgoyne, P. S., Buehr, M. and McLaren, A.** (1988). XY follicle cells in ovaries of XX----XY female mouse chimaeras. *Development* **104**, 683-8.

**Chaboissier, M. C., Kobayashi, A., Vidal, V. I., Lutzkendorf, S., van de Kant, H. J., Wegner, M., de Rooij, D. G., Behringer, R. R. and Schedl, A.** (2004). Functional analysis of Sox8 and Sox9 during sex determination in the mouse. *Development* **131**, 1891-901.

**Chambers, I., Colby, D., Robertson, M., Nichols, J., Lee, S., Tweedie, S. and Smith, A.** (2003). Functional expression cloning of Nanog, a pluripotency sustaining factor in embryonic stem cells. *Cell* **113**, 643-55.

**Chambers, I., Silva, J., Colby, D., Nichols, J., Nijmeijer, B., Robertson, M., Vrana, J., Jones, K., Grotewold, L. and Smith, A.** (2007). Nanog safeguards pluripotency and mediates germline development. *Nature* **450**, 1230-4.

**Chambers, I. and Tomlinson, S. R.** (2009). The transcriptional foundation of pluripotency. *Development* **136**, 2311-22.

**Chassot, A. A., Ranc, F., Gregoire, E. P., Roepers-Gajadien, H. L., Taketo, M. M., Camerino, G., de Rooij, D. G., Schedl, A. and Chaboissier, M. C.** (2008). Activation of beta-catenin signaling by Rspo1 controls differentiation of the mammalian ovary. *Hum Mol Genet* **17**, 1264-77.

**Chassot, A. A., Turchi, L., Virolle, T., Fitsialos, G., Batoz, M., Deckert, M., Dulic, V., Meneguzzi, G., Busca, R. and Ponzio, G.** (2007). Id3 is a novel regulator of p27kip1 mRNA in early G1 phase and is required for cell-cycle progression. *Oncogene* **26**, 5772-83.

**Choi, Y., Yuan, D. and Rajkovic, A.** (2008). Germ cell-specific transcriptional regulator sohlh2 is essential for early mouse folliculogenesis and oocyte-specific gene expression. *Biol Reprod* **79**, 1176-82.

**Chuma, S. and Nakatsuji, N.** (2001). Autonomous transition into meiosis of mouse fetal germ cells in vitro and its inhibition by gp130-mediated signaling. *Dev Biol* **229**, 468-79.

**Ciarrocchi, A., Jankovic, V., Shaked, Y., Nolan, D. J., Mittal, V., Kerbel, R. S., Nimer, S. D. and Benezra, R.** (2007). Id1 restrains p21 expression to control endothelial progenitor cell formation. *PLoS One* **2**, e1338.

**Colvin, J. S., Green, R. P., Schmahl, J., Capel, B. and Ornitz, D. M.** (2001). Male-to-female sex reversal in mice lacking fibroblast growth factor 9. *Cell* **104**, 875-89.

**Combes, A. N., Wilhelm, D., Davidson, T., Dejana, E., Harley, V., Sinclair, A. and Koopman, P.** (2009). Endothelial cell migration directs testis cord formation. *Dev Biol* **326**, 112-20.

**Cool, J., Carmona, F. D., Szucsik, J. C. and Capel, B.** (2008). Peritubular myoid cells are not the migrating population required for testis cord formation in the XY gonad. *Sex Dev* **2**, 128-33.

**Cory, A. T., Boyer, A., Pilon, N., Lussier, J. G. and Silversides, D. W.** (2007). Presumptive pre-Sertoli cells express genes involved in cell proliferation and cell signalling during a critical window in early testis differentiation. *Mol Reprod Dev* **74**, 1491-504.

**Cupp, A. S., Dufour, J. M., Kim, G., Skinner, M. K. and Kim, K. H.** (1999). Action of retinoids on embryonic and early postnatal testis development. *Endocrinology* **140**, 2343-52.

**De Santa Barbara, P., Bonneaud, N., Boizet, B., Desclozeaux, M., Moniot, B., Sudbeck, P., Scherer, G., Poulat, F. and Berta, P.** (1998). Direct interaction of SRY-related protein SOX9 and steroidogenic factor 1 regulates transcription of the human anti-Mullerian hormone gene. *Mol Cell Biol* **18**, 6653-65.

**Desprez, P. Y., Hara, E., Bissell, M. J. and Campisi, J.** (1995). Suppression of mammary epithelial cell differentiation by the helix-loop-helix protein Id-1. *Mol Cell Biol* **15**, 3398-404.

**Di Carlo, A. D., Travia, G. and De Felici, M.** (2000). The meiotic specific synaptonemal complex protein SCP3 is expressed by female and male primordial germ cells of the mouse embryo. *Int J Dev Biol* **44**, 241-4.

**DiNapoli, L., Batchvarov, J. and Capel, B.** (2006). FGF9 promotes survival of germ cells in the fetal testis. *Development* **133**, 1519-27.

**Donovan, P. J., Stott, D., Cairns, L. A., Heasman, J. and Wylie, C. C.** (1986). Migratory and postmigratory mouse primordial germ cells behave differently in culture. *Cell* **44**, 831-8.

**Durcova-Hills, G., Burgoyne, P. and McLaren, A.** (2004). Analysis of sex differences in EGC imprinting. *Dev Biol* **268**, 105-10.

**Eckner, R., Yao, T. P., Oldread, E. and Livingston, D. M.** (1996). Interaction and functional collaboration of p300/CBP and bHLH proteins in muscle and B-cell differentiation. *Genes Dev.* **10**, 2478-2490.

**Eguchi, N., Minami, T., Shirafuji, N., Kanaoka, Y., Tanaka, T., Nagata, A., Yoshida, N., Urade, Y., Ito, S. and Hayaishi, O.** (1999). Lack of tactile pain (allodynia) in lipocalin-type prostaglandin D synthase-deficient mice. *Proc Natl Acad Sci U S A* **96**, 726-30.

**Eicher, E. M., Shown, E. P. and Washburn, L. L.** (1995). Sex reversal in C57BL/6J-YPOS mice corrected by a Sry transgene. *Philos Trans R Soc Lond B Biol Sci* **350**, 263-8; discussion 268-9.

**Eicher, E. M. and Washburn, L. L.** (1986). Genetic control of primary sex determination in mice. *Annu Rev Genet* **20**, 327-60.

**Eicher, E. M., Washburn, L. L., Schork, N. J., Lee, B. K., Shown, E. P., Xu, X., Dredge, R. D., Pringle, M. J. and Page, D. C.** (1996). Sex-determining genes on mouse autosomes identified by linkage analysis of C57BL/6J-YPOS sex reversal. *Nat Genet* **14**, 206-9.

**Enders, G. C. and May, J. J., 2nd.** (1994). Developmentally regulated expression of a mouse germ cell nuclear antigen examined from embryonic day 11 to adult in male and female mice. *Dev Biol* **163**, 331-40.

**Farini, D., Scaldaferri, M. L., Iona, S., La Sala, G. and De Felici, M.** (2005). Growth factors sustain primordial germ cell survival, proliferation and entering into meiosis in the absence of somatic cells. *Dev Biol* **285**, 49-56.

**Fischer, A. and Gessler, M.** (2007). Delta-Notch--and then? Protein interactions and proposed modes of repression by Hes and Hey bHLH factors. *Nucleic Acids Res* **35**, 4583-96.

**Ford, C. E., Evans, E. P. and Gardner, R. L.** (1975). Marker chromosome analysis of two mouse chimaeras. *J Embryol Exp Morphol* **33**, 447-57.

**Foster, J. W., Dominguez-Steglich, M. A., Guioli, S., Kwok, C., Weller, P. A., Stevanovic, M., Weissenbach, J., Mansour, S., Young, I. D., Goodfellow, P. N. et al.** (1994). Campomelic dysplasia and autosomal sex reversal caused by mutations in an SRY-related gene. *Nature* **372**, 525-30.

**Fouchecourt, S., Castella, S., Dacheux, F. and Dacheux, J. L.** (2003). Prostaglandin D2 synthase secreted in the caput epididymidis displays spatial and temporal delay between messenger RNA and protein expression during postnatal development. *Biol Reprod* **68**, 174-9.

**Fraidenraich, D., Stillwell, E., Romero, E., Wilkes, D., Manova, K., Basson, C. T. and Benezra, R.** (2004). Rescue of cardiac defects in id knockout embryos by injection of embryonic stem cells. *Science* **306**, 247-52.

**Fujimori, K., Aritake, K. and Urade, Y.** (2008). Enhancement of prostaglandin D(2) production through cyclooxygenase-2 and lipocalin-type prostaglandin D synthase by upstream stimulatory factor 1 in human brain-derived TE671 cells under serum starvation. *Gene* **426**, 72-80.

**Fujimori, K., Fujitani, Y., Kadoyama, K., Kumanogoh, H., Ishikawa, K. and Urade, Y.** (2003). Regulation of lipocalin-type prostaglandin D synthase gene expression by Hes-1 through E-box and interleukin-1 beta via two NF-kappa B elements in rat leptomeningeal cells. *J Biol Chem* **278**, 6018-26.

**Fujimori, K., Kadoyama, K. and Urade, Y.** (2005). Protein kinase C activates human lipocalin-type prostaglandin D synthase gene expression through de-repression of notch-HES signaling and enhancement of AP-2 beta function in brain-derived TE671 cells. *J Biol Chem* **280**, 18452-61.

**Fujimori, K. and Urade, Y.** (2007). Cooperative activation of lipocalin-type prostaglandin D synthase gene expression by activator protein-2beta in proximal promoter and upstream stimulatory factor 1 within intron 4 in human brain-derived TE671 cells. *Gene* **397**, 143-52.

**Fujiwara, Y., Komiya, T., Kawabata, H., Sato, M., Fujimoto, H., Furusawa, M. and Noce, T.** (1994). Isolation of a DEAD-family protein gene that encodes a murine homolog of Drosophila vasa and its specific expression in germ cell lineage. *Proc Natl Acad Sci U S A* **91**, 12258-62.

**Garcia-Castro, M. I., Anderson, R., Heasman, J. and Wylie, C.** (1997). Interactions between germ cells and extracellular matrix glycoproteins during migration and gonad assembly in the mouse embryo. *J Cell Biol* **138**, 471-80.

**Garcia-Fernandez, L. F., Iniguez, M. A., Eguchi, N., Fresno, M., Urade, Y. and Munoz, A.** (2000). Dexamethasone induces lipocalin-type prostaglandin D synthase gene expression in mouse neuronal cells. *J Neurochem* **75**, 460-70.

**Garcia-Fernandez, L. F., Urade, Y., Hayaishi, O., Bernal, J. and Munoz, A.** (1998). Identification of a thyroid hormone response element in the promoter region of the rat lipocalin-type prostaglandin D synthase (beta-trace) gene. *Brain Res Mol Brain Res* **55**, 321-30.

**Garcia-Ortiz, J. E., Pelosi, E., Omari, S., Nedorezov, T., Piao, Y., Karmazin, J., Uda, M., Cao, A., Cole, S. W., Forabosco, A. et al.** (2009). Foxl2 functions in sex determination and histogenesis throughout mouse ovary development. *BMC Dev Biol* **9**, 36.

**Garrett-Engele, C. M., Tasch, M. A., Hwang, H. C., Fero, M. L., Perlmutter, R. M., Clurman, B. E. and Roberts, J. M.** (2007). A mechanism misregulating p27 in tumors discovered in a functional genomic screen. *PLoS Genet* **3**, e219.

**Gomperts, M., Garcia-Castro, M., Wylie, C. and Heasman, J.** (1994). Interactions between primordial germ cells play a role in their migration in mouse embryos. *Development* **120**, 135-41.

**Gradwohl, G., Dierich, A., LeMeur, M. and Guillemot, F.** (2000). neurogenin3 is required for the development of the four endocrine cell lineages of the pancreas. *Proc Natl Acad Sci U S A* **97**, 1607-11.

**Graham, P. L. and Kimble, J.** (1993). The mog-1 gene is required for the switch from spermatogenesis to oogenesis in Caenorhabditis elegans. *Genetics* **133**, 919-31.

**Gubbay, J., Collignon, J., Koopman, P., Capel, B., Economou, A., Munsterberg, A., Vivian, N., Goodfellow, P. and Lovell-Badge, R.** (1990). A gene mapping to the sex-determining region of the mouse Y chromosome is a member of a novel family of embryonically expressed genes. *Nature* **346**, 245-50.

**Guimera, J., Vogt Weisenhorn, D., Echevarria, D., Martinez, S. and Wurst, W.** (2006a). Molecular characterization, structure and developmental expression of Megane bHLH factor. *Gene* **377**, 65-76.

**Guimera, J., Weisenhorn, D. V. and Wurst, W.** (2006b). Megane/Heslike is required for normal GABAergic differentiation in the mouse superior colliculus. *Development* **133**, 3847-57.

**Hao, J., Yamamoto, M., Richardson, T. E., Chapman, K. M., Denard, B. S., Hammer, R. E., Zhao, G. Q. and Hamra, F. K.** (2008). Sohlh2 knockout mice are male-sterile because of degeneration of differentiating type A spermatogonia. *Stem Cells* **26**, 1587-97.

**Hara, E., Yamaguchi, T., Nojima, H., Ide, T., Campisi, J., Okayama, H. and Oda, K.** (1994). Id-related genes encoding helix-loop-helix proteins are required for G1 progression and are repressed in senescent human fibroblasts. *J Biol Chem* **269**, 2139-45.

**Harris, S. G., Padilla, J., Koumas, L., Ray, D. and Phipps, R. P.** (2002). Prostaglandins as modulators of immunity. *Trends Immunol* **23**, 144-50.

**Hatano, O., Takayama, K., Imai, T., Waterman, M. R., Takakusu, A., Omura, T. and Morohashi, K.** (1994). Sex-dependent expression of a transcription factor, Ad4BP, regulating steroidogenic P-450 genes in the gonads during prenatal and postnatal rat development. *Development* **120**, 2787-97.

**Hawkins, J. R.** (1993). The SRY gene. *Trends Endocrinol Metab* **4**, 328-32.

**Heikinheimo, M., Ermolaeva, M., Bielinska, M., Rahman, N. A., Narita, N., Huhtaniemi, I. T., Tapanainen, J. S. and Wilson, D. B.** (1997). Expression and hormonal regulation of transcription factors GATA-4 and GATA-6 in the mouse ovary. *Endocrinology* **138**, 3505-14.

**Henrique, D., Adam, J., Myat, A., Chitnis, A., Lewis, J. and Ish-Horowicz, D.** (1995). Expression of a Delta homologue in prospective neurons in the chick. *Nature* **375**, 787-90.

**Higgins, S., Wong, S. H., Richner, M., Rowe, C. L., Newgreen, D. F., Werther, G. A. and Russo, V. C.** (2009). FGF-2 RE-ACTIVATES G1-CHECKPOINT IN SK-N-MC CELLS VIA

REGULATION OF p21, INHIBITOR OF DIFFERENTIATION GENES (Id1-3), AND EMT-LIKE EVENTS. *Endocrinology*.

**Hiramatsu, R., Matoba, S., Kanai-Azuma, M., Tsunekawa, N., Katoh-Fukui, Y., Kurohmaru, M., Morohashi, K., Wilhelm, D., Koopman, P. and Kanai, Y.** (2009). A critical time window of Sry action in gonadal sex determination in mice. *Development* **136**, 129-38.

**Hoffmann, A., Conradt, H. S., Gross, G., Nimtz, M., Lottspeich, F. and Wurster, U.** (1993). Purification and chemical characterization of beta-trace protein from human cerebrospinal fluid: its identification as prostaglandin D synthase. *J Neurochem* **61**, 451-6.

**Hollnagel, A., Oehlmann, V., Heymer, J., Ruther, U. and Nordheim, A.** (1999). Id genes are direct targets of bone morphogenetic protein induction in embryonic stem cells. *J Biol Chem* **274**, 19838-45.

**Hooker, C. W. and Hurlin, P. J.** (2006). Of Myc and Mnt. *J Cell Sci* **119**, 208-16.

**Hosoya, T., Harada, N., Mimura, J., Motohashi, H., Takahashi, S., Nakajima, O., Morita, M., Kawauchi, S., Yamamoto, M. and Fujii-Kuriyama, Y.** (2008). Inducibility of cytochrome P450 1A1 and chemical carcinogenesis by benzo[a]pyrene in AhR repressor-deficient mice. *Biochem Biophys Res Commun* **365**, 562-7.

**Hua, H., Zhang, Y. Q., Dabernat, S., Kritzik, M., Dietz, D., Sterling, L. and Sarvetnick, N.** (2006). BMP4 regulates pancreatic progenitor cell expansion through Id2. *J Biol Chem* **281**, 13574-80.

**Huang, Z. L., Urade, Y. and Hayaishi, O.** (2007). Prostaglandins and adenosine in the regulation of sleep and wakefulness. *Curr Opin Pharmacol* **7**, 33-8.

**Hurlin, P. J., Queva, C. and Eisenman, R. N.** (1997). Mnt, a novel Max-interacting protein is coexpressed with Myc in proliferating cells and mediates repression at Myc binding sites. *Genes Dev* **11**, 44-58.

**Iizuka, K., Bruick, R. K., Liang, G., Horton, J. D. and Uyeda, K.** (2004). Deficiency of carbohydrate response element-binding protein (ChREBP) reduces lipogenesis as well as glycolysis. *Proc Natl Acad Sci U S A* **101**, 7281-6.

**Jeays-Ward, K., Dandonneau, M. and Swain, A.** (2004). Wnt4 is required for proper male as well as female sexual development. *Dev Biol* **276**, 431-40.

**Jeays-Ward, K., Hoyle, C., Brennan, J., Dandonneau, M., Alldus, G., Capel, B. and Swain, A.** (2003). Endothelial and steroidogenic cell migration are regulated by WNT4 in the developing mammalian gonad. *Development* **130**, 3663-70.

**Jen, Y., Weintraub, H. and Benezra, R.** (1992). Overexpression of Id protein inhibits the muscle differentiation program: in vivo association of Id with E2A proteins. *Genes Dev.* **6**, 1466-1479.

**Jeon, H. M., Jin, X., Lee, J. S., Oh, S. Y., Sohn, Y. W., Park, H. J., Joo, K. M., Park, W. Y., Nam, D. H., DePinho, R. A. et al.** (2008). Inhibitor of differentiation 4 drives brain tumor-initiating cell genesis through cyclin E and notch signaling. *Genes Dev* **22**, 2028-33.

**Jordan, B. K., Mohammed, M., Ching, S. T., Delot, E., Chen, X. N., Dewing, P., Swain, A., Rao, P. N., Elejalde, B. R. and Vilain, E.** (2001). Up-regulation of WNT-4 signaling and dosage-sensitive sex reversal in humans. *Am J Hum Genet* **68**, 1102-9.

**Kageyama, R., Ohtsuka, T., Hatakeyama, J. and Ohsawa, R.** (2005). Roles of bHLH genes in neural stem cell differentiation. *Exp Cell Res* **306**, 343-8.

**Kanekiyo, T., Ban, T., Aritake, K., Huang, Z. L., Qu, W. M., Okazaki, I., Mohri, I., Murayama, S., Ozono, K., Taniike, M. et al.** (2007). Lipocalin-type prostaglandin D synthase/beta-trace is a major amyloid beta-chaperone in human cerebrospinal fluid. *Proc Natl Acad Sci U S A* **104**, 6412-7.

**Kehler, J., Tolkunova, E., Koschorz, B., Pesce, M., Gentile, L., Boiani, M., Lomeli, H., Nagy, A., McLaughlin, K. J., Scholer, H. R. et al.** (2004). Oct4 is required for primordial germ cell survival. *EMBO Rep* **5**, 1078-83.

**Kent, J., Wheatley, S. C., Andrews, J. E., Sinclair, A. H. and Koopman, P.** (1996). A male-specific role for SOX9 in vertebrate sex determination. *Development* **122**, 2813-22.

**Kim, Y., Bingham, N., Sekido, R., Parker, K. L., Lovell-Badge, R. and Capel, B.** (2007). Fibroblast growth factor receptor 2 regulates proliferation and Sertoli differentiation during male sex determination. *Proc Natl Acad Sci U S A* **104**, 16558-63.

**Kim, Y., Kobayashi, A., Sekido, R., DiNapoli, L., Brennan, J., Chaboissier, M. C., Poulat, F., Behringer, R. R., Lovell-Badge, R. and Capel, B.** (2006). Fgf9 and Wnt4 act as antagonistic signals to regulate mammalian sex determination. *PLoS Biol* **4**, e187.

**Kimble, J. and Crittenden, S. L.** (2005). Germline proliferation and its control. *WormBook*, 1-14.

**Kobayashi, A., Chang, H., Chaboissier, M. C., Schedl, A. and Behringer, R. R.** (2005). Sox9 in testis determination. *Ann N Y Acad Sci* **1061**, 9-17.

**Kodaira, K., Takahashi, R., Hirabayashi, M., Suzuki, T., Obinata, M. and Ueda, M.** (1996). Overexpression of c-myc induces apoptosis at the prophase of meiosis of rat primary spermatocytes. *Mol Reprod Dev* **45**, 403-10.

**Koopman, P., Gubbay, J., Vivian, N., Goodfellow, P. and Lovell-Badge, R.** (1991). Male development of chromosomally female mice transgenic for Sry. *Nature* **351**, 117-21.

**Koshimizu, U., Taga, T., Watanabe, M., Saito, M., Shirayoshi, Y., Kishimoto, T. and Nakatsuji, N.** (1996). Functional requirement of gp130-mediated signaling for growth and survival of mouse primordial germ cells in vitro and derivation of embryonic germ (EG) cells. *Development* **122**, 1235-42.

**Koshimizu, U., Watanabe, M. and Nakatsuji, N.** (1995). Retinoic acid is a potent growth activator of mouse primordial germ cells in vitro. *Dev Biol* **168**, 683-5.

**Kostenis, E. and Ulven, T.** (2006). Emerging roles of DP and CRTH2 in allergic inflammation. *Trends Mol Med* **12**, 148-58.

**Koubova, J., Menke, D. B., Zhou, Q., Capel, B., Griswold, M. D. and Page, D. C.** (2006). Retinoic acid regulates sex-specific timing of meiotic initiation in mice. *Proc Natl Acad Sci U S A* **103**, 2474-9.

**Kwok, C., Weller, P. A., Guioli, S., Foster, J. W., Mansour, S., Zuffardi, O., Punnett, H. H., Dominguez-Steglich, M. A., Brook, J. D., Young, I. D. et al.** (1995). Mutations in SOX9, the gene responsible for Campomelic dysplasia and autosomal sex reversal. *Am J Hum Genet* **57**, 1028-36.

**Lasorella, A., Noseda, M., Beyna, M., Yokota, Y. and Iavarone, A.** (2000). Id2 is a retinoblastoma protein target and mediates signalling by Myc oncoproteins. *Nature* **407**, 592-8.

**Lawson, K. A., Dunn, N. R., Roelen, B. A., Zeinstra, L. M., Davis, A. M., Wright, C. V., Korving, J. P. and Hogan, B. L.** (1999). Bmp4 is required for the generation of primordial germ cells in the mouse embryo. *Genes Dev* **13**, 424-36.

**Lawson, K. A. and Hage, W. J.** (1994). Clonal analysis of the origin of primordial germ cells in the mouse. *Ciba Found Symp* **182**, 68-84; discussion 84-91.

**Li, B., Nair, M., Mackay, D. R., Bilanchone, V., Hu, M., Fallahi, M., Song, H., Dai, Q., Cohen, P. E. and Dai, X.** (2005a). Ovol1 regulates meiotic pachytene progression during spermatogenesis by repressing Id2 expression. *Development* **132**, 1463-73.

**Li, H. and Kim, K. H.** (2004). Retinoic acid inhibits rat XY gonad development by blocking mesonephric cell migration and decreasing the number of gonocytes. *Biol Reprod* **70**, 687-93.

**Li, X., Luo, Y., Starremans, P. G., McNamara, C. A., Pei, Y. and Zhou, J.** (2005b). Polycystin-1 and polycystin-2 regulate the cell cycle through the helix-loop-helix inhibitor Id2. *Nat Cell Biol* **7**, 1202-12.

**Lin, Y. and Page, D. C.** (2005). Dazl deficiency leads to embryonic arrest of germ cell development in XY C57BL/6 mice. *Dev Biol* **288**, 309-16.

**Liu, Y., Encinas, M., Comella, J. X., Aldea, M. and Gallego, C.** (2004). Basic helix-loop-helix proteins bind to TrkB and p21(Cip1) promoters linking differentiation and cell cycle arrest in neuroblastoma cells. *Mol.Cell Biol.* **24**, 2662-2672.

**Livera, G., Rouiller-Fabre, V., Durand, P. and Habert, R.** (2000). Multiple effects of retinoids on the development of Sertoli, germ, and Leydig cells of fetal and neonatal rat testis in culture. *Biol Reprod* **62**, 1303-14.

**Loveys, D. A., Streiff, M. B. and Kato, G. J.** (1996). E2A basic-helix-loop-helix transcription factors are negatively regulated by serum growth factors and by the Id3 protein. *Nucleic Acids Res* **24**, 2813-20.

**Lu, J. R., Bassel-Duby, R., Hawkins, A., Chang, P., Valdez, R., Wu, H., Gan, L., Shelton, J. M., Richardson, J. A. and Olson, E. N.** (2002). Control of facial muscle development by MyoR and capsulin. *Science* **298**, 2378-2381.

**Ludbrook, L. M. and Harley, V. R.** (2004). Sex determination: a 'window' of DAX1 activity. *Trends Endocrinol Metab* **15**, 116-21.

**Lyden, D., Young, A. Z., Zagzag, D., Yan, W., Gerald, W., O'Reilly, R., Bader, B. L., Hynes, R. O., Zhuang, Y., Manova, K. et al.** (1999). Id1 and Id3 are required for neurogenesis, angiogenesis and vascularization of tumour xenografts. *Nature* **401**, 670-7.

**Maatouk, D. M., DiNapoli, L., Alvers, A., Parker, K. L., Taketo, M. M. and Capel, B.** (2008). Stabilization of beta-catenin in XY gonads causes male-to-female sex-reversal. *Hum Mol Genet* **17**, 2949-55.

**MacLean, G., Li, H., Metzger, D., Chambon, P. and Petkovich, M.** (2007). Apoptotic extinction of germ cells in testes of Cyp26b1 knockout mice. *Endocrinology* **148**, 4560-7.

**Malki, S., Bibeau, F., Notarnicola, C., Roques, S., Berta, P., Poulat, F. and Boizet-Bonhoure, B.** (2007). Expression and biological role of the prostaglandin D synthase/SOX9 pathway in human ovarian cancer cells. *Cancer Lett* **255**, 182-93.

**Malki, S., Nef, S., Notarnicola, C., Thevenet, L., Gasca, S., Mejean, C., Berta, P., Poulat, F. and Boizet-Bonhoure, B.** (2005). Prostaglandin D2 induces nuclear import of the sex-determining factor SOX9 via its cAMP-PKA phosphorylation. *EMBO J* **24**, 1798-809.

**Mantani, A., Hernandez, M. C., Kuo, W. L. and Israel, M. A.** (1998). The mouse Id2 and Id4 genes: structural organization and chromosomal localization. *Gene* **222**, 229-35.

**Mark, M., Jacobs, H., Oulad-Abdelghani, M., Dennefeld, C., Feret, B., Vernet, N., Codreanu, C. A., Chambon, P. and Ghyselinck, N. B.** (2008). STRA8-deficient spermatocytes initiate, but fail to complete, meiosis and undergo premature chromosome condensation. *J Cell Sci* **121**, 3233-42.

**Martineau, J., Nordqvist, K., Tilmann, C., Lovell-Badge, R. and Capel, B.** (1997). Male-specific cell migration into the developing gonad. *Curr Biol* **7**, 958-68.

**Massari, M. E. and Murre, C.** (2000). Helix-loop-helix proteins: regulators of transcription in eucaryotic organisms. *Mol.Cell Biol.* **20**, 429-440.

**Matsui, Y., Toksoz, D., Nishikawa, S., Williams, D., Zsebo, K. and Hogan, B. L.** (1991). Effect of Steel factor and leukaemia inhibitory factor on murine primordial germ cells in culture. *Nature* **353**, 750-2.

**Matsui, Y., Zsebo, K. and Hogan, B. L.** (1992). Derivation of pluripotential embryonic stem cells from murine primordial germ cells in culture. *Cell* **70**, 841-7.

**McClive, P. J., Hurley, T. M., Sarraj, M. A., van den Bergen, J. A. and Sinclair, A. H.** (2003). Subtractive hybridisation screen identifies sexually dimorphic gene expression in the embryonic mouse gonad. *Genesis* **37**, 84-90.

**McLaren, A.** (1981). The fate of germ cells in the testis of fetal Sex-reversed mice. *J Reprod Fertil* **61**, 461-7.

**McLaren, A.** (1983). Studies on mouse germ cells inside and outside the gonad. *J Exp Zool* **228**, 167-71.

**McLaren, A.** (1984). Meiosis and differentiation of mouse germ cells. *Symp Soc Exp Biol* **38**, 7-23.

**McLaren, A.** (2000). Germ and somatic cell lineages in the developing gonad. *Mol Cell Endocrinol* **163**, 3-9.

**McLaren, A.** (2003). Primordial germ cells in the mouse. *Dev Biol* **262**, 1-15.

**McLaren, A. and Southee, D.** (1997). Entry of mouse embryonic germ cells into meiosis. *Dev Biol* **187**, 107-13.

**Meeks, J. J., Crawford, S. E., Russell, T. A., Morohashi, K., Weiss, J. and Jameson, J. L.** (2003a). Dax1 regulates testis cord organization during gonadal differentiation. *Development* **130**, 1029-36.

**Meeks, J. J., Weiss, J. and Jameson, J. L.** (2003b). Dax1 is required for testis determination. *Nat Genet* **34**, 32-3.

**Menke, D. B., Koubova, J. and Page, D. C.** (2003). Sexual differentiation of germ cells in XX mouse gonads occurs in an anterior-to-posterior wave. *Dev Biol* **262**, 303-12.

**Merchant-Larios, H., Moreno-Mendoza, N. and Buehr, M.** (1993). The role of the mesonephros in cell differentiation and morphogenesis of the mouse fetal testis. *Int J Dev Biol* **37**, 407-15.

**Mitsui, K., Tokuzawa, Y., Itoh, H., Segawa, K., Murakami, M., Takahashi, K., Maruyama, M., Maeda, M. and Yamanaka, S.** (2003). The homeoprotein Nanog is required for maintenance of pluripotency in mouse epiblast and ES cells. *Cell* **113**, 631-42.

**Molyneaux, K. and Wylie, C.** (2004). Primordial germ cell migration. *Int J Dev Biol* **48**, 537-44.

**Molyneaux, K. A., Schaible, K. and Wylie, C.** (2003). GP130, the shared receptor for the LIF/IL6 cytokine family in the mouse, is not required for early germ cell differentiation, but is required cell-autonomously in oocytes for ovulation. *Development* **130**, 4287-94.

**Molyneaux, K. A., Stallock, J., Schaible, K. and Wylie, C.** (2001). Time-lapse analysis of living mouse germ cell migration. *Dev Biol* **240**, 488-98.

**Moniot, B., Boizet-Bonhoure, B. and Poulat, F.** (2008). Male specific expression of lipocalin-type prostaglandin D synthase (cPTGDS) during chicken gonadal differentiation: relationship with cSOX9. *Sex Dev* **2**, 96-103.

**Moniot, B., Declosmenil, F., Barrionuevo, F., Scherer, G., Aritake, K., Malki, S., Marzi, L., Cohen-Solal, A., Georg, I., Klattig, J. et al.** (2009). The PGD2 pathway, independently of FGF9, amplifies SOX9 activity in Sertoli cells during male sexual differentiation. *Development* **136**, 1813-21.

**Morais da Silva, S., Hacker, A., Harley, V., Goodfellow, P., Swain, A. and Lovell-Badge, R.** (1996). Sox9 expression during gonadal development implies a conserved role for the gene in testis differentiation in mammals and birds. *Nat Genet* **14**, 62-8.

**Mori, S., Nishikawa, S. I. and Yokota, Y.** (2000). Lactation defect in mice lacking the helix-loop-helix inhibitor Id2. *EMBO J* **19**, 5772-81.

**Murre, C., McCaw, P. S., Vaessin, H., Caudy, M., Jan, L. Y., Jan, Y. N., Cabrera, C. V., Buskin, J. N., Hauschka, S. D. and Lassar, A. B.** (1989). Interactions between heterologous helix-loop-helix proteins generate complexes that bind specifically to a common DNA sequence. *Cell* **58**, 537-544.

**Nagamine, C. M. and Carlisle, C.** (1996). The dominant white spotting oncogene allele Kit(W-42J) exacerbates XY(DOM) sex reversal. *Development* **122**, 3597-605.

**Nakashima, K., Takizawa, T., Ochiai, W., Yanagisawa, M., Hisatsune, T., Nakafuku, M., Miyazono, K., Kishimoto, T., Kageyama, R. and Taga, T.** (2001). BMP2-mediated alteration in the developmental pathway of fetal mouse brain cells from neurogenesis to astrocytogenesis. *Proc Natl Acad Sci U S A* **98**, 5868-73.

**Nef, S., Schaad, O., Stallings, N. R., Cederroth, C. R., Pitetti, J. L., Schaer, G., Malki, S., Dubois-Dauphin, M., Boizet-Bonhoure, B., Descombes, P. et al.** (2005). Gene expression during sex determination reveals a robust female genetic program at the onset of ovarian development. *Dev Biol* **287**, 361-77.

**Nef, S., Verma-Kurvari, S., Merenmies, J., Vassalli, J. D., Efstratiadis, A., Accili, D. and Parada, L. F.** (2003). Testis determination requires insulin receptor family function in mice. *Nature* **426**, 291-5.

**Nichols, J., Zevnik, B., Anastassiadis, K., Niwa, H., Klewe-Nebenius, D., Chambers, I., Scholer, H. and Smith, A.** (1998). Formation of pluripotent stem cells in the mammalian embryo depends on the POU transcription factor Oct4. *Cell* **95**, 379-91.

**Nilsson, J. A., Maclean, K. H., Keller, U. B., Pendeville, H., Baudino, T. A. and Cleveland, J. L.** (2004). Mnt loss triggers Myc transcription targets, proliferation, apoptosis, and transformation. *Mol Cell Biol* **24**, 1560-9.

**Niwa, H., Miyazaki, J. and Smith, A. G.** (2000). Quantitative expression of Oct-3/4 defines differentiation, dedifferentiation or self-renewal of ES cells. *Nat Genet* **24**, 372-6.

**Ohinata, Y., Payer, B., O'Carroll, D., Ancelin, K., Ono, Y., Sano, M., Barton, S. C., Obukhanych, T., Nussenzweig, M., Tarakhovsky, A. et al.** (2005). Blimp1 is a critical determinant of the germ cell lineage in mice. *Nature* **436**, 207-13.

**Ohtani, N., Zebedee, Z., Huot, T. J., Stinson, J. A., Sugimoto, M., Ohashi, Y., Sharrocks, A. D., Peters, G. and Hara, E.** (2001). Opposing effects of Ets and Id proteins on p16INK4a expression during cellular senescence. *Nature* **409**, 1067-70.

**Okamura, D., Kimura, T., Nakano, T. and Matsui, Y.** (2003). Cadherin-mediated cell interaction regulates germ cell determination in mice. *Development* **130**, 6423-30.

**Ortega, S., Ittmann, M., Tsang, S. H., Ehrlich, M. and Basilico, C.** (1998). Neuronal defects and delayed wound healing in mice lacking fibroblast growth factor 2. *Proc Natl Acad Sci U S A* **95**, 5672-7.

**Ortega, S., Prieto, I., Odajima, J., Martin, A., Dubus, P., Sotillo, R., Barbero, J. L., Malumbres, M. and Barbacid, M.** (2003). Cyclin-dependent kinase 2 is essential for meiosis but not for mitotic cell division in mice. *Nat Genet* **35**, 25-31.

**Otsuki, M., Gao, H., Dahlman-Wright, K., Ohlsson, C., Eguchi, N., Urade, Y. and Gustafsson, J. A.** (2003). Specific regulation of lipocalin-type prostaglandin D synthase in mouse heart by estrogen receptor beta. *Mol Endocrinol* **17**, 1844-55.

**Ottolenghi, C., Pelosi, E., Tran, J., Colombino, M., Douglass, E., Nedorezov, T., Cao, A., Forabosco, A. and Schlessinger, D.** (2007). Loss of Wnt4 and Foxl2 leads to female-to-male sex reversal extending to germ cells. *Hum Mol Genet* **16**, 2795-804.

**Oulad-Abdelghani, M., Bouillet, P., Decimo, D., Gansmuller, A., Heyberger, S., Dolle, P., Bronner, S., Lutz, Y. and Chambon, P.** (1996). Characterization of a premeiotic germ cell-specific cytoplasmic protein encoded by Stra8, a novel retinoic acid-responsive gene. *J Cell Biol* **135**, 469-77.

**Palmer, S. J. and Burgoyne, P. S.** (1991). In situ analysis of fetal, prepuberal and adult XX----XY chimaeric mouse testes: Sertoli cells are predominantly, but not exclusively, XY. *Development* **112**, 265-8.

**Pangas, S. A., Choi, Y., Ballow, D. J., Zhao, Y., Westphal, H., Matzuk, M. M. and Rajkovic, A.** (2006). Oogenesis requires germ cell-specific transcriptional regulators Sohlh1 and Lhx8. *Proc Natl Acad Sci U S A* **103**, 8090-5.

**Parker, K. L., Schimmer, B. P. and Schedl, A.** (1999). Genes essential for early events in gonadal development. *Cell Mol Life Sci* **55**, 831-8.

**Parma, P., Radi, O., Vidal, V., Chaboissier, M. C., Dellambra, E., Valentini, S., Guerra, L., Schedl, A. and Camerino, G.** (2006). R-spondin1 is essential in sex determination, skin differentiation and malignancy. *Nat Genet* **38**, 1304-9.

**Payer, B., Saitou, M., Barton, S. C., Thresher, R., Dixon, J. P., Zahn, D., Colledge, W. H., Carlton, M. B., Nakano, T. and Surani, M. A.** (2003). Stella is a maternal effect gene required for normal early development in mice. *Curr Biol* **13**, 2110-7.

**Perk, J., Gil-Bazo, I., Chin, Y., de Candia, P., Chen, J. J., Zhao, Y., Chao, S., Cheong, W., Ke, Y., Al-Ahmadie, H. et al.** (2006). Reassessment of id1 protein expression in human mammary, prostate, and bladder cancers using a monospecific rabbit monoclonal anti-id1 antibody. *Cancer Res* **66**, 10870-7.

**Persson, J. L., Zhang, Q., Wang, X. Y., Ravnik, S. E., Muhlrad, S. and Wolgemuth, D. J.** (2005). Distinct roles for the mammalian A-type cyclins during oogenesis. *Reproduction* **130**, 411-22.

**Pesce, M., Wang, X., Wolgemuth, D. J. and Scholer, H.** (1998). Differential expression of the Oct-4 transcription factor during mouse germ cell differentiation. *Mech Dev* **71**, 89-98.

**Pierucci-Alves, F., Clark, A. M. and Russell, L. D.** (2001). A developmental study of the Desert hedgehog-null mouse testis. *Biol Reprod* **65**, 1392-402.

**Polanco, J. C. and Koopman, P.** (2007). Sry and the hesitant beginnings of male development. *Dev Biol* **302**, 13-24.

**Popov, N., Wahlstrom, T., Hurlin, P. J. and Henriksson, M.** (2005). Mnt transcriptional repressor is functionally regulated during cell cycle progression. *Oncogene* **24**, 8326-37.

**Prabhu, S., Ignatova, A., Park, S. T. and Sun, X. H.** (1997). Regulation of the expression of cyclin-dependent kinase inhibitor p21 by E2A and Id proteins. *Mol.Cell Biol.* **17**, 5888-5896.

**Qin, Y. and Bishop, C. E.** (2005). Sox9 is sufficient for functional testis development producing fertile male mice in the absence of Sry. *Hum Mol Genet* **14**, 1221-9.

**Resnick, J. L., Ortiz, M., Keller, J. R. and Donovan, P. J.** (1998). Role of fibroblast growth factors and their receptors in mouse primordial germ cell growth. *Biol Reprod* **59**, 1224-9.

**Riley, P., nson-Cartwright, L. and Cross, J. C.** (1998). The Hand1 bHLH transcription factor is essential for placentation and cardiac morphogenesis. *Nat.Genet.* **18**, 271-275.

**Roberts, C., Weith, A., Passage, E., Michot, J. L., Mattei, M. G. and Bishop, C. E.** (1988). Molecular and cytogenetic evidence for the location of Tdy and Hya on the mouse Y chromosome short arm. *Proc Natl Acad Sci U S A* **85**, 6446-9.

**Rosner, M. H., Vigano, M. A., Ozato, K., Timmons, P. M., Poirier, F., Rigby, P. W. and Staudt, L. M.** (1990). A POU-domain transcription factor in early stem cells and germ cells of the mammalian embryo. *Nature* **345**, 686-92.

**Ross, A., Munger, S. and Capel, B.** (2007). Bmp7 regulates germ cell proliferation in mouse fetal gonads. *Sex Dev* **1**, 127-37.

**Rothschild, G., Zhao, X., Iavarone, A. and Lasorella, A.** (2006). E Proteins and Id2 converge on p57Kip2 to regulate cell cycle in neural cells. *Mol Cell Biol* **26**, 4351-61.

**Rozenblatt-Rosen, O., Mosonego-Ornan, E., Sadot, E., Madar-Shapiro, L., Sheinin, Y., Ginsberg, D. and Yayon, A.** (2002). Induction of chondrocyte growth arrest by FGF: transcriptional and cytoskeletal alterations. *J Cell Sci* **115**, 553-62.

**Ruggiu, M., Saunders, P. T. and Cooke, H. J.** (2000). Dynamic subcellular distribution of the DAZL protein is confined to primate male germ cells. *J Androl* **21**, 470-7.

**Ruggiu, M., Speed, R., Taggart, M., McKay, S. J., Kilanowski, F., Saunders, P., Dorin, J. and Cooke, H. J.** (1997). The mouse Dazla gene encodes a cytoplasmic protein essential for gametogenesis. *Nature* **389**, 73-7.

**Ruzinova, M. B. and Benezra, R.** (2003). Id proteins in development, cell cycle and cancer. *Trends Cell Biol* **13**, 410-8.

**Sablitzky, F., Moore, A., Bromley, M., Deed, R. W., Newton, J. S. and Norton, J. D.** (1998). Stage- and subcellular-specific expression of Id proteins in male germ and Sertoli cells implicates distinctive regulatory roles for Id proteins during meiosis, spermatogenesis, and Sertoli cell function. *Cell Growth Differ* **9**, 1015-24.

**Saga, Y., Miyagawa-Tomita, S., Takagi, A., Kitajima, S., Miyazaki, J. and Inoue, T.** (1999). MesP1 is expressed in the heart precursor cells and required for the formation of a single heart tube. *Development* **126**, 3437-47.

**Saito, S., Tsuda, H. and Michimata, T.** (2002). Prostaglandin D2 and reproduction. *Am J Reprod Immunol* **47**, 295-302.

**Saitou, M., Barton, S. C. and Surani, M. A.** (2002). A molecular programme for the specification of germ cell fate in mice. *Nature* **418**, 293-300.

**Saitou, M., Payer, B., Lange, U. C., Erhardt, S., Barton, S. C. and Surani, M. A.** (2003). Specification of germ cell fate in mice. *Philos Trans R Soc Lond B Biol Sci* **358**, 1363-70.

**Samy, E. T., Li, J. C., Grima, J., Lee, W. M., Silvestrini, B. and Cheng, C. Y.** (2000). Sertoli cell prostaglandin D2 synthetase is a multifunctional molecule: its expression and regulation. *Endocrinology* **141**, 710-21.

**Sato, M., Kimura, T., Kurokawa, K., Fujita, Y., Abe, K., Masuhara, M., Yasunaga, T., Ryo, A., Yamamoto, M. and Nakano, T.** (2002). Identification of PGC7, a new gene expressed specifically in preimplantation embryos and germ cells. *Mech Dev* **113**, 91-4.

**Satyanarayana, A. and Kaldis, P.** (2009). Mammalian cell-cycle regulation: several Cdks, numerous cyclins and diverse compensatory mechanisms. *Oncogene* **28**, 2925-39.

**Schmahl, J. and Capel, B.** (2003). Cell proliferation is necessary for the determination of male fate in the gonad. *Dev Biol* **258**, 264-76.

**Schmahl, J., Eicher, E. M., Washburn, L. L. and Capel, B.** (2000). Sry induces cell proliferation in the mouse gonad. *Development* **127**, 65-73.

**Schmahl, J., Kim, Y., Colvin, J. S., Ornitz, D. M. and Capel, B.** (2004). Fgf9 induces proliferation and nuclear localization of FGFR2 in Sertoli precursors during male sex determination. *Development* **131**, 3627-36.

**Sekido, R., Bar, I., Narvaez, V., Penny, G. and Lovell-Badge, R.** (2004). SOX9 is up-regulated by the transient expression of SRY specifically in Sertoli cell precursors. *Dev Biol* **274**, 271-9.

**Sekido, R. and Lovell-Badge, R.** (2008). Sex determination involves synergistic action of SRY and SF1 on a specific Sox9 enhancer. *Nature* **453**, 930-4.

**Sekido, R. and Lovell-Badge, R.** (2009). Sex determination and SRY: down to a wink and a nudge? *Trends Genet* **25**, 19-29.

**Seligman, J. and Page, D. C.** (1998). The Dazh gene is expressed in male and female embryonic gonads before germ cell sex differentiation. *Biochem Biophys Res Commun* **245**, 878-82.

**Siep, M., Sleddens-Linkels, E., Mulders, S., van Eenennaam, H., Wassenaar, E., Van Cappellen, W. A., Hoogerbrugge, J., Grootegoed, J. A. and Baarends, W. M.** (2004). Basic helix-loop-helix transcription factor Tcfl5 interacts with the Calmegin gene promoter in mouse spermatogenesis. *Nucleic Acids Res* **32**, 6425-36.

**Soyal, S. M., Amleh, A. and Dean, J.** (2000). FIGalpha, a germ cell-specific transcription factor required for ovarian follicle formation. *Development* **127**, 4645-54.

**Spotila, L. D., Spotila, J. R. and Hall, S. E.** (1998). Sequence and expression analysis of WT1 and Sox9 in the red-eared slider turtle, Trachemys scripta. *J Exp Zool* **281**, 417-27.

**Stallock, J., Molyneaux, K., Schaible, K., Knudson, C. M. and Wylie, C.** (2003). The pro-apoptotic gene Bax is required for the death of ectopic primordial germ cells during their migration in the mouse embryo. *Development* **130**, 6589-97.

**Steingrimsson, E., Tessarollo, L., Reid, S. W., Jenkins, N. A. and Copeland, N. G.** (1998). The bHLH-Zip transcription factor Tfeb is essential for placental vascularization. *Development* **125**, 4607-16.

**Stewart, C. L., Kaspar, P., Brunet, L. J., Bhatt, H., Gadi, I., Kontgen, F. and Abbondanzo, S. J.** (1992). Blastocyst implantation depends on maternal expression of leukaemia inhibitory factor. *Nature* **359**, 76-9.

**Stinson, J., Inoue, T., Yates, P., Clancy, A., Norton, J. D. and Sharrocks, A. D.** (2003). Regulation of TCF ETS-domain transcription factors by helix-loop-helix motifs. *Nucleic Acids Res* **31**, 4717-28.

**Sugiyama, A., Kume, A., Nemoto, K., Lee, S. Y., Asami, Y., Nemoto, F., Nishimura, S. and Kuchino, Y.** (1989). Isolation and characterization of s-myc, a member of the rat myc gene family. *Proc.Natl.Acad.Sci.U.S.A* **86**, 9144-9148.

**Sun, H., Lu, B., Li, R. Q., Flavell, R. A. and Taneja, R.** (2001). Defective T cell activation and autoimmune disorder in Stra13-deficient mice. *Nat Immunol* **2**, 1040-7.

**Suzuki, A. and Saga, Y.** (2008). Nanos2 suppresses meiosis and promotes male germ cell differentiation. *Genes Dev* **22**, 430-5.

**Swain, A. and Lovell-Badge, R.** (1999). Mammalian sex determination: a molecular drama. *Genes Dev* **13**, 755-67.

**Swain, A., Narvaez, V., Burgoyne, P., Camerino, G. and Lovell-Badge, R.** (1998). Dax1 antagonizes Sry action in mammalian sex determination. *Nature* **391**, 761-7.

**Swain, A., Zanaria, E., Hacker, A., Lovell-Badge, R. and Camerino, G.** (1996). Mouse Dax1 expression is consistent with a role in sex determination as well as in adrenal and hypothalamus function. *Nat Genet* **12**, 404-9.

**Swarbrick, A., Akerfeldt, M. C., Lee, C. S., Sergio, C. M., Caldon, C. E., Hunter, L. J., Sutherland, R. L. and Musgrove, E. A.** (2005). Regulation of cyclin expression and cell cycle progression in breast epithelial cells by the helix-loop-helix protein Id1. *Oncogene* **24**, 381-9.

**Takeda, K., Yokoyama, S., Aburatani, H., Masuda, T., Han, F., Yoshizawa, M., Yamaki, N., Yamamoto, H., Eguchi, N., Urade, Y. et al.** (2006). Lipocalin-type prostaglandin D synthase as a melanocyte marker regulated by MITF. *Biochem Biophys Res Commun* **339**, 1098-106.

**Takeuchi, Y., Molyneaux, K., Runyan, C., Schaible, K. and Wylie, C.** (2005). The roles of FGF signaling in germ cell migration in the mouse. *Development* **132**, 5399-409.

**Tam, P. P. and Snow, M. H.** (1981). Proliferation and migration of primordial germ cells during compensatory growth in mouse embryos. *J Embryol Exp Morphol* **64**, 133-47.

**Tanaka, K., Tamura, H., Tanaka, H., Katoh, M., Futamata, Y., Seki, N., Nishimune, Y. and Hara, T.** (2002). Spermatogonia-dependent expression of testicular genes in mice. *Dev Biol* **246**, 466-79.

**Tanaka, S. S., Toyooka, Y., Akasu, R., Katoh-Fukui, Y., Nakahara, Y., Suzuki, R., Yokoyama, M. and Noce, T.** (2000). The mouse homolog of Drosophila Vasa is required for the development of male germ cells. *Genes Dev* **14**, 841-53.

**Tanaka, T., Urade, Y., Kimura, H., Eguchi, N., Nishikawa, A. and Hayaishi, O.** (1997). Lipocalin-type prostaglandin D synthase (beta-trace) is a newly recognized type of retinoid transporter. *J Biol Chem* **272**, 15789-95.

**Tian, H., Hammer, R. E., Matsumoto, A. M., Russell, D. W. and McKnight, S. L.** (1998). The hypoxia-responsive transcription factor EPAS1 is essential for catecholamine homeostasis and protection against heart failure during embryonic development. *Genes Dev.* **12**, 3320-3324.

**Tilmann, C. and Capel, B.** (1999). Mesonephric cell migration induces testis cord formation and Sertoli cell differentiation in the mammalian gonad. *Development* **126**, 2883-90.

**Tokudome, S., Sano, M., Shinmura, K., Matsuhashi, T., Morizane, S., Moriyama, H., Tamaki, K., Hayashida, K., Nakanishi, H., Yoshikawa, N. et al.** (2009). Glucocorticoid protects rodent hearts from ischemia/reperfusion injury by activating lipocalin-type prostaglandin D synthase-derived PGD2 biosynthesis. *J Clin Invest* **119**, 1477-88.

**Tomizuka, K., Horikoshi, K., Kitada, R., Sugawara, Y., Iba, Y., Kojima, A., Yoshitome, A., Yamawaki, K., Amagai, M., Inoue, A. et al.** (2008). R-spondin1 plays an essential role in ovarian development through positively regulating Wnt-4 signaling. *Hum Mol Genet* **17**, 1278-91.

**Toyoda, S., Miyazaki, T., Miyazaki, S., Yoshimura, T., Yamamoto, M., Tashiro, F., Yamato, E. and Miyazaki, J.** (2009). Sohlh2 affects differentiation of KIT positive oocytes and spermatogonia. *Dev Biol* **325**, 238-48.

**Trautmann, E., Guerquin, M. J., Duquenne, C., Lahaye, J. B., Habert, R. and Livera, G.** (2008). Retinoic acid prevents germ cell mitotic arrest in mouse fetal testes. *Cell Cycle* **7**, 656-64.

**Trimarchi, J. M. and Lees, J. A.** (2002). Sibling rivalry in the E2F family. *Nat Rev Mol Cell Biol* **3**, 11-20.

**Tsuda, M., Sasaoka, Y., Kiso, M., Abe, K., Haraguchi, S., Kobayashi, S. and Saga, Y.** (2003). Conserved role of nanos proteins in germ cell development. *Science* **301**, 1239-41.

**Urade, Y. and Hayaishi, O.** (2000). Biochemical, structural, genetic, physiological, and pathophysiological features of lipocalin-type prostaglandin D synthase. *Biochim Biophys Acta* **1482**, 259-71.

**Vainio, S., Heikkila, M., Kispert, A., Chin, N. and McMahon, A. P.** (1999). Female development in mammals is regulated by Wnt-4 signalling. *Nature* **397**, 405-9.

**Van Wayenbergh, R., Taelman, V., Pichon, B., Fischer, A., Kricha, S., Gessler, M., Christophe, D. and Bellefroid, E. J.** (2003). Identification of BOIP, a novel cDNA highly expressed during spermatogenesis that encodes a protein interacting with the orange domain of the hairy-related transcription factor HRT1/Hey1 in Xenopus and mouse. *Dev Dyn* **228**, 716-25.

**Vidal, V. P., Chaboissier, M. C., de Rooij, D. G. and Schedl, A.** (2001). Sox9 induces testis development in XX transgenic mice. *Nat Genet* **28**, 216-7.

**Walker, W., Zhou, Z. Q., Ota, S., Wynshaw-Boris, A. and Hurlin, P. J.** (2005). Mnt-Max to Myc-Max complex switching regulates cell cycle entry. *J Cell Biol* **169**, 405-13.

**Ware, C. B., Horowitz, M. C., Renshaw, B. R., Hunt, J. S., Liggitt, D., Koblar, S. A., Gliniak, B. C., McKenna, H. J., Papayannopoulou, T., Thoma, B. et al.** (1995). Targeted disruption of the low-affinity leukemia inhibitory factor receptor gene causes placental, skeletal, neural and metabolic defects and results in perinatal death. *Development* **121**, 1283-99.

**Webb, S. E. and Miller, A. L.** (2003). Calcium signalling during embryonic development. *Nat Rev Mol Cell Biol* **4**, 539-51.

**Western, P., Maldonado-Saldivia, J., van den Bergen, J., Hajkova, P., Saitou, M., Barton, S. and Surani, M. A.** (2005). Analysis of Esg1 expression in pluripotent cells and the germline reveals similarities with Oct4 and Sox2 and differences between human pluripotent cell lines. *Stem Cells* **23**, 1436-42.

**Western, P. S., Miles, D. C., van den Bergen, J. A., Burton, M. and Sinclair, A. H.** (2008). Dynamic regulation of mitotic arrest in fetal male germ cells. *Stem Cells* **26**, 339-47.

**White, D. M., Takeda, T., DeGroot, L. J., Stefansson, K. and Arnason, B. G.** (1997). Beta-trace gene expression is regulated by a core promoter and a distal thyroid hormone response element. *J Biol Chem* **272**, 14387-93.

**Wilhelm, D., Hiramatsu, R., Mizusaki, H., Widjaja, L., Combes, A. N., Kanai, Y. and Koopman, P.** (2007). SOX9 regulates prostaglandin D synthase gene transcription in vivo to ensure testis development. *J Biol Chem* **282**, 10553-60.

**Wilhelm, D., Martinson, F., Bradford, S., Wilson, M. J., Combes, A. N., Beverdam, A., Bowles, J., Mizusaki, H. and Koopman, P.** (2005). Sertoli cell differentiation is induced both cell-autonomously and through prostaglandin signaling during mammalian sex determination. *Dev Biol* **287**, 111-24.

**Wilhelm, D., Washburn, L. L., Truong, V., Fellous, M., Eicher, E. M. and Koopman, P.** (2009). Antagonism of the testis- and ovary-determining pathways during ovotestis development in mice. *Mech Dev* **126**, 324-36.

**Wilson, M. J., Jeyasuria, P., Parker, K. L. and Koopman, P.** (2005). The transcription factors steroidogenic factor-1 and SOX9 regulate expression of Vanin-1 during mouse testis development. *J Biol Chem* **280**, 5917-23.

**Wolfes, H., Kogawa, K., Millette, C. F. and Cooper, G. M.** (1989). Specific expression of nuclear proto-oncogenes before entry into meiotic prophase of spermatogenesis. *Science* **245**, 740-3.

**Xie, T. and Spradling, A. C.** (1998). decapentaplegic is essential for the maintenance and division of germline stem cells in the Drosophila ovary. *Cell* **94**, 251-60.

**Yabuta, Y., Kurimoto, K., Ohinata, Y., Seki, Y. and Saitou, M.** (2006). Gene expression dynamics during germline specification in mice identified by quantitative single-cell gene expression profiling. *Biol Reprod* **75**, 705-16.

**Yamaguchi, S., Kimura, H., Tada, M., Nakatsuji, N. and Tada, T.** (2005). Nanog expression in mouse germ cell development. *Gene Expr Patterns* **5**, 639-46.

**Yao, H. H. and Capel, B.** (2002). Disruption of testis cords by cyclopamine or forskolin reveals independent cellular pathways in testis organogenesis. *Dev Biol* **246**, 356-65.

**Yao, H. H., DiNapoli, L. and Capel, B.** (2003). Meiotic germ cells antagonize mesonephric cell migration and testis cord formation in mouse gonads. *Development* **130**, 5895-902.

**Yao, H. H., Matzuk, M. M., Jorgez, C. J., Menke, D. B., Page, D. C., Swain, A. and Capel, B.** (2004). Follistatin operates downstream of Wnt4 in mammalian ovary organogenesis. *Dev Dyn* **230**, 210-5.

**Ying, Q. L., Nichols, J., Chambers, I. and Smith, A.** (2003). BMP induction of Id proteins suppresses differentiation and sustains embryonic stem cell self-renewal in collaboration with STAT3. *Cell* **115**, 281-92.

**Ying, Y., Liu, X. M., Marble, A., Lawson, K. A. and Zhao, G. Q.** (2000). Requirement of Bmp8b for the generation of primordial germ cells in the mouse. *Mol Endocrinol* **14**, 1053-63.

**Ying, Y. and Zhao, G. Q.** (2001). Cooperation of endoderm-derived BMP2 and extraembryonic ectoderm-derived BMP4 in primordial germ cell generation in the mouse. *Dev Biol* **232**, 484-92.

**Yokota, Y.** (2001). Id and development. *Oncogene* **20**, 8290-8.

**Yoshida, S., Takakura, A., Ohbo, K., Abe, K., Wakabayashi, J., Yamamoto, M., Suda, T. and Nabeshima, Y.** (2004). Neurogenin3 delineates the earliest stages of spermatogenesis in the mouse testis. *Dev Biol* **269**, 447-58.

**Yoshimizu, T., Sugiyama, N., De Felice, M., Yeom, Y. I., Ohbo, K., Masuko, K., Obinata, M., Abe, K., Scholer, H. R. and Matsui, Y.** (1999). Germline-specific expression of the Oct-4/green fluorescent protein (GFP) transgene in mice. *Dev Growth Differ* **41**, 675-84.

**Zamboni, L. and Upadhyay, S.** (1983). Germ cell differentiation in mouse adrenal glands. *J Exp Zool* **228**, 173-93.

**Zebedee, Z. and Hara, E.** (2001). Id proteins in cell cycle control and cellular senescence. *Oncogene* **20**, 8317-25.

**Zhang, H. and Bradley, A.** (1996). Mice deficient for BMP2 are nonviable and have defects in amnion/chorion and cardiac development. *Development* **122**, 2977-86.

**Zhao, G. Q. and Hogan, B. L.** (1996). Evidence that mouse Bmp8a (Op2) and Bmp8b are duplicated genes that play a role in spermatogenesis and placental development. *Mech Dev* **57**, 159-68.

**Zheng, W., Wang, H., Xue, L., Zhang, Z. and Tong, T.** (2004). Regulation of cellular senescence and p16(INK4a) expression by Id1 and E47 proteins in human diploid fibroblast. *J Biol Chem* **279**, 31524-32.

# Acknowledgements

I'd like to say a general thank you to all in E3 and around the HGU who helped me out in various small, but kind ways, lending me reagents when needed etc. Thanks especially go to Ian Adams, my supervisor, for helping me to conceive of the experiments and analyse data during my research and also in writing this thesis. And warm appreciations go to my fellow lab members – Diana Best, Rupert Ollinger and Ayhan Kocher. Many thank yous go to Howard Cooke for letting me use his Dazl antibody, and big thanks to Gabriella Durcova-Hills for generating, dissecting, preparing and sending *Sry* transgenic/knockout embryos.